

Climate Change Adaptation of Urban Stormwater Infrastructure

John Gulliver, Principal Investigator

St. Anthony Falls Laboratory
University of Minnesota

JUNE 2023

Research Report
Final Report 2023-21

To request this document in an alternative format, such as braille or large print, call [651-366-4718](tel:651-366-4718) or [1-800-657-3774](tel:1-800-657-3774) (Greater Minnesota) or email your request to ADArequest.dot@state.mn.us. Please request at least one week in advance.

Technical Report Documentation Page

1. Report No. MN 2023-21	2.	3. Recipients Accession No.	
4. Title and Subtitle Climate Change Adaptation of Urban Stormwater Infrastructure		5. Report Date June 2023	
		6.	
7. Author(s) Andrew J. Erickson, William R. Herb, Noah D. Gallagher, Peter T. Weiss, Bruce N. Wilson, John S. Gulliver		8. Performing Organization Report No.	
9. Performing Organization Name and Address St. Anthony Falls Laboratory University of Minnesota 2 Third Ave SE Minneapolis, MN 55414		10. Project/Task/Work Unit No. CTS #2021003	
		11. Contract (C) or Grant (G) No. (c) 1036217	
12. Sponsoring Organization Name and Address Minnesota Department of Transportation Office of Research & Innovation 395 John Ireland Boulevard, MS 330 St. Paul, Minnesota 55155-1899		13. Type of Report and Period Covered Final Report	
		14. Sponsoring Agency Code	
15. Supplementary Notes http://mdl.mndot.gov/			
16. Abstract (Limit: 250 words) <p>The final analysis of historical (TP-40), current (Atlas 14), and future predicted storm events for three watersheds in Minnesota (Duluth, Minneapolis, Rochester) has shown that current design philosophy is not sufficient to prevent flooding from 10-year and larger design storm events and that flood depth and duration will increase given current climate projections. Several stormwater infrastructure adaptation strategies were assessed for reducing flood depth and duration: Baseline (existing conditions), adding rain gardens (aka, Infiltration Basins), adding new wet ponds, retrofitting existing stormwater ponds to be "Smart Ponds, adding new Smart Ponds while also converting existing ponds into Smart Ponds, or upsizing of stormwater pipes to convey more water. In watersheds that are mixed urban, suburban, and rural like Rochester's Kings Run or Duluth's Miller Creek sub-watersheds, the most cost-effective climate change adaptation strategy was to build new stormwater wet ponds (Extra Ponds strategy) to treat the impervious surfaces not currently treated by existing wet ponds and other stormwater BMPs. In the fully developed urban 1NE watershed in Minneapolis, the most cost-effective (excluding land costs) climate change adaptation strategy was building wet ponds (Extra Ponds). Securing property for building new stormwater infrastructure in fully developed urban watersheds like 1NE may be a substantial cost compared to other watersheds. Smart Ponds do not require additional land for implementation and thus represent a relatively low-cost alternative that will be more beneficial in watersheds with numerous existing wet ponds.</p>			
17. Document Analysis/Descriptors Climate change adaptation, Runoff, Floods, Ponding, Watersheds		18. Availability Statement No restrictions. Document available from: National Technical Information Services, Alexandria, Virginia 22312	
19. Security Class (this report) Unclassified	20. Security Class (this page) Unclassified	21. No. of Pages 163	22. Price

Climate Change Adaptation of Urban Stormwater Infrastructure

Final Report

Prepared by:

Andrew J. Erickson¹

William R. Herb¹

Noah D. Gallagher^{1,2}

Peter T. Weiss³

Bruce N. Wilson⁴

John S. Gulliver^{1,2}

¹St. Anthony Falls Laboratory, University of Minnesota

²Department of Civil, Environmental, Geo-engineering

³Department of Civil & Environmental Engineering, Valparaiso University

⁴Department of Department of Bioproducts and Biosystems Engineering, University of Minnesota

June 2023

Published by:

Minnesota Department of Transportation

Office of Research and Innovation

395 John Ireland Boulevard, MS 330

St. Paul, Minnesota 55155-1899

This report represents the results of research conducted by the authors and does not necessarily represent the views or policies of the Minnesota Department of Transportation or University of Minnesota. This report does not contain a standard or specified technique.

The authors, the Minnesota Department of Transportation, and University of Minnesota do not endorse products or manufacturers. Trade or manufacturers' names appear herein solely because they are considered essential to this report because they are considered essential to this report.

Acknowledgements

The authors thank the Minnesota Department of Transportation (MnDOT) and the Local Road Research Board (LRRB) for funding this research. The authors thank Elizabeth Klemann (MnDOT), Leif Halverson (MnDOT), and Jackie Jiran (MnDOT) for serving as project coordinators. The authors also thank Erik Brenna (MnDOT) for serving as the technical liaison and project champion.

The authors thank numerous individuals from MnDOT, cities, counties, state agencies, and other entities for serving on the Technical Advisory Panel and providing input, review, and comment on task deliverables and the final report, including but not limited to Troy Erickson (Rochester), Ryan Granlund (Duluth), Andrea Hendrickson (MnDOT), Brian Jastram (MnDOT), Stephanie Johnson (Barr Engineering), Kris Langlie (MnDOT), Jeffrey Meek (MnDOT), Randy Neprash (Stantec), Beth Neuendorf (MnDOT), Nick Olson (MnDOT), Brent Rusco (MnDOT), and Micaela Resh (MnDOT).

Table of Contents

Chapter 1. Estimation Techniques for the Cost of Adapting Stormwater Management Systems to Future Climate Change Scenarios: A Literature Review	1
1.1 Introduction	1
1.2 Climate Change Literature	1
1.2.1 Global Climate Models	1
1.2.2 Spatially Downscaled Global Climate Model Projections	2
1.2.3 Evaluation of Model Projections	3
1.2.4 Sub-daily Precipitation Depths from Global Climate Model Projections.....	4
1.2.4.1 Overview	4
1.2.4.2 Downscaling Methods.....	5
1.3 Cost of Stormwater Infrastructure.....	7
1.3.1 Tools and Calculators	7
1.3.1.1 WERF Spreadsheet Calculators.	7
1.3.1.2 USEPA SUSTAIN.....	7
1.3.1.3 USEPA National Stormwater Calculator.....	8
1.3.1.4 National Green Values Calculator.....	8
Chapter 2. Potential Adaptation to Climate Change Predictions	9
2.1 Introduction	9
2.2 U.S. EPA SWMM Models.....	9
2.2.1 Miller Creek.....	10
2.2.1.1 Calibration.....	12
2.2.1.2 Modifications	16
2.2.2 Minneapolis.....	17
2.2.2.1 Calibration.....	17
2.2.3 Rochester	18
2.2.3.1 Calibration.....	19
2.3 Historical and Future Climate Inputs to SWMM	19
2.4 Stormwater Infrastructure Adaptation Strategies.....	23
2.5 Adaptation Strategy Simulation Results	25
2.5.1 Miller Creek.....	25

2.5.1.1	Upstream – Node J14.....	27
2.5.1.2	Kohl’s Wetland – Node J23 & link main25	29
2.5.1.3	Miller Creek Outlet.....	31
2.5.2	Minneapolis.....	32
2.5.2.1	Upstream Manhole - MH420743	33
2.5.2.2	Downstream Node - SA999039.....	35
2.5.2.3	1NE Outlet.....	37
2.5.3	Rochester	38
2.5.3.1	Mid-watershed – Node RN176248	39
2.5.3.2	Lower-watershed – Node SP113.....	40
2.5.3.3	Kings Run Outlet.....	41
2.6	Designing For Storms	43
2.7	Discussion.....	45
2.7.1	Miller Creek, Duluth.....	45
2.7.2	1NE, Minneapolis	46
2.7.3	Kings Run, Rochester.....	46
Chapter 3.	Cost of Adaptation.....	48
3.1	Introduction	48
3.2	Calculating Costs	48
3.2.1	Cost Assumptions – CLASIC.....	48
3.2.2	Cost Assumptions – Smart Ponds	50
3.2.3	Cost Assumptions – More Smart Ponds.....	51
3.2.4	Cost Assumptions – Pipe Upsizing	51
3.2.5	Comparing CLASIC to other cost models	51
3.3	Cost Effectiveness Analysis	55
3.3.1	Total Cost of Stormwater Infrastructure Adaptation Strategies	55
3.3.2	Flood Mitigation Effectiveness.....	56
3.3.3	Cost & Effectiveness.....	58
Chapter 4.	Summary and Conclusions.....	62
Appendix A: SWMM Simulation Results		
Appendix B: Climate Predictions		

List of Figures

Figure 1: Equivalent CO2 emissions for the RCP 2.6, 4.5, 6.0 and 8.5 scenarios using in CMIP5 (Source epa.gov).	2
Figure 2: Illustration of Quantile Method for Sub-daily Depths.	6
Figure 3: Illustration of Equidistant Quantile Mapping for Daily Depths.	6
Figure 4. The Miller Creek and Coffee Creek watersheds. The 44 subcatchments of Miller Creek are shaded green and the six subcatchments of Coffee Creek are shaded purple. The main storm sewers and channels that convey water from the subcatchments to the main channel, along with the main channel itself, are shown as blue lines.	11
Figure 5: Details of the Miller Creek SWMM model in the vicinity of the combined Miller Creek and Coffee Creek outlets. The subcatchments of Miller Creek are shaded green and the subcatchments of Coffee Creek are shaded purple. The combined culvert outlet to Lake Superior is labeled main68.	12
Figure 6. Observed and simulated daily average flow rates for the Miller Creek outlet, May 1 to October 31, 2008.	13
Figure 7. Observed and simulated flow exceedance probabilities for the Miller Creek outlet for daily averaged data.	13
Figure 8. Simulated flood extent for the June 19-20, 2012 storm in Duluth (7.25 in., see Figure 10). The water elevation in the middle of the Kohl’s wetland is 1338 ft above mean sea level (MSL), and the elevation of Highway 53 adjacent to the wetland is 1337 ft above MSL. The simulated flood extent was approximated using piece-wise flat water levels between the model nodes and 1-foot contours from the Minnesota state LiDAR data.	14
Figure 9. Observed flood inundation map for the June 2012 storm in Duluth (7.25 in.), from Czuba et al. 2012.	15
Figure 10. Hourly rainfall at Duluth International Airport on June 19 and 20, 2012, totaling 7.25 in.....	16
Figure 11: The 1NE watershed in Minneapolis shown as the grey area with subcatchments outlined in grey lines. The Columbia Golf Course is outlined in green. Storm sewer and surface channels are shown in blue.	17
Figure 12: The Kings Run watershed shown as the grey area with subcatchments outlined in grey lines. Rochester City boundaries shown as red lines. Primary surface channels are shown in blue.	18
Figure 13: Storm depth (in) increasing from smallest (top) to largest (bottom) for TP-40, Atlas-14, and the 50th percentile future projections in Duluth, Minneapolis, and Rochester.	21
Figure 14: Projected % change in the 100-year storm size for the time period 2070-2099 for the mpi-esm mr RCP8.5 GCM model outputs, as supplied by the WSP products.	22

Figure 15: Projected 24-hour precipitation distribution for 32 RCP8.5 GCM outputs for Rochester, MN (solid lines) using the quantile method and the MSE-3 rainfall distribution (open circles).	23
Figure 16. Approximate flood extent and area of inundation during the 2012 flood in Duluth, MN (light blue shading) and points of interest for comparing stormwater adaptation strategies (red dots) with labels in white rectangles.	26
Figure 17: Node Depth in ft (top) and flood duration in hours (bottom) for the 2-, 10-, and 100-year storms at node J14 in Duluth.	28
Figure 18: Node Depth in ft (top), flood duration in hours (middle), and peak flow rate in cfs (bottom) for the 2-, 10-, and 100-year storms at node J23 (depth and duration) and link main25 (flow rate) in Duluth.	30
Figure 19: Peak flow rate (cfs) at the outlet from Miller Creek and Coffee Creek sub-watersheds (main68).	31
Figure 20: Miller Creek Outlet (main68) Hydrograph (flow in cfs) for the 100-year Atlas 14 event (6.31 inches)	32
Figure 21: Nodes of Interest in the 1NE Watershed. The four nodes and two outlets discussed are labeled with yellow circles. Additionally, existing wet ponds are identified with light blue circles and the sewer lines are depicted as blue lines. Two of the nodes of interest, SA35C350 and SS512682, are existing wet ponds so are represented with both yellow and blue circles.	33
Figure 22: Node Depth in ft (top) and flood duration in hours (bottom) for the 2-, 10-, and 100-year storms at MH420743 in Minneapolis.	34
Figure 23: Node Depth in ft (top) and flood duration in hours (bottom) for the 2-, 10-, and 100-year storms at SA999039 in Minneapolis.	36
Figure 24: Maximum Flow Rate (cfs) for OF441017 in Minneapolis for all storms.	37
Figure 25: 1NE Outlet (OF441017) Hydrograph (flow in cfs) for the 100-year Atlas 14 event (7.5 inches)	38
Figure 26: Nodes of Interest in the Kings Run Watershed. The node and outlet discussed are labeled with yellow circles. Additionally, existing wet ponds are identified with light blue circles Three of the nodes of interest SP113, SP64, and SP105, are existing wet ponds so are represented with both yellow and light blue circles.	39
Figure 27: Node Depth in ft (top) and flood duration in hours (bottom) for the 2-, 10-, and 100-year storms at node RN176248 in Rochester.	40
Figure 28: Node Depth in ft (top) and flood duration in hours (bottom) for the 2-, 10-, and 100-year storms at node SP113 in Rochester.	41
Figure 29: Maximum Flow Rate (cfs) for the outlet (Temp) in Rochester for all storms.	42

Figure 30: Kings Run Outlet (Temp) Hydrograph (flow in cfs) for the 100-year Atlas 14 event (7.85 inches).....	42
Figure 31: Ratio of Wet Pond Area to Catchment Area for the Miller Creek sub-watershed in Duluth (a), the 1NE sub-watershed in Minneapolis (b), and the Kings Run sub-watershed in Rochester (c), for Atlas 14 storms including 2-yr, 10-yr, 25-yr, 50-yr, and 100-year. Note: x-axis logarithmic scale.	44
Figure 32: Influence of rainfall distribution over 24 hours on water balance in the 1NE Minneapolis watershed for the 100-year storm.....	45
Figure 33: 50-year life-cycle cost for a bioretention (aka Infiltration Basins) as predicted by CLASIC, iDST, and Weiss et al. (2005, 2007). WQV = Water Quality Volume.	53
Figure 34: 50-year life-cycle cost for a wet pond as predicted by CLASIC, iDST, and Weiss et al. (2005, 2007). WQV = Water Quality Volume.....	54
Figure 35: Total cost of adaptation strategies compared to change in flood depth (Δ Depth (ft)) for strategies that provide at least 0.5 ft of flood depth reduction. Note: Land costs excluded.....	60
Figure 36: Total cost of adaptation strategies compared to change in peak outflow (Δ Peak Flow (cfs)) for strategies that provide at least 0.5 ft of flood depth reduction. Note: Land costs excluded.....	61
Figure A-1: Node Depth in ft for the 2-, 10-, 25-, 50-, 100-, and 500-year storms at node Temp8 in Duluth	1
Figure A-2: Node Depth in ft for the 2-, 10-, 25-, 50-, 100-, and 500-year storms at node J21 in Duluth....	2
Figure A-3: Node Depth in ft for the 2-, 10-, 25-, 50-, 100-, and 500-year storms at node J23 in Duluth....	3
Figure A-4: Node Depth in ft for the 2-, 10-, 25-, 50-, 100-, and 500-year storms at node J14 in Duluth....	4
Figure A-5: Maximum Flow Rate (cfs) for the 2-, 10-, 25-, 50-, 100-, and 500-year storms at the outlet (main25) of the Kohl's Wetland in Duluth.	5
Figure A-6: Maximum Flow Rate (cfs) for the 2-, 10-, 25-, 50-, 100-, and 500-year storms at the outlet (main65) of the Miller Creek sub-watershed in Duluth.....	6
Figure A-7: Maximum Flow Rate (cfs) for the 2-, 10-, 25-, 50-, 100-, and 500-year storms at the outlet (main68) of the combined Miller Creek and Coffee Creek watershed in Duluth.	7
Figure A-8: Flood duration in hours for the 2-, 10-, 25-, 50-, 100-, and 500-year storms at node Temp8 in Duluth.	8
Figure A-9: Flood duration in hours for the 2-, 10-, 25-, 50-, 100-, and 500-year storms at node J21 in Duluth.	9
Figure A-10: Flood duration in hours for the 2-, 10-, 25-, 50-, 100-, and 500-year storms at node J23 in Duluth.	10

Figure A-11: Flood duration in hours for the 2-, 10-, 25-, 50-, 100-, and 500-year storms at node J14 in Duluth.	11
Figure A-12: Miller Creek Kohl’s wetland inlet (Node Temp8) Hydrograph (depth in ft) for the 100-year Atlas 14 event (6.31 inches).....	13
Figure A-13: Miller Creek Kohl’s wetland channel (main25) Hydrograph (flow in cfs) for the 100-year Atlas 14 event (6.31 inches).....	14
Figure A-14: Miller Creek Kohl’s wetland outlet (Node J23) Hydrograph (depth in ft) for the 100-year Atlas 14 event (6.31 inches).....	15
Figure A-15: Miller Creek Outlet (main68) Hydrograph (flow in cfs) for the 100-year Atlas 14 event (6.31 inches).....	16
Figure A-16: Node Depth in ft for the 2-, 10-, 25-, 50-, 100-, and 500-year storms at node MH420743 in Minneapolis.	17
Figure A-17: Node Depth in ft for the 2-, 10-, 25-, 50-, 100-, and 500-year storms at node SA35C350 in Minneapolis.	18
Figure A-18: Node Depth in ft for the 2-, 10-, 25-, 50-, 100-, and 500-year storms at node SS512682 in Minneapolis.	19
Figure A-19: Node Depth in ft for the 2-, 10-, 25-, 50-, 100-, and 500-year storms at node SA999039 in Minneapolis.	20
Figure A-20: Cumulative Node volume in million ft ³ for the 2-, 10-, 25-, 50-, 100-, and 500-year storms at MH420743 in Minneapolis.....	21
Figure A-21: Cumulative Node volume in million ft ³ for the 2-, 10-, 25-, 50-, 100-, and 500-year storms at SA35C350 in Minneapolis.	22
Figure A-22: Cumulative Node volume in million ft ³ for the 2-, 10-, 25-, 50-, 100-, and 500-year storms at SS512682 in Minneapolis.....	23
Figure A-23: Cumulative Node volume in million ft ³ for the 2-, 10-, 25-, 50-, 100-, and 500-year storms at SA999039 in Minneapolis.	24
Figure A-24: Maximum Flow Rate (cfs) for the 2-, 10-, 25-, 50-, 100-, and 500-year storms at the outlet (OF441017) of the 1NE watershed in Minneapolis.....	25
Figure A-25: Maximum Flow Rate (cfs) for the 2-, 10-, 25-, 50-, 100-, and 500-year storms at the outlet (OF441270) of the 1NE watershed in Minneapolis.....	26
Figure A-26: Flood duration in hours for the 2-, 10-, 25-, 50-, 100-, and 500-year storms at node MH420743 in Minneapolis.....	27

Figure A-27: Flood duration in hours for the 2-, 10-, 25-, 50-, 100-, and 500-year storms at node SA35C350 in Minneapolis.	28
Figure A-28: Flood duration in hours for the 2-, 10-, 25-, 50-, 100-, and 500-year storms at node SS5120682 in Minneapolis.	29
Figure A-29: Flood duration in hours for the 2-, 10-, 25-, 50-, 100-, and 500-year storms at node SA999039 in Minneapolis.	30
Figure A-30: 1NE Outlet (OF441017) Hydrograph (flow in cfs) for the 100-year Atlas 14 event (7.5 inches)	31
Figure A-31: 1NE Outlet (OF441270) Hydrograph (flow in cfs) for the 100-year Atlas 14 event (7.5 inches)	32
Figure A-32: Node Depth in ft for the 2-, 10-, 25-, 50-, 100-, and 500-year storms at node SP105 in Rochester.	33
Figure A-33: Node Depth in ft for the 2-, 10-, 25-, 50-, 100-, and 500-year storms at node SP64 in Rochester.	34
Figure A-34: Node Depth in ft for the 2-, 10-, 25-, 50-, 100-, and 500-year storms at node RN176248 in Rochester.	35
Figure A-35: Node Depth in ft for the 2-, 10-, 25-, 50-, 100-, and 500-year storms at node SP113 in Rochester.	36
Figure A-36: Cumulative Node volume in million ft ³ for the 2-, 10-, 25-, 50-, 100-, and 500-year storms at SP105 in Rochester.	37
Figure A-37: Cumulative Node volume in million ft ³ for the 2-, 10-, 25-, 50-, 100-, and 500-year storms at SP64 in Rochester.	38
Figure A-38: Cumulative Node volume in million ft ³ for the 2-, 10-, 25-, 50-, 100-, and 500-year storms at RN176248 in Rochester.	39
Figure A-39: Cumulative Node volume in million ft ³ for the 2-, 10-, 25-, 50-, 100-, and 500-year storms at SP113 in Rochester.	40
Figure A-40: Maximum Flow Rate (cfs) for the 2-, 10-, 25-, 50-, 100-, and 500-year storms at the outlet (Temp) of the Kings Run watershed in Rochester.	41
Figure A-41: Flood duration in hours for the 2-, 10-, 25-, 50-, 100-, and 500-year storms at node SP105 in Rochester.	42
Figure A-42: Flood duration in hours for the 2-, 10-, 25-, 50-, 100-, and 500-year storms at node SP64 in Rochester.	43

Figure A-43: Flood duration in hours for the 2-, 10-, 25-, 50-, 100-, and 500-year storms at node RN176248 in Rochester.	44
Figure A-44: Flood duration in hours for the 2-, 10-, 25-, 50-, 100-, and 500-year storms at node SP113 in Rochester.	45
Figure B-1: Illustration of the Quantile Method	5
Figure B-2: Ratio of total annual precipitation calculated from hourly and daily precipitation data for Minneapolis.	7
Figure B-3: Equivalent CO ₂ emissions for the RCP 2.6, 4.5, 6.0 and 8.5 scenarios using in CMIP5 (source epa.gov).	8
Figure B-4: Observed and simulated (mpi-esm-mr rcp8.5) annual total precipitation, 1950-2020, and linear trend fits, Minneapolis.....	10
Figure B-5: Observed and simulated (mpi-esm-mr rcp8.5) annual maximum daily precipitation time series and fitted trendlines, for Minneapolis.	12
Figure B-6: GEV distributions of observed and simulated annual maximum daily precipitation for the time periods 1950-1979 and 1988-2017, Minneapolis.....	12
Figure B-7: GEV distributions of observed and simulated annual maximum daily precipitation for the time periods 1950-1979 and 1988-2017, Rochester.	13
Figure B-8: GEV distributions of observed and simulated annual maximum daily precipitation for the time periods 1950-1979 and 1988-2017, Duluth.....	13
Figure B-9: Historical and future GEV precipitation distributions for 50-year blocks of data, MPI-ESM-MR, RCP4.5 (left) and RPC8.5 (right), Minneapolis.	14
Figure B-10: Historical and future GEV precipitation distributions for 50-year blocks of data, MPI-ESM-MR, RCP4.5 (left) and RPC8.5 (right), Rochester.	14
Figure B-11: Historical and future GEV precipitation distributions for 50-year blocks of data, MPI-ESM-MR, RCP4.5 (left) and RPC8.5 (right), Duluth.....	14
Figure B-12: Probability of a wet day (P(W)) and probability of a wet day following a wet day (P(W/W)) for the mpi-esm-mr RCP4.5 and RCP8.5 GCM outputs, for 30-year blocks from 1950 through 2099.	16
Figure B-13: 90th, 99th, and 99.9th percentile hourly (left panel) and daily (right panel) precipitation depth vs. mean daily air temperature based on observed MSP data, 1950-2020	16
Figure B-14: Frequency Analysis for 1-h Duration.	18
Figure B-15: Frequency Analysis for 6-h Duration.	19
Figure B-16: Frequency Analysis for 1-h Duration for Pre-Change and Current Conditions.	20

Figure B-17: Frequency Analysis for 24-h Duration for Pre-Change and Current Conditions	21
Figure B-18: Mean and Standard Deviation Trends with Duration for pre-climate change Conditions.....	22
Figure B-19: Trends in 100-hr Depths with Durations for Pre-climate change Conditions	22
Figure B-20: Original and Adjusted GEV for 6-h, 12-h and 24-h Durations.	23
Figure B-21: Frequency Analysis of Daily Depths Using GCM simulations mpi-esm-mr rcp4.5 and mpi-esm-mr rcp8.5.....	24
Figure B-22: DDF Depths Using Quantile Method and Depths from Atlas 14.	25
Figure B-23: Summary of Normalized Depths for Different Durations.....	25
Figure B-24: DDF Analysis for MSP using RCP8.5 for 2040 to 2069.	26
Figure B-25: Normalized Sub-daily Depths Using GCM for 2040 to 2069.	27
Figure B-26: Design Storms for 2-yr, 10-yr and 100-yr Return Periods for 2040 to 2069.	27

List of Tables

Table 1: Historical and Projected 24-hour storm size verses return period for Duluth, MN from the EPA CREAT database, for the 30-year period 2045-2074. Data are given for three GCM outputs; W/W = warm and wet, H/D = hot and dry, Med = median. 5

Table 2. Summary of flow rate and water elevation in the Kohl’s wetland and the flow at the Miller Creek outlet for the June 2012 storm and synthetic storms of 10-to-500-year return periods, as determined using corresponding precipitation events from Hershfield (1961) and Atlas 14 (NOAA 2021). Flows at the Miller Creek outlet tops out at 1124 cfs due to a culvert. 16

Table 3: Summary of historical and future 24-hour duration storm sizes (precipitation depth, inches) used in this study for Duluth, Minneapolis, and Rochester, MN. n/a = not available. 20

Table 4: Summary of percent total connected impervious area treated by Ponds, Infiltration Basins (Infil.), and Smart Ponds (Smart) for the six adaptation strategies. 25

Table 5: Node and Link Descriptions for Miller Creek SWMM model, as shown in Figure 16. 26

Table 6: Unit life-cycle costs for 10,000 ft² infiltration basins as predicted by CLASIC. Costs for 2018 were updated to 2022 using the consumer price index. Note: Land costs excluded. 49

Table 7: Unit life-cycle cost for medium wet ponds as predicted by CLASIC. Costs for 2018 were updated to 2022 using the consumer price index. Note: Land costs excluded. 50

Table 8: Unit life-cycle cost (2022 \$) for upgrading existing wet ponds with ‘smart’ technology. Note: Land costs excluded. 51

Table 9: Summary of infrastructure adaptation strategies and total 20-year life-cycle cost of each strategy. Note: Land costs excluded. 56

Table 10: Average flood depth (ft) improvement (negative values) or detriment (positive values) for Minneapolis, Rochester, and Duluth sub-watersheds for TP-40, Atlas-14, 2069-50th, 2069-75th, and 2069-90th predicted storms and 2-Yr, 10-Yr, 25-Yr, 50-Yr, 100-Yr, and 500-Yr return period, compared to the Baseline. 57

Table 11: Average peak outflow (cfs) improvement (negative values) or detriment (positive values) for Minneapolis, Rochester, and Duluth sub-watersheds. 58

Table 12: Average change in flood depth and peak flow with total cost for adaptation strategies in Minneapolis, Rochester, and Duluth. Note: Land costs excluded. 59

Table A-1: Time to Peak (hours) and +/- change in Time to Peak for Atlas-14, 100-year storm event for Temp8, J21, J23, J14, main25, main65, and main68 in Duluth. 12

Table B-1: Summary of observed and simulated annual precipitation statistics for the three study sites. . 9

Table B-2: Summary of observed and simulated annual precipitation statistics for the three study sites, based on observed and simulated daily precipitation.....	11
Table B-3: Probability of a wet day P(W) and probability of a wet day following a wet day P(W/W) for the GCM outputs and observations at Minneapolis, Duluth, and Rochester.	15
Table B-4: Ratios Used to Compute Depths for Sub-hour Durations	19
Table B-5: Comparison of P_x/P_{24} Using Annual and Partial Duration Series for MSP.	28

Executive Summary

This document is the final report of the project funded by the Minnesota Department of Transportation titled *Climate Change Adaptation of Urban Stormwater Infrastructure*. The objectives of the project involve predicting future climate affected design rainfall events and determining the cost-effectiveness of adaptation strategies for stormwater infrastructure in response to future-predicted events. The project consists of several tasks, which are represented by the sections of this final report and are described below.

Section 1 is a literature review that summarizes published reports, studies, and tools that have reported on or enables users to estimate the cost of traditional gray stormwater infrastructure, green stormwater infrastructure, or low impact development (GSI or LID). The literature review focuses on the latest information related to available global climate models, climate model uncertainty, downscaling techniques, and available downscaled climate data sets, in addition to available information and tools related to the costs associated with adaptation to climate change.

Section 2 provides a description of modeling for various stormwater infrastructure adaptation strategies. To determine the cost-effectiveness of stormwater infrastructure adaptations, the U.S. EPA's SWMM software is used to model stormwater infrastructure in existing Minnesota watersheds in response to past, current, and predicted future design storms. The final analysis of historical (TP-40), current (Atlas 14), and future predicted storm events for three watersheds in Minnesota (Duluth, Minneapolis, Rochester) has shown that current design philosophy is not sufficient to prevent flooding from 10-year and larger design storm events and that flood depth and duration will increase given current climate projections. Several stormwater infrastructure adaptation strategies were assessed for reducing flood depth and duration: Baseline (existing conditions), adding rain gardens (aka, Infiltration Basins), adding new wet ponds, retrofitting existing stormwater ponds to be "Smart Ponds, adding new Smart Ponds while also converting existing ponds into Smart Ponds, or upsizing of stormwater pipes to convey more water.

Section 3 is an analysis of the cost of possible strategies for adapting stormwater infrastructure to manage potential future storms. In addition to the adaptation strategies described in Section 2, Underground Storage is also included in the cost analysis. Freely available cost tools are used to estimate the cost of adaptation strategies, which are converted to 2022 dollars and then combined with performance data to determine cost-effectiveness. Performance data of the adaptation strategies included the reduction in flood depth, peak flow, and flood duration. In watersheds that are mixed urban, suburban, and rural like Rochester's Kings Run or Duluth's Miller Creek sub-watersheds, the most cost-effective climate change adaptation strategy of those evaluated in this project was to build new stormwater wet ponds (Extra Ponds strategy) to treat the impervious surfaces not currently treated by existing wet ponds and other stormwater BMPs. It is expected that land costs and acquisition may be less difficult in these watersheds compared to watersheds like 1NE in Minneapolis.

In the fully developed urban 1NE watershed in Minneapolis, the most cost-effective (excluding land costs) climate change adaptation strategy was building wet ponds (Extra Ponds), compared to all the strategies evaluated in this project. Securing property for building new stormwater infrastructure in fully developed urban watersheds like 1NE may be a substantial cost compared to other watersheds. Smart Ponds do not require additional land for implementation and thus represent a relatively low-cost alternative that will be more beneficial in watersheds with numerous existing wet ponds.

When considering climate change mitigation, one measure of success was whether flooding was the same or less for future-predicted storms compared to current condition(s). It was observed that the node depth, flood duration, and/or peak outflow at several nodes and outfalls was less for future-predicted storms (2069 50th) compared to current Baseline conditions (Atlast-14) when the More Smart Ponds adaptation strategy was implemented. This observation was true for all three watersheds and for upstream, downstream, and watershed outfalls.

Section 4 is a summary of our findings and the conclusions we drew from the results. The next section contains references cited, Appendix A contains relevant SWMM results excluded from Section 2, and Appendix B contains our analysis of climate predictions under a constantly changing climate and an estimate of storms at durations less than 24 hours.

Chapter 1. Estimation Techniques for the Cost of Adapting Stormwater Management Systems to Future Climate Change Scenarios: A Literature Review

1.1 Introduction

This section is a literature review that summarizes published reports, studies, and tools that have reported on or enables users to estimate the cost of traditional gray stormwater infrastructure and/or green stormwater infrastructure (GSI or LID). It focuses on the latest information related to available global climate models, climate model uncertainty, downscaling techniques, and available downscaled climate data sets, in addition to available information and tools related to the costs associated with adaptation to climate change.

1.2 Climate Change Literature

1.2.1 Global Climate Models

There are numerous research groups worldwide that publish climate projections from global climate models (GCMs) that are compiled by the Intergovernmental Panel on Climate Change (<http://www.ipcc-data.org/>). These models provide future climate projections (air temperature, precipitation, etc.) at a spatial resolution of 100 to 300 km. CMIP6 (Climate Model Intercomparison Project, 6th exercise) is the most recently published GCM data set, however, CMIP5 data (Climate Model Intercomparison Project, 5th exercise) was more readily available in downscaled form at the time of this study. Data are compiled by the IPCC for modeling results from 23 different climate research centers. Data are compiled for a wide range of atmospheric, land surface, and ocean variables over a range of time scales from sub-daily time series to long-term summaries. A key feature of the CMIP5 climate projections are the CO₂ emission scenarios (Figure 1) – each climate modeling group runs at least 2 of the emission scenarios, most commonly Representative Concentration Pathway (RCP) 4.5 and RCP8.5, representing relatively low and relatively high CO₂ emissions, respectively.

Projected Atmospheric Greenhouse Gas Concentrations

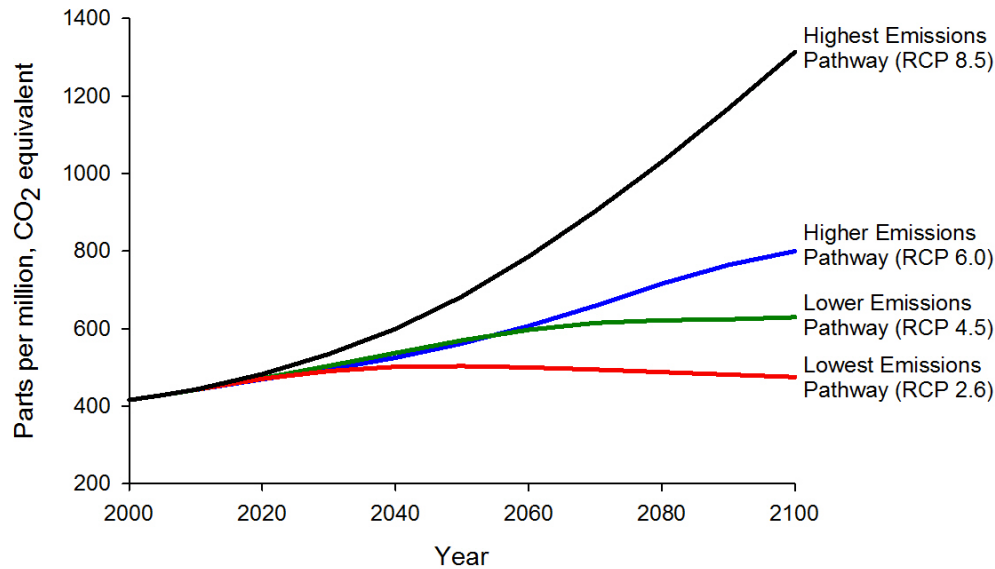


Figure 1: Equivalent CO₂ emissions for the RCP 2.6, 4.5, 6.0 and 8.5 scenarios using in CMIP5 (Source epa.gov).

1.2.2 Spatially Downscaled Global Climate Model Projections

The spatial resolution of raw GCM model outputs (~100 km grid) are typically insufficient for regional or local hydrologic modeling studies. Finer resolution climate projections are available from research groups that downscale subsets of the GCM outputs to spatial scales closer to 10 km. Downscaling methods include statistical downscaling, which uses historical weather data to characterize spatial relationships between large scale atmospheric variables to local weather, and dynamic downscaling, where physics-based models are used to downscale the GCM outputs for a more specific region. For Minnesota, there are several downscaled GCM projections available for the CMIP5 projections. In all cases, GCM downscaled GCM outputs are available for historical periods (back to 1950) to future periods up to 2099.

1. University of Wisconsin (<https://nelson.wisc.edu/ccr/resources/dynamical-downscaling/index.php>). The UW Center for Climatic Research has published dynamically downscaled GCM data for the U.S. Midwest, including Minnesota. Data are available for six GCMs at 25 km grid resolution. In addition to conventional climate variables such as air temperature and precipitation, the modeling process also includes secondary variables such as soil moisture, snowfall, and more detailed summaries of precipitation, such as number of days per decade with precipitation greater than 3 inches.
2. University of Idaho (<https://climate.northwestknowledge.net/MACA/>). The University of Idaho provides a statistically downscaled data set (Abatzoglou et al. 2012) which includes projections for humidity, solar radiation, and wind speed, in addition to precipitation and air temperature, at a spatial resolution of 4 to 6 km. Downscaled data are available for 20 GCMs using the RCP4.5

and RCP8.5 emission scenarios. These data were used in a climate change study to project the changes in flows and sediment loads in a tributary of the Minnesota River (Butcher et al. 2015).

3. Downscaled CMIP3 and CMIP5 Climate and Hydrology Projections (https://gdo-dcp.ucllnl.org/downscaled_cmip_projections/). A collaborative effort of many institutions provides statistically downscaled climate and hydrology projections for 20 GCMs (some with multiple versions or runs) and multiple CO₂ emission scenarios (RCP2.6, 4.5, 6.0, and 8.5). The most recent product (LOCA) gives variables including precipitation, air temperature, wind speed, soil moisture content, total runoff, and evapotranspiration on a 1/16-degree spatial grid at daily time steps. These downscaled data were used by WSP for projecting future storm sizes in Minnesota. The Federal Highway Association is developing a tool for downloading and analyzing the LOCA data to calculate projected changes in air temperature and precipitation statistics for transportation planners:
https://www.fhwa.dot.gov/engineering/hydraulics/software/cmip_processing_tool_version2.cfm
4. The University of Minnesota has an ongoing effort to create dynamically downscaled GCM data for Minnesota. These data were not available for the timeframe of this study.
<https://climate.umn.edu/climate-projections>

1.2.3 Evaluation of Model Projections

A comprehensive review of the uncertainty in GCMs was completed by the IPCC (Flato et al., 2013). Several weather variables were considered in this report. They concluded that large-scale mean surface temperatures were predicted with a very high level of confidence. However, systematic errors were found in regions of high topography and near the ice edge in North America. They were less confident of temperature predictions at sub-continental or smaller scales with the spread among models of $\pm 3^{\circ}$ C. The IPCC report concluded that prediction of precipitation at large-scale was not as accurate as surface temperature. At smaller spatial scales, the simulation of precipitation becomes less accurate. However, the accuracy at these smaller scales is more difficult to assess because of uncertainty in observations. IPCC found that the GCMs underestimated the sensitivity of extreme precipitation to temperature variability. This trend implied the models may underestimate the increase in extreme precipitation events.

The IPCC report also examined the effectiveness of regional downscaling methods to provide climate data at smaller scales. They concluded that these methods improved predictions in regions with highly variable topography and were better able to capture small-scale processes. However, the downscaling methods used global models for boundary conditions and are therefore limited by the biases of these larger scale models. They cited studies of regional downscaling methods improving the prediction of regional climate variables because of improved resolution of topography and coastline features and providing a better representation of (small-scale) convective processes that are important for precipitation predictions.

1.2.4 Sub-daily Precipitation Depths from Global Climate Model Projections

1.2.4.1 Overview

GCM outputs, even when spatially downscaled, typically give daily precipitation data averaged over 5-10 km grids and 1-day time steps. These data do not give direct information on future changes in precipitation intensity and duration at the scale of small to medium sized watersheds and are unsuitable for hydrologic analysis of urban watersheds (Maimone et al. 2019). As a result, further work is necessary to temporally downscale GCM projections to sub-daily durations. Methods for downscaling GCM precipitation projections to sub-daily time steps and finer spatial resolution is a subject of ongoing research. A key focus of this work is to develop methods to update Intensity-Duration-Frequency (IDF) curves to incorporate information from future GCM projections. Careful consideration of GCM model biases must be included, as model biases in precipitation intensity distributions may exceed the projected future changes (Arnbjerg-Nielson, 2012).

Two general approaches have been used for temporal downscaling precipitation from GCMs daily projections. Some studies (e.g., Lee and Jeong, 2014; Lee and Park, 2017) use the downscaling methods for each precipitation event. These methods estimate the hourly depths corresponding to the daily depth of the GCMs projections. The other approaches (e.g., Butcher and Zi, 2019; Srivastav et al., 2014) limit the downscaling method to annual maxima. Both of these approaches are discussed in greater detail later.

Instead of using downscaling methods, Maimone et al. (2019) used a combination of GCM-derived change factors and a stochastic weather generator to synthesize future hourly precipitation time series for Philadelphia, PA. Average change factors were calculated based on the outputs of 9 GCMs. Arnbjerg-Nielson (2012) evaluated two methods, one based on partial duration series and the other based on a stochastic rainfall generator and found the projected increase in precipitation intensities tended to be larger with increasing return period and decreasing duration.

The US Environmental Protection Agency has published a nationwide analysis of changes in future storm sizes, as a part of the risk analysis toolset CREAT for water utilities (<https://www.epa.gov/crwu/creat-risk-assessment-application-water-utilities>). Future storm sizes for return periods up to 100 years are estimated for the entire country. Example CREAT storm data for the Duluth area are given in Table 1. The CREAT database gives storm sizes for three future climate scenarios, to encompass the range of GCM climate projections. Future storm projections are also available in proprietary risk analysis tools such as SimCLIM (<https://www.climsystems.com/simclim>), which were used in several MnDOT climate change studies (Parsons Brinckerhoff, 2014).

Table 1: Historical and Projected 24-hour storm size verses return period for Duluth, MN from the EPA CREAT database, for the 30-year period 2045-2074. Data are given for three GCM outputs; W/W = warm and wet, H/D = hot and dry, Med = median.

Return Period (Years)	Storm Size (inches)			
	Historical	2060 W/W	2060 H/D	2060 Med
5	2.87	3.33	3.15	3.08
10	3.19	3.69	3.53	3.36
15	3.35	3.87	3.74	3.49
30	3.58	4.15	4.07	3.69
50	3.7	4.29	4.26	3.78
100	3.9	4.52	4.57	3.94

1.2.4.2 Downscaling Methods

Lee and Jeong (2014) and Lee and Park (2017) have developed algorithms to convert daily precipitation data from GCMs to hourly depths. The first step is to identify weather stations near to the target site that have daily and hourly observed data. For a GCM daily depth, possible observed storms for downscaling are prioritized by using the smallest square distance between the GCM's depth and those storms in the observed data set. The initial hourly depths are obtained by selecting randomly from the prioritized list. A genetic algorithm is then used to refine these initial depths by considering other storms in the observed weather station database. The genetic algorithm is an adaptive stochastic optimization algorithm. They reported that the approach was able to reproduce the key statistics of the historical data and obtained downscaled probability distributions that are similar to those observed.

Instead of downscaling all precipitation events, Srivastav et al. (2014) and Butcher and Zi (2019) have developed methods that are applied to only the annual maxima data. The annual maximum daily depths are used from GCM projections; and daily and sub-daily depths are used for observational data. Cumulative probability distribution functions (CDFs) are computed for all depths. Quantile mapping methods are used in the downscaling approach. The general approach of quantile mapping is illustrated in Figure 2. The CDFs correspond to the GCM daily projections (left-graph) and those obtained from observed sub-daily 1-h and 12-h depths (right-side graphs). The quantile for each of the annual maximum daily depth of the GCM is obtained from its CDF. The corresponding 1-h and 12-h depths are obtained by assuming equal quantile values. Let's consider the 90th percentile precipitation depth obtained from the analysis of an annual series of maximum daily depths from a GCM under current conditions. We are interested in the percentile of this depth under future conditions as predicted by the GCM. For illustration purposes, let's say that the depth for future conditions now corresponds to the 80th percentile. The sub-daily depths are now adjusted using this change in percentiles. The future 1-h depth of the 80th percentile equals the 90th percentile of the current (observed) distribution. This trend is duplicated for all sub-daily durations and is repeated for different percentiles corresponding to the current and future GCM predictions. If the CDFs are defined by the extreme value type I distribution, it can be shown that the adjustment for sub-daily depth is defined by a linear relationship.

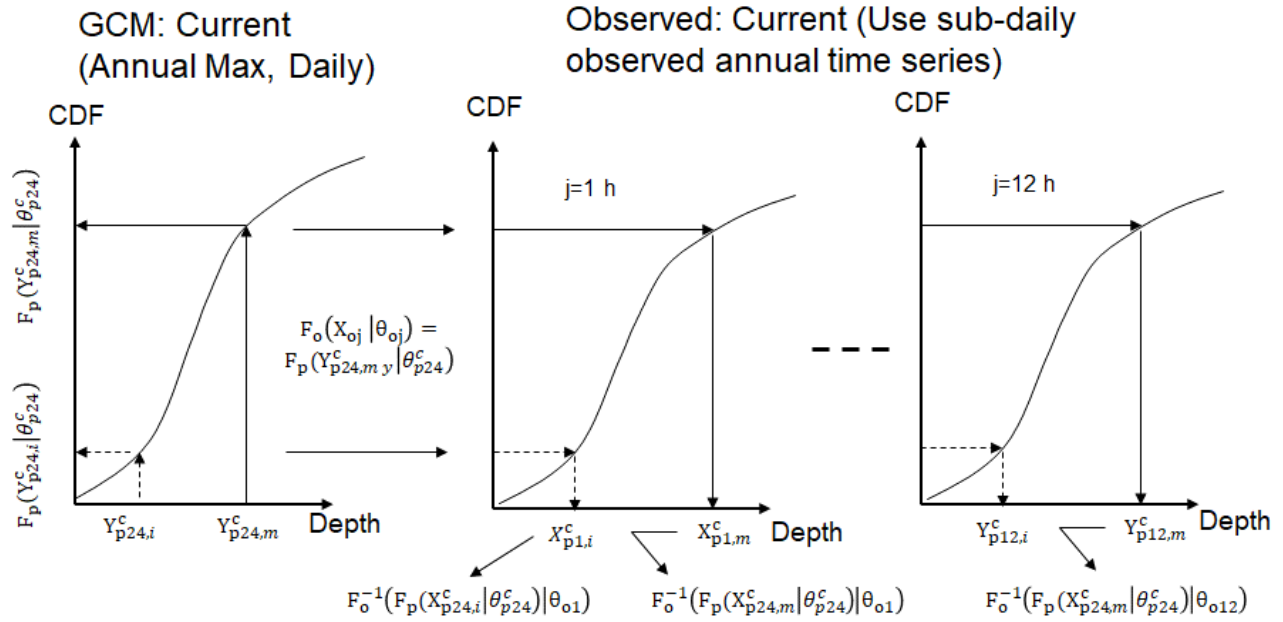


Figure 2: Illustration of Quantile Method for Sub-daily Depths.

Equidistance quantile mapping is used by Srivastav et al. (2014), Butcher and Zi (2019) and Medeiros de Saboia et al. (2020) for adjusting for the difference between daily depths of GCMs and observed depths. An illustration of the equidistance quantile mapping is shown in Figure 3. Here the quantile of GCM's daily depth for future conditions is shown. For the same quantile, a corresponding depth can be obtained from the historical observation ($X_{o,adj}$), and the depth from the GCMs ($X_{p,c}$) corresponding to the same time period as the observed data. The projected maximum daily depth for future conditions is then defined as:

$$X_{p,adj} = X_{o,adj} + \Delta X_p \quad (1)$$

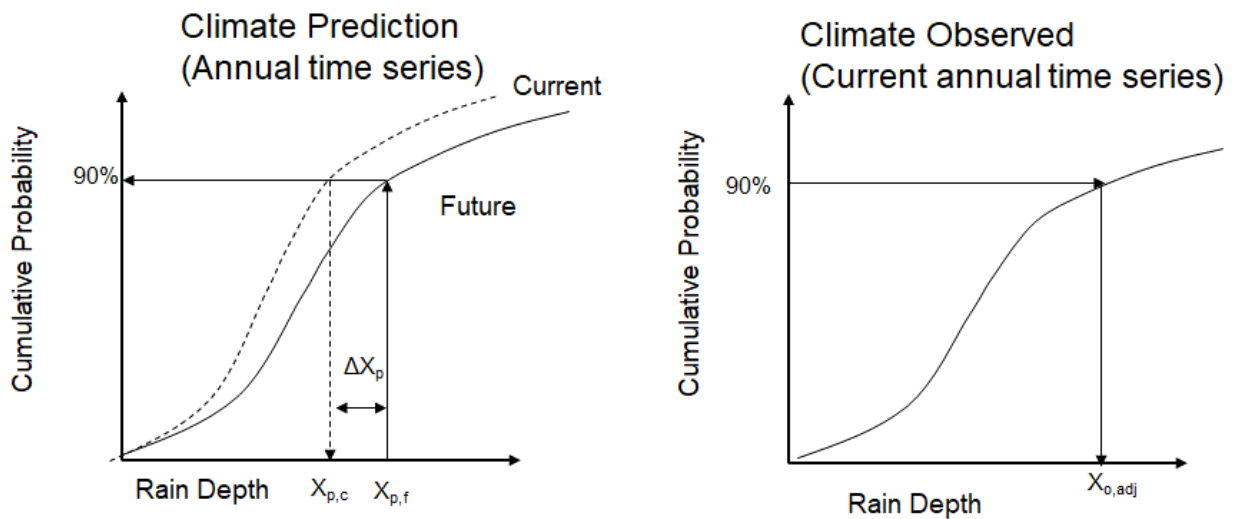


Figure 3: Illustration of Equidistant Quantile Mapping for Daily Depths.

1.3 Cost of Stormwater Infrastructure

An early study of the cost of stormwater treatment practices was by Heaney et al. (2002) and Sample, et al. (2003), who utilized literature on site-specific cost curves for stormwater treatment practices and other control options for wet weather flows. Weiss et al. (2005, 2007) used values of total construction and operation and maintenance costs of stormwater treatment practices throughout the United States collected from published literature to develop cost curves with uncertainty estimates for stormwater treatment practice construction, operation and maintenance, and total present costs. Narayanan and Pitt (2006) included the published cost of the conventional drainage systems and stormwater treatment practices to develop a cost module for the Source Loading and Management Model (WinSLAMM). Montaldo, et al. (2007) also utilized known cost curves to assess the cost-effectiveness of low impact development for CSO control. Houle, et al. (2013) compared maintenance cost estimates for seven stormwater treatment practice maintenance demands in the context of personnel hours, costs, and system pollutant removal. Bixler, et al. (2020) developed a cost estimating methodology for the seven stormwater treatment practices to determine the equivalent annual cost of these practices in five cities across the U.S.

There were thus two studies that created new general cost curves for stormwater treatment practices from literature data, those of Sample et al. (2003) and Weiss et al. (2005, 2007). The other sources, however, identified more recent data that can be used in the analysis of the cost of stormwater treatment practices and stormwater handling facilities such as storm sewers and underground storage facilities.

1.3.1 Tools and Calculators

1.3.1.1 WERF Spreadsheet Calculators.

The Water Environment Research Foundation (WERF) has a set of spreadsheet tools that can be used to estimate and combine capital costs and yearly maintenance costs to estimate whole life costs for various stormwater management systems. The models provide a framework for calculating capital and long-term maintenance costs of individual best management practices and low impact development techniques. Models are included for: retention ponds, extended detention basins, swales, permeable pavement, green roofs, large commercial cisterns, residential rain gardens, curb-contained bioretention, and in-curb planter vaults (WERF 2009). The spreadsheets allow users to enter detailed information about the situation such as the size of the stormwater management practice, rainfall, unit costs, maintenance actions/costs, etc. or, for some fields, use default values. The tool then calculates the whole life costs for the practice.

1.3.1.2 USEPA SUSTAIN.

SUSTAIN is a computer tool developed by the USEPA with the most recent version released in 2014. The USEPA is no longer developing or supporting SUSTAIN and there are no plans for updated versions. The software is, however, still available on the USEPA website (USEPA 2014) and, according to the website,

requires ESRI's ArcGIS 9.3 and the Spatial Analyst extension. SUSTAIN is a hydrologic and water quality model for watersheds and urban streams. Based on water quality objectives, it seeks to optimize the cost-effectiveness of possible water management solutions. Users are informed of what solutions are most cost-effective, what type of stormwater management practices should be used along with their size and location, and how effective the practices are in reducing runoff and pollutant loads.

1.3.1.3 USEPA National Stormwater Calculator.

The USEPA also has a National Stormwater Calculator (USEPA 2019). This software estimates the amount and frequency of runoff from a user defined site and user selected stormwater BMPs. Estimates are based on user supplied site conditions such as soil type and conditions, land cover/use, design storm depth, and software including historical rainfall records. The user may select any of the seven green infrastructure stormwater BMPs that are available in the software along with a climate change scenario (no change, hot/dry, medium change, warm/wet) and the time period to which the climate change applies (years 2020 to 2049 or 2045 to 2074). The calculator then estimates the fraction of annual rainfall that infiltrates, runs off, and evaporates. It also estimates costs of the selected green infrastructure stormwater BMPs.

1.3.1.4 National Green Values Calculator.

The National Green Values™ Calculator (CNT 2020) compares the performance, costs, and benefits of green stormwater infrastructure to conventional gray stormwater management systems. Users enter the zip code, lot area, hydrologic soil type (A, B, C, D), then choose the desired rainfall percentile to use in the modeling. Additional information entered by the user includes the predevelopment land conditions, the desired depth of rain captured, and details corresponding to conventional development such as the percent impervious area and the condition of pervious areas. After selecting green stormwater infrastructure improvements, the calculator estimates how much volume capture will be achieved by each green infrastructure component. Construction, annual O&M, and life-cycle costs for the green and conventional infrastructure are also estimated and presented.

Chapter 2. Potential Adaptation to Climate Change Predictions

2.1 Introduction

This section provides a description of modeling for various stormwater infrastructure adaptation strategies. To determine the cost-effectiveness of stormwater infrastructure adaptations, the U.S. EPA's SWMM software was used to model stormwater infrastructure in existing Minnesota watersheds in response to past, current, and predicted future design storms. The final analysis described in this section includes three sub-watersheds, Miller Creek watershed in Duluth, MN, the 1NE watershed in Minneapolis, MN, and the Kings Run Watershed in Rochester, MN using the following infrastructure adaptations: Baseline (existing conditions), adding rain gardens (aka Infiltration Basins), adding new wet ponds, retrofitting existing stormwater ponds to be "smart" ponds, adding new "smart" ponds while also converting existing ponds into "smart" ponds, or upsizing of stormwater pipes to convey more water.

The purpose of this analysis is not to develop specific climate adaptation plans for Minneapolis, Duluth, and Rochester, but rather to generate guidelines for Minnesota watersheds in general. These watersheds were used to reflect real and diverse watersheds and the results are intended to inform a broad audience of stormwater managers. Thus, the authors' intent is to use the watershed models for relative comparisons between watersheds and adaptation strategies. Also, the feasibility of implementation is not considered in this analysis. For example, the number of rain gardens or stormwater ponds that are proposed by the adaptation strategies may not be feasible for watersheds like Minneapolis. The purpose is to demonstrate the response of these strategies to future possible events. With an understanding of the relative impact of the strategies, stormwater managers can then begin to weigh the cost and feasibility of implementation. It's also important to note that this analysis reflects a snapshot in time. For example, pipe upsizing will likely occur during street reconstruction projects and not all at once. Watersheds will also likely continue to develop and sprawl across the landscape, increasing the impervious surface, potentially compacting the pervious surfaces, and otherwise altering the variables that affect runoff. Implementation of strategies at the scale proposed in this section will likely require years or decades during which stormwater managers will need to continuously adapt their strategy in response to changes and opportunities within the watershed.

2.2 U.S. EPA SWMM Models

The analysis described in this section involved an adaptation of existing U.S. EPA-SWMM models to the purposes of this study for three sub-watersheds; Miller Creek watershed in Duluth, MN, the 1NE watershed in northeast Minneapolis, MN, and the Kings Run Watershed in northwest Rochester, MN. These sub-watershed models will be described in more detail in the following sub-sections.

2.2.1 Miller Creek

The Miller Creek watershed has an area of approximately 10 square miles (6,400 acres) of which 23% is impervious. Duluth International Airport is within the watershed as are portions of the City of Duluth and Hermantown, MN. The Miller Creek watershed is shown schematically in Figure 4 and Figure 5. The main channel runs from the border of subcatchment 1 (SC1) and subcatchment 2 (SC2) in the north to the outlet near St. Louis Bay in subcatchment 39 (SC39). The major storm sewers and channels that convey water from the subcatchments to the main channel, along with the main channel itself, were modeled and are shown as blue lines in Figure 4 and Figure 5 and are labeled with blue text. The Miller Creek SWMM model used in this study was based on a model that was originally developed by the University of Minnesota Natural Resources Research Institute, and further developed by the St. Anthony Falls Lab for a series of projects, most recently a project funded by the Minnesota Lake Superior Coastal Program studying infiltration characteristics of undeveloped land in the Duluth area (Herb et al. 2020) and a project funded by Minnesota Sea Grant studying climate change adaptation (Herb 2021). Revisions to the Miller Creek model were last made in 2023. Further details of the Miller Creek SWMM model, including its calibration, are given in the following subsection.

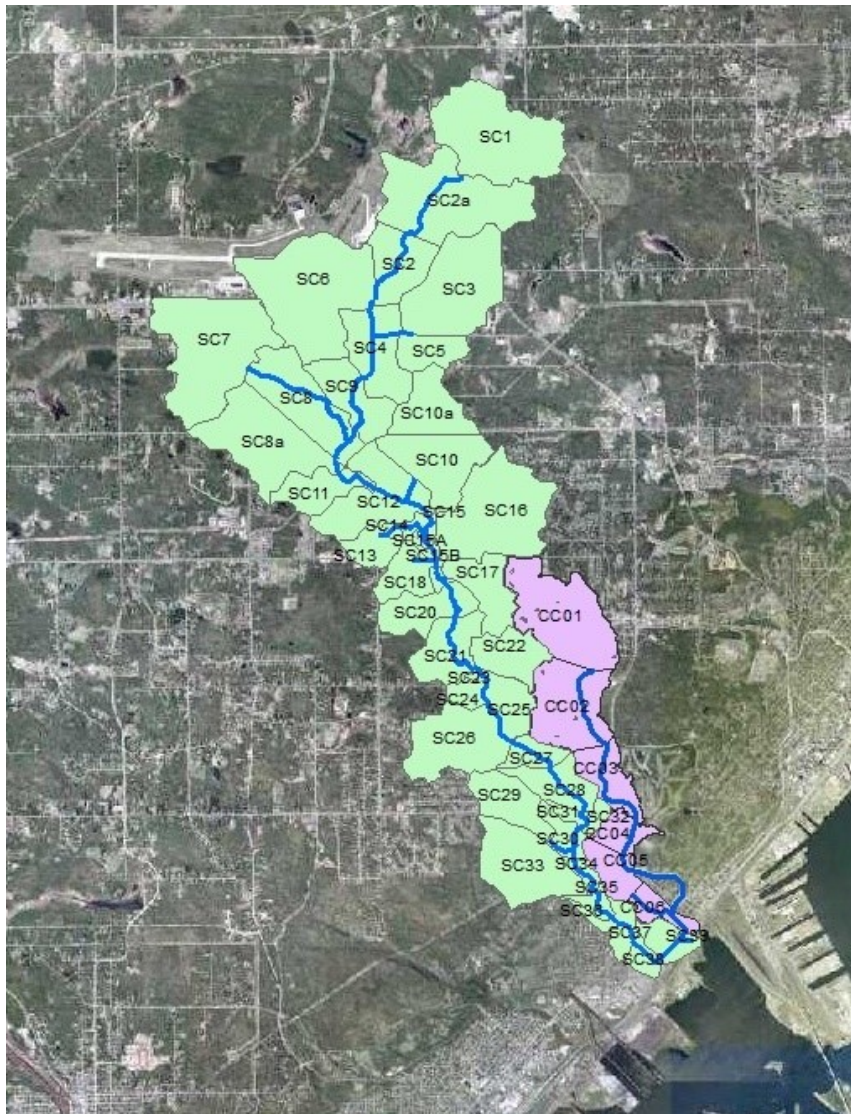


Figure 4. The Miller Creek and Coffee Creek watersheds. The 44 subcatchments of Miller Creek are shaded green and the six subcatchments of Coffee Creek are shaded purple. The main storm sewers and channels that convey water from the subcatchments to the main channel, along with the main channel itself, are shown as blue lines.

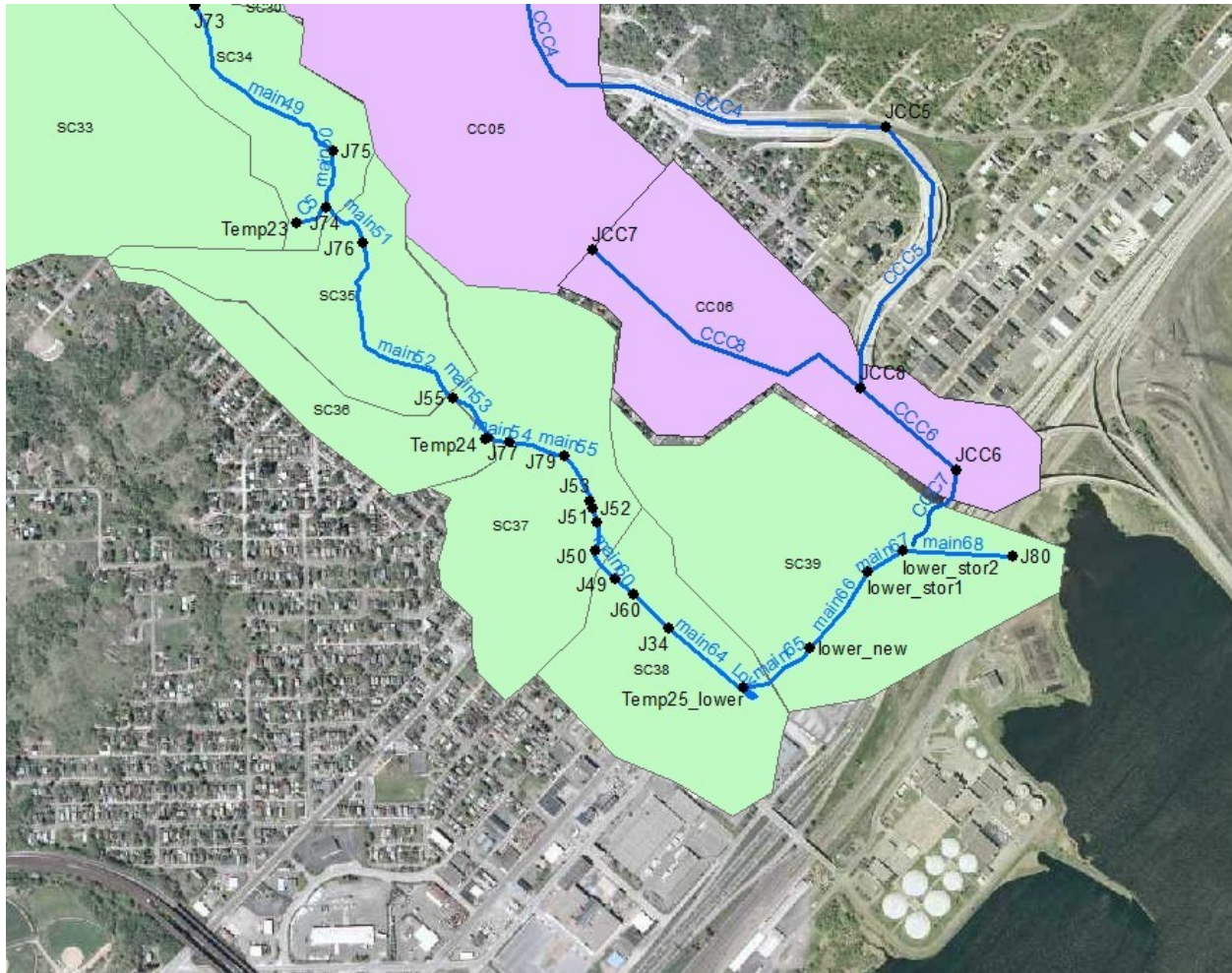


Figure 5: Details of the Miller Creek SWMM model in the vicinity of the combined Miller Creek and Coffee Creek outlets. The subcatchments of Miller Creek are shaded green and the subcatchments of Coffee Creek are shaded purple. The combined culvert outlet to Lake Superior is labeled main68.

2.2.1.1 Calibration

The U.S. EPA SWMM model developed in previous studies (Herb et al., 2020, Herb 2021) was used as the basis for this project. Several modifications were made in this study to eliminate inappropriate flow restrictions in the upper part of the watershed for very large storms (e.g., 100-year return period), including adding weir models to allow overtopping of roads and sewer pipe overflow routing of stormwater to Miller Creek via curbed streets. The model modifications did not significantly alter the model calibration, which was for more typical flow conditions. The U.S. EPA SWMM model was originally calibrated based on 2008 flow and weather data. The main calibration parameters were the groundwater aquifer time constants (indicative of groundwater flow) and the surface detention storage of each catchment. The observed and simulated flow rates at the Miller Creek outlet are shown in Figure 6, and the observed and simulated flow duration curves are shown in Figure 7. The Nash-Sutcliffe model efficiency coefficient of the calibrated model was 0.74.

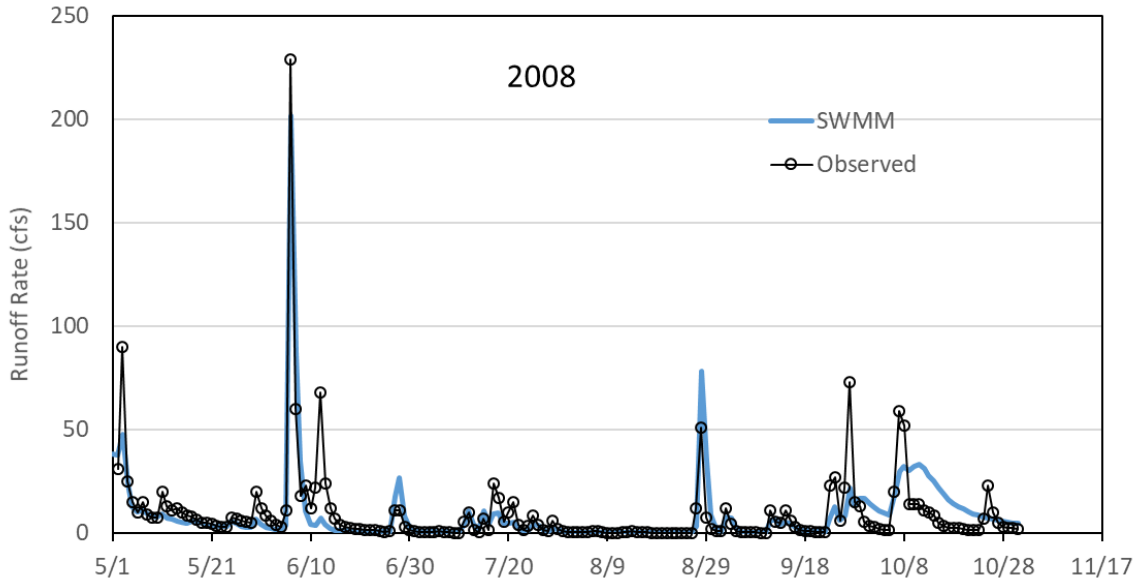


Figure 6. Observed and simulated daily average flow rates for the Miller Creek outlet, May 1 to October 31, 2008.

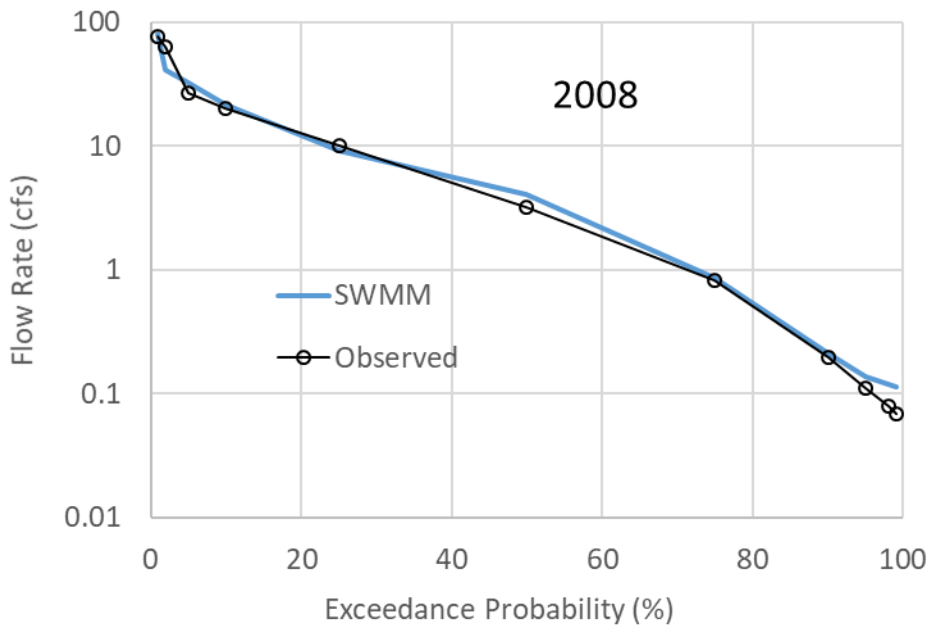


Figure 7. Observed and simulated flow exceedance probabilities for the Miller Creek outlet for daily averaged data.

The modifications of the groundwater aquifer time constants and the surface detention storage of each catchment resulted in higher storm flows through the Kohl's wetland and better reproduction of the observed flood extent (Figure 8 and Figure 9) during the June 2012 storm (Figure 10), which includes flooding of portions of Highway 53 and Haines Road. The main flooding in and around the Kohl's

wetland is due to the low slope and high roughness of the wetland itself, rather than a restrictive culvert. Although the flood extent was documented, there is no flow gaging data available for the storm.

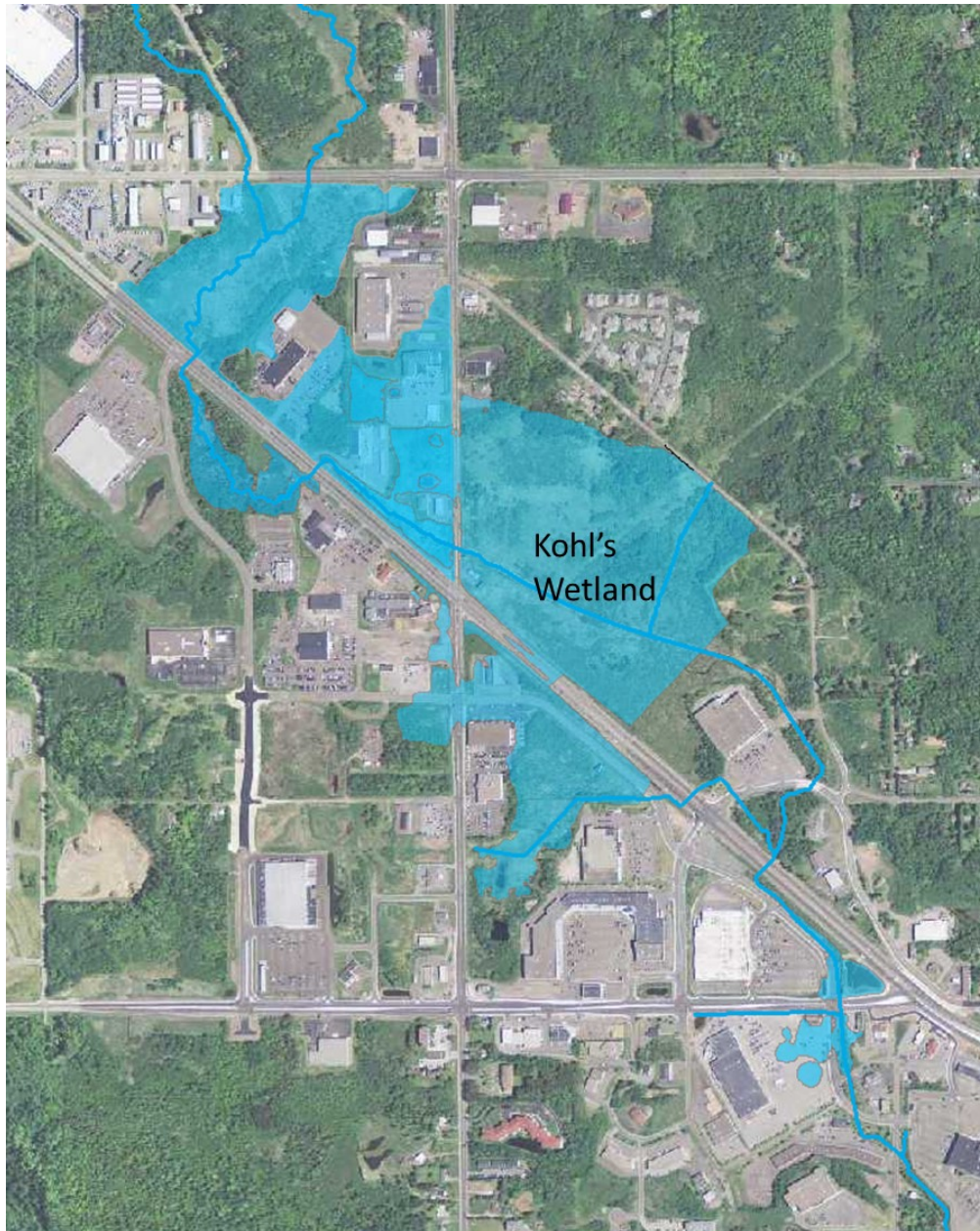


Figure 8. Simulated flood extent for the June 19-20, 2012 storm in Duluth (7.25 in., see Figure 10). The water elevation in the middle of the Kohl's wetland is 1338 ft above mean sea level (MSL), and the elevation of Highway 53 adjacent to the wetland is 1337 ft above MSL. The simulated flood extent was approximated using piece-wise flat-water levels between the model nodes and 1-foot contours from the Minnesota state LiDAR data.



Figure 9. Observed flood inundation map for the June 2012 storm in Duluth (7.25 in.), from Czuba et al. 2012.

The flow rates and water levels in the Kohl's wetland during the 2012 storm (NWS 2021) are compared to synthetic storms of 10-year to 500-year return periods as specified in the TP-40 document (Hershfield 1961) or Atlas 14 (NOAA 2021) and shown in Table 2. The water elevation for the 2012 storm (1338.0 ft) falls between the 100-year (1337.5 ft) and 500-year storms (1338.5 ft). The results also suggest that a 25-year return period storm produces flooding that approaches the elevation of Highway 53 (1337 ft).

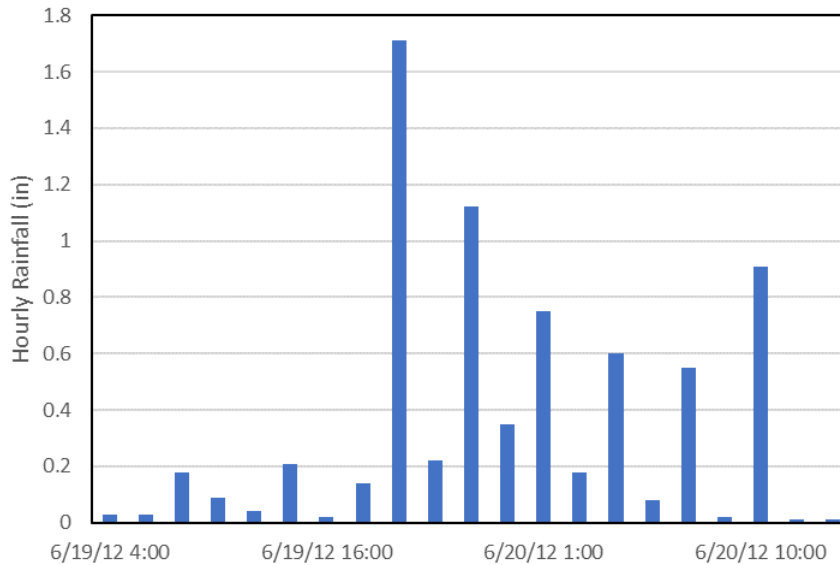


Figure 10. Hourly rainfall at Duluth International Airport on June 19 and 20, 2012, totaling 7.25 in.

Table 2. Summary of flow rate and water elevation in the Kohl’s wetland and the flow at the Miller Creek outlet for the June 2012 storm and synthetic storms of 10-to-500-year return periods, as determined using corresponding precipitation events from Hershfield (1961) and Atlas 14 (NOAA 2021). Flows at the Miller Creek outlet tops out at 1124 cfs due to a culvert.

Event	Peak Flow at Miller Creek Outlet (cfs)	Peak flow in Kohl’s Wetland (cfs)	Peak Elevation at Kohl’s Wetland (ft)	Duration of Road Flooding (hours)
June 2012	983	410	1338.0	26
10-year	729	243	1336.6	0
25-year	932	285	1337.0	0
50-year	1124	318	1337.3	11
10- year	1124	348	1337.5	16
500-year	1124	482	1338.5	25

2.2.1.2 Modifications

The Miller Creek SWMM model was modified to include a new culvert being constructed at the outlet of Miller Creek, passing under Interstate 35 to Lake Superior. The new culvert, with four rectangular barrels each 8 x 12 ft, will serve as a combined outlet for both Miller Creek and Coffee Creek. The Miller Creek SWMM model was modified to add six subcatchments and the associated drainage network for Coffee Creek, which adds approximately 20% to the total watershed area draining to the Miller Creek outlet, including a heavily developed section of downtown Duluth (Figure 4 and Figure 5).

2.2.2 Minneapolis

The 1NE watershed (Figure 11) is primarily located in the north-eastern corner of Minneapolis, MN and contains part of southern Columbia Heights. The watershed has an area of approximately 3.25 square miles (2,100 Acres) of which 47% is impervious. The watershed includes a variety of land uses, including residential neighborhoods, industrial areas, a railyard and a golf course. The Columbia Golf Course is located at the watershed's center and makes up over 9% of the total watershed area. The watershed has 723 modeled subcatchments. The watershed is relatively flat and relies on a sewer network to transmit stormwater to several outlet structures which discharge into the Mississippi River. Most of the watershed east of the railroad discharges into one main sewer pipe which runs westward under the railroad.

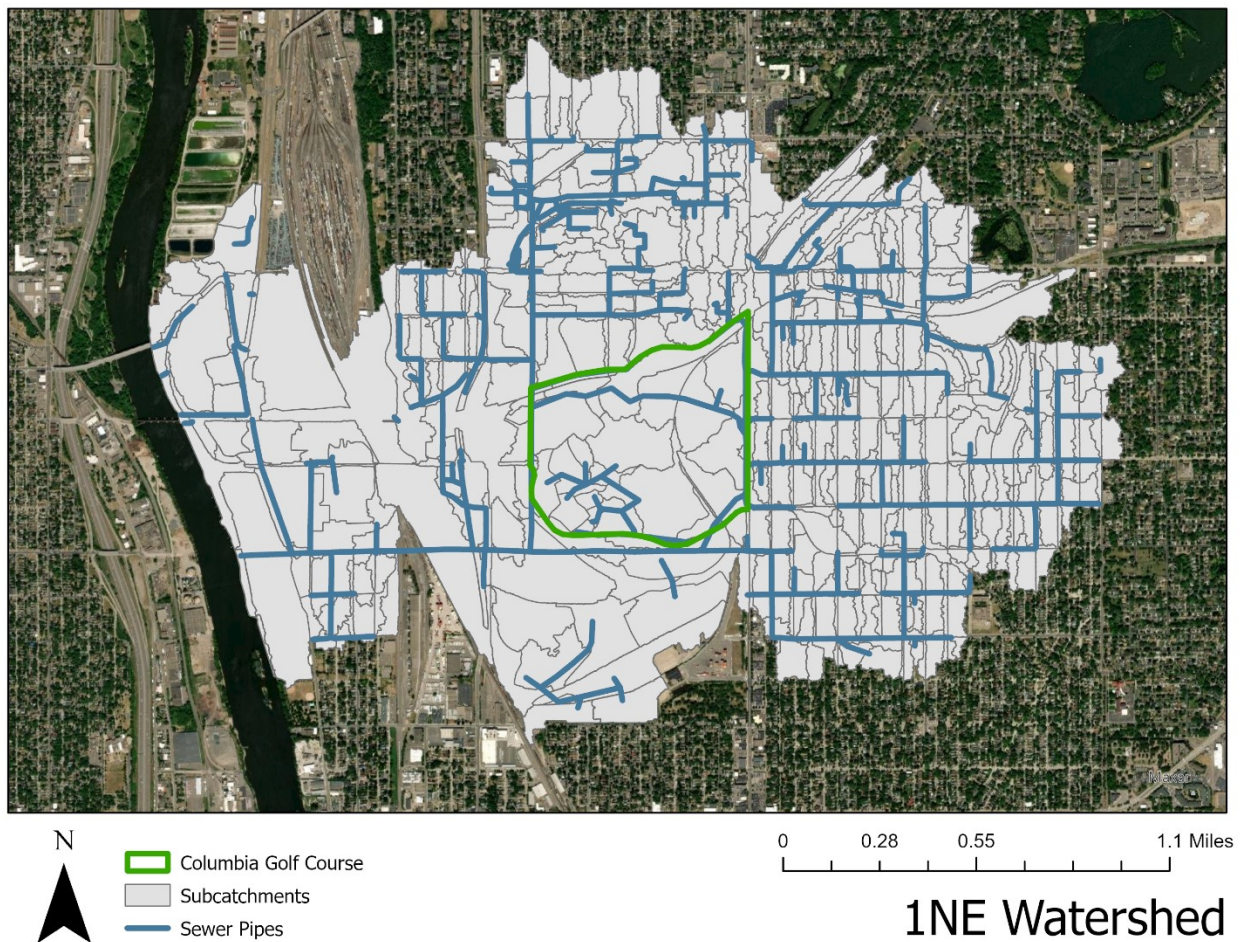


Figure 11: The 1NE watershed in Minneapolis shown as the grey area with subcatchments outlined in grey lines. The Columbia Golf Course is outlined in green. Storm sewer and surface channels are shown in blue.

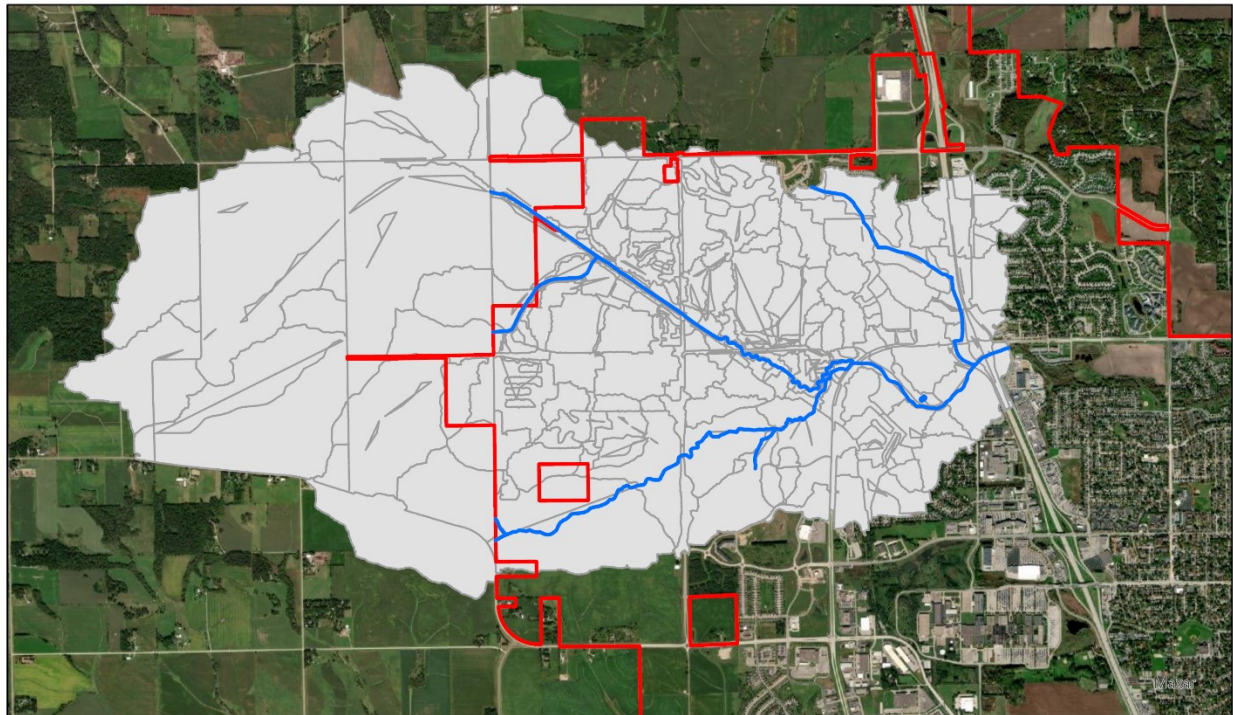
2.2.2.1 Calibration




The Minneapolis 1NE XP-SWMM model was updated by Barr Engineering in 2019 (Barr Engineering 2019a, 2019b). The model was calibrated using three monitoring stations with data beginning in January

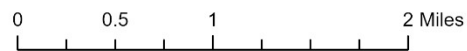
of 2016 and ending between December of 2018 and February of 2019. The model was converted from XP-SWMM to EPA-SWMM by Barr Engineering who performed quality assurance to ensure all modeled elements were properly converted. Minor modifications were made as part of this research project in 2022 and 2023, but in general the model has not been significantly updated since 2019.

2.2.3 Rochester

The Kings Run watershed (Figure 12) contains the northwestern corner of Rochester and the East side of Kalmar Township and has an area of approximately 8.75 square miles (5,600 Acres) of which ~17% is impervious. The watershed has 285 modeled subcatchments. The watershed has significant changes in elevation, dropping over 250ft from the highest point to the outlet. The western half of the model is primarily agricultural land connected by ditches which connect to two main channels. One channel runs southeast, parallel to the Douglas State Trail, the other runs northeast through Northern Hills Golf Course before merging with the other channel and running east, passing under Highway 52. Shortly after flowing under Highway 52, the combined channel exits the watershed.



-  Kings Run Subcatchments
-  Rochester City Limits
-  Channels



Kings Run Watershed

Figure 12: The Kings Run watershed shown as the grey area with subcatchments outlined in grey lines. Rochester City boundaries shown as red lines. Primary surface channels are shown in blue.

2.2.3.1 Calibration

The Kings Run model was originally developed by Houston Engineering Inc in 2019, then expanded by EOR in 2022. The model was calibrated using stage data at Kresbach Pond and aerial photographs comparison from storm events in June and July 2019.

2.3 Historical and Future Climate Inputs to SWMM

Storm events were compiled for both historical and future time periods. Historical storm information for Duluth, Minneapolis, and Rochester, MN were compiled from both the TP-40 report (Herschfield, 1961) and Atlas-14 (Perica, et al., 2013). Total storm depths were compiled for storm durations ranging from 15 minutes to 24 hours, and for return periods of 2, 5, 10, 25, 50, 100 and 500 years. The analysis given in this report used only the 24 storm durations. For the TP-40 storms, the sub-daily precipitation distribution was set using the SCS Type II distribution, while the MSE-3 distribution was used for the Atlas-14 storms. The compiled TP-40 and Atlas-14 storm depths for Duluth, Minneapolis, and Rochester are summarized in Table 3. The TP-40, Atlas-14, and the 50th percentile future-projected storms were sorted from smallest to largest for Duluth, MN were plotted and compared to Minneapolis and Rochester in Figure 13. These are the storms for which the analysis in Section 2.5: Adaptation Strategy Simulation Results is based.

Table 3: Summary of historical and future 24-hour duration storm sizes (precipitation depth, inches) used in this study for Duluth, Minneapolis, and Rochester, MN. n/a = not available.

Duluth Precipitation Depth (inches) in 24 hours											
Return Period (years)	TP-40	Atlas -14	50th Percentile			75th Percentile			90th Percentile		
			2010-2039	2040-2069	2070-2099	2010-2039	2040-2069	2070-2099	2010-2039	2040-2069	2070-2099
2	2.51	2.47	2.77	3.04	3.31	2.89	3.27	3.65	3.04	3.55	4.07
10	3.80	3.89	4.21	4.50	4.79	4.33	4.73	5.13	4.49	5.03	5.58
25	4.30	4.81	5.16	5.46	5.77	5.28	5.7	6.13	5.44	6.01	6.6
50	4.80	5.55	5.91	6.23	6.55	6.04	6.5	6.95	6.21	6.80	7.41
100	5.30	6.34	6.72	7.06	7.39	6.87	7.35	7.83	7.02	7.64	8.27
500	n/a	8.35	8.77	9.14	9.51	8.95	9.48	10.03	9.1	9.77	10.46
Minneapolis Precipitation Depth (inches) in 24 hours											
Return Period (years)	TP-40	Atlas-14	50th Percentile			75th Percentile			90th Percentile		
			2010-2039	2040-2069	2070-2099	2010-2039	2040-2069	2070-2099	2010-2039	2040-2069	2070-2099
2	2.80	2.64	2.82	2.97	3.13	3.00	3.32	3.63	3.05	3.42	3.79
10	4.20	4.18	4.37	4.54	4.71	4.59	4.94	5.30	4.64	5.05	5.46
25	4.75	5.34	5.55	5.74	5.93	5.79	6.2	6.60	5.86	6.32	6.78
50	5.30	6.36	6.59	6.79	6.99	6.86	7.31	7.75	6.93	7.43	7.93
100	6.00	7.50	7.75	7.97	8.19	8.05	8.54	9.03	8.12	8.68	9.23
500	n/a	10.6	10.9	11.17	11.43	11.25	11.84	12.42	11.36	12.04	12.72
Rochester											
Return Period (years)	TP-40	Atlas-14	50th Percentile			75th Percentile			90th Percentile		
			2010-2039	2040-2069	2070-2099	2010-2039	2040-2069	2070-2099	2010-2039	2040-2069	2070-2099
2	2.90	2.72	2.83	2.92	3.02	2.96	3.18	3.39	3.09	3.41	3.74
10	4.30	4.41	4.51	4.61	4.69	4.64	4.84	5.04	4.75	5.06	5.37
25	4.90	5.62	5.72	5.81	5.90	5.84	6.04	6.23	5.97	6.27	6.58
50	5.45	6.66	6.75	6.84	6.91	6.88	7.07	7.26	7.02	7.33	7.65
100	6.10	7.81	7.9	7.98	8.05	8.02	8.21	8.39	8.18	8.5	8.82
500	n/a	10.9	10.98	11.06	11.13	11.09	11.26	11.42	11.28	11.62	11.96

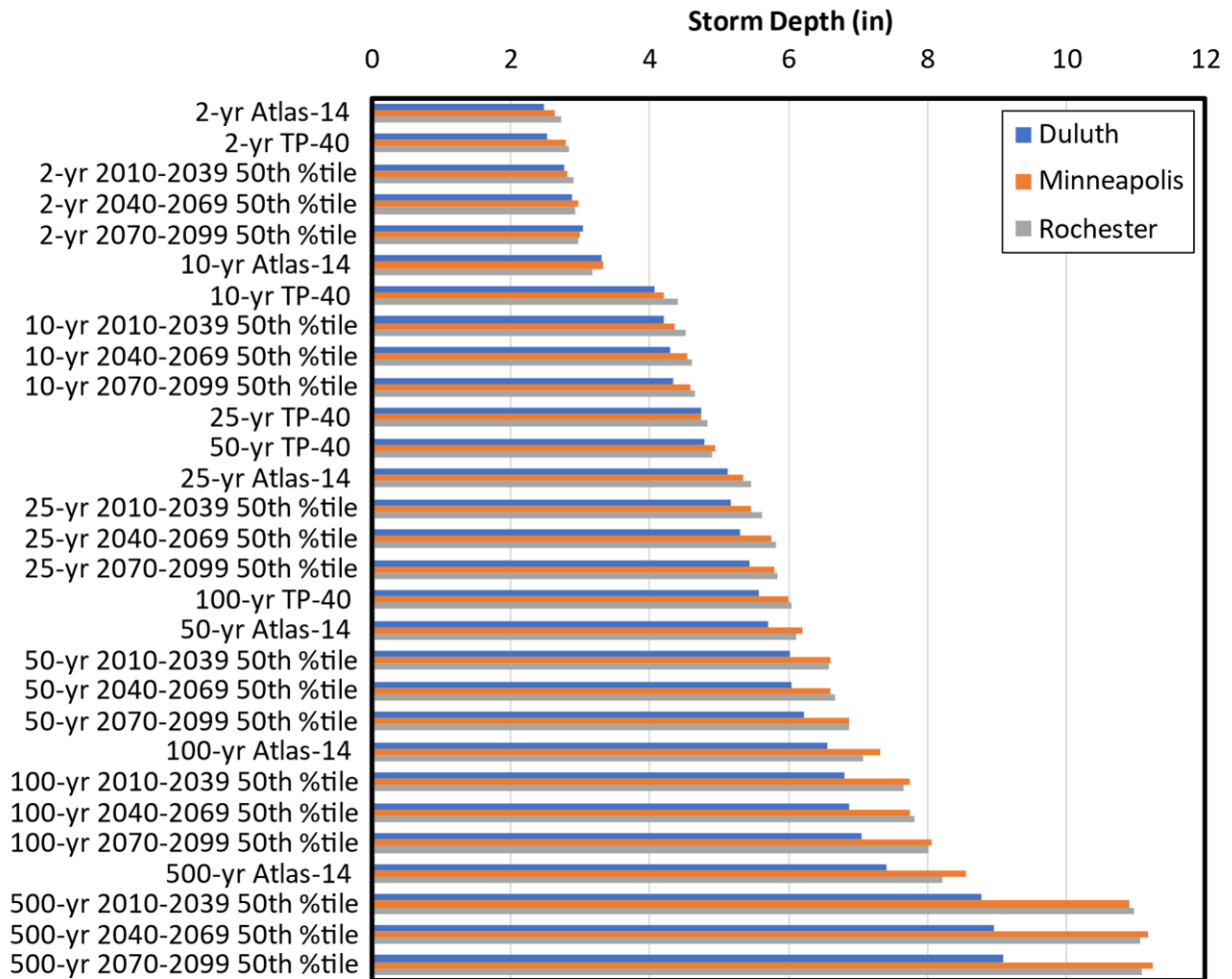


Figure 13: Storm depth (in) increasing from smallest (top) to largest (bottom) for TP-40, Atlas-14, and the 50th percentile future projections in Duluth, Minneapolis, and Rochester.

Future storms were compiled based on the future storm map products created by WSP in their MnDOT-funded project (Dorney and Miller, 2020). The WSP products include maps of future storms sizes for two GCM runs (mpi-esm-mr RCP4.5 and mpi-esm-mr RCP8.5) and maps of the % change in storm size for a much larger set of 64 GCM runs (32 GCMs X 2 CO₂ emission scenarios), with both products covering return periods of 2 to 500 years and 3 time periods (2010-2039, 2040-2069, 2070-2099). The mpi-esm-mr RCP4.5 and mpi-esm-mr RCP8.5 GCM products represent the projected 50th and 75th percentile increase in storm size over Minnesota. However, locally, these two GCM products do not represent the 50th and 75th percentile increase due to the fine scale spatial variability in the GCM outputs over the state (Figure 14). For example, the mpi-esm-mr RCP8.5 product in Minneapolis represents about a 90th percentile increase in storm size amongst the 64 GCMs outputs. To achieve consistent future storm analysis for the three sites in this study, we chose to calculate the 50th, 75th, and 90th percentile increase in storm size locally for each site and each return period, based on the WSP maps for %change in storm size for 64 GCM runs. The 50th, 75th, and 90th percentile increase in storm sizes were then used to calculate future storm depths, based on the Atlas-14 storm sizes as shown in Equation (1):

$$x_{i,j} = x_{o,j} \cdot (1 + c_{i,j}/100) \quad (1)$$

where $x_{i,j}$ is the 24-hour storm size for the i^{th} future time period and j^{th} return period, $x_{o,j}$ is the 24-hour Atlas-14 storm depth, and $c_{i,j}$ is the percent change in storm size.

To mimic the process that WSP used, we ranked the % change in storm size for a combined list of RCP4.5 and RCP8.5 outputs. Based on recently published commentary by Hausfather and Peters (2020), the most likely future scenario falls somewhere between the RCP4.5 and RCP8.5 emission scenarios; thus, ranking of a combined list is a reasonable approach. Note that the change in precipitation for the larger storms between TP-40 and Atlas-14 was greater than the change in precipitation between Atlas-14 and the 50th percentile future storms (see Table 3).

The sub-daily distribution of precipitation was also calculated using daily time series of precipitation for each GCM output, using the quantile method described in Appendix B. It was found that the quantile method fails for approximately 5% of the GCM outputs, for cases where the annual maxima of precipitation time series of a GCM for the historical period (1950-2020) are not well matched to the annual maxima of the observed precipitation at a site. For cases where the quantile method gave reasonable results, the resulting 24-hour distribution was similar to MSE-3 distribution (Figure 15). As a result, we chose to use the MSE-3 distribution for all projected storms.

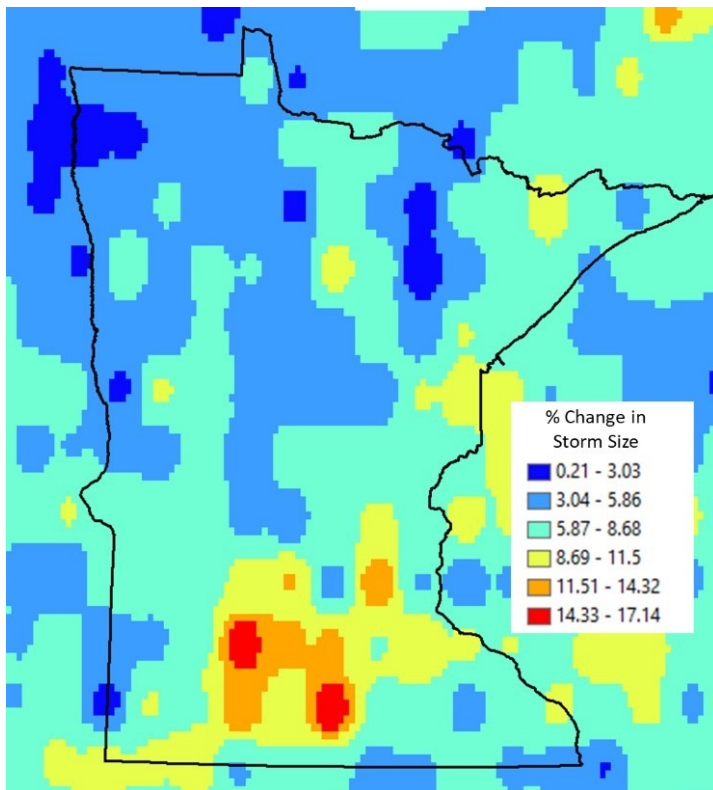


Figure 14: Projected % change in the 100-year storm size for the time period 2070-2099 for the mpi-esm mr RCP8.5 GCM model outputs, as supplied by the WSP products.

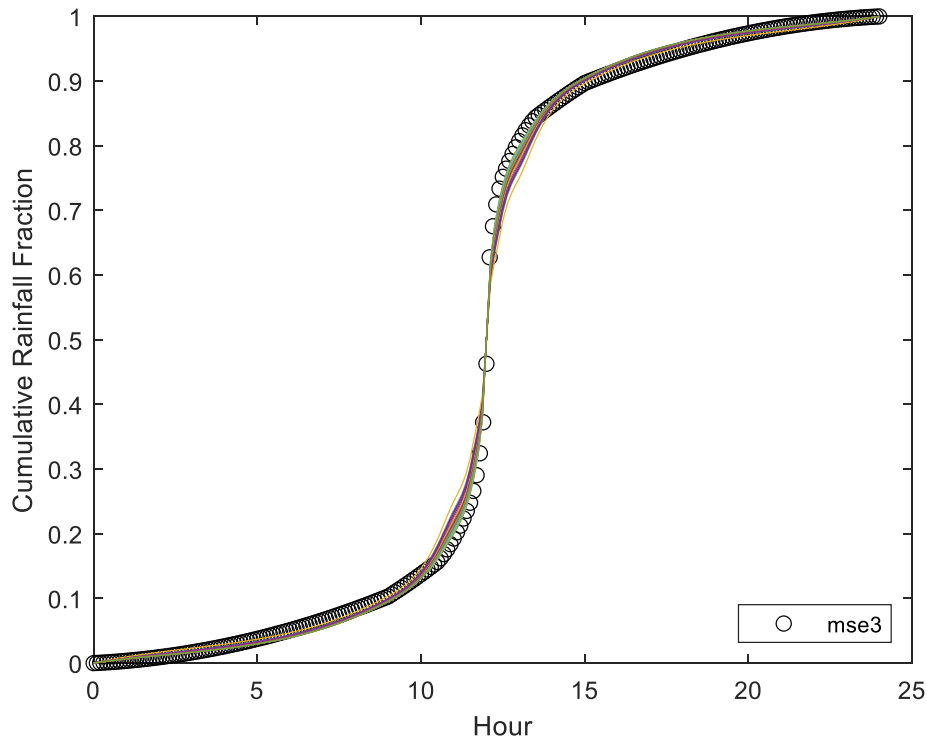


Figure 15: Projected 24-hour precipitation distribution for 32 RCP8.5 GCM outputs for Rochester, MN (solid lines) using the quantile method and the MSE-3 rainfall distribution (open circles).

2.4 Stormwater Infrastructure Adaptation Strategies

Six potential stormwater infrastructure adaptation strategies were considered in this analysis, as described below and summarized in Table 4:

1. **Baseline:** In general, the “baseline” adaptation strategy represents the ‘no change’ option in which the existing watershed stormwater management infrastructure is used without modification.
 - a. The existing stormwater treatment infrastructure within the Miller Creek watershed mainly consists of stormwater retention ponds and grassed swales. Currently, approximately 50% of the connected impervious surface within the watershed is treated by stormwater ponds and runoff is conveyed by stormwater pipes or grassed swales. These existing conditions are denoted as the Baseline stormwater adaptation strategy.
 - b. The existing stormwater treatment infrastructure within the Minneapolis 1NE watershed is a combination of stormwater retention ponds and dry detention basins. Currently, approximately 11% of the connected impervious surface within the watershed is immediately routed to and treated by stormwater ponds and runoff is conveyed by stormwater pipes. These existing conditions are denoted as the Baseline stormwater adaptation strategy.
 - c. The existing stormwater treatment infrastructure within the Kings Run watershed mainly consists of stormwater retention ponds and grassed swales. Currently,

approximately 40% of the connected impervious surface within the watershed is treated by stormwater ponds and runoff is conveyed by stormwater pipes or grassed swales. These existing conditions are denoted as the Baseline stormwater adaptation strategy.

2. **Extra Ponds:** new stormwater ponds were installed such that 100% of the connected impervious area is treated by the combination of existing ponds (no modifications) and new stormwater ponds. The new ponds were designed as follows:
 - a. A standard size with a 5-foot-deep permanent pool with 91,000 ft³ permanent pool volume and a permanent pool surface area of 20,000 ft². The temporary pool (above the permanent pool) is 4 feet deep with a volume of 100,000 ft³ and a surface area of 30,500 ft². A 300 ft² forebay was included for each pond to account for pretreatment.
 - b. The cost analysis (Section 4) includes cost estimates for Underground Storage. Underground storage vaults were not modeled using SWMM but were assumed to provide identical adaptation benefit as the 'Extra Ponds' case.
3. **Infiltration Basins:** small infiltration basins, or rain gardens, were modeled throughout the watershed such that the untreated connected impervious surface is treated by these basins, in addition to the existing ponds (no modifications) from the Baseline condition. For Miller Creek, the infiltration basins were modeled with underdrains, recognizing that many areas of Duluth have soil unsuitable for standard infiltration practices. An infiltration rate of 1 inch/hour was specified at the base of the infiltration basins. The rain gardens were designed as follows:
 - a. A standard size with a surface area of 10,000 ft², a ponding depth of 12 inches, and a total media depth of 24 inches. This standard rain garden size represents the combination of large and medium rain gardens, infiltration basins, and swales.
4. **Smart Ponds:** To reflect recent advances in remote sensing and remote automated control of stormwater infrastructure, this strategy modeled the retrofit adaptation of 'smart' stormwater ponds. In this strategy, the existing stormwater ponds are drained to half depth prior to the storm event, which provides additional storage within the pond when the storm arrives. For existing ponds, as built bathymetry information was used to calculate the draw down depth. For ponds without bathymetric data, it is assumed that 2 feet of storage is available for prior-to-the-storm drainage in the permanent pool.
5. **Combination of Extra Ponds and Smart Ponds (aka More Smart Ponds):** The Extra Ponds case (#2 above) was modified such that all stormwater ponds (existing and new) are Smart Ponds. For new ponds, it is assumed that 3 feet of storage is available for prior-to-the-storm drainage in the permanent pool.
6. **Pipe Upsizing:** In this strategy, the existing storm sewer pipes were replaced with new pipes in which the cross-sectional area is 30% larger (pipe dimensions rounded up to 1' intervals). This was applied to all circular, rectangular, trapezoidal, and arch pipe structures.

Table 4: Summary of percent total connected impervious area treated by Ponds, Infiltration Basins (Infil.), and Smart Ponds (Smart) for the six adaptation strategies.

Scenario	Duluth			Minneapolis			Rochester		
	Ponds	Infil.	Smart	Ponds	Infil.	Smart	Ponds	Infil.	Smart
Baseline	50%	0%	0%	11%	0%	0%	40%	0%	0%
Extra Ponds	100%	0%	0%	100%	0%	0%	100%	0%	0%
Infiltration Basins	50%	50%	0%	11%	89%	0%	40%	60%	0%
Smart Ponds	0%	0%	50%	0%	0%	11%	0%	0%	40%
Extra Ponds + Smart Ponds	0%	0%	100%	0%	0%	100%	0%	0%	100%
Pipe Upsizing	50%	0%	0%	11%	0%	0%	40%	0%	0%

2.5 Adaptation Strategy Simulation Results

2.5.1 Miller Creek

To measure impact of stormwater infrastructure adaptations, the following metrics were chosen for Miller Creek: 1) the depth of flooding at two locations, 2) the flood duration at two locations, and 3) the peak flow at the outlet of Miller Creek. For comparison, the water level will be compared to the approximate crown elevation of US Highway 53 and several cross-roads because flooding on this highway is a major concern within the Miller Creek watershed. The four locations in which flood depth was tracked within the model (J14, J21, J23, and Temp8) were chosen because they are locations in which flooding was identified during previous large rain events, including the historic June 2012 flood (Figure 16, Table 5). The wetland of interest is known as the “Kohl’s wetland” because of its proximity to a local retail store, near Miller Creek mall. The two drainage channels of interest represent the open-channel flow through Kohl’s wetland (main25) and the arch-culvert outlet from Miller Creek into the St. Louis Bay (main65). The SWMM model results suggest that flooding in the main basin of Kohl’s wetland is caused by the low slope and high vegetation roughness of the wetland, rather than a downstream flow restriction.



Figure 16. Approximate flood extent and area of inundation during the 2012 flood in Duluth, MN (light blue shading) and points of interest for comparing stormwater adaptation strategies (red dots) with labels in white rectangles.

Table 5: Node and Link Descriptions for Miller Creek SWMM model, as shown in Figure 16.

Model Component	Physical Significance
J14	Water levels at Highway 53 culverts
J21	
Temp8	Water levels in Kohl's wetland adjacent to Highway 53
J23	
Main25	Flow rate in Kohl's wetland

2.5.1.1 Upstream – Node J14

The node depth (ft) and duration of flooding (hr) for Node J14 in the Miller Creek sub-watershed in Duluth is shown in Figure 17 (top and bottom, respectively) and illustrates the advantages of the adaptation strategies compared to the Baseline (i.e., current conditions) strategy for the 2-year, 10-year, and 100-year storms. For these storms, this structure will overtop for the Baseline TP-40 10-year events and larger. Node flooding is eliminated for all 10-year events (TP-40, Atlas 14, 2069-50th) when the More Smart Ponds strategy is implemented. This is expected because the More Smart Ponds strategy provides substantial storage for flood volume due to existing ponds being converted to Smart Ponds (~50% additional storage) and new ponds built as Smart Ponds (~50% additional storage). Extra Ponds and Pipe Upsizing also eliminated node flooding for the TP-40 and Atlas 10-year event, but not the 2069-50th. Extra Ponds provide extra storage, though not as much as Smart Ponds. Pipe Upsizing conveys water downstream faster, which benefits upstream nodes like J14. Though Extra Ponds, More Smart Ponds, and Pipe Upsizing reduce the node flooding depth for the 100-year events, the depths still exceed the overtopping level.

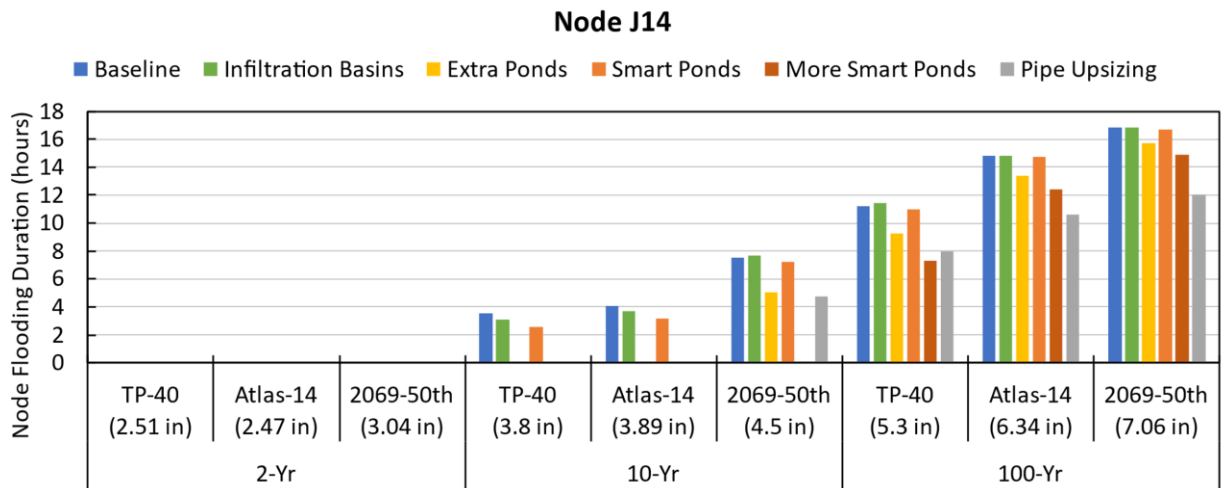
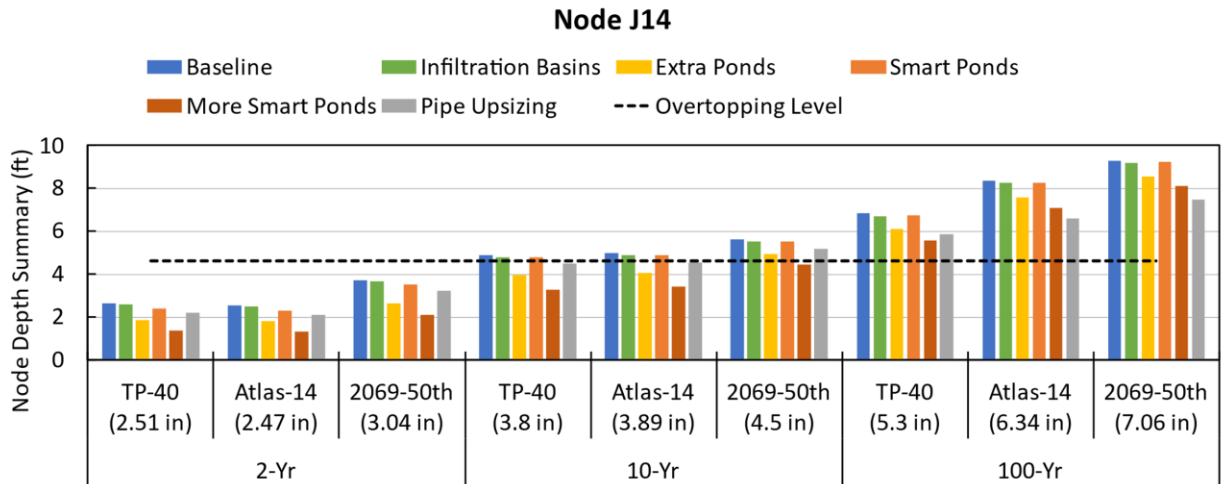


Figure 17: Node Depth in ft (top) and flood duration in hours (bottom) for the 2-, 10-, and 100-year storms at node J14 in Duluth.

When considering climate change mitigation, one measure of success is whether flooding is the same or less for future-predicted storms compared to the current condition(s). For example, the node depth for J14 for the 2-year, 10-year-, and 100-year Atlas-14 storms and the Baseline scenario represents the ‘current’ conditions and amount of potential flooding at this location. An adaptation strategy could be considered successful at mitigating future-predicted flooding if the node depth and flood duration for the adaptation strategy during the future-predicted storm (e.g., 2069 50th) is the same or less than the node depth and flood duration for the current conditions. The node depth (Figure 17, top) and node flooding duration (Figure 17, bottom) is less for the More Smart Ponds and Pipe Upsizing strategies for the 2069-50th predicted storms when compared to the Baseline Atlas-14 storms. In other words, flooding at J14 will be less for future-predicted storms compared to the current conditions if More Smart Ponds or Pipe Upsizing are implemented.

The length of time that the node depth exceeds the overtopping level is termed the ‘flood duration’ and is shown for node J14 in in Figure 17 (bottom). When node J14 floods (10-yr events and above), the

duration ranges from 2 to 16+ hours. The relative benefits of the adaptation strategies are similar for node depth and flooding duration (Figure 17 top and bottom, respectively). The order of best to worst strategies for reducing node depth and flood duration for node J14 is: 1) Pipe Upsizing, 2) More Smart Ponds, 3) Extra Ponds, 4) Smart Ponds, 5) Infiltration Basins, and 6) Baseline. Pipe Upsizing is the most beneficial at this node because it is upstream in the watershed and Pipe Upsizing provides the benefit of quickly sending excess runoff volume downstream, resulting in reduced flood depth and flood duration.

2.5.1.2 Kohl's Wetland – Node J23 & link main25

Further downstream from J14 is the Kohl's wetland. Node J23 and link main25 represent the roughly the outlet from Kohl's wetland. The node depth, duration, and link flow for this location are shown in Figure 18 (top, middle, and bottom, respectively). Flooding at this location begins with the 2069-50th predicted 10-yr event. While the flooding depth is minimal, the duration is nearly 10 hours. The flooding depth for the 100-year events range from less than one foot for TP-40 up to two feet for the 2069-50th storm with durations ranging from 8 to 23 hours. For all events at this node, the More Smart Ponds strategy provides the most reduction in node depth and flood duration compared to the Baseline.

The order of best to worst strategies for reducing node depth, flood duration, and peak flow for the Kohl's wetland is: 1) More Smart Ponds, 2) Extra Ponds, 3) Smart Ponds, 4) Infiltration Basins, 5) Baseline, and 6) Pipe Upsizing. There are more ponds built in the Extra Ponds strategy compared to the existing ponds in the Baseline strategy, which is why Extra Ponds provides more benefits than Smart Ponds. In Miller Creek, the Infiltration Basins are designed with underdrains because the soils are poor for infiltration. Thus, there is minimal volume reduction and limited peak flow reduction for the Infiltration Basin strategy. Unlike the upstream node J14, Pipe Upsizing is not beneficial at node J23 because it increases node depth and peak flow rate compared to the Baseline.

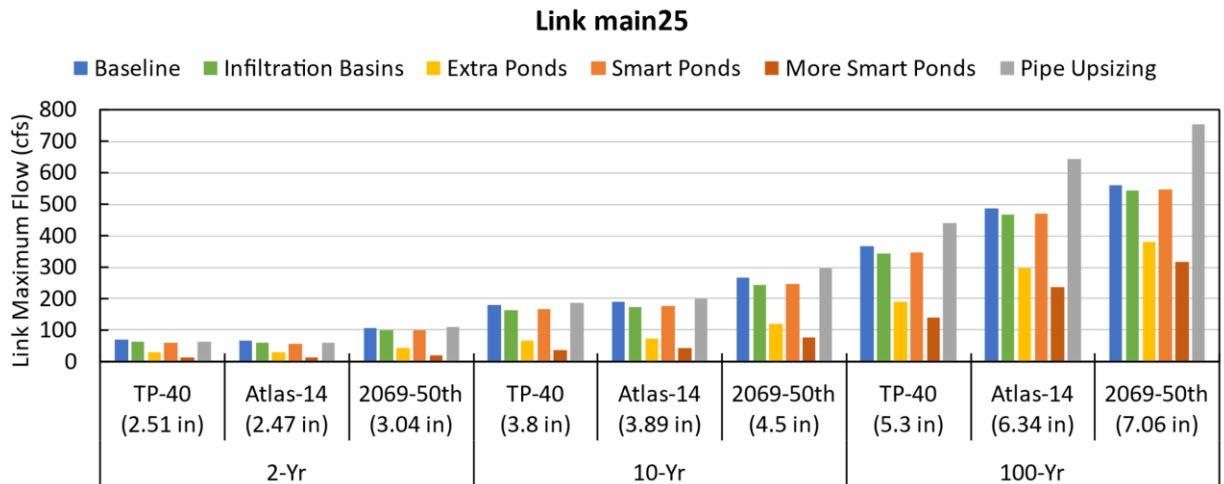
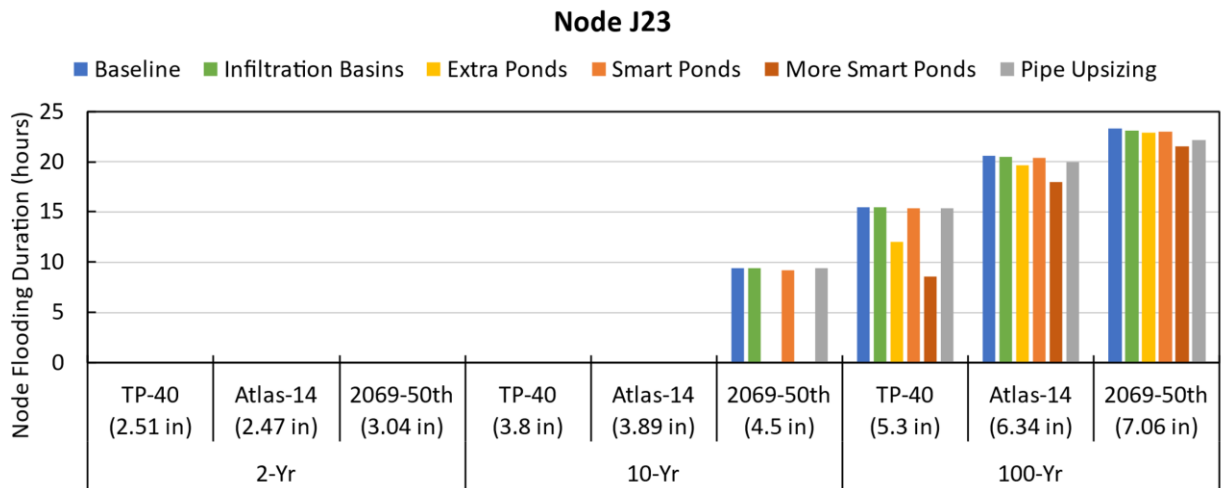
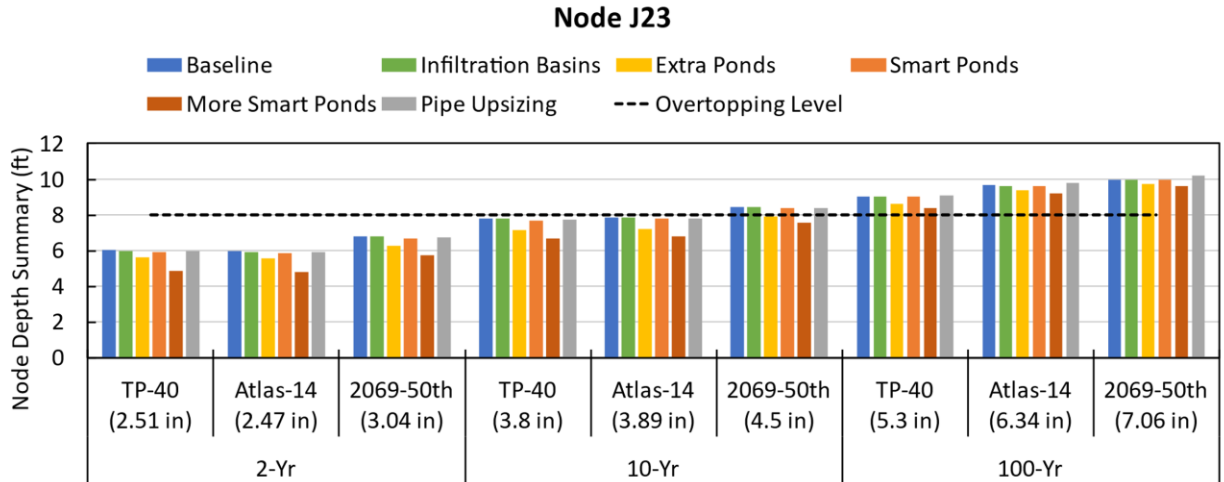


Figure 18: Node Depth in ft (top), flood duration in hours (middle), and peak flow rate in cfs (bottom) for the 2-, 10-, and 100-year storms at node J23 (depth and duration) and link main25 (flow rate) in Duluth.

2.5.1.3 Miller Creek Outlet

The outlet from Miller Creek including the newly added Coffee creek sub-watershed is the link main68. Using the new outlet culvert design for combined outlet of Miller and Coffee Creeks, the capacity of the outlet was not exceeded, even for future 500 years storms. Simulations were run with the culvert backwatered at a 50-year mean lake elevation for Lake Superior (602 ft). Flows at the outlet were largely limited by the capacity of the stormwater tunnel upstream of the outlet (e.g., main64, Figure 5), however, these capacity limits were not predicted to cause flooding upstream of the tunnel. The peak flow rate at this location is shown in Figure 19. The peak flow rate is reduced substantially for the 2-yr and 10-yr events when the More Smart Ponds (> 50% reduction) or Extra Ponds (~50% reduction) strategies are implemented in the watershed. As observed for upstream nodes, More Smart Ponds and Extra Ponds provide substantial storage for flood volume which also reduces the peak outflow at the watershed outlet for smaller storms. The benefits of these strategies diminish for the 100-year events because the cumulative effects of larger events overwhelm the storage capacity of the strategies presented herein. Similar to upstream nodes, the Smart Ponds and Infiltration Basins strategies provide minimal benefit to outflow from the watershed. Pipe Upsizing substantially increased the peak outflow at the outlet from Miller Creek due to the cumulative effect of increased conveyance capacity throughout the watershed. The peak outflow for the 100-year event is up to 30% greater for Pipe Upsizing compared to the Baseline. The order of best to worst strategies for reducing node depth, flood duration, and peak flow for the Miller Creek watershed is: 1) More Smart Ponds, 2) Extra Ponds, 3) Smart Ponds, 4) Infiltration Basins, 5) Baseline, and 6) Pipe Upsizing.

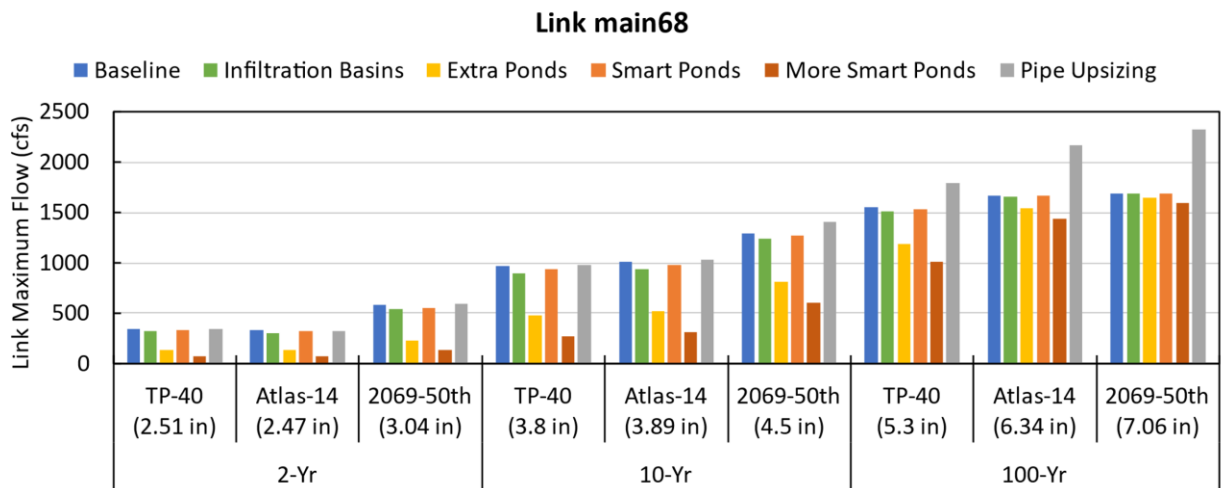


Figure 19: Peak flow rate (cfs) at the outlet from Miller Creek and Coffee Creek sub-watersheds (main68).

In terms of climate change mitigation, the max flow rate (Figure 19) is less for the More Smart Ponds strategy for the 2069-50th predicted storms when compared to the Baseline Atlas-14 storms. In other words, peak flow at the primary outlet will be less for future-predicted storms compared to the current conditions if More Smart Ponds are implemented within Miller Creek.

The flow hydrograph at the outlet of Miller Creek for the Atlas 14 100-yr event is shown in Figure 20. The Baseline, Infiltration Basins, and Smart Ponds strategies overlap and are difficult to distinguish from each other. As expected, the Pipe Upsizing strategy increases the peak outflow by ~30%. The More Smart Ponds and Extra Ponds strategies reduce the peak flow by ~6-12% and delay the peak by ~2 hours.

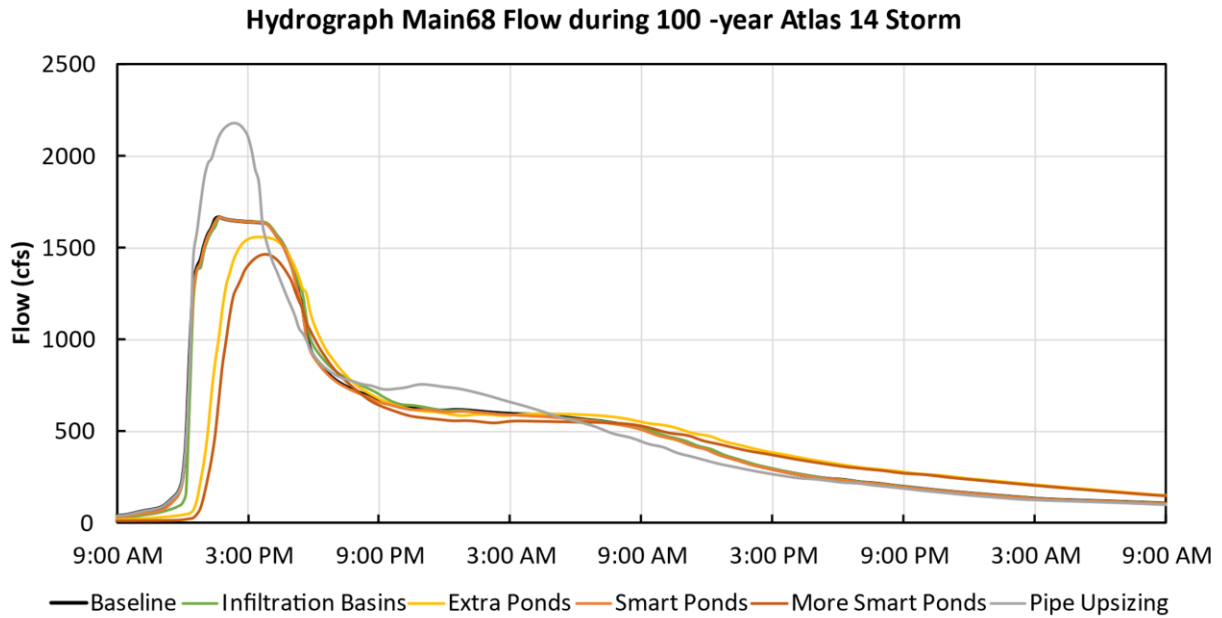


Figure 20: Miller Creek Outlet (main68) Hydrograph (flow in cfs) for the 100-year Atlas 14 event (6.31 inches)

2.5.2 Minneapolis

To measure impact of stormwater infrastructure adaptations, the following metrics were chosen for Minneapolis: 1) the depth of flooding, 2) the flood duration, and 3) the peak flow at the outlet to the Mississippi River. For comparison, the water level will be compared to the approximate surface elevation at which the nodes would overtop with water. Four nodes and two outlets of interest are shown in Figure 21. The nodes were selected because model results showed flooding which would impact neighborhood or infrastructure function during extreme events. MH420743 is a manhole in a residential neighborhood which is prone to flooding during extreme events. SA35C350 is an existing wet pond at the intersection of Huset Parkway & 5th Street which can overtop and flood that intersection. SS512682 is along NE Central Ave and SA999039 is a Railway Overpass crossing with NE Main Street.

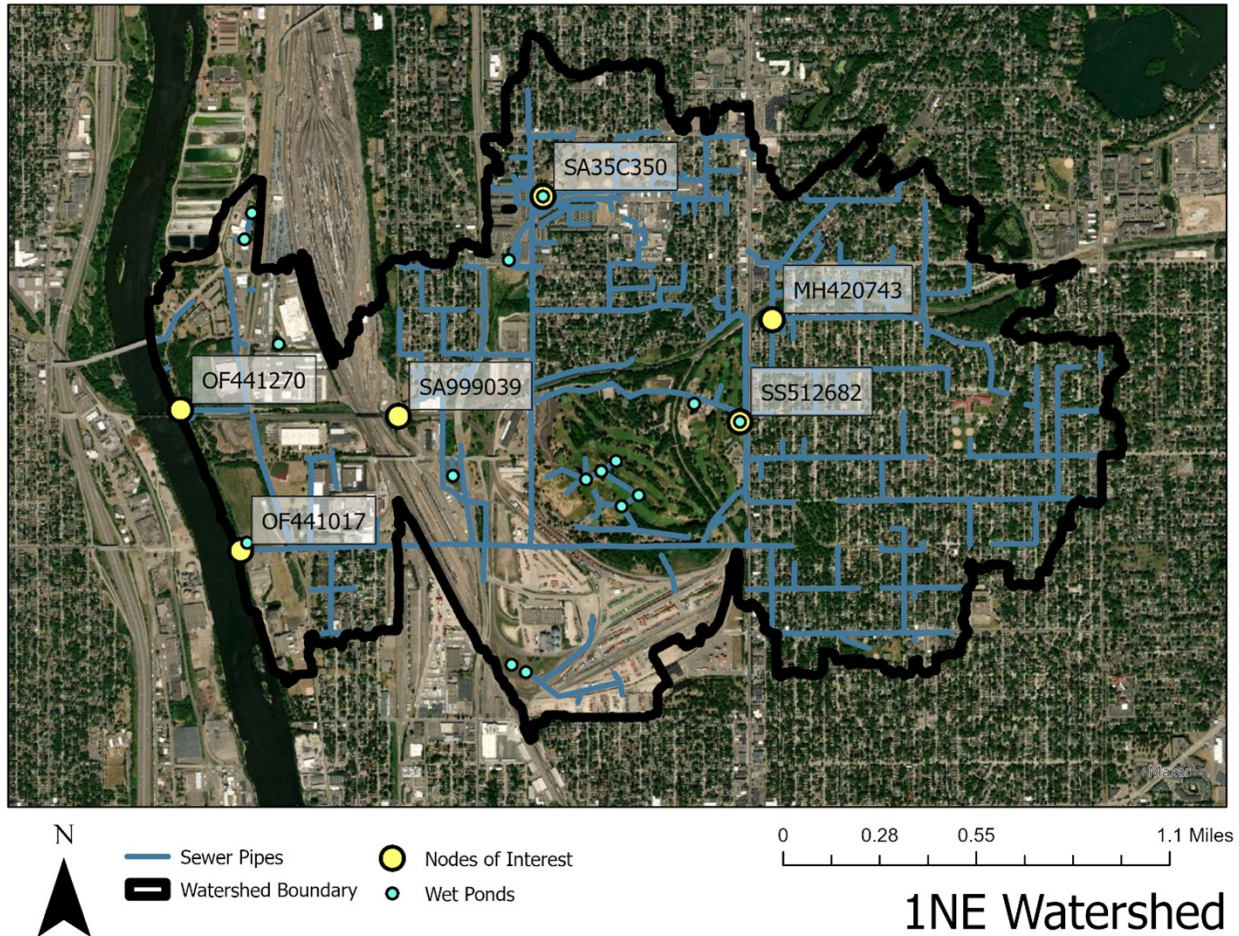


Figure 21: Nodes of Interest in the 1NE Watershed. The four nodes and two outlets discussed are labeled with yellow circles. Additionally, existing wet ponds are identified with light blue circles and the sewer lines are depicted as blue lines. Two of the nodes of interest, SA35C350 and SS512682, are existing wet ponds so are represented with both yellow and blue circles.

2.5.2.1 Upstream Manhole - MH420743

The node depth for MH420743 in Minneapolis is shown in Figure 22 (top) and illustrates the advantages of the adaptation strategies compared to the Baseline (i.e., current conditions) for the 2-yr, 10-yr, and 100-yr storms. For these storms, the Baseline case will overtop this structure by between two feet and seven feet of water. The More Smart Ponds and Extra Ponds adaptation strategies prevent overtopping for the 2-yr and 10-yr storm events. Pipe Upsizing and Infiltration Basins eliminate flooding for the 2-yr storms compared to the Baseline but provide minimal benefit for the 10-yr and 100-yr storms. The Smart ponds strategy does not provide benefit at this node because there are no existing stormwater ponds upstream of the node, thus no changes compared to the Baseline condition.

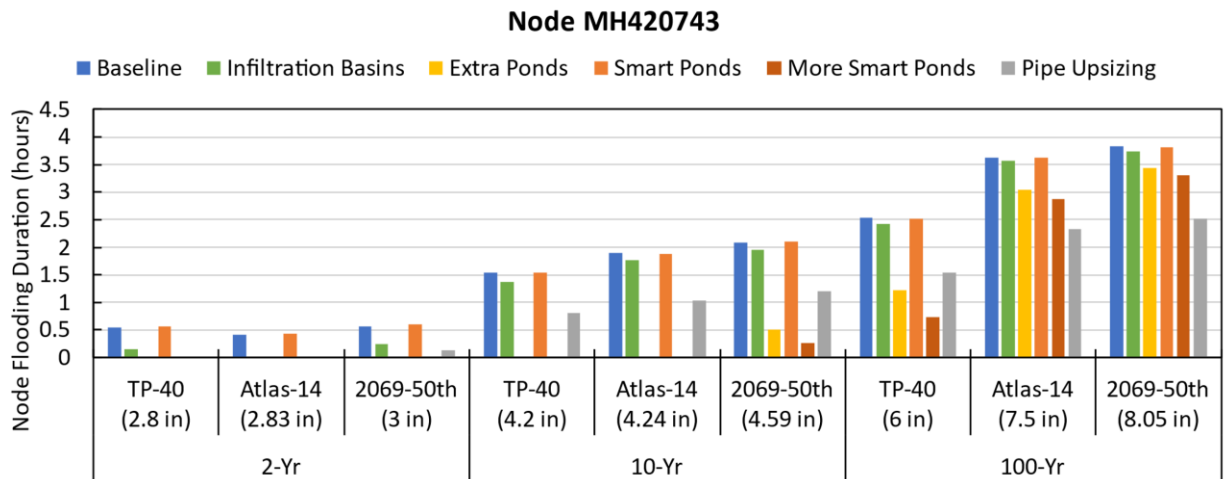
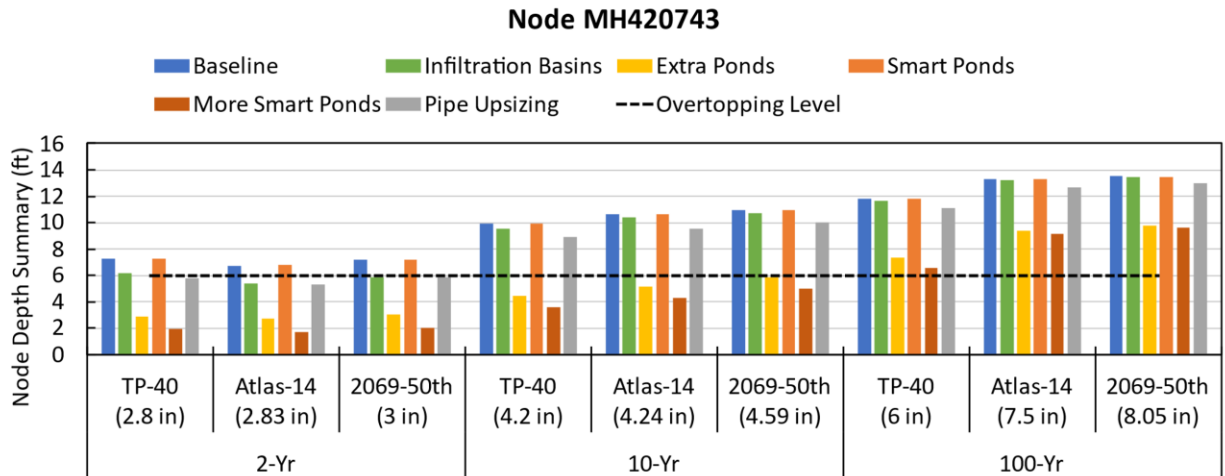


Figure 22: Node Depth in ft (top) and flood duration in hours (bottom) for the 2-, 10-, and 100-year storms at MH420743 in Minneapolis.

None of the adaptation strategies can eliminate flooding during the 100-yr event. It should be noted, though, that flood depth at this node (MH420743) is predicted to be approximately seven feet above the street elevation for the 100-year event. To the authors’ knowledge, this depth of flooding has not been observed in this area of Minneapolis, but rainfall events have exceeded the 100-year rainfall depth for this area. According to state precipitation records (Minnesota State Climatology Office 2023), at least two events of approximately this depth or more have been recorded in Minneapolis (Aug 30, 1977 = 7.28 inches; Jul 23, 1987 = 9.15 inches). This suggests that the EPA-SWMM models have not been adequately calibrated and tested for large rainfall events. They can be used, however, for relative comparisons between adaptation strategies.

The flood duration at node MH420743 (Figure 22, bottom) shows similar relative trends between the adaptation strategies, except for Pipe Upsizing. For node depth, Pipe Upsizing provided benefit for the 2-yr event and minimal benefit (<10%) for the 10-yr and 100-yr. For flood duration, however, Pipe Upsizing reduces the flood duration ~30-50% for the 10-yr and 100-yr events. Pipe Upsizing conveys

more water downstream, but the storage of flood water is unaltered. The street-storage of flood water at this location is wide and flat such that large changes in volume may not produce large changes in depth. The duration of flooding, however, is reduced because Pipe Upsizing can convey the flood water away from the site more quickly.

2.5.2.2 Downstream Node - SA999039

Node SA999039 is further down in the watershed (see Figure 21) and thus the adaptation strategies will affect the node depth and flood duration more than they did at the upstream node MH420743. The node depth for SA999039 in Minneapolis is shown in Figure 23 (top). Node flooding occurs in the Baseline condition for the 2-yr, 10-yr, and 100-yr events. As observed in other watersheds and nodes, More Smart Ponds and Extra Ponds reduce the flood depth the most and eliminate flooding for the 2-yr event. More Smart Ponds almost eliminates flooding for the 10-yr event and reduces flood depth by ~50% for the 100-yr event. Because SA999039 is downstream in the watershed, the cumulative effects of More Smart Ponds and Extra Ponds upstream in the watershed provide substantial storage benefit. Pipe Upsizing slightly increases flood depth for the 2-yr and 10-year events but reduces flood depth slightly for the 100-year events.

Smart Ponds and Infiltration Basins provide no benefit to flood depth at SA999039. The general flow path in 1NE is south and then west. While further west than other nodes, SA999039 is relatively upstream and there are not many contributing subcatchments that are routed through SA999039 before joining the main flow path. As such, there are no ponds upstream so Smart Ponds have minimal effect. Infiltration Basins have minimal effect because few upstream catchments also mean few Infiltration Basins will be added upstream, thus providing minimal effect.

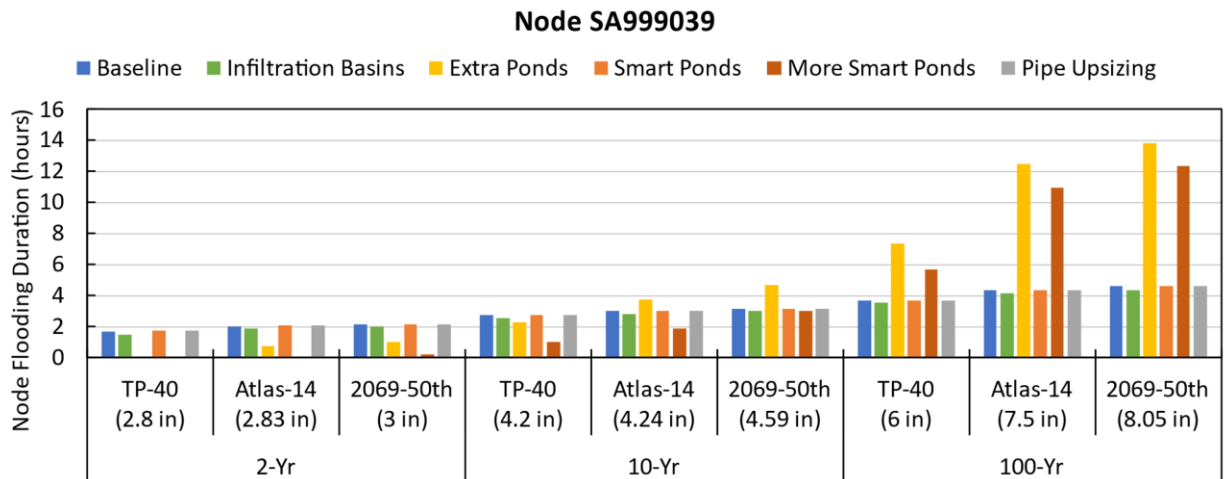
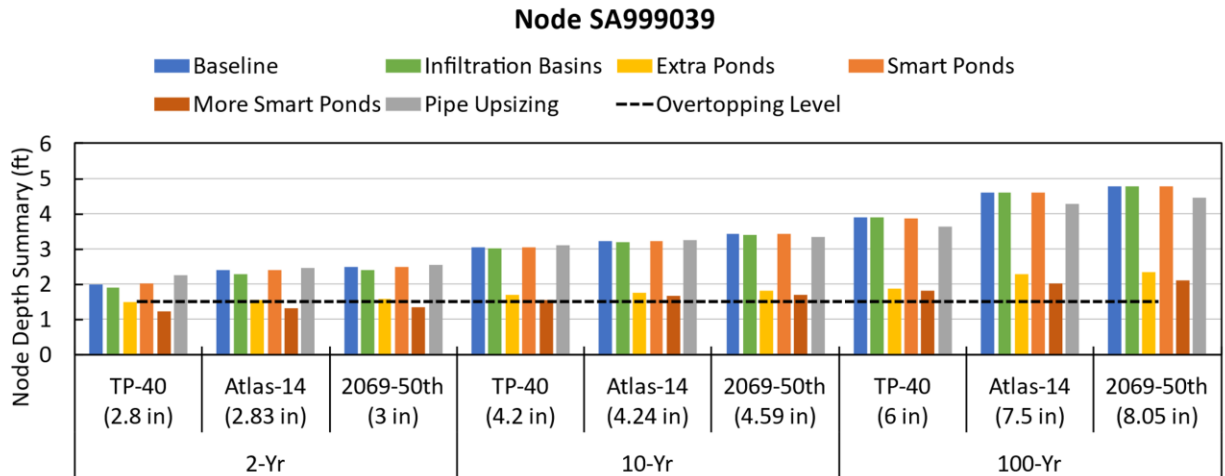


Figure 23: Node Depth in ft (top) and flood duration in hours (bottom) for the 2-, 10-, and 100-year storms at SA999039 in Minneapolis.

Flood duration ranges from approximately 2 to nearly 14 hours (Figure 23 bottom). More Smart Ponds eliminate or reduce flood duration for the 2-yr and 10-yr storms, as expected and as observed for other watersheds and nodes. Extra Ponds, however, increases flood duration for the 10-yr storm under Atlas 14 and 2069-50th, while also reducing the flood depth (Figure 23 top). More Smart Ponds and Extra Ponds both increase flood duration for the 100-yr events. Extra Ponds and More Smart Ponds increase the flood duration for large events because the purpose of these new ponds is to capture and slowly release flood water. While these strategies decrease the flood depth substantially, they can also increase the duration over which the flood depths persist due to the slow release of the stored flood volume. One must, however, consider the relative magnitude of the tradeoff. The Baseline, Infiltration Basins, Smart Ponds, and Pipe Upsizing strategies at this node produce a peak flood depth above the overtopping level of ~3.5 feet and maintains flooding for ~4 hours (not continuously at the peak flood depth). By contrast, the More Smart Ponds and Extra Ponds strategies reduce the flood depth to approximately 6 inches to 1 ft, but maintains flooding for between 10 and 14 hours (again, not continuously at the peak flood depth).

In terms of climate change mitigation, the node depth (Figure 23, top) is less for the Extra Ponds and More Smart Ponds strategies for the 2069-50th predicted storms when compared to the Baseline Atlas-14 storms. The flood duration (Figure 23, bottom), however, is increased for both the 10-year and 100-year storms when the Extra Ponds or More Smart Ponds strategies are implemented. As discussed above, however, the flood depth is minimal and is a substantial reduction when these strategies are implemented. In other words, flooding at this location will be less for future-predicted storms compared to the current conditions if Extra Ponds or More Smart Ponds are implemented.

2.5.2.3 1NE Outlet

The maximum flow rate from the primary outfall from the 1NE model (Figure 24) shows that Pipe Upsizing will substantially increase the outflow from the watershed to the Mississippi River. Compared to the Baseline and the other adaptation strategies, Pipe Upsizing increases the maximum flow rate by ~50% for nearly all storms, including the smallest 2-year events. This represents the tradeoff of Pipe Upsizing; reducing flooding upstream in the watershed by conveying it more quickly to the outlet. This, however, can exacerbate flooding downstream of the watershed. The reduction in flooding in the watershed by Pipe Upsizing was ~10% for this watershed, but the increase in peak flow at the outlet was ~50% more than the Baseline condition. The order of best to worst strategies for reducing node depth, flood duration, and peak flow for the Minneapolis 1NE watershed is: 1) More Smart Ponds, 2) Extra Ponds, 3) Infiltration Basins, 4) Smart Ponds, 5) Baseline, and 6) Pipe Upsizing.

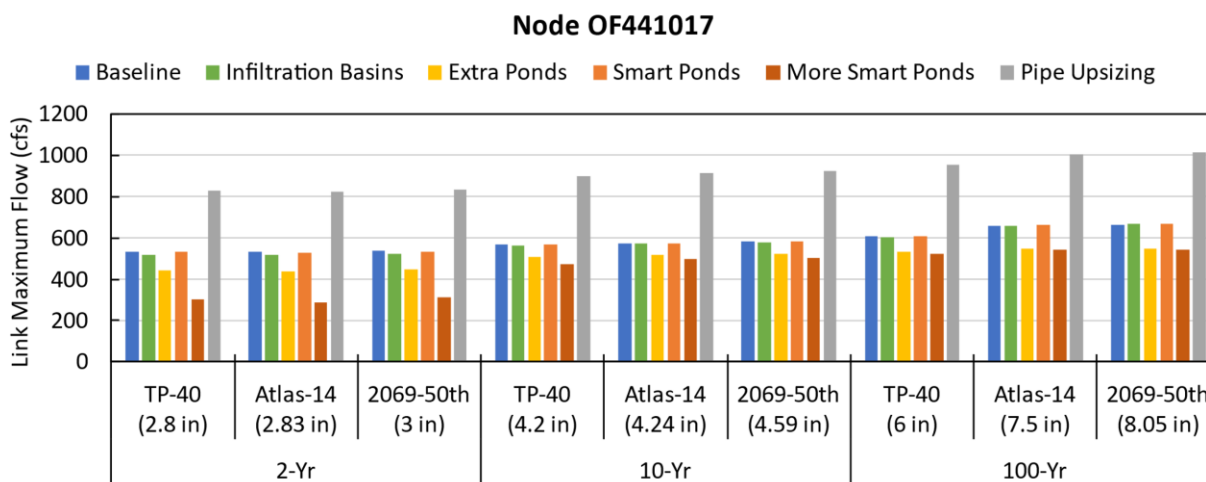


Figure 24: Maximum Flow Rate (cfs) for OF441017 in Minneapolis for all storms.

The flow hydrograph at the outlet of the 1NE watershed in Minneapolis for the Atlas 14 100-yr event is shown in Figure 25. The Baseline, Infiltration Basins, and Smart Ponds strategies overlap and are difficult to distinguish from each other. The Infiltration Basins strategy delays the rising limb of the hydrograph by ~8 hours but then the hydrographs quickly become similar and peak at the same time. As expected, and observed in other watersheds and nodes, the Pipe Upsizing strategy increases the peak flow substantially (~50% for 1NE) and does not delay the peak. In contrast, the More Smart Ponds and the Extra Ponds strategies decrease the peak by ~17% and delay the peak by ~1 hour.

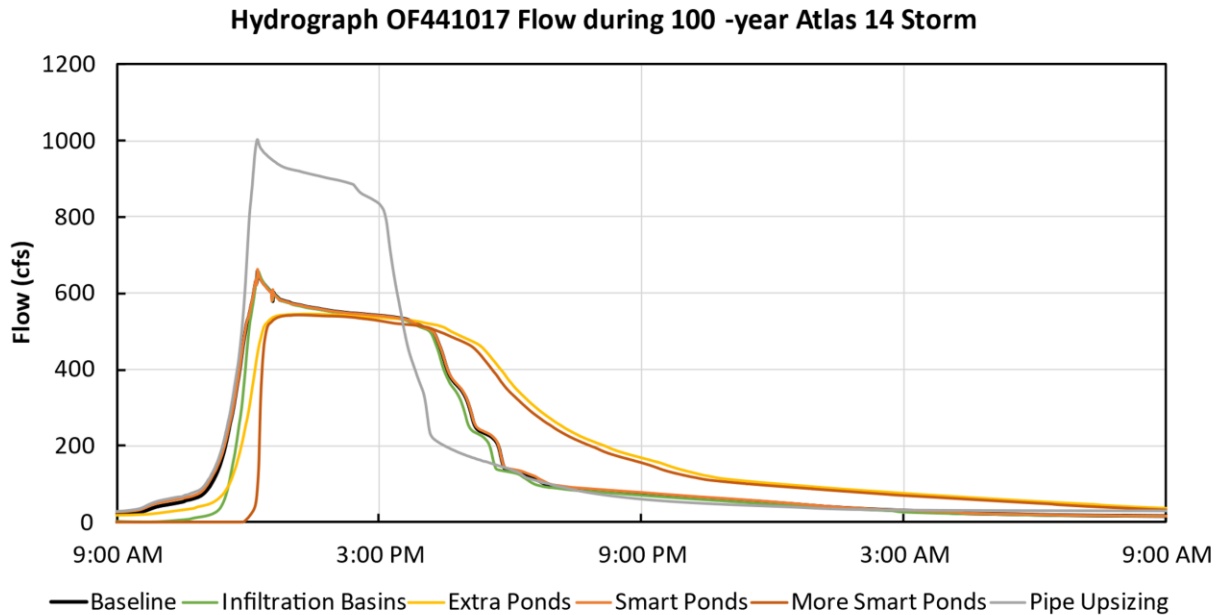


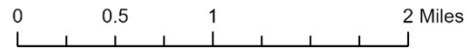
Figure 25: 1NE Outlet (OF441017) Hydrograph (flow in cfs) for the 100-year Atlas 14 event (7.5 inches)

2.5.3 Rochester

To measure impact of stormwater infrastructure adaptations, the following metrics were chosen for Kings Run in Rochester: 1) the depth of flooding, 2) the flood duration, and 3) the peak flow at the outlet to a tributary of the Zumbro River. For comparison, the water level will be compared to the approximate surface elevation at which the nodes selected would overtop with water. Four nodes of interest and outlet location are shown in Figure 26. The nodes were selected based on model results that would substantially impact infrastructure. RN176248 represents a culvert that can surcharge during large rain events and overtop onto 55th St NW which is a key connection between the residential neighborhoods in the watershed and the rest of Rochester. SP113 is an existing wet pond next to a neighborhood composed of multifamily residences which can overtop during large events and floods substantial portions of the residences. SP64 is an existing wet storage pond next to a commercial center, which can overtop and flood the parking lot as well as surrounding businesses. SP105 is an existing wet pond located in the interchange between 55th St NW and Highway 52. This is a local low point for Highway 52, and overtopping of SP105 indicates flooding of the highway, obstructing a regional artery. The only outlet in the watershed is labeled “Temp” which discharges into a surface channel that merges with the Zumbro River outside the watershed.



- Nodes of Interest
- Watershed Boundary
- WetPonds



Kings Run Watershed

Figure 26: Nodes of Interest in the Kings Run Watershed. The node and outlet discussed are labeled with yellow circles. Additionally, existing wet ponds are identified with light blue circles. Three of the nodes of interest, SP113, SP64, and SP105, are existing wet ponds so are represented with both yellow and light blue circles.

2.5.3.1 Mid-watershed – Node RN176248

The node depth and flood duration for RN176248 in Rochester are shown in Figure 27 top, and bottom, respectively. Flooding at this node does not occur except for the Atlas 14 and 2069-50th 100-yr storms, but flood depth and flood duration are 2.5 feet and between 2 and 6 hours, respectively, for these storms. This is because the Atlas 14 (7.85 inches) and 2069-50th (8.02 inches) 100-yr events are substantially larger than the TP-40 100-year event (6.1 inches) and smaller events (e.g., 2069-50th 10-yr = 4.64 inches).

Similar to other upstream nodes, the More Smart Ponds, Extra Ponds, and Pipe Upsizing strategies reduce flood depth and/or duration at this node due to their ability to store flood water or convey flood water downstream. Node RN176248 is approximately mid-watershed such that there are upstream ponds, but the storage volume within those ponds is relatively small compared to the flood volume generated by the modeled rainfall events. Thus, the Smart Ponds strategy provided minimal benefit for this node.

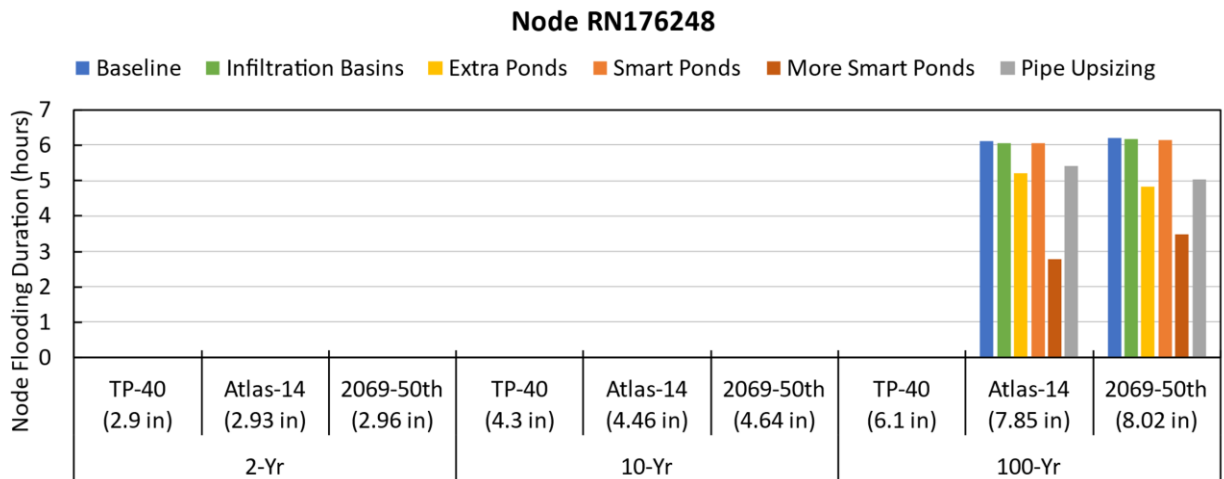
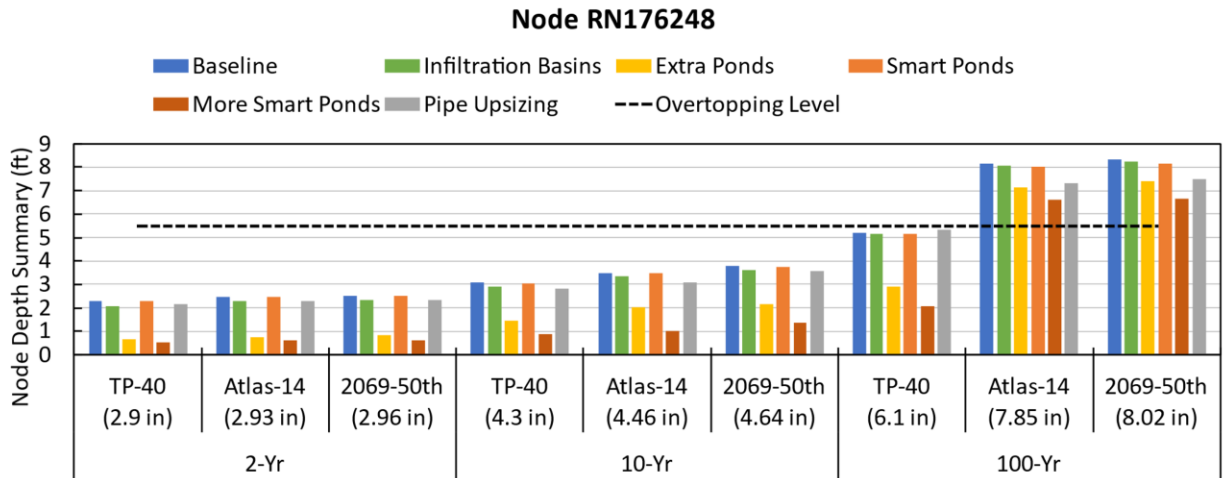


Figure 27: Node Depth in ft (top) and flood duration in hours (bottom) for the 2-, 10-, and 100-year storms at node RN176248 in Rochester.

2.5.3.2 Lower-watershed – Node SP113

The node depth and flood duration for SP113 in Rochester are shown in Figure 28 top, and bottom, respectively. Overtopping at this node begins with 10-yr events. The Pipe Upsizing strategy is the only strategy to flood during the TP-40 10-yr event, which occurs because SP113 is downstream in the watershed and the cumulative effects of Pipe Upsizing throughout the watersheds results in more flood water delivered to the downstream nodes more quickly, exacerbating flooding. Pipe Upsizing also causes the deepest flood depths and longest flood durations for all 10-yr and 100-yr events at Node SP113. Flooding at this node results in inundation of numerous residents in the adjacent multifamily residential neighborhood.

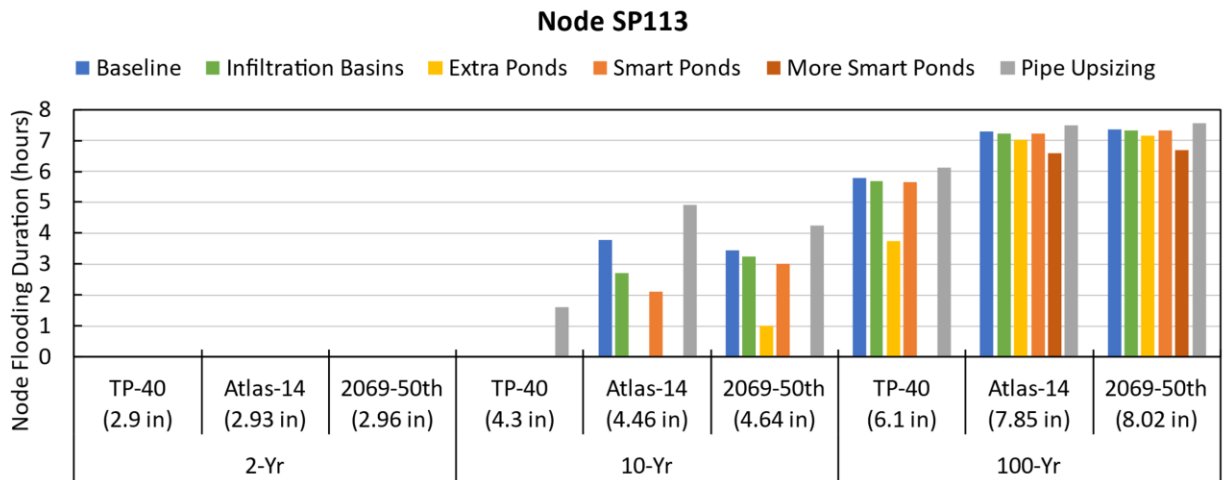
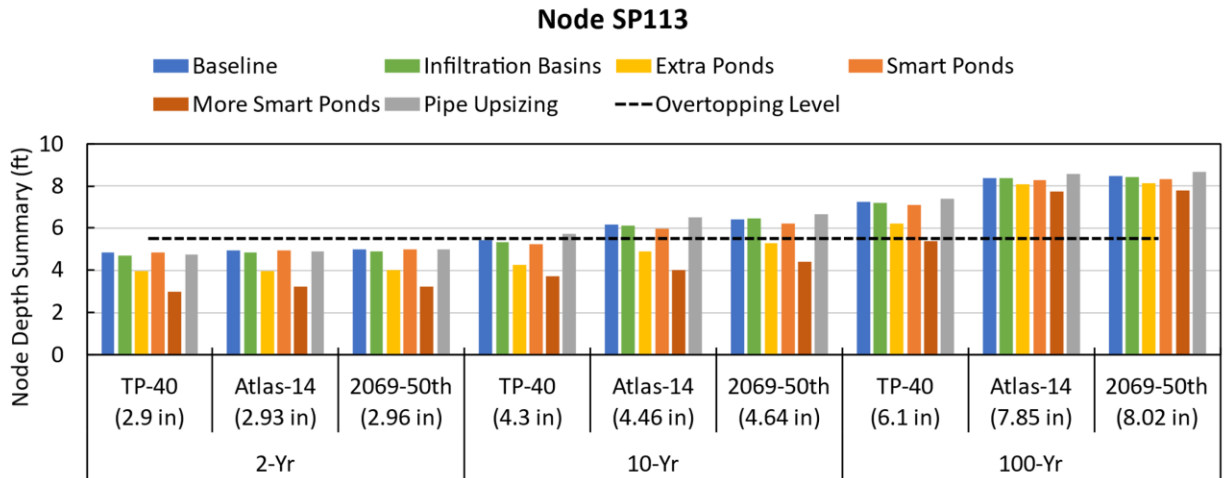


Figure 28: Node Depth in ft (top) and flood duration in hours (bottom) for the 2-, 10-, and 100-year storms at node SP113 in Rochester.

More Smart Ponds and Extra Ponds provide the most benefit in reducing peak depth and flood duration but have less effect on the largest 100-year storms because of SP113’s location at the bottom of the watershed. Flooding is eliminated at this node for the 10-yr events and the TP-40 100-year with More Smart Ponds.

2.5.3.3 Kings Run Outlet

The maximum flow rate from the primary outfall from the Kings Run model (Figure 29) shows that most adaptation strategies will decrease the peak flow from the watershed to the outlet, but Pipe Upsizing will increase the outflow, as expected. More Smart Ponds and Extra Ponds provide reduction in peak outflow while Infiltration Basins and Smart Ponds provide minimal benefit. The flow hydrograph at the outlet of the Kings Run watershed in Rochester for the Atlas 14 100-yr event is shown in Figure 30. The Baseline, Infiltration Basins, and Smart Ponds strategies overlap and are difficult to distinguish from each other, which corresponds well with the peak outflow data shown in Figure 29. Pipe Upsizing increases

the peak flow of the Atlas 14 100-year event by ~6% and the peak occurs ~10 minutes earlier than the Baseline strategy. Extra ponds decrease the peak by ~10% and delays the peak by ~25 minutes, whereas the More Smart Ponds strategy reduces the peak by ~20% and delays the peak by ~45 minutes. The order of best to worst strategies for reducing node depth, flood duration, and peak flow for the Rochester Kings Run watershed is: 1) More Smart Ponds, 2) Extra Ponds, 3) Smart Ponds, 4) Infiltration Basins, 5) Baseline, and 6) Pipe Upsizing.

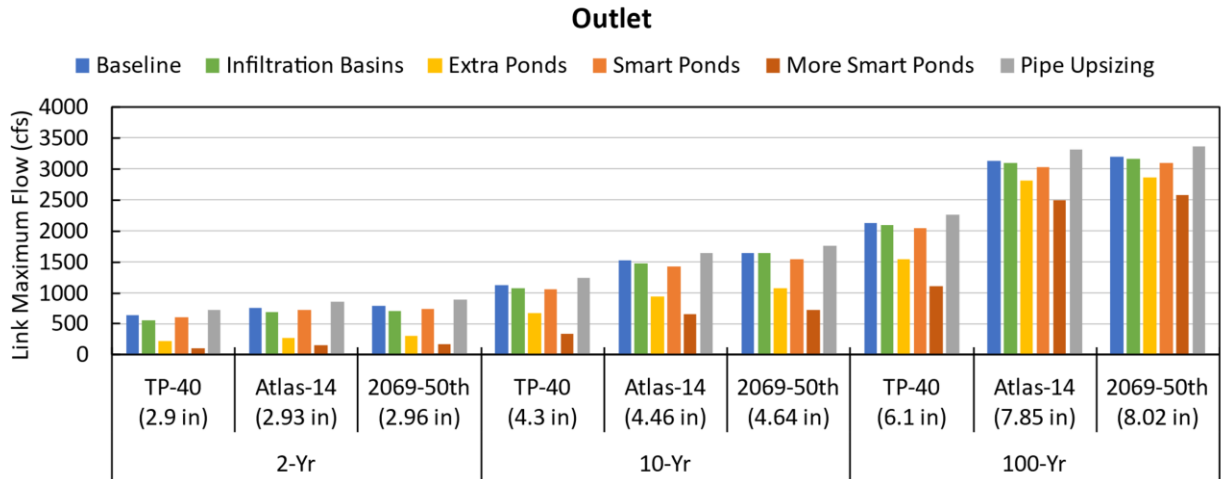


Figure 29: Maximum Flow Rate (cfs) for the outlet (Temp) in Rochester for all storms.

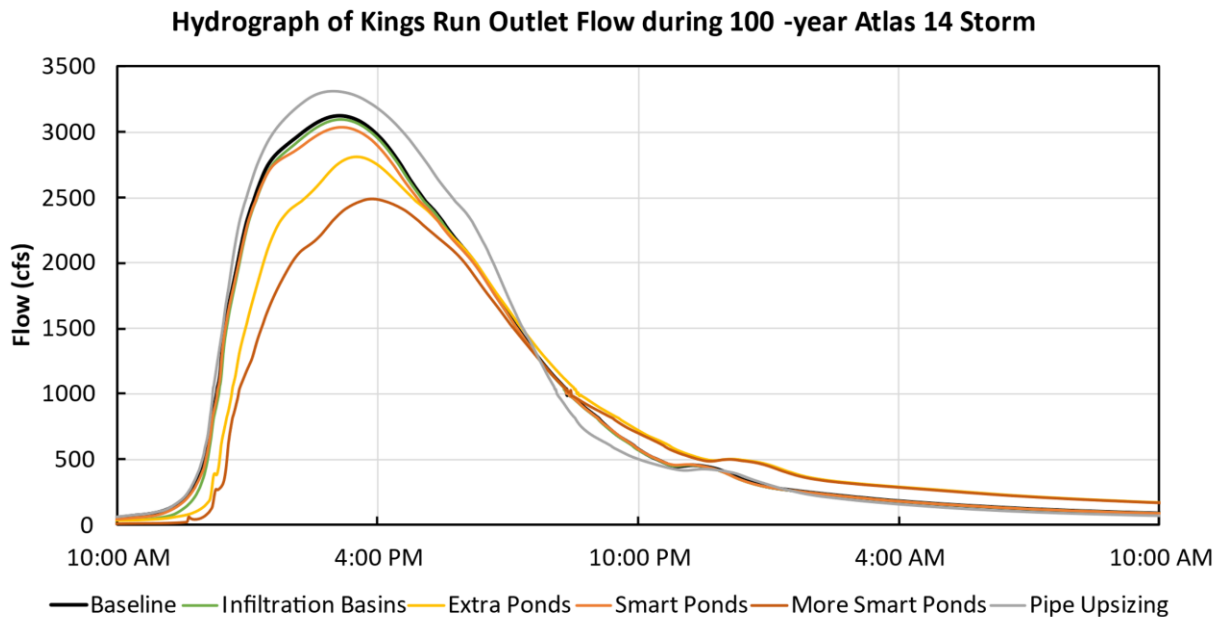


Figure 30: Kings Run Outlet (Temp) Hydrograph (flow in cfs) for the 100-year Atlas 14 event (7.85 inches).

2.6 Designing For Storms

The results in section 2.5: Adaptation Strategy Simulation Results demonstrate that existing design paradigms are not sufficient to eliminate flooding in many of our watersheds and neighborhoods for the design MSE-3 storms (Figure 15). Designing for future potential rainfall events requires more substantial investment in stormwater control infrastructure. The results above were used to estimate how much infrastructure would be required to prevent flooding from low probability events such as the 100-year storm. To do this, the number of Extra Ponds, More Smart Ponds, or Infiltration Basins was increased until all the runoff generated by the Atlas-14 storms were stored by the adaptation strategies. Then, the surface area required to install the number of Extra Ponds, More Smart Ponds, or Infiltration Basins was estimated based on the standard design described above. Finally, the Watershed Area Needed was calculated, which is the land area for each strategy divided by the total watershed area.

The Watershed Area Needed for Duluth, Minneapolis, and Rochester is shown in Figure 31a, b, and c, respectively. This demonstrates that ~40% of the watershed would need to be converted to Infiltration Basins (Figure 31a), ~10% of the watershed to Extra Ponds, or ~6% of the watershed to Smart Ponds to prevent flooding from the 6-inch event in Duluth. One acre of wet pond for every 10 acres of contributing area is a substantial implementation plan. Similar plots for Minneapolis and Rochester are shown in Figure 31b and Figure 31c, respectively. Infiltration basins are limited in their design to one foot of depth above the ground and 40% void space within the media (assumed 2-foot depth) to store runoff. As such, they provide less potential storage per square foot of surface area than stormwater ponds. The amount of area required to store runoff within Infiltration Basins and prevent flooding for the 2-yr to 500-yr Atlas 14 storms (Figure 31) ranges from ~5% to ~40%. It is important to note that this is the percent of the entire watershed, not just the impervious surface.

However, not all storms have the temporal distribution of the MSE-3, shown in Figure 15. The June 20-21, 2012 Duluth storm, for example, officially distributed 7.25 inches (and locally 8-10 inches) of precipitation over two days (National Weather Service 2021). In order to examine the effectiveness of adaptation strategies at remediating flooding for storms of longer duration, we examined the SWMM result for a hypothetical 24 hour-uniform storm with a 100-year return interval in the 1NE Minneapolis watershed (7.97-inch precipitation). The storm would have dropped 0.33 inches of rainfall each hour for 24 hours. The results, shown in Figure 32, indicate that infiltration into pervious areas can act as a remediation strategy for this type of storm. Thus, the response of the watershed is dependent on the temporal distribution of the storm, and soil health is an important factor for more uniform storm distributions. This means that the encouragement of deep-rooted grasses and other plants on lawns could be helpful in developing soils that can absorb an extreme event storm with a temporal distribution that is more uniform than the MSE-3 storm.

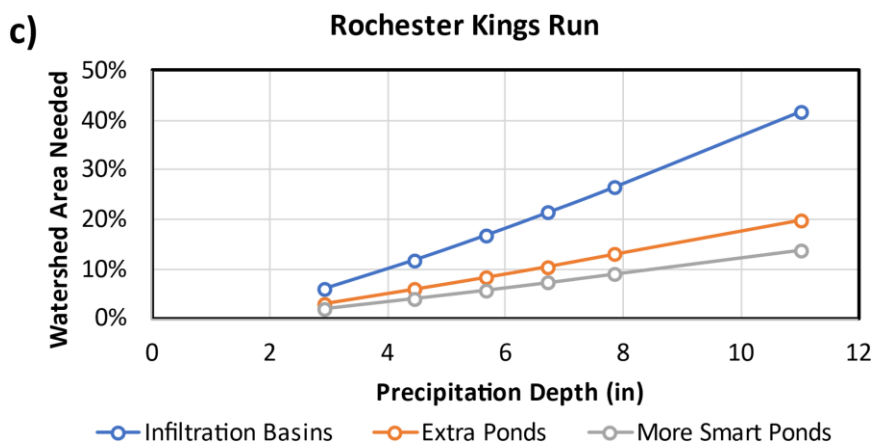
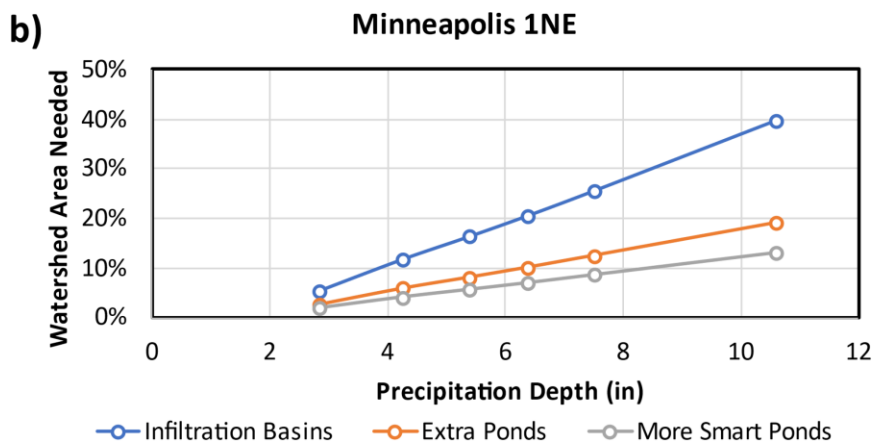
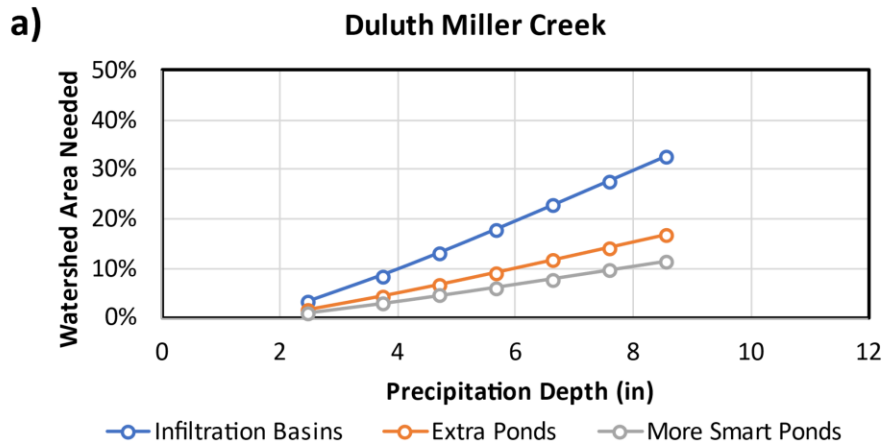


Figure 31: Ratio of Wet Pond Area to Catchment Area for the Miller Creek sub-watershed in Duluth (a), the 1NE sub-watershed in Minneapolis (b), and the Kings Run sub-watershed in Rochester (c), for Atlas 14 storms including 2-yr, 10-yr, 25-yr, 50-yr, and 100-year. Note: x-axis logarithmic scale.

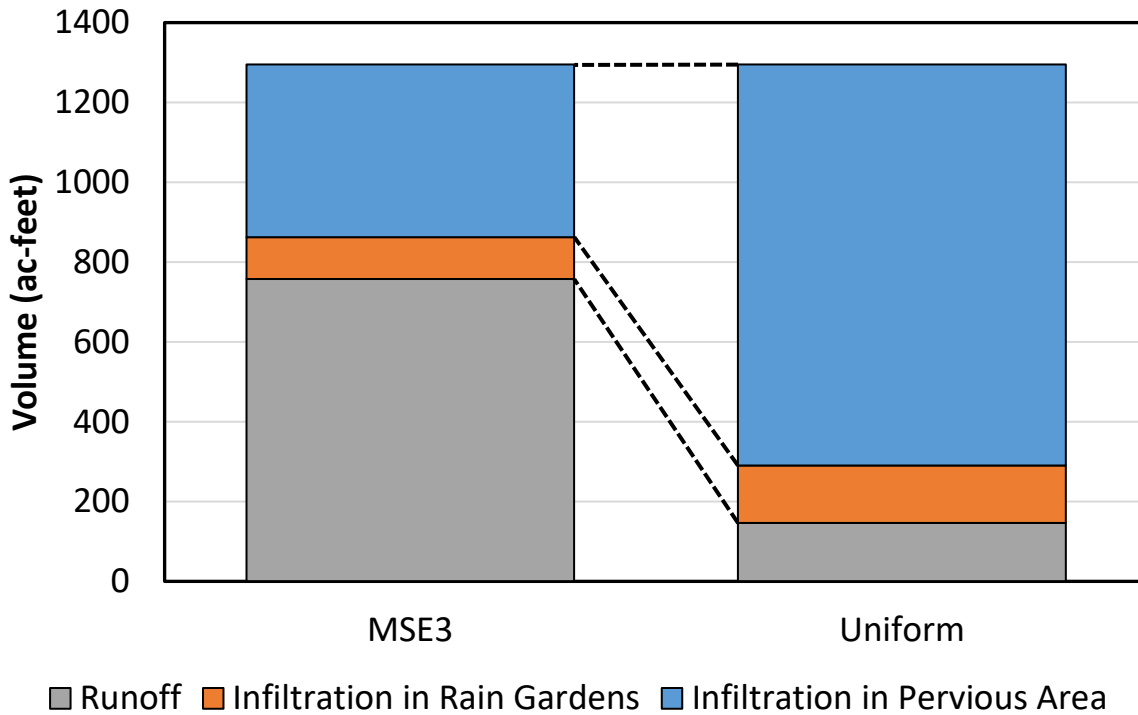


Figure 32: Influence of rainfall distribution over 24 hours on water balance in the 1NE Minneapolis watershed for the 100-year storm.

2.7 Discussion

2.7.1 Miller Creek, Duluth

Our adaptation strategies addressed treatment of connected impervious surfaces. In the Miller Creek watershed, much of the drainage network includes pervious ditches. For increasing storm size, impervious areas with ditch drainage become more connected. In addition, pervious areas contribute significant runoff during large storms, due to the limited infiltration capacity of the soil. For example, for an Atlas-14, 100-year design storm (6.3 inches), approximately 47% of the total runoff volume is from pervious surfaces. The results given in this report suggest that designing stormwater BMPs to treat 1” of runoff from connected impervious surfaces (typical rain garden design) or the 2-year storm (typical NURP pond design) will not be sufficient to offset future increases in storm depths and that more aggressive adaptation strategies will be needed.

The location of additional stormwater BMPs is also an important consideration. The existing Baseline condition of stormwater ponds treating ~50% of the connected impervious area is not enough to address the increasing rainfall amount associated with climate change. Pipe Upsizing can reduce flood depth and duration upstream in the watershed but will exacerbate flooding downstream, both within and beyond the watershed. In addition, placement of treatment practices upstream of flood-prone areas or places in which flooding should be minimized (e.g., major highways) is the best approach to minimizing flooding at critical locations. For the Miller Creek sub-watershed, the order of best to worst

strategies for reducing node depth, flood duration, and peak flow is: 1) More Smart Ponds, 2) Extra Ponds, 3) Smart Ponds, 4) Infiltration Basins, 5) Baseline, and 6) Pipe Upsizing.

2.7.2 1NE, Minneapolis

The Minneapolis 1NE sub-watershed is a fully built sub-watershed with few ponds, a large golf course (~9% of the watershed), and challenging locations that are prone to flooding. Because Minneapolis is fully developed, it can be difficult to find areas to build new stormwater management and flood control structures. If flood prone areas are upstream in the watershed, there is less opportunity to mitigate flooding with upstream practices. This is made more challenging with the limited available land for implementation, potentially high land costs, and underground utilities and obstacles. Minneapolis has been redeveloped for 150+ years, which has led to a legacy of uncertain soil conditions, buried debris, and other factors that force stormwater managers to carefully consider how and where they implement infiltration practices.

Similar to Miller Creek in Duluth, the order of best to worst strategies for reducing node depth, flood duration, and peak flow in the Minneapolis 1NE sub-watershed is: 1) More Smart Ponds, 2) Extra Ponds, 3) Infiltration Basins, 4) Smart Ponds, 5) Baseline, and 6) Pipe Upsizing. The results of our analysis are a good relative comparison, but may not be accurate predictions of flood elevations, durations, or peak flows. For example, one node in a residential area of Minneapolis is predicted to have up to seven feet of flooding depth for the 100-year event (Atlas 14, 7.5 inches), though this depth of flooding has not been observed in this area of Minneapolis to the authors' knowledge. According to state precipitation records (Minnesota State Climatology Office 2023), at least two events of approximately this depth or more have been recorded in Minneapolis (Aug 30, 1977 = 7.28 inches; Jul 23, 1987 = 9.15 inches). This suggests that the EPA-SWMM models have not been adequately calibrated and tested for large rainfall events. As reconstruction for new practices is complete and more monitoring data is acquired, the SWMM models can be updated and calibrated to real data to ensure accurate predictions of response to storm events.

2.7.3 Kings Run, Rochester

Like Duluth and Minneapolis, the order of best to worst strategies for reducing node depth, flood duration, and peak flow for the Rochester Kings Run watershed is: 1) More Smart Ponds, 2) Extra Ponds, 3) Smart Ponds, 4) Infiltration Basins, 5) Baseline, and 6) Pipe Upsizing. A difference observed in the Kings Run sub-watershed is the outlet hydrograph, which did not peak as sharply as Duluth or Minneapolis. This is partly due to the number of existing ponds within Kings Run but also due to the increased size and amount of pervious area compared to Minneapolis. Pipe Upsizing increased the peak flow rate from the outlet much less in Kings Run (+6%) compared to Duluth (+30%) and Minneapolis (+50%).

Rochester, like Duluth, has the most potential for future development. Minneapolis is fully developed, but large portions of the Kings Run and Miller Creek watersheds are undeveloped. It will be important to

consider potential climate change adaptation strategies as these areas develop because current design standards are not adequate to prevent or limit flooding from potential events.

Chapter 3. Cost of Adaptation

3.1 Introduction

This section is an analysis of the cost of possible strategies for adapting stormwater infrastructure to manage potential future storms. Section 3 describes the SWMM modeling of three sub-watersheds: Miller Creek watershed in Duluth and Hermantown, MN, the 1NE watershed at the border between Minneapolis and Columbia Heights, MN, and the Kings Run Watershed in the northwestern portion of Rochester, MN. The potential infrastructure adaptations modeled in Section 3 include the Baseline (existing conditions), adding rain gardens (aka Infiltration Basins), adding new wet ponds, retrofitting existing stormwater ponds to be “smart” ponds, adding new “smart” ponds, and upsizing of stormwater pipes to convey more water. In addition to the adaptation strategies described in Section 3, Underground Storage was also included in the cost analysis described in this section. Freely available cost tools were used to estimate the cost of adaptation strategies, which were converted to 2022 dollars, and then combined with performance data to determine cost effectiveness. Performance data of the adaptation strategies included the reduction in flood depth, peak flow, and flood duration.

3.2 Calculating Costs

For accessibility and transparency, the publicly available Community-enabled Lifecycle Analysis of Stormwater Infrastructure Costs (CLASIC, Colorado State University, 2021) tool was used whenever possible to estimate life-cycle costs for the infrastructure adaptation strategies proposed by this project. CLASIC is based upon historical costs for stormwater practices up to 2018, including data from the Urban Stormwater BMP Database. CLASIC, however, did not have cost estimates for all infrastructure strategies. Thus, other estimation tools were necessary to complete the life-cycle cost analysis. It is important to note that none of the cost estimation tools incorporate land costs as part of the life-cycle costs. Land costs are site-specific and change quickly with the economy such that values would become outdated between the time of writing and publication. It is important, however, for decision makers to consider land costs because it could substantially affect total costs. The assumptions for the life-cycle costs estimates are described in the sections below.

3.2.1 Cost Assumptions – CLASIC

CLASIC was used to estimate costs for adding Infiltration Basins to simulate all infiltration practices (hereafter called the Infiltration Basins scenario) and adding new wet ponds (Extra Ponds scenario). To simulate the SWMM modeling performed in Section 3, the watersheds were delineated in CLASIC, and the watershed properties were used as inputs into CLASIC. The number of infiltration basins or wet ponds recommended by CLASIC (based on watershed area, impervious surfaces, and design storm) was compared to the number of infiltration basins or wet ponds modeled in SWMM. If needed, small changes to input parameters in CLASIC were made to match the number of infiltration basins or wet ponds between CLASIC and SWMM. Then the 20-year life-cycle costs for construction, operation, and

maintenance were predicted by CLASIC. Note that CLASIC assumes an Annual Discount Rate of 4%, which was used for all calculations.

Infiltration basins were assumed to have a surface area of 10,000 ft², a ponding depth of 12 inches, and a total media depth of 24 inches. CLASIC allows for infiltration basin surface areas to be 100 ft², 1,000 ft², and 10,000 ft². The project team decided that a standard infiltration basin size of 10,000 ft² would represent the combination of large and medium rain gardens, infiltration basins, and swales that could be installed to address climate change impacts in the watersheds. CLASIC differentiates between the type of vegetation planted in rain gardens and infiltration practices. For the reported cost estimates, we used grasses rather than flowering plants and seeded installation rather than sod or plug installation as this is the most cost-effective combination. CLASIC also offers multiple optional design parameters for rain gardens. An impermeable liner, irrigation system, trees, and routine mowing were all excluded in the cost estimate. In Duluth, infiltration basins were modeled with underdrains in CLASIC and SWMM because of the prevalence of soils unsuitable to standard infiltration practices. When the costs were estimated in CLASIC, the additional cost for underdrains was included in the Duluth estimates. CLASIC adjusts cost based on geographic location and proximity to urban areas. As such, the 20-year life-cycle costs for construction, operation, and maintenance per infiltration basin in Minneapolis, Rochester, and Duluth are provided in Table 6.

Table 6: Unit life-cycle costs for 10,000 ft² infiltration basins as predicted by CLASIC. Costs for 2018 were updated to 2022 using the consumer price index. Note: Land costs excluded.

Location	Construction Cost	Operation and Maintenance Cost (20-years)	Total Life-cycle Cost (20-years)
Minneapolis	\$421,674	\$60,368	\$482,042
Rochester	\$439,243	\$62,882	\$502,125
Duluth	\$427,727	\$69,678	\$542,405

The ‘medium’ size wet pond in CLASIC was assumed to be the standard size for this cost analysis. Medium wet ponds have a 5-foot-deep permanent pool with 91,000 ft³ permanent pool volume and a permanent pool surface area of 20,000 ft². The temporary pool (above the permanent pool) is 4 feet deep with a volume of 100,000 ft³ and a surface area of 30,500 ft². A 300 ft² forebay was included for each pond to account for pretreatment BMP costs. The 20-year life-cycle costs for construction, operation, and maintenance per medium wet pond in Minneapolis, Rochester, and Duluth are provided in Table 7.

Table 7: Unit life-cycle cost for medium wet ponds as predicted by CLASIC. Costs for 2018 were updated to 2022 using the consumer price index. Note: Land costs excluded.

Location	Construction Cost	Operation and Maintenance Cost (20-years)	Total Life-cycle Cost (20-years)
Minneapolis	\$139,911	\$118,154	\$258,065
Rochester	\$145,740	\$123,074	\$268,814
Duluth	\$145,740	\$123,074	\$268,814

When aboveground solutions are not feasible or possible, then underground solutions must be considered. CLASIC provides estimated costs for Underground Storage for structures of default nominal dimensions: 200 ft length and 10 ft height (small), 20 ft height (medium), and 30 ft height (large). A width is not specified, and the ‘height’ is not otherwise defined. It was assumed that the ‘height’ is the diameter of a circular storage structure, which corresponds well with the estimated storage volume provided by CLASIC. In general, the cost for Underground Storage is approximately \$311 per ft³ in Minneapolis, and \$324 per ft³ in Rochester and Duluth.

3.2.2 Cost Assumptions – Smart Ponds

CLASIC does not have cost estimate for Smart Ponds because the technology is relatively new and cost data is limited. Therefore, the project team obtained cost estimate data from a private company with 8 years of experience designing, installing, and servicing smart water management technology (Personal Communication, 2022). Estimates from other companies or for alternative installation methods such as Do-It-Yourself (DIY) and/or open-source technology were not obtained. The cost estimates obtained for this project represent the costs incurred by many municipal, public, and private entities that have installed Smart Pond systems, including several in Minnesota.

The unit cost breakdown for Smart Ponds is provided in Table 8 below. The private company provided a range of values for each category (e.g., professional services, equipment, permitting, etc.), which reflects the variability in site conditions, accessibility, cost of local services, and other factors. The average value for each range was used in the life-cycle cost analysis for Smart Ponds.

Table 8: Unit life-cycle cost (2022 \$) for upgrading existing wet ponds with ‘smart’ technology. Note: Land costs excluded.

	Single Site		Subsequent Sites	
	Range	Average	Range	Average
Professional Services	\$45,000 - \$65,000	\$55,000	\$25,000 - \$35,000	\$30,000
Equipment	\$30,000 - \$45,000	\$37,500	\$30,000 - \$45,000	\$37,500
Permitting	\$20,000 - \$75,000	\$47,500	\$20,000 - \$75,000	\$47,500
Installation	\$25,000 - \$50,000	\$37,500	\$25,000 - \$50,000	\$37,500
Total Construction		\$177,500		\$152,500
Subscription Services	\$25,000/yr	\$25,000/yr	\$5,000 - \$6,500/yr	\$5,750
Operation and Maintenance	\$2,500 - \$7,500/yr	\$5,000/yr	\$2,500 - \$7,500/yr	\$5,000
Total Recurring Cost*		\$424,018		\$151,940
Total 20-year Cost		\$601,518		\$304,440

*NOTE: Recurring costs calculated assuming 20-year life cycle and 4% discount rate.

3.2.3 Cost Assumptions – More Smart Ponds

In order to estimate the costs for an adaptation scenario where existing new Smart Ponds were constructed in addition to existing ponds being retrofit into Smart Ponds, a combination of methods from Sections 4.2.1 (wet ponds) and 4.2.2 (Smart Ponds) were used. The cost for Smart Pond adaptations and new pond adaptations within each watershed were summed and converting the extra ponds to Smart Ponds was calculated at the “Subsequent Site” rate from Section 4.2.2.

3.2.4 Cost Assumptions – Pipe Upsizing

Cost estimates for Pipe Upsizing was not available in CLASIC, so estimates were obtained through personal communication with the City of Minneapolis (2016), as given in Eq (1).

$$\text{Cost of Pipe Upsizing (2016 \$)} = (12.4D + 1100) \times L \quad (1)$$

where:

D = pipe diameter (inches) & $12'' < D < 144''$ for standard pipe diameters of 12, 15, 18, 24, 30, 36, 42, 48, 54, 60, 72, 84, 96, 108, 120, 132, 144

L = pipe length (feet)

3.2.5 Comparing CLASIC to other cost models

CLASIC is not the only life-cycle cost analysis tool available. Two other cost tools were evaluated as part of this analysis: Weiss et al. (2005, 2007) and the Integrated Decision Support Tool (iDST) (Grubert and Krieger 2020). Weiss et al. (2005, 2007) developed 20-year life-cycle cost equations for dry extended detention basins, wet basins, sand filters, constructed wetlands, bioretention filters, and infiltration trenches, including construction, operation, and maintenance as well as 67% confidence intervals to

illustrate the variability in cost data (2005 \$). CLASIC is based upon similar data as Weiss, et al., but with more recent information. Grubert and Krieger (2020) developed the iDST tool, which is a self-described “bottom-up, process and inventory-based approach to estimating financial and monetized environmental costs for distributed stormwater control measures (SCMs).” The iDST tool includes 50-year life-cycle cost estimates including design and planning, construction, operations and maintenance, and end of life costs for porous pavement, green roof, constructed wetland, bioretention, rain barrel, buffer strip, infiltration trench, vegetated swale, dry pond, wet pond, perforated pipe, cistern, above-ground storage tank, underground detention structure, underground retention structure, underground gravel bed, and a user-defined SCM. The iDST tool, however, is based upon traditional building construction practices, and not based upon stormwater practice data. Results from CLASIC, Weiss et al. (2005, 2007), and iDST are compared in the remainder of this section.

The total present cost (2022 \$) for a bioretention practice as estimated by CLASIC, iDST, and Weiss et al. (2005, 2007) are shown in Figure . For the full range of water quality volume (WQV), the costs predicted by iDST are greater than the costs predicted by CLASIC and Weiss et al. (2005, 2007). In fact, the low range of iDST is greater than the high range for Weiss et al. (2005, 2007) for nearly all WQV. The estimates from CLASIC are approximately equal to the low predictions of iDST. At a WQV of 75,000 gal (10026 ft³ = 0.23 ac-ft), the average iDST cost is ~50% more than CLASIC and more than double the estimate from Weiss et al. (2005, 2007). At 200,000 gal (26,736 ft³ = 0.61 ac-ft), the iDST cost prediction is approximately three times larger than the average from Weiss et al. (2005, 2007). For bioretention, the iDST predicts much greater costs than CLASIC and Weiss et al. (2005, 2007). The cost estimated by CLASIC is approximately equal to the high range predicted by Weiss et al. (2005, 2007).

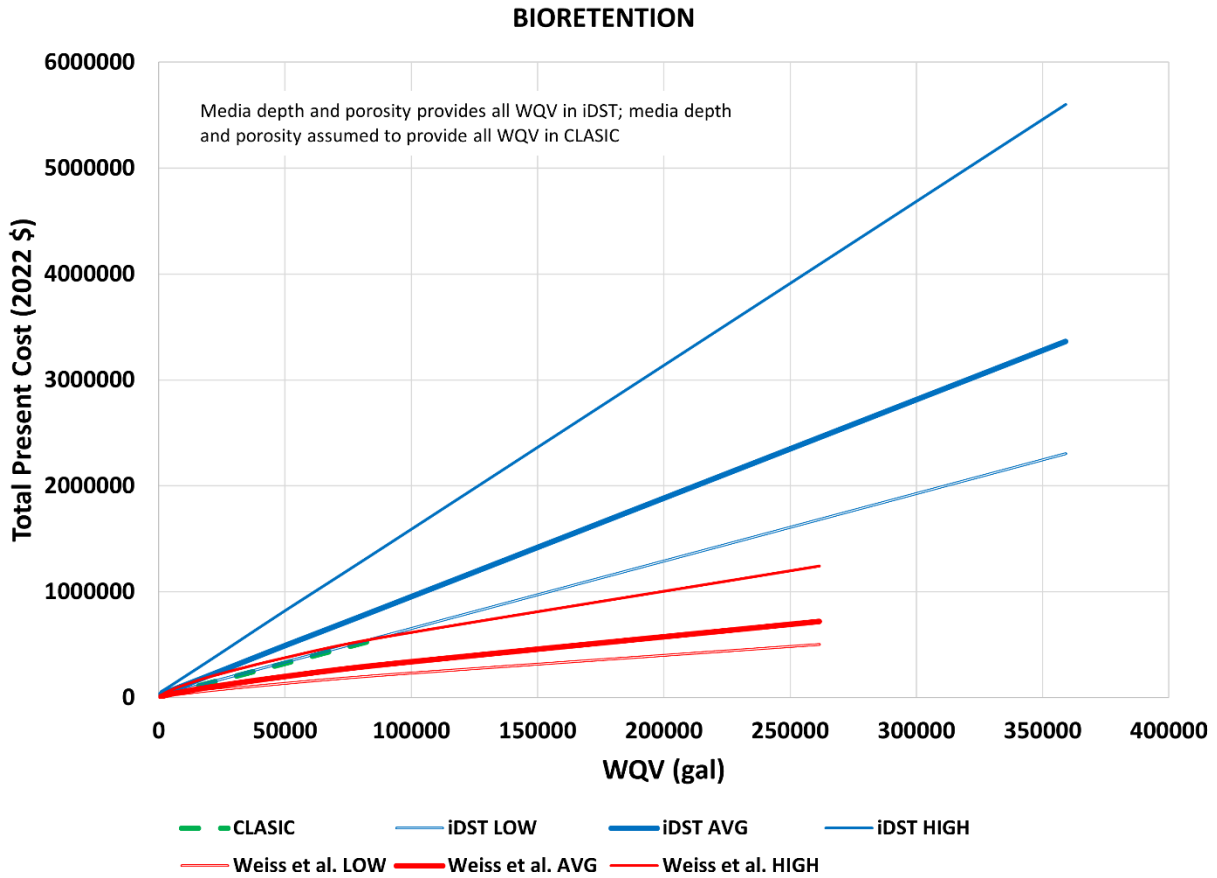


Figure 33: 50-year life-cycle cost for a bioretention (aka Infiltration Basins) as predicted by CLASIC, iDST, and Weiss et al. (2005, 2007). WQV = Water Quality Volume.

The total present cost (2022 \$) for a wet pond practice as estimated by CLASIC, iDST, and Weiss et al. (2005, 2007) are shown in Figure 34. For the full range of water quality volume (WQV), the costs predicted by CLASIC are less than the low costs predicted by iDST and Weiss et al. (2005, 2007). Except for very low WQV, the average iDST cost prediction is approximately equal to the high prediction from Weiss et al. (2005, 2007). The average cost prediction from Weiss et al. (2005, 2007) is approximately equal to the low estimate from iDST. The cost predictions from CLASIC are approximately equal to the low range predicted by Weiss et al. (2005, 2007). For wet ponds, the iDST predicts costs equivalent to the high range of Weiss et al. (2005, 2007) and higher than CLASIC, while CLASIC predicts costs equivalent to the low range of Weiss et al. (2005, 2007).

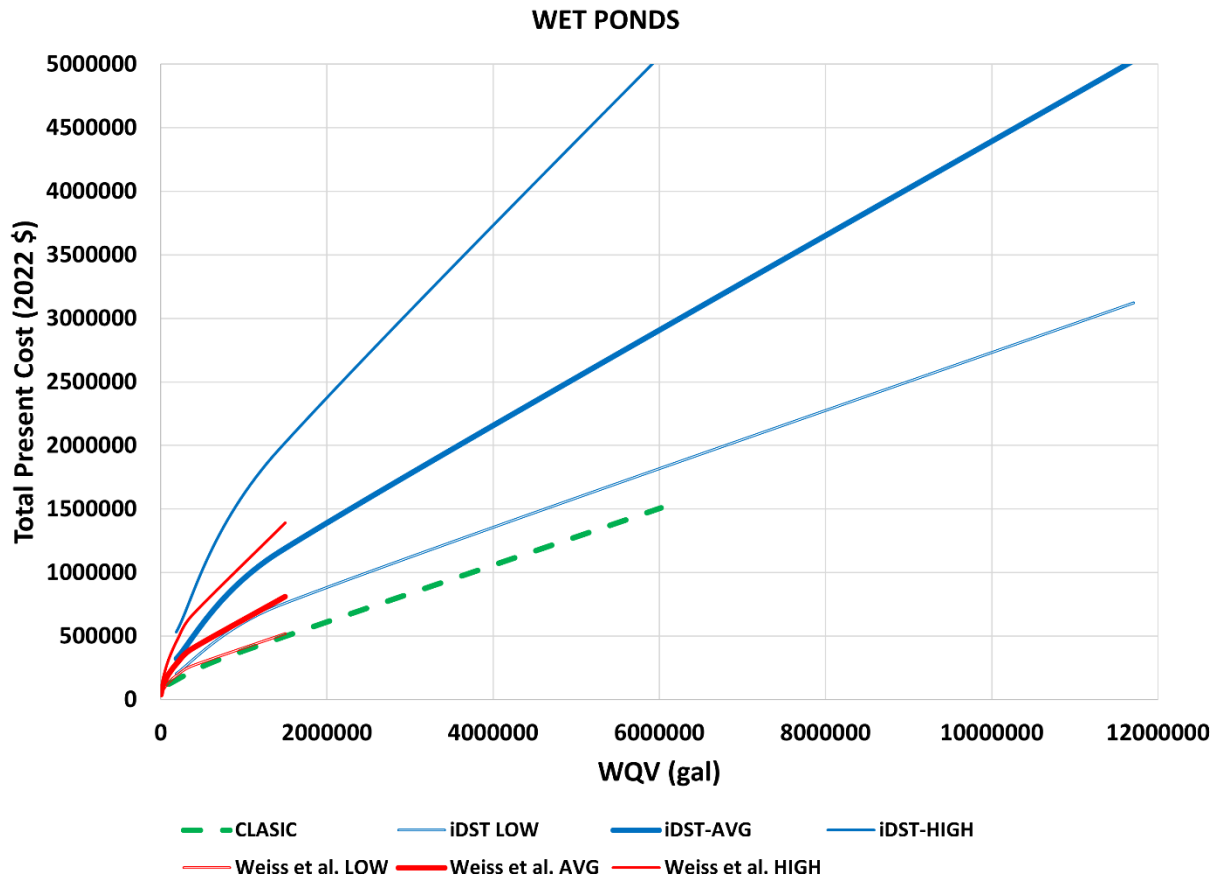


Figure 34: 50-year life-cycle cost for a wet pond as predicted by CLASIC, iDST, and Weiss et al. (2005, 2007). WQV = Water Quality Volume.

For both bioretention and wet ponds, the iDST tool predicts higher costs than both CLASIC and Weiss et al. (2005, 2007). For bioretention, the CLASIC tool predicts lower costs than the iDST tool and higher costs than the Weiss et al. (2005, 2007) tool. For wet ponds, CLASIC predicts lower costs than both iDST and Weiss et al. (2005, 2007), though CLASIC’s prediction is approximately equal to the low costs predicted by Weiss et al. (2005, 2007). Cost estimates vary substantially based on several factors not often included in cost prediction models (proximity to construction resources such as materials and equipment, complexity of site conditions, etc.), so it can be challenging to select and rely on a single tool for cost predictions. For this analysis, CLASIC was chosen for the following reasons:

- 1) CLASIC cost estimates were consistent with other cost estimate tools. iDST’s costs were consistently greater than other tools. Weiss et al. (2005, 2007)’s costs were consistent with CLASIC.
- 2) CLASIC is based on recent cost data. The iDST tool was published in 2020 but does not describe the data upon which it was based. Weiss et al. (2005, 2007) is based on data up to ~2004, and thus does not incorporate the most recent cost data.
- 3) CLASIC has a built-in user interface. The iDST is a spreadsheet tool and Weiss et al. (2005, 2007) are cost equations provided in the report and journal article. The Weiss, et al. equations must be entered into a software package such as a spreadsheet or programming script to predict costs.

3.3 Cost Effectiveness Analysis

3.3.1 Total Cost of Stormwater Infrastructure Adaptation Strategies

The Baseline condition for the three watersheds includes the existing stormwater management infrastructure, primarily consisting of wet ponds, some infiltration practices, swales, pipes, and other conveyance structures (see Section 3). The expected operation and maintenance cost of the existing infrastructure (i.e., Baseline conditions) was also estimated because it is assumed that the ‘status quo’ (aka Baseline) option would require maintenance of the existing infrastructure. To compare the cost effectiveness of the climate changes adaptation strategies, the 20-year life-cycle cost (excluding land costs) for each strategy was estimated using the tools and assumptions described above and then presented alongside the performance for each strategy and watershed.

A summary of the total cost of infrastructure adaptation is provided in Table 9, including the number of units added for each adaptation strategy (e.g., 171 new Infiltration Basins added in Minneapolis). A Baseline option of operation and maintenance of the existing stormwater management infrastructure was calculated using operation and maintenance costs for wet ponds (see Figure 34) and the number of existing wet ponds for each watershed. When comparing adaptation strategies, more infiltration basins are required than wet ponds because infiltration basins are smaller than wet ponds and provide less volume storage. This is reflected in the number of practices proposed by the SWMM modeling in Section 3 when comparing these two strategies (e.g., 171 new Infiltration Basins vs. 74 Extra Ponds for Minneapolis). In addition, the number of existing stormwater ponds, which is reflected in the number of Smart Ponds added (e.g., 16 for Minneapolis), is different than the number of Extra Ponds necessary to treat the current untreated impervious surface (e.g., 16 existing ponds vs. 74 Extra Ponds for Minneapolis). It is important to note the differing number of units for different strategies and watersheds because the total cost is based on the unit cost and total number of units (e.g., Infiltration Basins). For Pipe Upsizing, there were various sizes (1 ft to 15+ ft diameter) and lengths (2 ft to 2700+ ft) of pipes that were upsized. For Underground Storage, the storage volume used to determine the number of Extra Ponds was also used to determine the amount of Underground Storage.

Table 9: Summary of infrastructure adaptation strategies and total 20-year life-cycle cost of each strategy. Note: Land costs excluded.

Strategy	Duluth (Miller Creek)		Minneapolis (1NE)		Rochester (Kings Run)	
	Number Added	Total Cost (\$ Million)	Number Added	Total Cost (\$ Million)	Number Added	Total Cost (\$ Million)
Baseline	(O&M)	\$7.6 M	(O&M)	\$1.9 M	(O&M)	\$5.8 M
Smart Ponds	62	\$19.2 M	16	\$5.2 M	47	\$14.6 M
Extra Ponds	145	\$40.0 M	74	\$19.6 M	180	\$49.7 M
More Smart Ponds	62 Retrofit + 145 New	\$104 M	16 Retrofit + 74 New	\$47.7 M	47 Retrofit + 180 New	\$120 M
Infiltration Basins	241	\$152.4 M	171	\$96.1 M	127	\$74.3 M
Pipe Upsizing	(various)	\$53.9 M	(various)	\$256.6 M	(various)	\$71.1 M
Underground Storage	(various)	\$5,468 M	(various)	\$2,679 M	(various)	\$6,788 M

Overall, the order of adaptation strategies for all watersheds from least expensive total cost (excluding land costs) to most expensive was 1) retrofitting existing ponds into Smart Ponds, 2) adding Extra Ponds, 3) retrofitting existing ponds into Smart Ponds AND adding More Smart Ponds, 4) adding new rain gardens or Infiltration Basins, 5) Upsizing existing stormwater conveyance Pipes, and 6) installing Underground Storage units instead of aboveground options. There are fewer existing ponds (16 – 62) than Extra Ponds (74 – 180), which explains why the Smart Ponds are less expensive than building Extra Ponds and More Smart Ponds strategies. The unit costs for Infiltration Basins (\$482k – \$542k) and the larger number of infiltration basins (127 – 241) compared to wet ponds (\$258k - \$269k and 74 – 180) explains the substantial cost increase for the Infiltration Basin adaptation strategy. The cost for Pipe Upsizing can be substantial based on Eq (1) above, which equates to approximately \$1550 per linear foot for a 3-foot diameter pipe (average pipe size for Minneapolis) and \$2440 per linear foot for a 9-foot diameter pipe (average pipe size for Duluth). The total length of pipes that were upsized ranged from 16,400 ft in Duluth to over 134,000 ft in Minneapolis, which explains the range of total cost for Pipe Upsizing (\$54 M – \$257 M). The cost of Underground Storage is \$311-\$324 per ft³ and the storage requirements in Minneapolis, Rochester and Duluth range from 7.4 – 18 million ft³, which explains the substantial cost of storing stormwater underground.

3.3.2 Flood Mitigation Effectiveness

To determine cost effectiveness of the adaptation strategies, the total cost must be combined with one or more performance metrics. For this report, quantifying effectiveness of climate change adaptation strategies consisted of 1) flood depth for important locations and 2) peak outflow from the sub-watershed. Reduction of or increase in flood depth at important locations within the watershed will reflect the ability of an adaptation strategy to minimize flooding from extreme events within the watershed. Reduction (or increase) in peak outflow reflects the impact that an adaptation strategy will

have on downstream watersheds and water bodies. For example, the purpose of Pipe Upsizing is to increase the conveyance of flow from the watershed for discharge out of the watershed, and thus the flood depth within the watershed may decrease but the outflow from the watershed will likely increase. Thus, both flood depth and peak outflow are important metrics for determining effectiveness of an adaptation strategy.

Four SWMM nodes (typically storm sewer manhole structures) were selected from each SWMM model that represented important locations for flooding within each sub-watershed. These nodes were selected because they were either points of recurring historical flooding or near important civil infrastructure (e.g., large commercial shopping centers, interstate highways, etc.). The flood depth at each node was determined using for the existing conditions and for each adaptation strategy for the TP-40, Atlas-14, 2069-50th, 2069-75th, and 2069-90th predicted storms and 2-Yr, 10-Yr, 25-Yr, 50-Yr, 100-Yr, and 500-Yr return periods. The difference between the existing condition and the adaptation strategy represents the improvement (or detriment) caused by the adaptation strategy. For each strategy, the flood depth improvement was averaged for all storms and return periods and listed in Table 10.

Table 10: Average flood depth (ft) improvement (negative values) or detriment (positive values) for Minneapolis, Rochester, and Duluth sub-watersheds for TP-40, Atlas-14, 2069-50th, 2069-75th, and 2069-90th predicted storms and 2-Yr, 10-Yr, 25-Yr, 50-Yr, 100-Yr, and 500-Yr return period, compared to the Baseline.

<i>Duluth (ft)</i>				
	Temp8	J21	J23	J14
More Smart Ponds	-0.65	-1.32	-0.66	-1.27
Extra Ponds	-0.32	-0.85	-0.37	-0.79
Smart Ponds	-0.09	-0.11	-0.05	-0.09
Infiltration Basins	-0.03	-0.11	-0.01	-0.09
Pipe Upsizing	+0.16	-0.73	+0.12	-1.11
<i>Minneapolis (ft)</i>				
	MH420743	SA35C350	SS512682	SA999039
More Smart Ponds	-4.83	-2.13	-2.52	-2.12
Extra Ponds	-4.29	-1.05	-1.97	-2.00
Pipe Upsizing	-0.78	-0.55	-0.11	-0.19
Infiltration Basins	-0.29	-0.46	-0.19	-0.02
Smart Ponds	-0.01	-0.02	-0.02	0
<i>Rochester (ft)</i>				
	SP105	SP64	RN176248	SP113
More Smart Ponds	-1.60	-1.98	-2.17	-1.34
Extra Ponds	-0.93	-1.48	-1.38	-0.73
Infiltration Basins	-0.11	-0.18	-0.12	-0.04
Smart Ponds	-0.14	-0.01	-0.08	-0.13
Pipe Upsizing	+0.24	-0.85	-0.33	+0.16

Considering the average change in flood depth compared to the Baseline for all storms, the order of adaptation strategies from best (1 = largest flood depth reduction) to worst (5 = least flood depth reduction) are 1) More Smart ponds, 2) Extra Ponds, 3) Pipe Upsizing, 4) Infiltration Basins, and 5) Smart Ponds in Minneapolis. In Rochester and Duluth, 1) and 2) were the same as Minneapolis, but Pipe Upsizing was 5) because it caused an increase (+) in flood depth for two of the four nodes. The peak flow at the outlet for the Minneapolis, Rochester, and Duluth watersheds is the other metric used to quantify performance of the adaptation strategies for mitigating impacts from climate change. Similar to the assessment of flood depth, the Baseline peak outflow for existing conditions for the TP-40, Atlas-14, 2069-50th, 2069-75th, and 2069-90th predicted storms and 2-Yr, 10-Yr, 25-Yr, 50-Yr, 100-Yr, and 500-Yr return periods and then compared to the peak outflow for each of the adaptation strategies. For each strategy, the difference in peak flow was averaged for all storms and return periods and listed in Table 11.

Table 11: Average peak outflow (cfs) improvement (negative values) or detriment (positive values) for Minneapolis, Rochester, and Duluth sub-watersheds.

	<i>Duluth</i>			<i>Minneapolis</i>		<i>Rochester</i>
	main25	main65	main68	OF441017	OF441270	Outlet
More Smart Ponds	-184	-391	-381	-122.9	-20.3	-752
Extra Ponds	-139	-284	-262	-96.3	-19.2	-443
Infiltration Basins	-15	-37	-28	-1.1	-0.2	-34
Smart Ponds	-12	-18	-13	+3.0	+0.5	-86
Pipe Upsizing	+98	+173	+324	+337.4	+13.1	+146

The order of best (1 = largest reduction in peak flow) to worst (5 = least reduction in peak flow) adaptation strategies are 1) More Smart Ponds, 2) Extra Ponds, 3) Smart Ponds, 4) Infiltration Basins, and 5) Pipe Upsizing for all storms. The More Smart Ponds strategy increases the number of stormwater ponds within the watershed and converts all ponds into Smart Ponds, which provides substantial additional storage to mitigate the impacts of these storm events. As a result, the flood depth and peak outflow are decreased the most by More Smart Ponds compared to all other adaptation strategies. Extra Ponds will be NURP-sized ponds to treat any untreated connected impervious, which provides storage to handle large storm events and results in reduced flood depth and peak outflow. The Smart Ponds and Infiltration Basin strategies provided minimal benefit in flood depth and peak flow. In contrast, Pipe Upsizing increases conveyance in the watershed towards the outlet, resulting in a substantial increase in peak outflow at the outlet from the watershed. Thus, More Smart Ponds will reduce the potential for flooding in downstream watersheds while Pipe Upsizing will exacerbate downstream flooding.

3.3.3 Cost & Effectiveness

Table 12 shows the average change in flood depth and peak flow with the total cost for each adaptation strategies in Minneapolis, Rochester, and Duluth. First, the Baseline case is performing operation and maintenance on the existing infrastructure, which provides no benefit to flood depth or peak flow but

costs \$2 – \$8 million for these three sub-watersheds. It is important to note that the Underground Storage option is assumed to perform identical to the Extra Ponds scenario for both flood depth and peak flow benefit because the storage characteristics are identical.

Table 12: Average change in flood depth and peak flow with total cost for adaptation strategies in Minneapolis, Rochester, and Duluth. Note: Land costs excluded.

<i>Duluth Miller Creek</i>			
#Rank. Strategy	Δ Depth (ft)	Δ Peak Flow (cfs)	Total Cost (\$)
0. Baseline (O&M existing)	0	0	\$8 M
1. More Smart Ponds	-0.98	-319	\$115 M
2. Extra Ponds	-0.58	-228	\$45 M
2. Underground Storage	-0.58	-228	\$6,185 M
3. Infiltration Basins	-0.08	-27	\$152 M
4. Smart Ponds	-0.06	-14	\$19 M
5. Pipe Upsizing	-0.39	+199	\$54 M
<i>Minneapolis 1NE</i>			
#Rank. Strategy	Δ Depth (ft)	Δ Peak Flow (cfs)	Total Cost (\$)
0. Baseline (O&M existing)	0	0	\$2 M
1. More Smart Ponds	-2.90	-72	\$48 M
2. Extra Ponds	-2.33	-58	\$20 M
2. Underground Storage	-2.33	-58	\$2,679 M
3. Infiltration Basins	-0.41	-1	\$96 M
4. Smart Ponds	-0.24	+2	\$5 M
5. Pipe Upsizing	-0.01	+175	\$257 M
<i>Rochester Kings Run</i>			
#Rank. Strategy	Δ Depth (ft)	Δ Peak Flow (cfs)	Total Cost (\$)
0. Baseline (O&M existing)	0	0	\$6 M
1. More Smart Ponds	-1.77	-752	\$120 M
2. Extra Ponds	-1.13	-443	\$50 M
2. Underground Storage	-1.13	-443	\$6,788 M
3. Infiltration Basins	-0.11	-34	\$74 M
4. Smart Ponds	-0.09	-86	\$15 M
5. Pipe Upsizing	-0.20	+146	\$71 M

Overall, Smart Ponds are the least expensive strategy but also provided the second least benefit, and thus is inexpensive and ineffective. The next least expensive strategy was Extra Ponds, which was the second most beneficial for depth and peak flow. This represents a cost-effective strategy because it is relatively low cost but relatively high benefit. More Smart Ponds were the next more expensive option and the most beneficial for mitigation flooding impacts. The costs, however, were more than twice the cost of Extra Ponds but provided less than twice the benefit for flood depth and peak flow reduction. Thus, More Smart Ponds are less cost effective than Extra Ponds. Underground storage is assumed to perform identical to Extra Ponds, but the costs are over 100 times more expensive than Extra Ponds, which reflects the cost associated with building large Underground Storage vaults for stormwater. After

More Smart Ponds, the next more expensive strategy was Infiltration Basins, which provided minimal benefit in flood depth and peak flow reduction. In this analysis, Infiltration Basins were expensive and ineffective. Pipe upsizing was more expensive than Infiltration Basins in Minneapolis but less expensive than Infiltration Basins in Rochester and Duluth but was the least effective at reducing flood depth and peak flow.

Another way to compare the benefits to flood depth and the cost of implementation for the adaptation strategies is shown in Figure 35. A cost-effective strategy provides a large negative change in flood depth (Δ Depth (ft)) at a relatively low total cost, which is the lower left portion of Figure 35. For all three watersheds, More Smart Ponds and Extra Ponds provided the most benefit for flood depth reduction. More Smart Ponds cost more than twice the cost of Extra Ponds but did not provide twice the reduction in flood depth. Thus, it could be argued that Extra Ponds are more cost effective than More Smart Ponds. A similar analysis of cost-effectiveness can be made based on peak flow, as shown in Figure 36. Again, More Smart Ponds and Extra Ponds provide the most benefit while Extra Ponds cost less than More Smart Ponds.

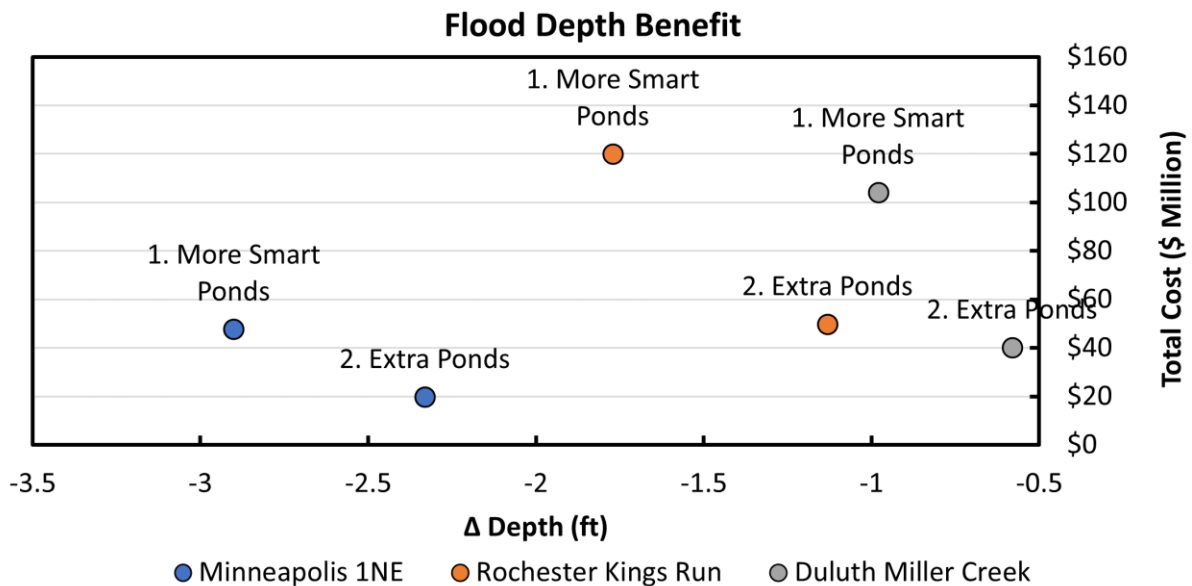


Figure 35: Total cost of adaptation strategies compared to change in flood depth (Δ Depth (ft)) for strategies that provide at least 0.5 ft of flood depth reduction. Note: Land costs excluded.

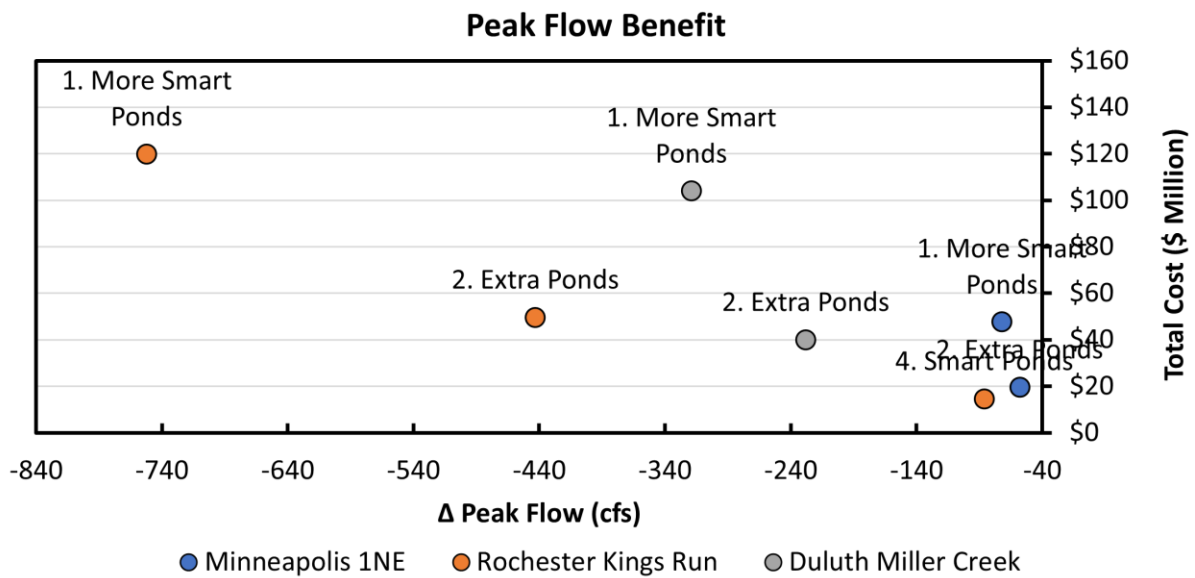


Figure 36: Total cost of adaptation strategies compared to change in peak outflow (Δ Peak Flow (cfs)) for strategies that provide at least 0.5 ft of flood depth reduction. Note: Land costs excluded.

While More Smart Ponds and Extra Ponds were the most cost-effective adaptation strategies in all three watersheds, it is important to note that it may be challenging and expensive to obtain land for installing new stormwater ponds in a fully developed and dense watershed such as Minneapolis’s 1NE. As mentioned above, none of the cost estimation tools consider land costs. Securing property for building new stormwater infrastructure in some watersheds may be a substantial cost compared to other watersheds. This is also important when comparing Smart Ponds to other strategies. Converting existing wet ponds to Smart Ponds requires no additional land for implementation, unlike Extra Ponds, Infiltration Basins, and More Smart Ponds. Thus, converting existing ponds to Smart Ponds may become more cost-effective compared to the strategies that also require land acquisition.

Chapter 4. Summary and Conclusions

Analysis of historical (TP-40), current (Atlas 14), and future predicted storm events for three watersheds in Minnesota (Duluth, Minneapolis, Rochester) has shown that current design philosophy is not sufficient to prevent flooding from 10-year and larger design storm events and that flood depth and duration will increase given current climate projections. Several stormwater infrastructure adaptation strategies were assessed for reducing flood depth and duration and the cost of implementing these strategies was estimated (see summary in Table 12). Several important conclusions can be drawn from the results of this study.

In watersheds that are mixed urban, suburban, and rural like Rochester's Kings Run or Duluth's Miller Creek sub-watersheds, the most cost-effective climate change adaptation strategy of those evaluated in this project was to build new stormwater wet ponds (Extra Ponds strategy) to treat the impervious surfaces not currently treated by existing wet ponds and other stormwater BMPs. It is expected that land costs and acquisition may be less difficult in these watersheds compared to watersheds like 1NE in Minneapolis. A difference observed in the Kings Run sub-watershed is the outlet hydrograph, which did not peak as sharply as in Duluth or Minneapolis. This is partly due to the number of existing ponds within Kings Run but also to the increased size and amount of pervious area compared to Minneapolis. Pipe Upsizing increased the peak flow rate from the outlet much less in Kings Run (+6%) compared to Duluth (+30%) and Minneapolis (+50%).

In the fully developed urban 1NE watershed in Minneapolis, the most cost-effective (excluding land costs) climate change adaptation strategy was building wet ponds (Extra Ponds), compared to all the strategies evaluated in this project. New wet ponds were the second least expensive and the second most effective and thus struck the balance between cost and effectiveness. Securing property for building new stormwater infrastructure in fully developed urban watersheds like 1NE may be a substantial cost compared to other watersheds. Smart Ponds are relatively inexpensive but also relatively ineffective. Smart Ponds, however, do not require additional land for implementation and thus represent a relatively low-cost alternative that will be more beneficial in watersheds with numerous existing wet ponds. Land costs are not considered in this analysis, so the value of Smart Ponds is greater than reported here when compared to other strategies that require land acquisition for implementation (e.g., Extra Ponds and Infiltration Basins).

When considering climate change mitigation, one measure of success was whether flooding was the same or less for future-predicted storms compared to current condition(s). It was observed that the node depth, flood duration, and/or peak outflow at several nodes and outfalls was less for future-predicted storms (2069 50th) compared to current Baseline conditions (Atlas-14) when the More Smart Ponds adaptation strategy was implemented. This observation was true for all three watersheds and for upstream, downstream, and watershed outfalls.

The location of additional stormwater BMPs is also an important consideration. Placement of treatment practices upstream of flood-prone areas or places in which flooding should be minimized (e.g., major highways) is the best approach to minimizing flooding at critical locations. For some watersheds like

1NE, it may be more difficult to find places to implement flood-control stormwater infrastructure upstream of flood-prone areas due to limitations in available land or constructable spaces. Minneapolis has been redeveloped for 150-plus years, which has led to a legacy of uncertain soil conditions, buried debris, and other factors that force stormwater managers to carefully consider how and where infiltration practices and underground structures can be implemented.

The results of our analysis are a good relative comparison but may not be accurate predictions of flood elevations, durations, or peak flows. For example, one node in a residential area of Minneapolis is predicted to have up to seven feet of flooding depth for the 100-year event (Atlas 14, 7.5 inches), though this depth of flooding has not been observed in this area of Minneapolis, to the authors' knowledge. According to state precipitation records (Minnesota State Climatology Office 2023), at least two events of approximately this depth or more have been recorded in Minneapolis (Aug 30, 1977 = 7.28 inches; Jul 23, 1987 = 9.15 inches). The temporal distribution of storms, however, is important in flooding events, and these storms may not have been as intense as the design MSE-3 storm. It is also possible that the EPA-SWMM models were not adequately calibrated and tested for large rainfall events, because these events are rare and it is more difficult to achieve the appropriate measurements. As reconstruction for new practices is completed and more monitoring data is acquired, the SWMM models can be updated and calibrated to real data to ensure accurate predictions of response to storm events.

It should be noted that not all storms have the temporal distribution of the MSE-3 design storm. The June 20-21, 2012, Duluth storm, for example, officially distributed 7.25 inches (and locally 8-10 inches) of precipitation over two days (National Weather Service 2021). Our examination of the effectiveness of adaptation strategies at remediating flooding for a hypothetical 24-hour, uniform storm with a 100-year return interval in the Rochester watershed indicated that infiltration into pervious areas can act as a remediation strategy for this type of storm. Thus, the response of the watershed is dependent on the temporal distribution of the storm and the encouragement of deep-rooted grasses and other plants on lawns could be helpful in developing soils that can absorb an extreme storm event with a temporal distribution that is more uniform than the MSE-3 design storm.

Watersheds like those modeled in Rochester and Duluth have the most potential for future development. It will be important to consider potential climate change adaptation strategies as these areas develop because current design standards are not adequate to prevent or limit flooding from potential events. Proactive implementation of flood control structures while development occurs will reduce long-term costs of implementing adaptation strategies and potentially reduce flooding in downstream, developed portions of the watershed.

In general, for all three watersheds, the order of most effective strategies for reducing node depth, flood duration, and peak flow during the MSE-3 design storm distributions is: 1) More Smart Ponds, 2) Extra Ponds, 3) Smart Ponds, 4) Infiltration Basins, 5) Baseline (keep existing conditions), 6) Pipe Upsizing, and 7) Underground Storage. Considering cost, the order of strategies from least expensive to most expensive is: 1) Baseline, 2) Smart Ponds, 3) Extra Ponds, 4) Pipe Upsizing, 5) More Smart Ponds, 6) Infiltration Basins, and 7) Underground Storage. An important consideration for selecting adaptation

strategies for mitigating climate change impacts is the potential cost of doing nothing (keep existing conditions) or selecting a low-cost, minimally effective strategy. The Baseline cost of operating and maintaining the existing stormwater wet ponds is \$2 million to \$8 million for these three sub-watersheds. While this may save money today compared to implementing adaptation strategies, the potential cost of damage to infrastructure, loss of life and property, and damage to ecosystems and natural resources may far eclipse the upfront and 20-year, life-cycle cost of the adaptation strategies presented herein. The most cost-effective strategy from Table 12 was Extra Ponds, which cost between \$20 million and \$50 million for Minneapolis, Rochester, and Duluth. For comparison, the impacts of the 2012 storm in Duluth was estimated at more than \$100 million, with damage to MnDOT infrastructure alone estimated to be \$20 million (*New York Times* 2022). It's important to note that the estimated damage from the 2012 storm in Duluth is from a much larger area than the Miller Creek sub-watershed, so these costs are not intended for direct comparison. While preventing all damage from extreme events may be infeasible, minimizing impacts through cost-effective adaptation strategies can save millions of dollars.

The risks to communities and transportation due to large rainfall events is a serious issue and a primary purpose of this project. The analysis of adaptation strategies illustrated the conventional design philosophy is not adequate to mitigate impacts of current design (Atlas 14), future predicted storms (e.g., 2030 - 2069 50th percentile median), or low-frequency storms (e.g., 100-year). With this knowledge, stormwater managers can reevaluate their watershed and stormwater management plans to discern vulnerable locations, prioritize resiliency improvements to armor and protect overland flow paths, and understand the watershed to find optimal locations to implement stormwater infrastructure adaptation strategies when opportunities arise. One possible methodology is the concept of a "check storm," which is an event larger than the design storm and used to evaluate the response of proposed conditions for flows that exceed the design storm. An event with a 1 percent annual probability of occurrence (100-year frequency) is commonly used as a check storm. It is not intended that design criteria are upheld for the check storm, but rather that vulnerable areas and unanticipated flow paths or outcomes are identified for extreme low-frequency events. Vulnerable areas or unanticipated flow paths identified during check storm analysis can be protected or reinforced such that damage risk is reduced. Going beyond conventional or permit-required designs for the purpose of mitigating large storm events will reduce flood risk in flood prone areas and prevent other areas from being impacted by larger future storms.

While this research project produced numerous results and conclusions, more research is needed to fully realize resilient stormwater management systems. This research illustrated how current management strategies respond to future design storms, but strategies that could mitigate flooding from future predicted storms or the feasibility of adopting such aggressive strategies was not fully investigated. Research is also needed to document the uncertainty in 1) rainfall quantity and temporal distribution predictions, 2) response of stormwater infrastructure to increased runoff, and 3) flood risk potential. As noted in the final report, the models used were limited in their accuracy to predict flooding for low frequency events because most are not calibrated for such events. More research is needed to quantify the true risk of event probability and potential risk of damage to infrastructure. Our initial

investigations suggest that flood water finds alternative routes to watershed outlets or new outlets during extreme events — routes and outlets not incorporated in current watershed models. More research is needed to develop tools to improve our watershed models for low-frequency events and ascertain true risk of flood damage and impacts.

More research into other possible adaptation strategies is also needed. The strategies proposed by this research need additional iterations and combinations thereof to find more optimized watershed-scale resiliency plans. New and innovative solutions to the challenge of climate resilience need to be investigated and combined with the knowledge of existing mitigation strategies. One example of a new and innovative resiliency strategy is the scale of improvement in natural storage that can be gained by improving soil health on all the pervious surfaces in a watershed via deep-rooted grasses and other plants, mulching, and topsoil amendments, among other things. Preliminary estimates of response to a uniform rainfall distribution suggest that soil permeability can be important and that runoff could be substantially reduced for less intense rainfall distributions. The pervious areas in most watersheds, including highly urbanized areas, can be substantial and improving soil health and surface permeability in the pervious areas could provide “natural” storage within the watershed without large stormwater ponds or underground storage vaults. The scale of potential improvement and actions necessary to realize improvement (e.g., deep-rooted grasses and other plants, mulching, and topsoil amendments) must be studied. Given the strategies, cost and feasibility of implementing such strategies, and accurate watershed models calibrated to extreme events, stormwater managers will need to be informed and prepared to develop robust and resilient stormwater management plans.

References and Bibliography

- Abatzoglou, J.T., & Brown, T.J. (2012). A comparison of statistical downscaling methods suited for wildfire applications. *International Journal of Climatology*, 32(5), 772-780.
- Arnbjerg-Nielsen, K. (2012). Quantification of climate change effects on extreme precipitation used for high resolution hydrologic design. *Urban Water Journal*, 9(2), 57-65.
- Barr Engineering. (2019a). 1NE model update and calibration summary (Technical memorandum to Mississippi Watershed Management Organization and city of Minneapolis).
- Barr Engineering. (2019b), 1NE XPSWMM model conversion (Technical memorandum to Mississippi Watershed Management Organization).
- UBoer, G.J. (1993). Climate change and the regulation of the surface moisture and energy budgets. *Climate Dynamics*, 8(5), 225-239.
- Bixler, T.S., Houle, J., Ballesterio, T.P. & Mo, W. (2020). A spatial life-cycle cost assessment of stormwater management systems. *Science of the Total Environment*, 728, 138787.
- Butcher, J.B., & Zi, T. (2019). Efficient method for updating IDF curves to future climate projections. arXiv preprint arXiv:1906.04802.
- Butcher, J., Sarkar, S., & Zi, T. (2015). *Climate change adaptation modeling in the Chippewa River Watershed, MN*. St. Paul, MN: Minnesota Pollution Control Agency.
- City of Minneapolis. (2016). Cost estimates for pipe upsizing construction projects. Personal Communication.
- CNT (Center for Neighborhood Technology). (2020). Retrieved from <http://greenvalues.cnt.org/national/calculator.php>
- Colorado State University One Water Solutions Institute. (2021). Community-enabled life-cycle analysis of stormwater infrastructure costs (CLASIC). Retrieved from <https://clasic.erams.com/> and <https://www.waterrf.org/CLASIC>
- Czuba, C.R., Fallon, J.D., & Kessler, E.W. (2012). *Floods of June 2012 in Northeastern Minnesota*. (Scientific Investigations Report 2012–5283, 52 pp). Reston, VA: USGS.
- Dorney, C., & Miller, R. (2020). Climate projections of precipitation events (Task 4 technical memorandum). St. Paul, MN: Minnesota Department of Transportation.
- EOR (Emmons and Olivier Resources, Inc.). (2022). Kings run model calibration, revised (Technical memorandum to City of Rochester).

- Flato, G., Marotzke, J., Abiodun, B., Braconnot, P., Chou, S.C., Collins, W. & Rummukainen, M. (2013). Evaluation of climate models. In T. F. Stocker, D. Qin, G.-K. Plattner, M. Tignor, S.K. Allen, J. Boschung, ...& P.M. Midgley (eds.), *Climate change 2013: The physical science basis*. (Contribution of Working Group I to the fifth assessment report of the Intergovernmental Panel on Climate Change). Cambridge, UK: Cambridge University Press.
- Grubert, E., & Krieger, J. (2020). *Integrated decision support tool (iDST) life-cycle costing module for distributed stormwater control measures (SCMs)*. Georgia Institute of Technology Library. Retrieved from <https://smartech.gatech.edu/handle/1853/62873>
- Hausfather, Z., & Peters, G.P. (2020). Emissions—the ‘business as usual’ story is misleading. *Nature*, 577, 618-620.
- Heaney, J.P., Sample, D., & Wright, L. (2002). *Cost of urban stormwater control (EPA-600/R-02/021)*. Cincinnati, OH, US Environmental Protection Agency,
- Herb, W., Johnson, L., & Gulliver, J. (2020). *Detailed hydrology for stormwater BMPs (St. Anthony Falls Laboratory Project Report No. 592)*. Minneapolis, MN: Minnesota Lake Superior Coastal Program, University of Minnesota.
- Herb, W. (2021). Analysis of stormwater runoff best management practices in Miller Creek, Duluth, MN, (St. Anthony Falls Laboratory Project Report No. 596). Minneapolis, MN: Minnesota Sea Grant, University of Minnesota.
- Hershfield, D.M. (1961). *Rainfall frequency atlas of the United States for durations from 30 minutes to 24 hours and return periods from 1 to 100 years (Technical Paper No. 40)*. Washington, DC: Department of Commerce.
- Hosking, J.R.M. (1990). L-moments: Analysis and estimation of distributions using linear combinations of order statistics, *J. R. Statist. Soc. B*, 52(1), 105-124.
- Houle, J.J., Roseen, R.M., Ballesterio, T.P., Plus, T.A., & Sherrard, Jr., J. (2013). Comparison of maintenance cost, labor demands, and system performance for LID and conventional stormwater management. *Journal of Environmental Engineering*, 139(7), 932-938.
- Houston Engineering, Inc. (2019). *Flood mitigation and water quality analysis for portions of Cascade Township, city of Rochester*. Maple Grove: Houston Engineering, Inc.
- Huff, F.A., & Angel, J.R. (1992). Rainfall frequency atlas of the Midwest (Bulletin 71). Champaign, IL: Midwestern Climate Center.
- Landwehr, J.M., Matalas, N.C., & Wallis, J.R. (1979). Probability weighted moments compared with some traditional techniques in estimating Gumbel parameters and quantiles. *Water Resource Research*, 15(5), 1055-1064.

- Lee, T., & Jeong, C. (2014). Nonparametric statistical temporal downscaling of daily precipitation to hourly precipitation and implications for climate change scenarios. *Journal of Hydrology*, 510, 182-196.
- Lee, T., & Park, T. (2017). Nonparametric temporal downscaling with event-based population generating algorithm for RCM daily precipitation to hourly: Model development and performance evaluation. *Journal of Hydrology*, 547, 498-516.
- Lenderink, G., & Van Meijgaard, E. (2010). Linking increases in hourly precipitation extremes to atmospheric temperature and moisture changes. *Environmental Research Letters*, 5(2), 025208.
- Lepore, C., Veneziano, D., & Molini, A. (2015). Temperature and CAPE dependence of rainfall extremes in the eastern United States. *Geophysical Research Letters*, 42(1), 74-83.
- Maimone, M., Malter, S., Rockwell, J., & Raj, V. (2019). Transforming global climate model precipitation output for use in urban stormwater applications. *Journal of Water Resources Planning and Management*, 145(6), 04019021.
- Medeiros de Saboia, M.A., de Souza Filho, F.D.A., Helfer, F., & Rolim, L.Z.R. (2020). Robust strategy for assessing the costs of urban drainage system designs under climate change scenarios. *Journal of Water Resources Planning and Management*, 146(11), 05020022.
- Minnesota State Climatology Office. (2023). Nearest station precipitation data retrieval. Retrieved from https://climateapps.dnr.state.mn.us/HIDradius/radius_new.asp
- Montaldo, F., Behr, C. Alfredo, K., Wolf, M. Arye, M., & Walsh, M. (2007). Rapid assessment of the cost-effectiveness of low-impact development for CSO control. *Landscape and Urban Planning*, 82, 117–131.
- Narayanan, A., & Pitt, R. (2006). Costs of urban stormwater control practices. Tuscaloosa, AL: Department of Civil, Construction, and Environmental Engineering, University of Alabama.
- National Oceanic and Atmospheric Association (NOAA). (2021). Hydrometeorological design studies center precipitation frequency data server, Retrieved from https://hdsc.nws.noaa.gov/hdsc/pfds/pfds_map_cont.html
- National Weather Service (NWS). (2021). June 2012 flood in Duluth and the Northland. Retrieved from https://www.weather.gov/dlh/june2012_duluth_flood#:~:text=Two%20day%20rainfall%20amounts%20of,rivers%20and%20streams%20to%20flood.&text=The%20official%20Duluth%20total%20rainfall%20for%20the%20event%20was%207.25%E2%80%9D
- New York Times*. (2022). Cost of Minnesota flood estimated at \$100 Million, June 22, 2012. Retrieved from <https://www.nytimes.com/2012/06/23/us/millions-in-damage-from-duluth-flooding.html>
- Parsons Brinckerhoff. (2014). *Flash flood vulnerability and adaptation assessment pilot project: District 1 Silver Creek case study*. St. Paul, MN: Minnesota Department of Transportation.

- Perica, S., Martin, D., Pavlovic, S., Roy, I., St. Laurent, M., Trypaluk C., ... & Bonnin, G. (2013). *NOAA atlas 14 precipitation-frequency atlas of the United States*, Vol. 8 Version 2.0. Silver Spring, MD, NOAA.
- Personal Communication. (2022). Cost estimate and typical design parameters for “smart” ponds. Personal Communication with Anonymous company.
- Pierce, D.W., Cayan, D.R., & Thrasher, B.L. (2014). Statistical downscaling using localized constructed analogs (LOCA) > *Journal of Hydrometeorology*, 15(6), 2558-2585.
- Sample, J.J., Heaney, J.P., Wright, L.T., Fan, C.Y., Lai, F.H., & Field, R. (2003). Costs of best management practices and associated land for urban stormwater control, *Journal of Water Resources Planning and Management*, 129(1) 59-68.
- Soil Conservation Service. (1972). Section 4: Hydrology. In *National engineering handbook*,. Washington DC: USDA.
- Srivastav, R.K., Schardong, A., & Slobodan, P. (2014). Equidistance quantile matching method for updating IDF curves under climate change. *Water Resources Management*, 28, 2539–2562. DOI: 10.1007/s11269-014-0626-y
- USEPA. (2014). System for urban stormwater treatment and analysis integration (SUSTAIN). Retrieved from <https://www.epa.gov/water-research/system-urban-stormwater-treatment-and-analysis-integration-sustain>
- USEPA, (2016). Climate resilience evaluation and awareness tool, Version 3.0 methodology guide. Retrieved from https://www.epa.gov/sites/default/files/2016-05/documents/creat_3_0_methodology_guide_may_2016.pdf
- USEPA. (2019). National stormwater calculator. Retrieved from <https://www.epa.gov/water-research/national-stormwater-calculator>
- Weiss, P.T., Erickson, A.J., & Gulliver, J.S. (2007). Cost and pollutant removal of storm-water treatment practices. *Journal of Water Resources Planning and Management*, 133(3), 218–229. [http://dx.doi.org/10.1061/\(ASCE\)0733-9496\(2007\)133:3\(218\)](http://dx.doi.org/10.1061/(ASCE)0733-9496(2007)133:3(218))
- Weiss, P.T., Gulliver, J.S., & Erickson, A.J. (2005). *The cost and effectiveness of stormwater management practices*. St. Paul, MN: Minnesota Department of Transportation. <https://www.cts.umn.edu/publications/report/the-cost-and-effectiveness-of-stormwater-management-practices>
- WERF (2009). BMP and LID whole life cost models: Version 2.0. (Project 1757). Retrieved from <https://www.waterrf.org/research/projects/bmp-and-lid-whole-life-cost-models-version-20>
- Wilson, B.N., & Sheshukov, A. Y. (2011). *Precipitation parameters of stochastic climate models for a changing climate*. Anchorage, AK: ASABE International Symposium on Erosion and Landscape Evolution.

Appendix A: SWMM Simulation Results

A.1 SWMM Simulation Results for Miller Creek, Duluth

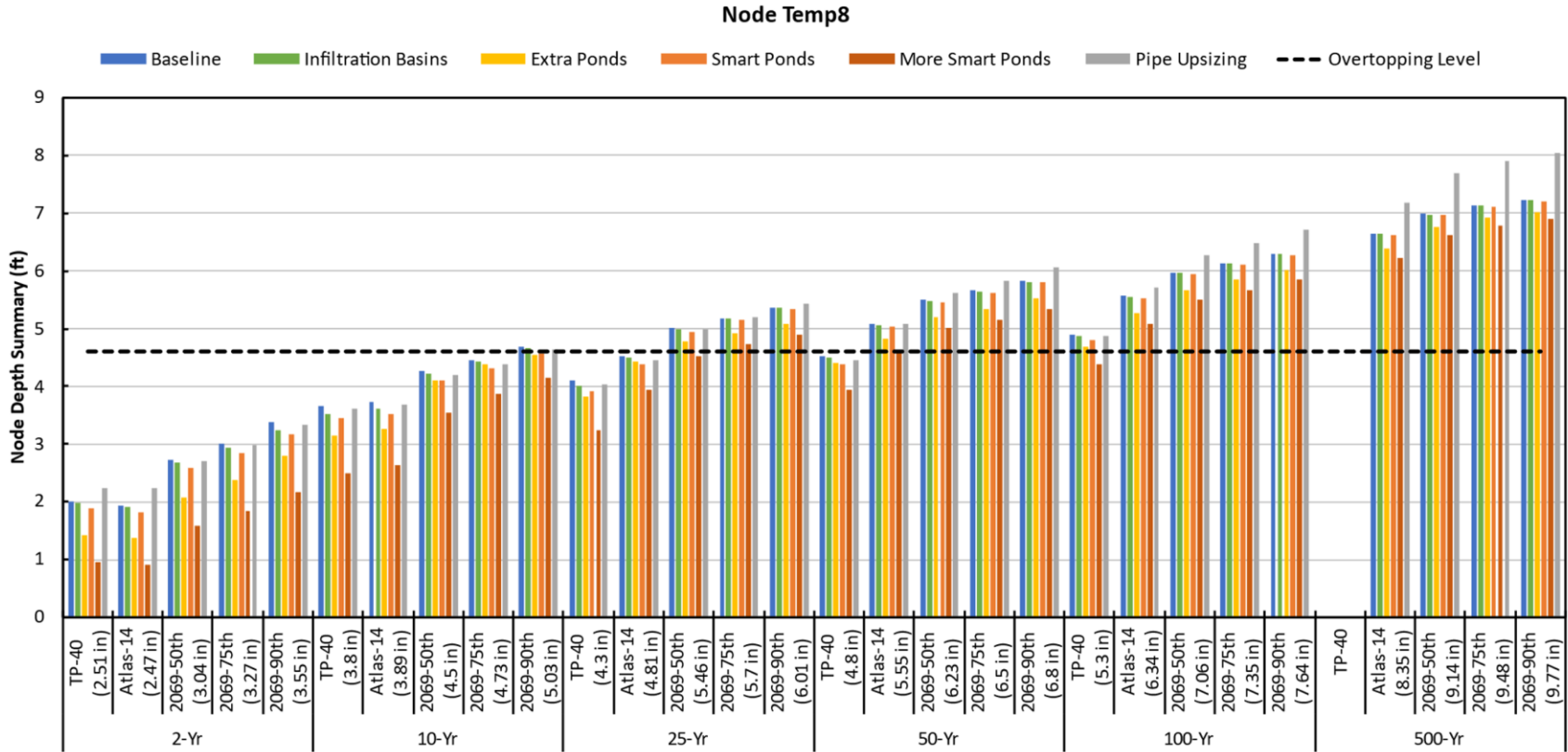


Figure A-1: Node Depth in ft for the 2-, 10-, 25-, 50-, 100-, and 500-year storms at node Temp8 in Duluth

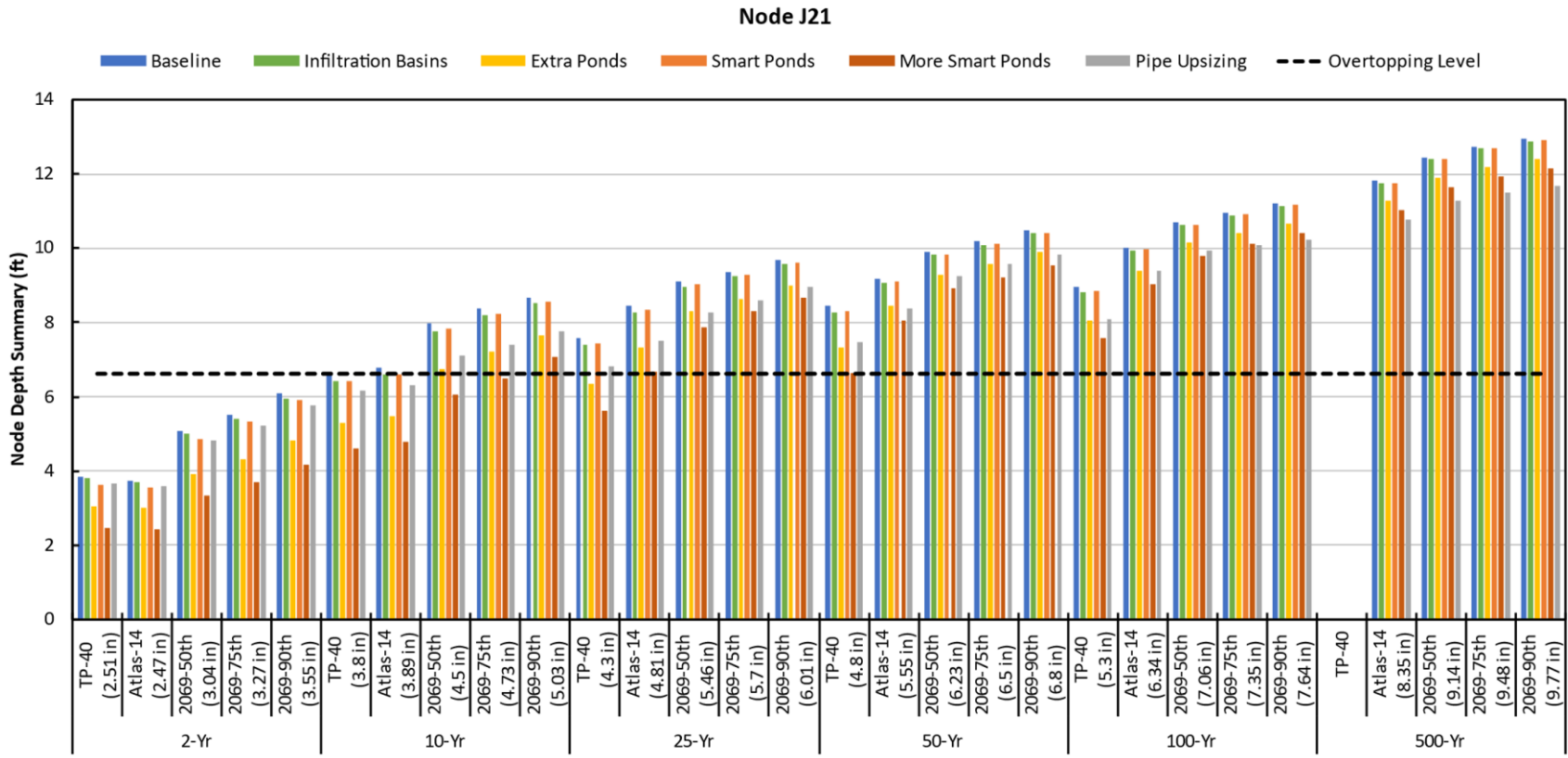


Figure A-2: Node Depth in ft for the 2-, 10-, 25-, 50-, 100-, and 500-year storms at node J21 in Duluth

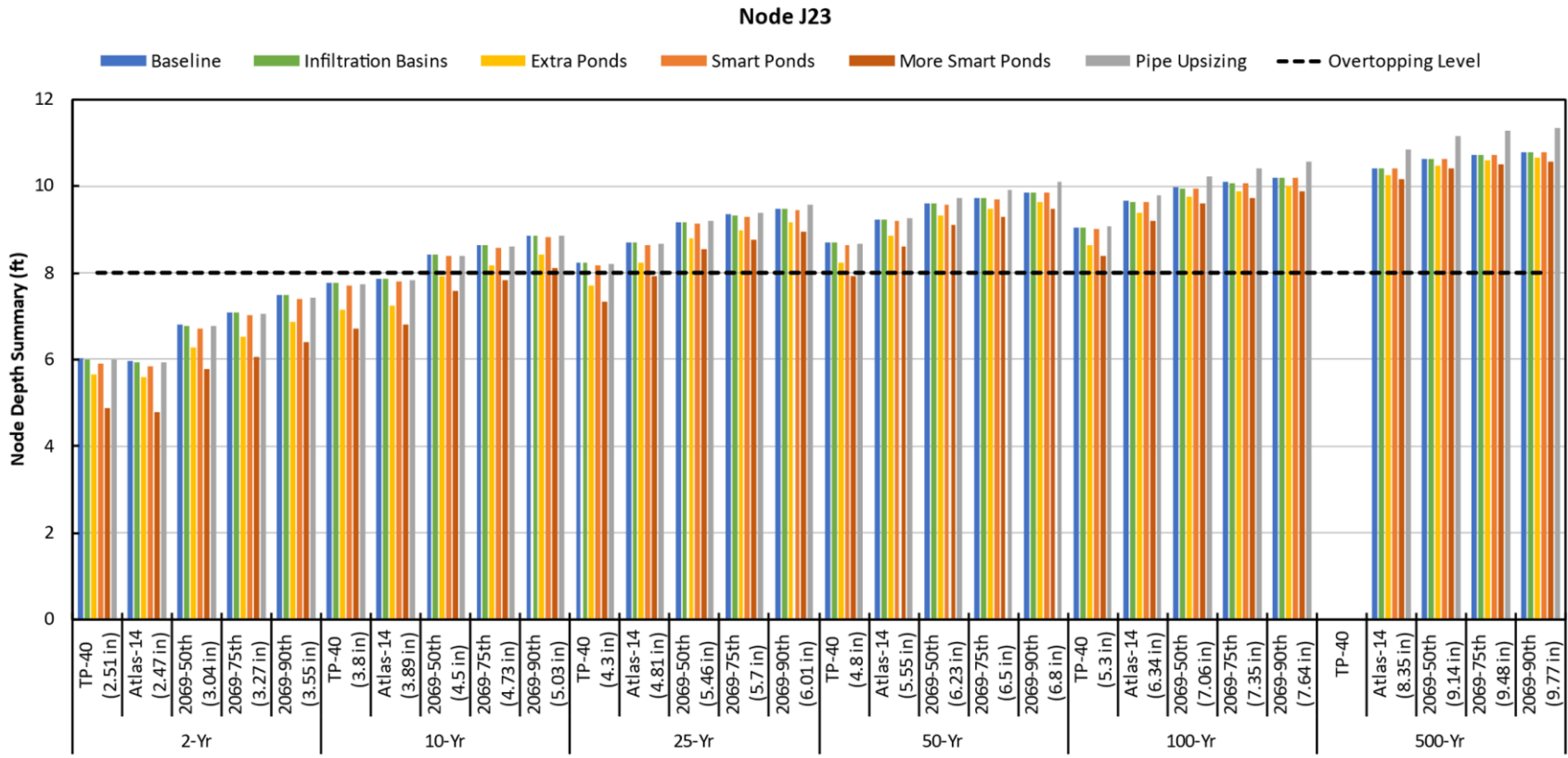


Figure A-3: Node Depth in ft for the 2-, 10-, 25-, 50-, 100-, and 500-year storms at node J23 in Duluth

Node J14

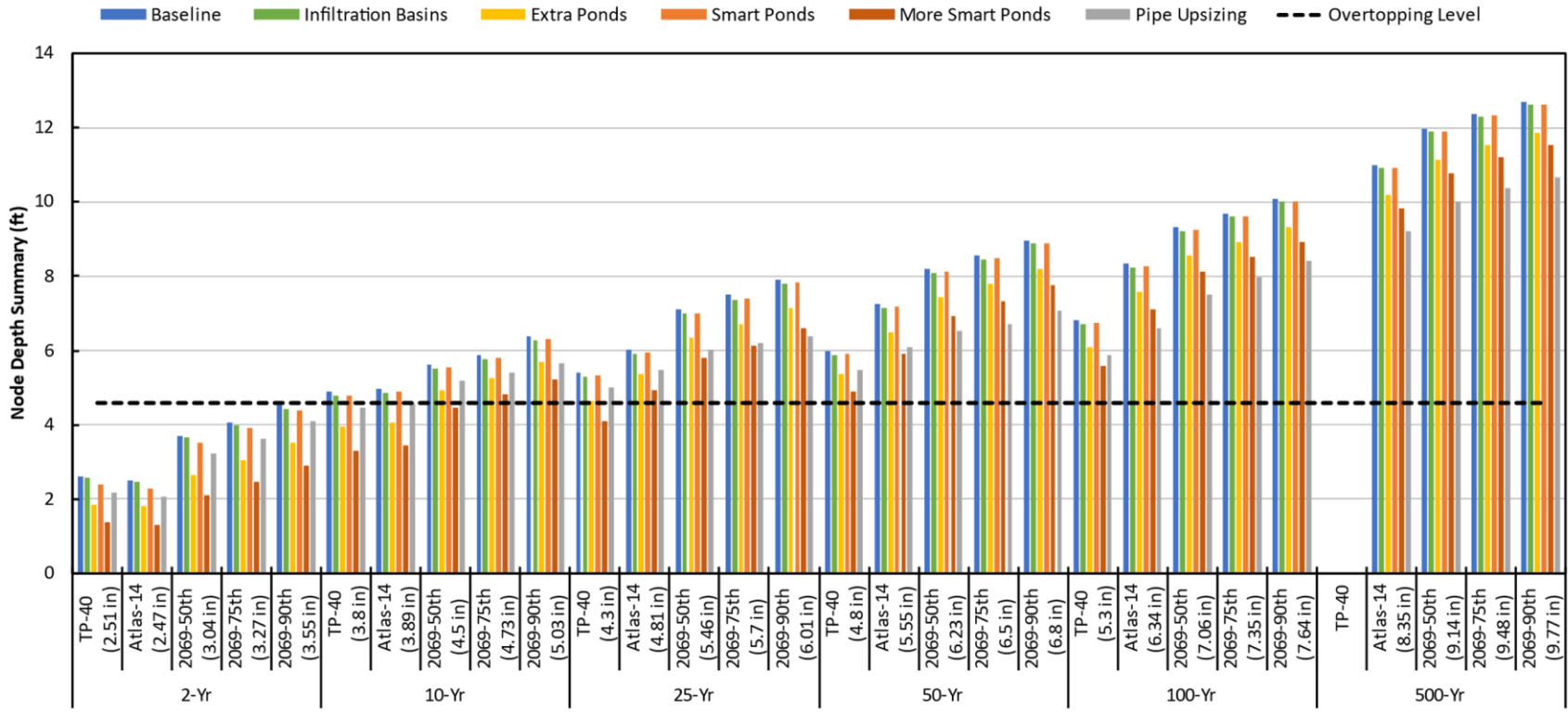


Figure A-4: Node Depth in ft for the 2-, 10-, 25-, 50-, 100-, and 500-year storms at node J14 in Duluth

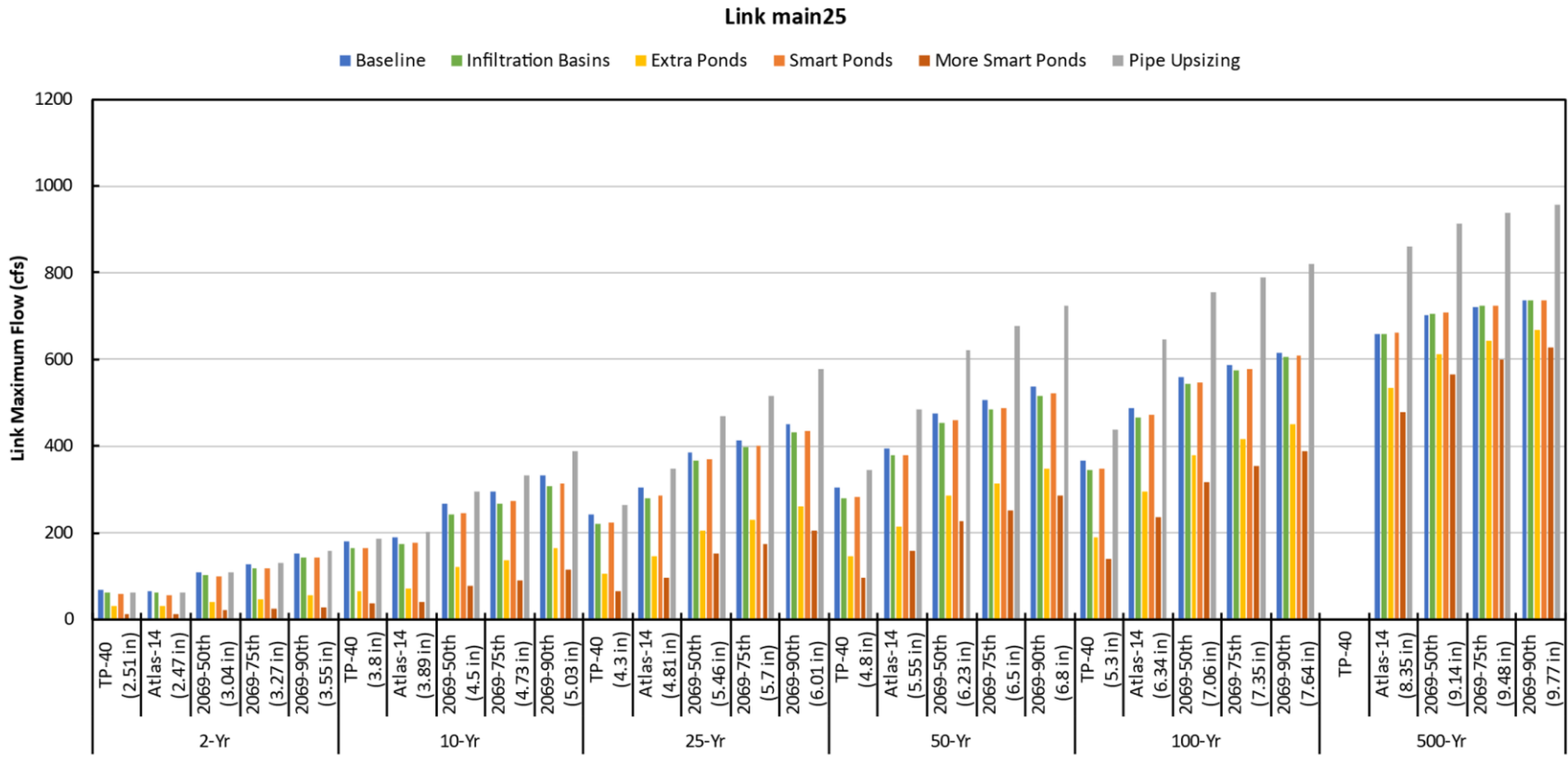


Figure A-5: Maximum Flow Rate (cfs) for the 2-, 10-, 25-, 50-, 100-, and 500-year storms at the outlet (main25) of the Kohl's Wetland in Duluth.

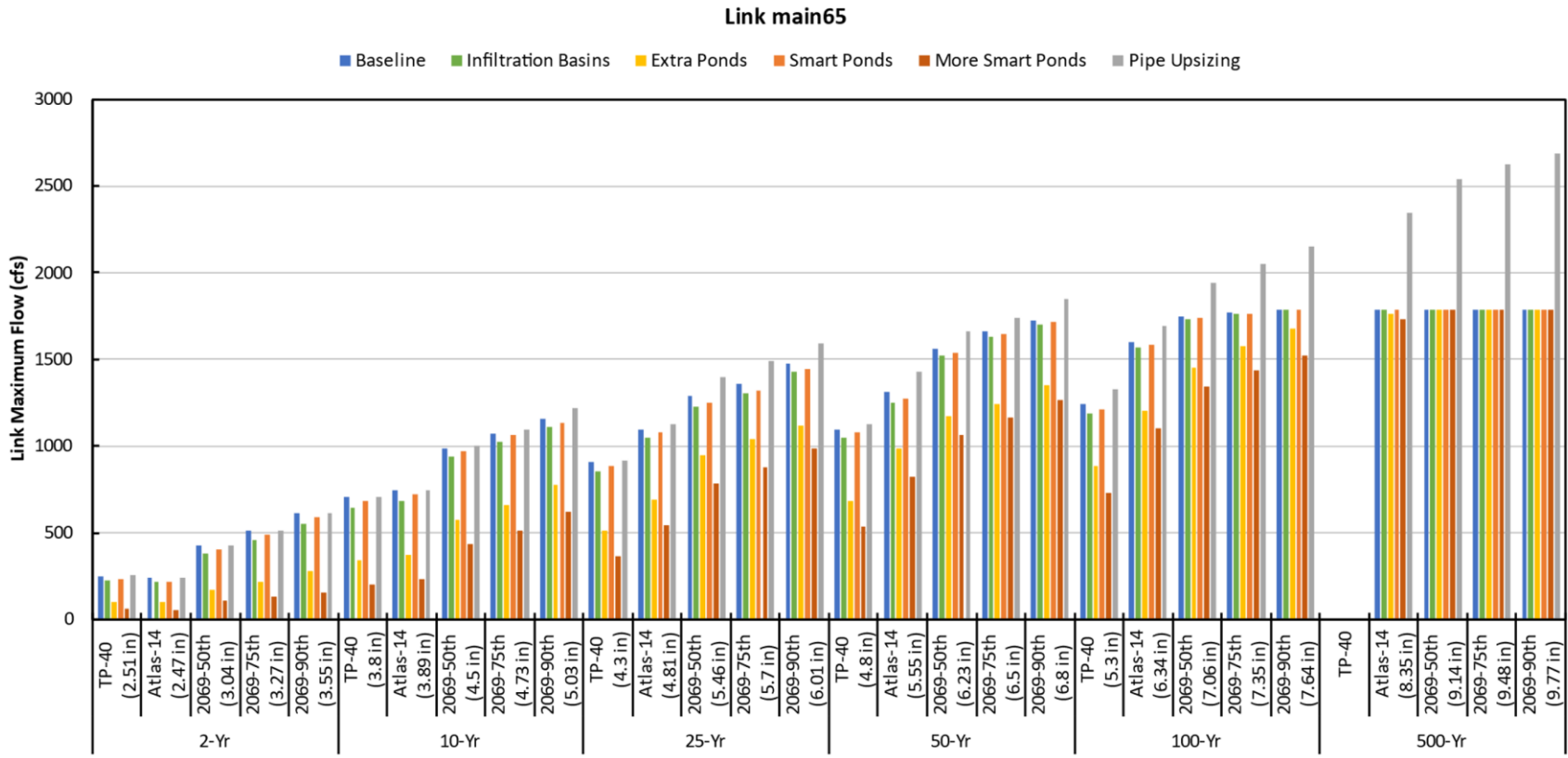


Figure A-6: Maximum Flow Rate (cfs) for the 2-, 10-, 25-, 50-, 100-, and 500-year storms at the outlet (main65) of the Miller Creek sub-watershed in Duluth.

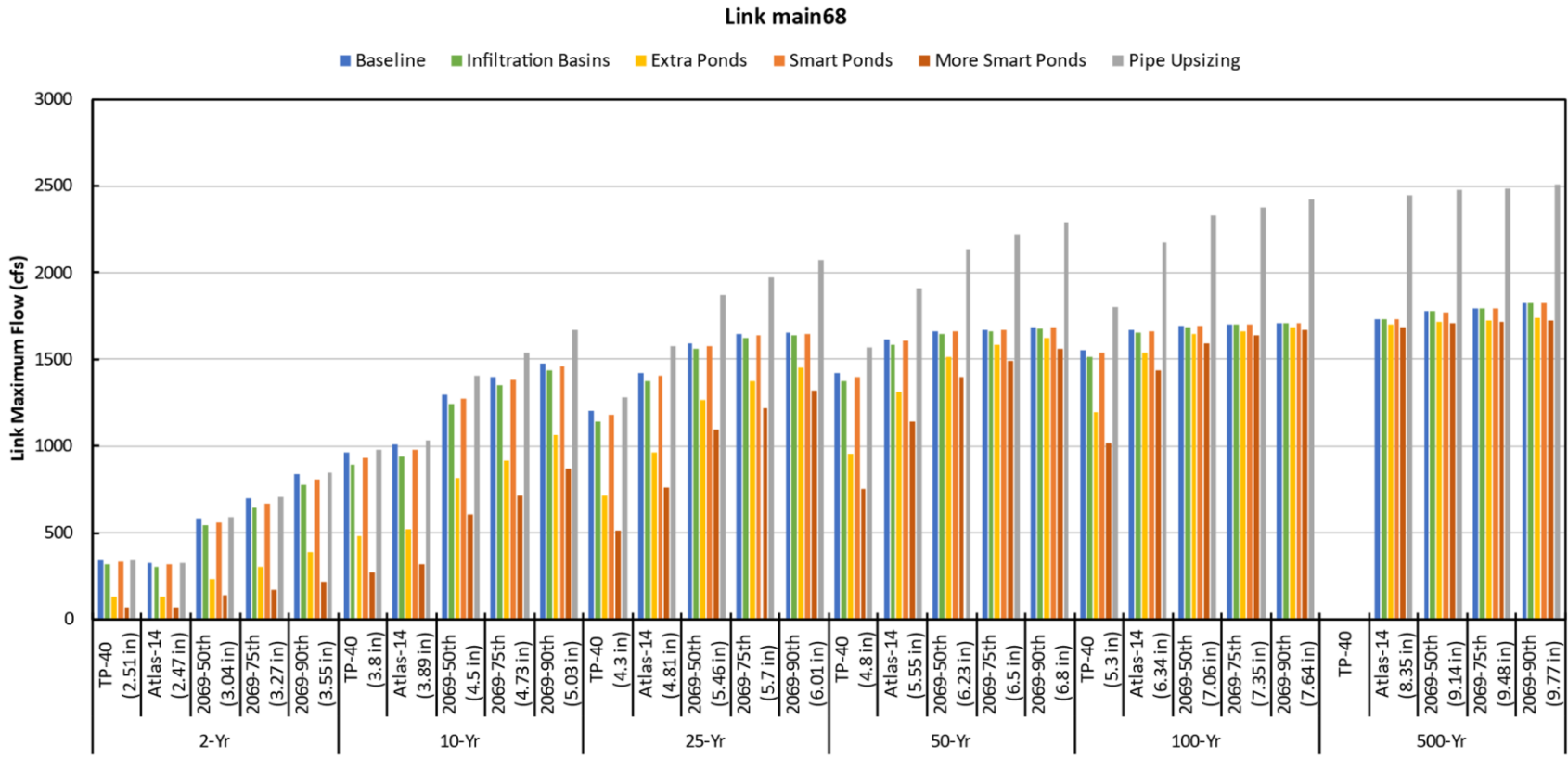


Figure A-7: Maximum Flow Rate (cfs) for the 2-, 10-, 25-, 50-, 100-, and 500-year storms at the outlet (main68) of the combined Miller Creek and Coffee Creek watershed in Duluth.

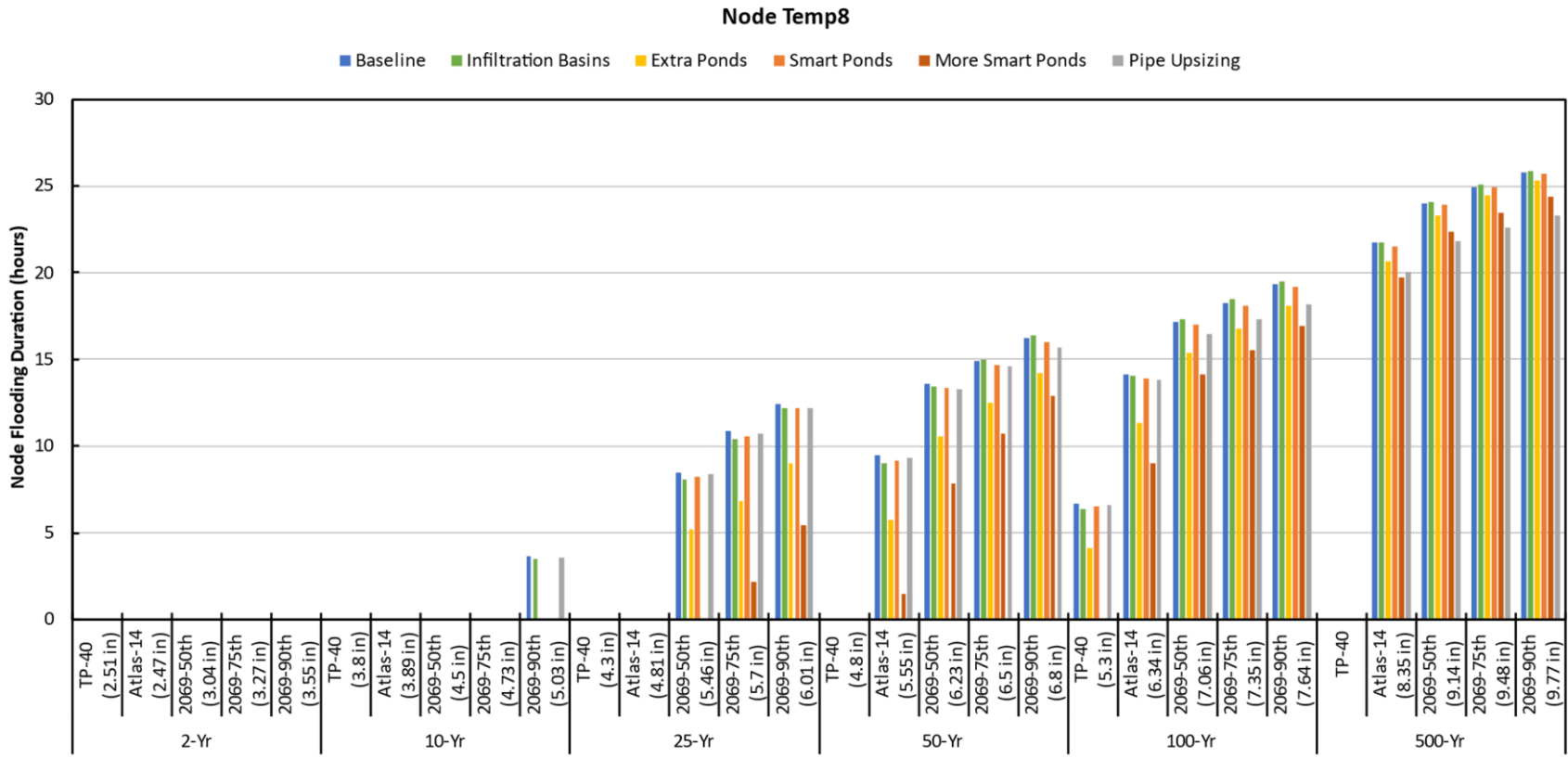


Figure A-8: Flood duration in hours for the 2-, 10-, 25-, 50-, 100-, and 500-year storms at node Temp8 in Duluth.

Node J21

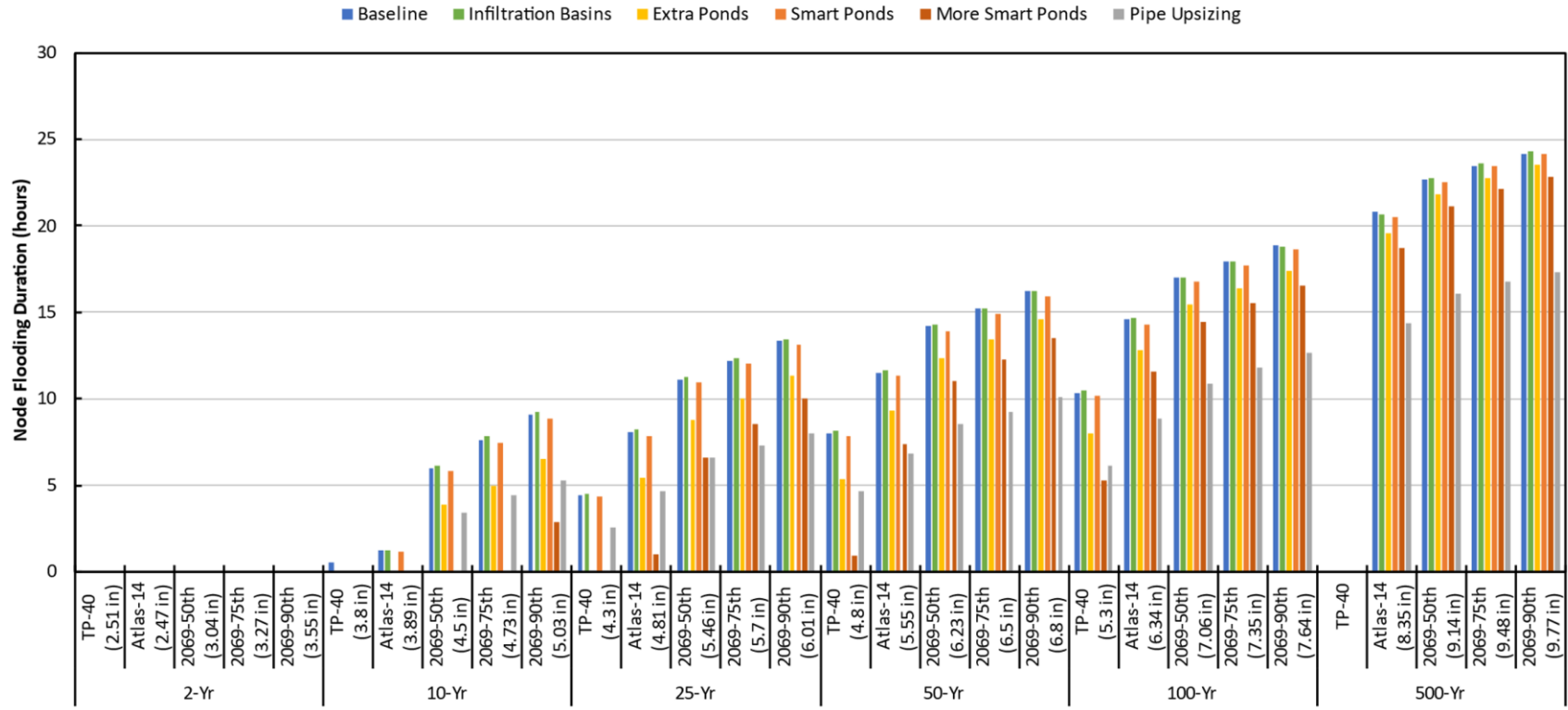


Figure A-9: Flood duration in hours for the 2-, 10-, 25-, 50-, 100-, and 500-year storms at node J21 in Duluth.

Node J23

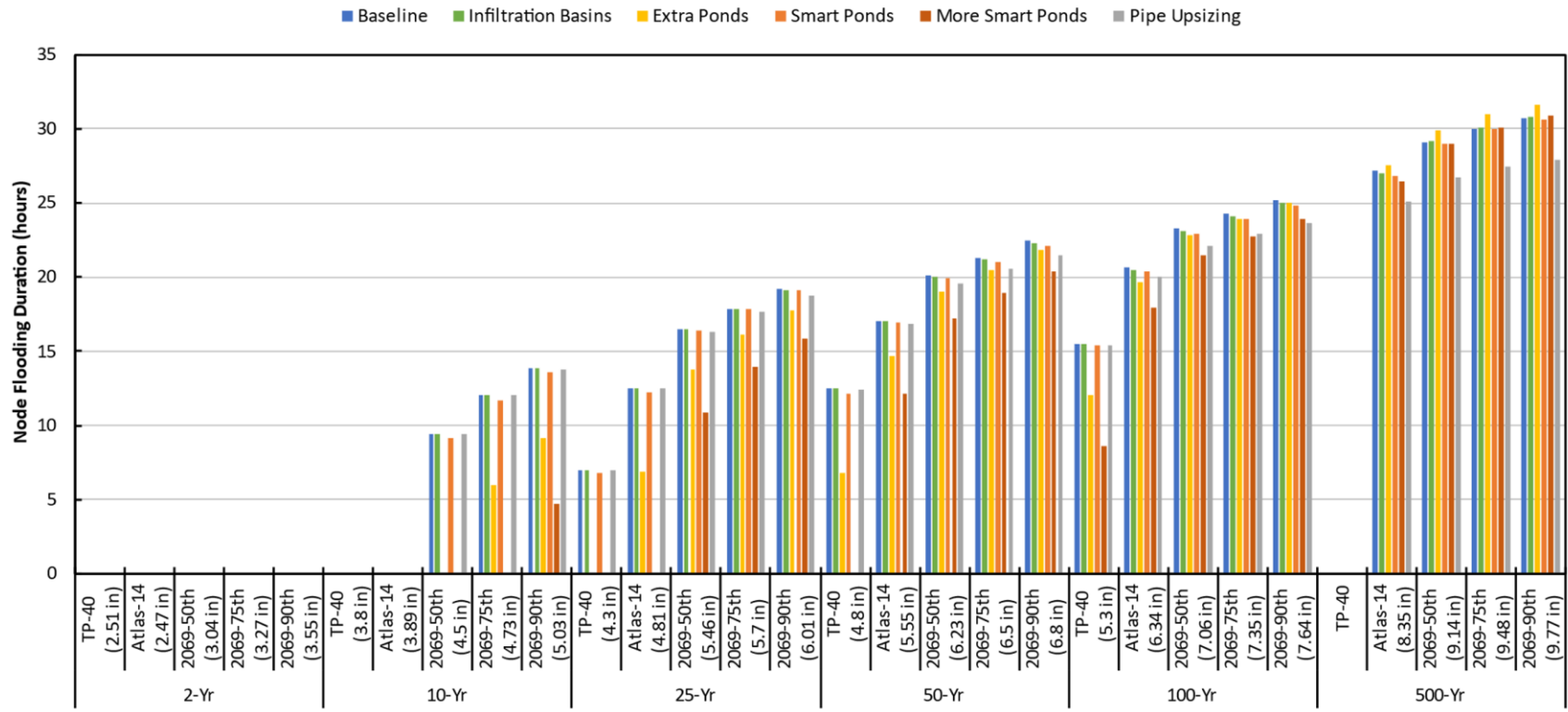


Figure A-10: Flood duration in hours for the 2-, 10-, 25-, 50-, 100-, and 500-year storms at node J23 in Duluth.

Node J14

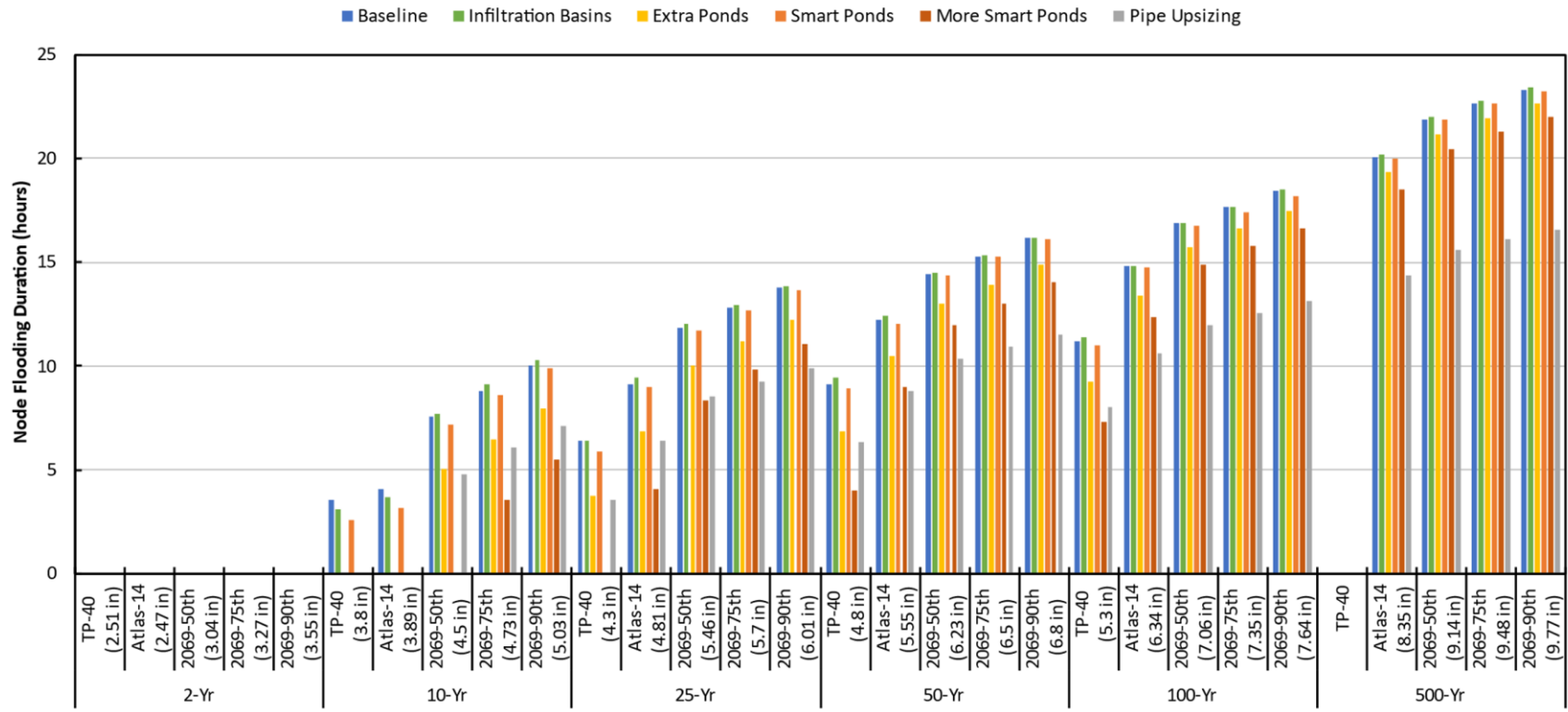


Figure A-11: Flood duration in hours for the 2-, 10-, 25-, 50-, 100-, and 500-year storms at node J14 in Duluth.

Table A-1: Time to Peak (hours) and +/- change in Time to Peak for Atlas-14, 100-year storm event for Temp8, J21, J23, J14, main25, main65, and main68 in Duluth.

Location	Quantity	Time to Peak (Hours)	+/- Change in Time to Peak (Hours)				
		Baseline	Infiltration	Extra Ponds	Smart Ponds	More Smart Ponds	Upsize
Temp8	Depth	26.69	+0.17	+0.51	-0.16	+0.83	-2.86
J21	Depth	19.34	+0.16	+1.33	+0.00	+1.18	-1.50
J23	Depth	27.20	+0.49	+0.82	+0.16	+1.15	-2.54
J14	Depth	19.02	+0.33	+1.32	+0.16	+2.30	-1.69
main25	Flow	18.15	+0.17	+1.82	+0.17	+2.65	-0.33
main65	Flow	14.67	0.16	0.68	0.16	1.15	-0.82
main68	Flow	14.47	0.32	1.03	0.32	1.36	-0.46

Node Temp8 Depth during 100-year Atlas 14 Storm

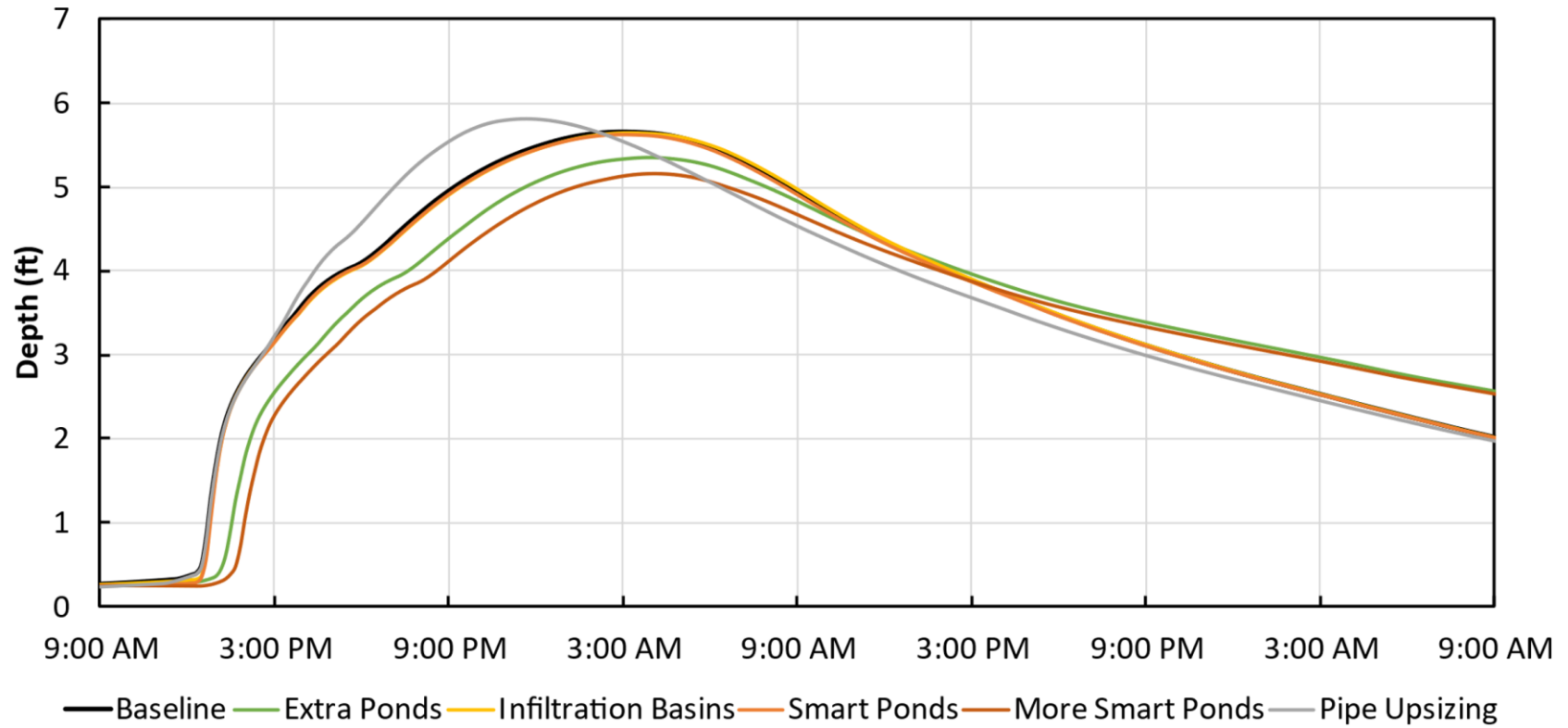


Figure A-12: Miller Creek Kohl's wetland inlet (Node Temp8) Hydrograph (depth in ft) for the 100-year Atlas 14 event (6.31 inches)

Hydrograph Main25 Flow during 100 -year Atlas 14 Storm

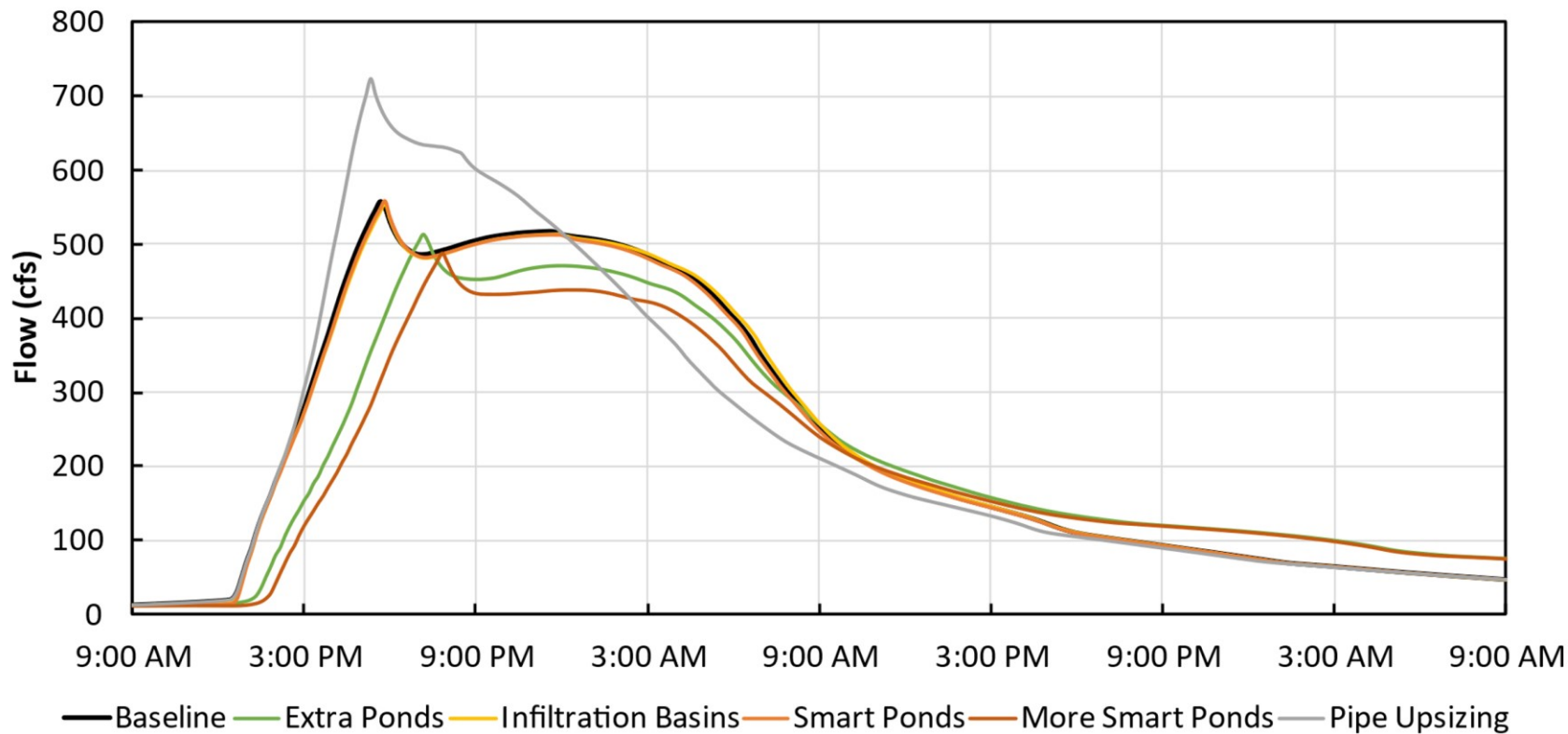


Figure A-13: Miller Creek Kohl's wetland channel (main25) Hydrograph (flow in cfs) for the 100-year Atlas 14 event (6.31 inches)

Node J23 Depth during 100 -year Atlas 14 Storm

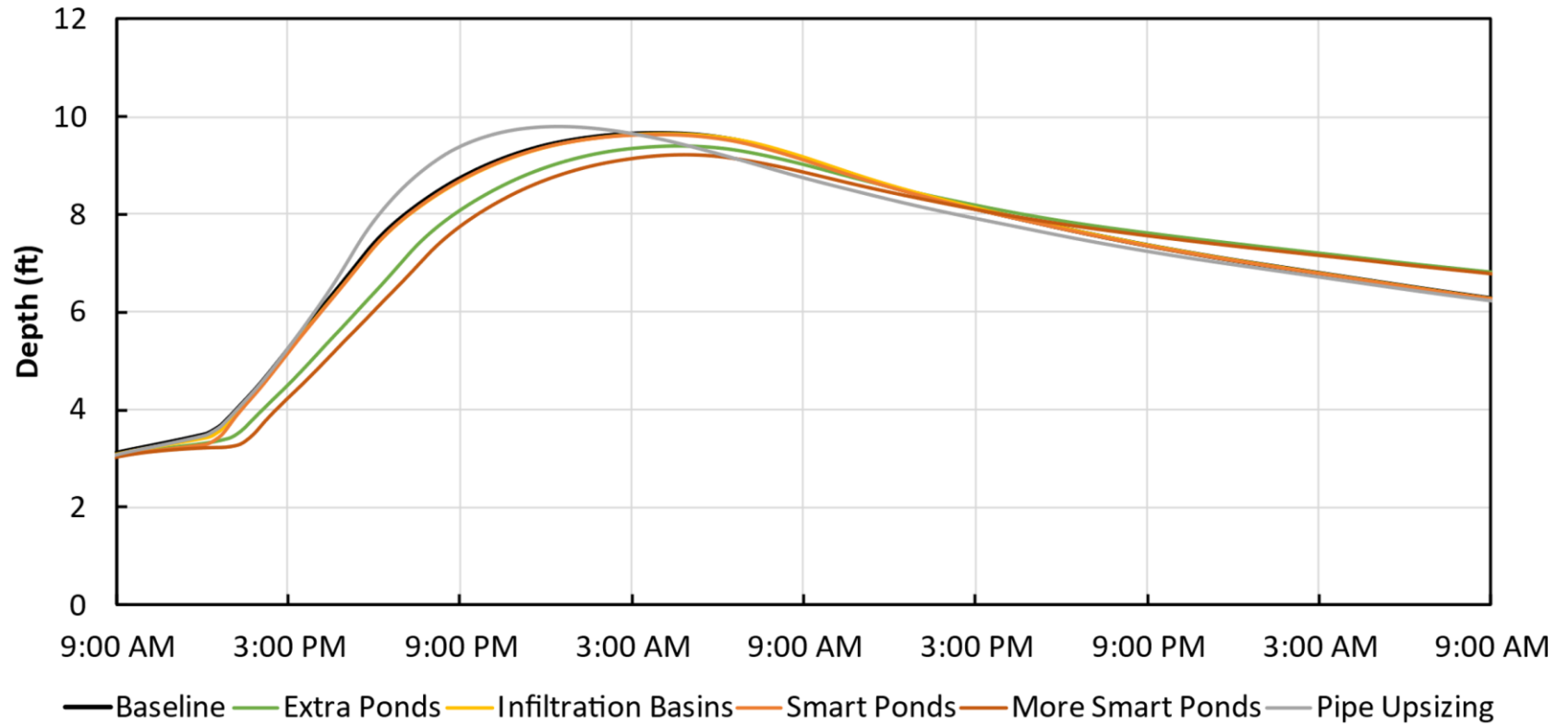


Figure A-14: Miller Creek Kohl's wetland outlet (Node J23) Hydrograph (depth in ft) for the 100-year Atlas 14 event (6.31 inches)

Hydrograph Main68 Flow during 100 -year Atlas 14 Storm

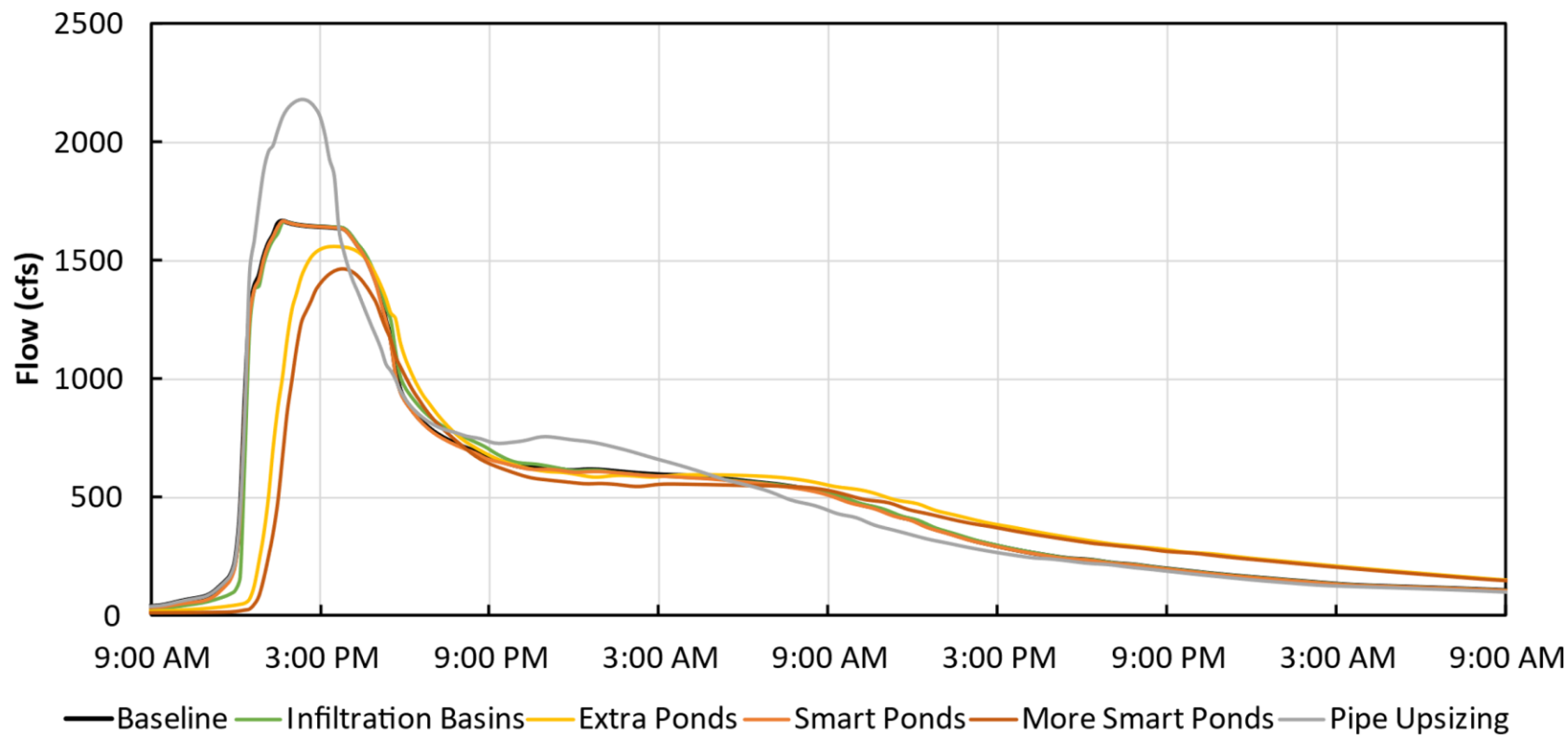


Figure A-15: Miller Creek Outlet (main68) Hydrograph (flow in cfs) for the 100-year Atlas 14 event (6.31 inches)

A.2 SWMM Simulation Results For 1NE, Minneapolis

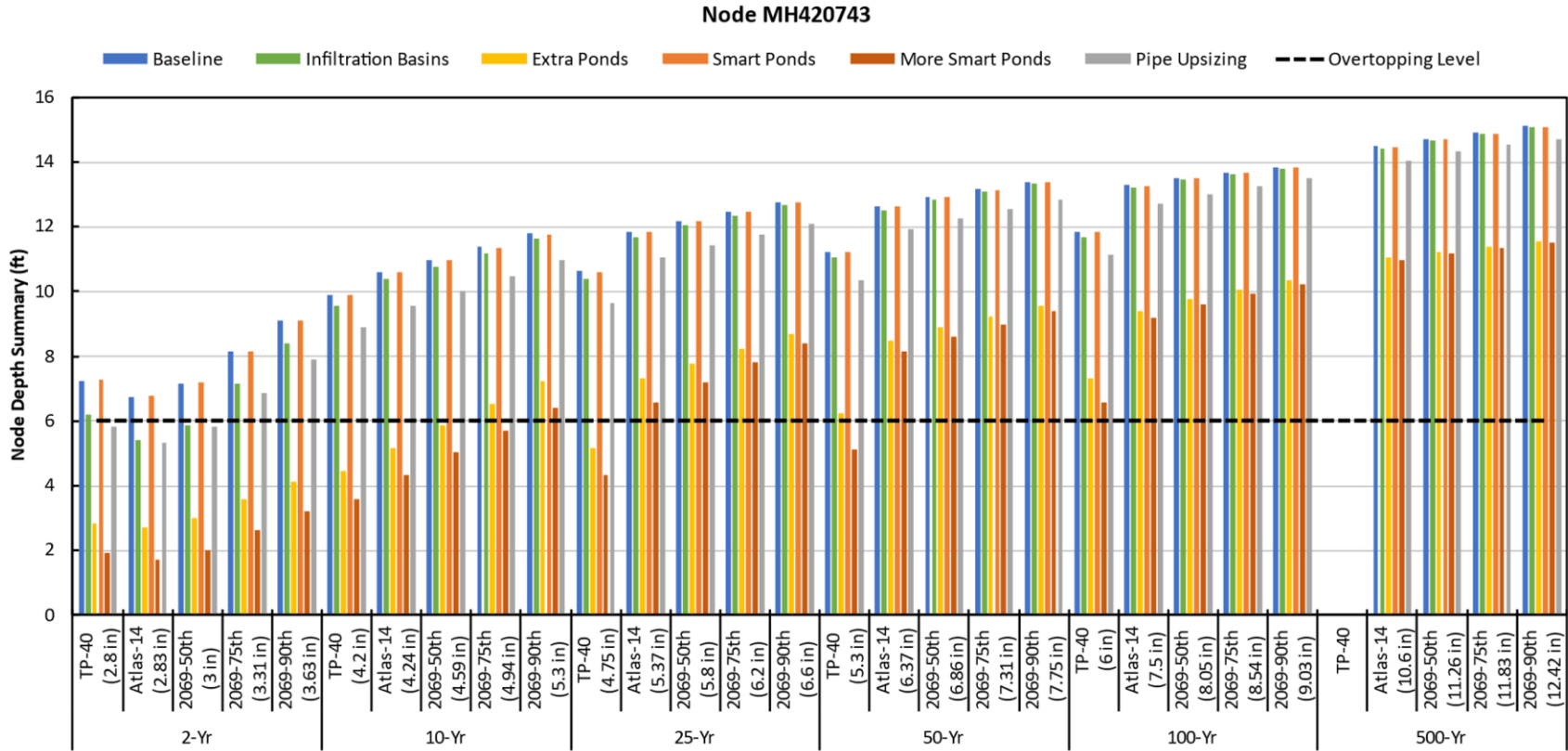


Figure A-16: Node Depth in ft for the 2-, 10-, 25-, 50-, 100-, and 500-year storms at node MH420743 in Minneapolis.

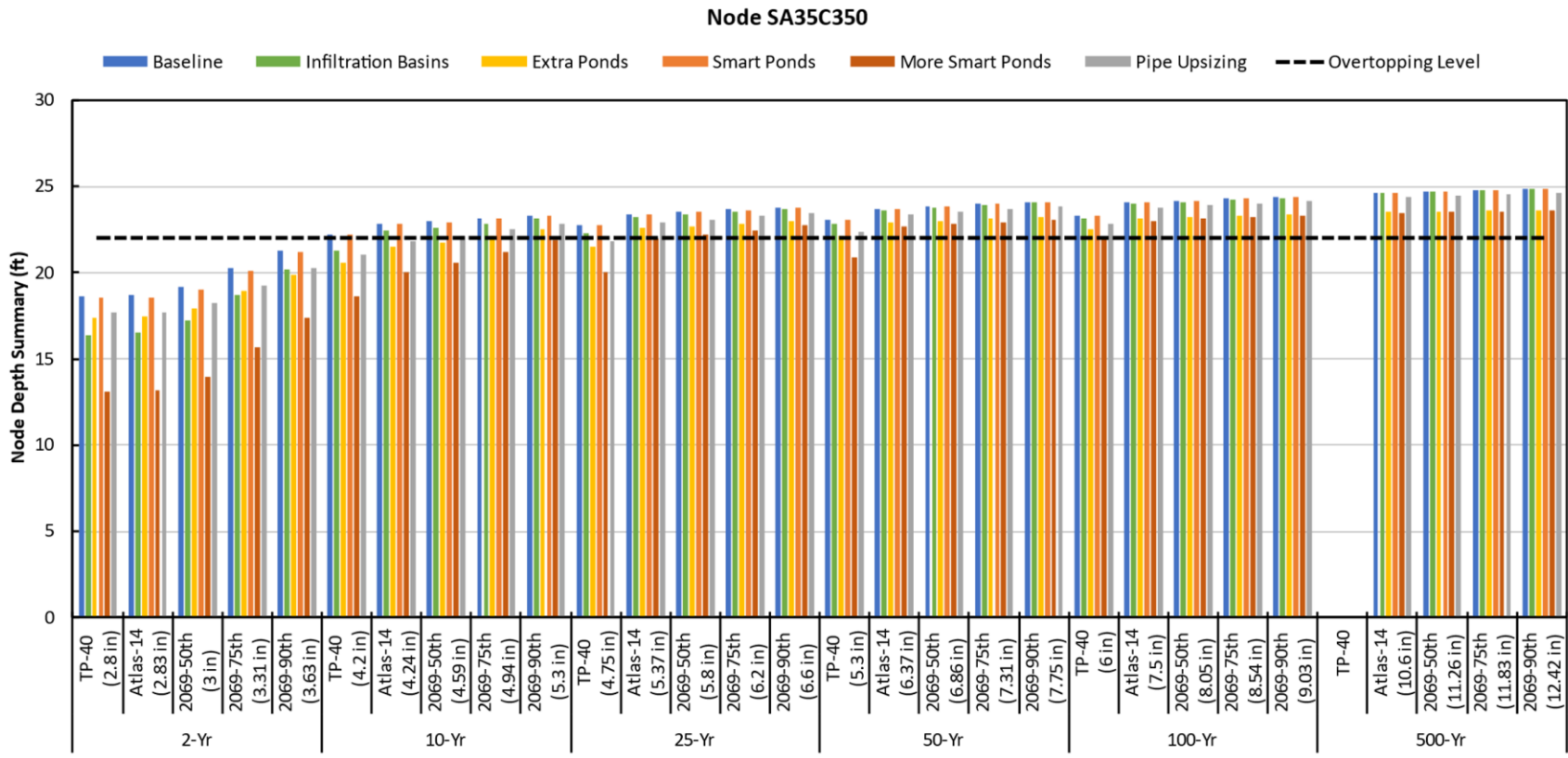


Figure A-17: Node Depth in ft for the 2-, 10-, 25-, 50-, 100-, and 500-year storms at node SA35C350 in Minneapolis.

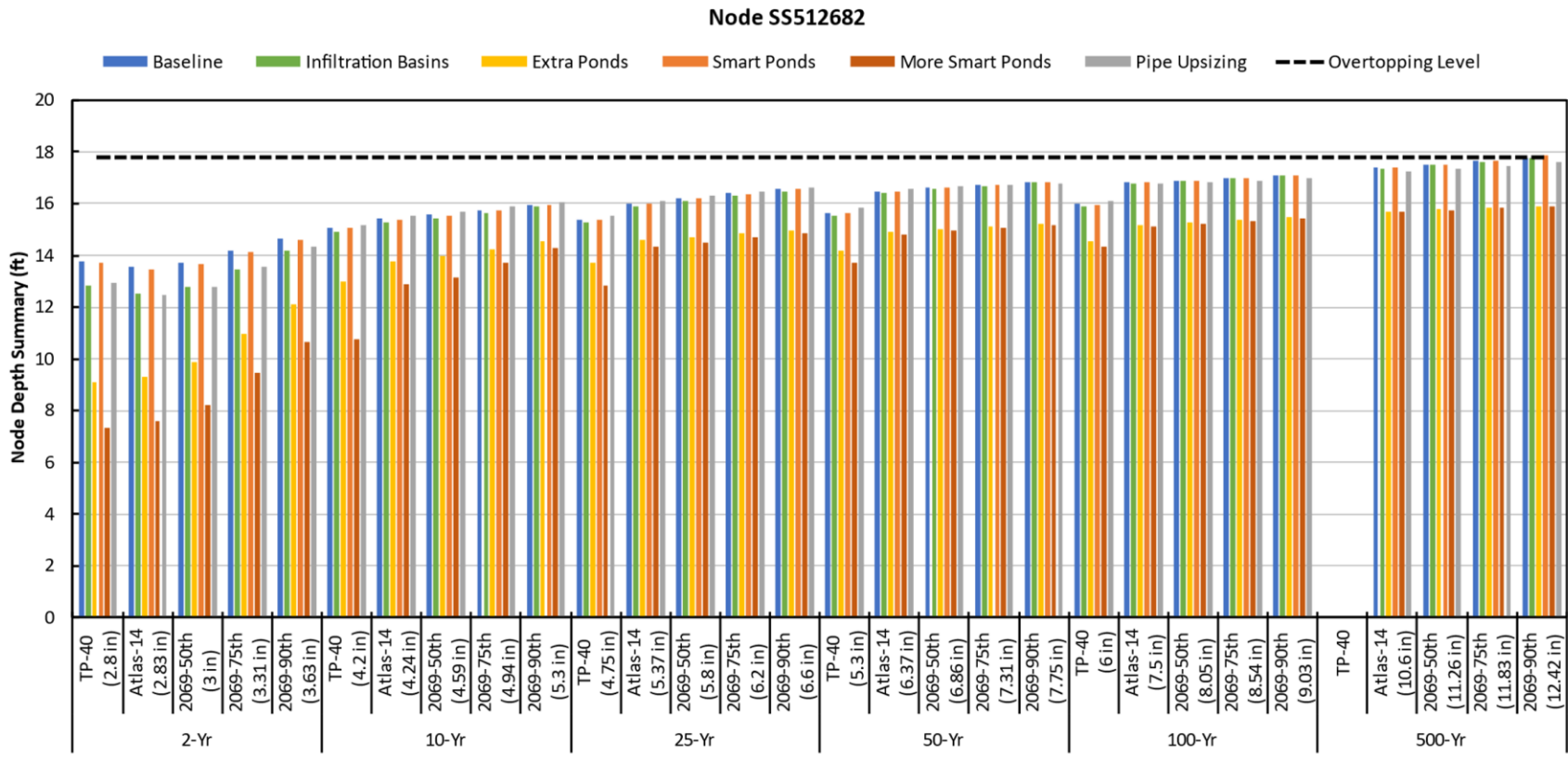


Figure A-18: Node Depth in ft for the 2-, 10-, 25-, 50-, 100-, and 500-year storms at node SS512682 in Minneapolis.

Node SA999039

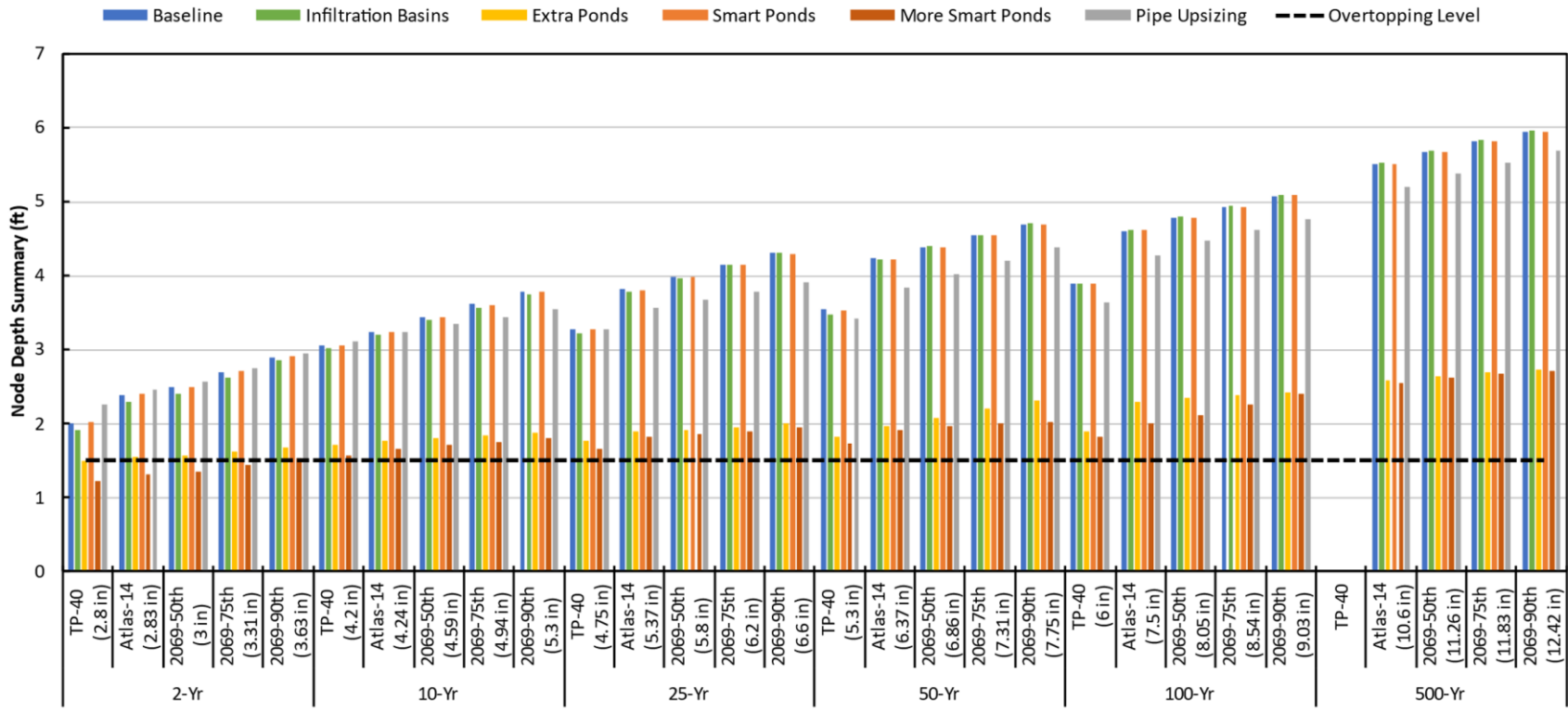


Figure A-19: Node Depth in ft for the 2-, 10-, 25-, 50-, 100-, and 500-year storms at node SA999039 in Minneapolis.

Node MH420743

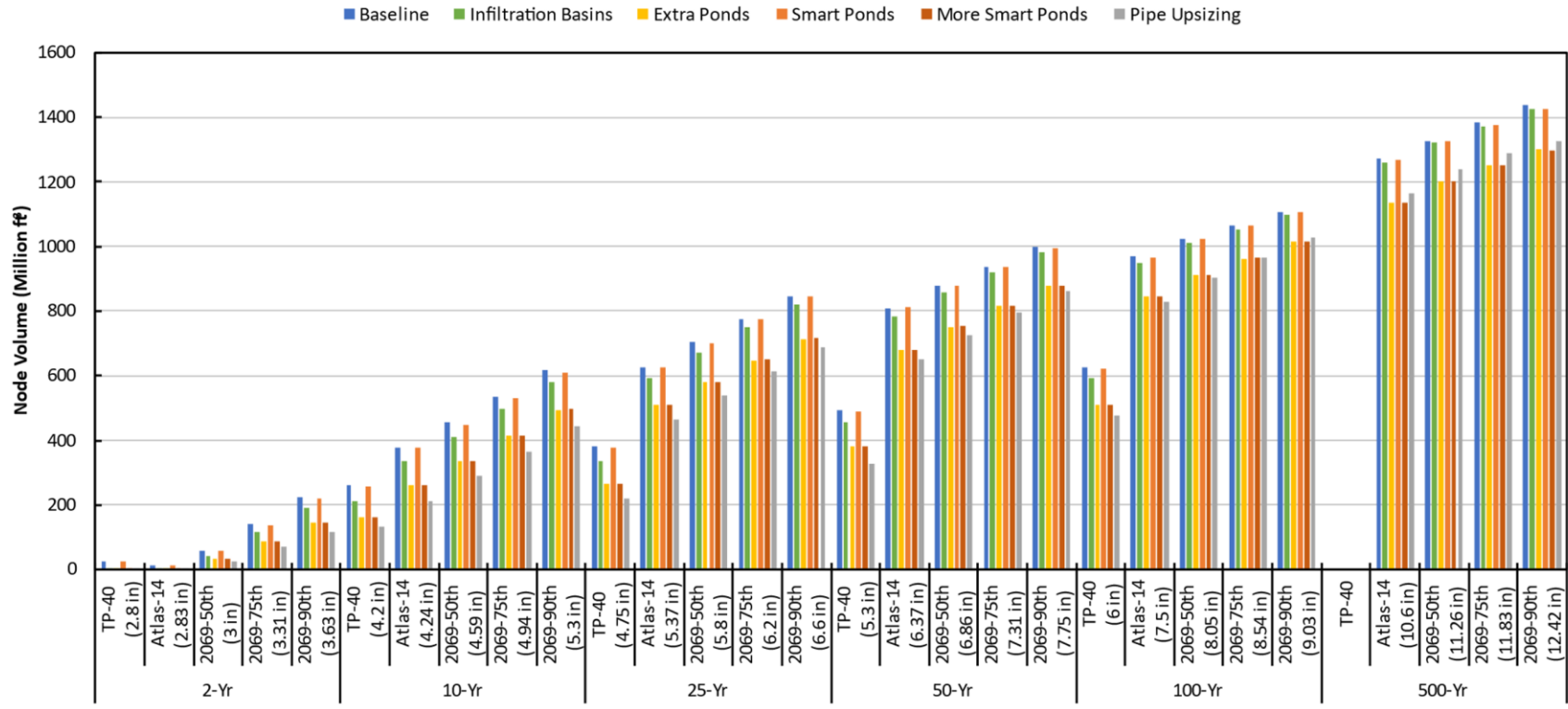


Figure A-20: Cumulative Node volume in million ft³ for the 2-, 10-, 25-, 50-, 100-, and 500-year storms at MH420743 in Minneapolis.

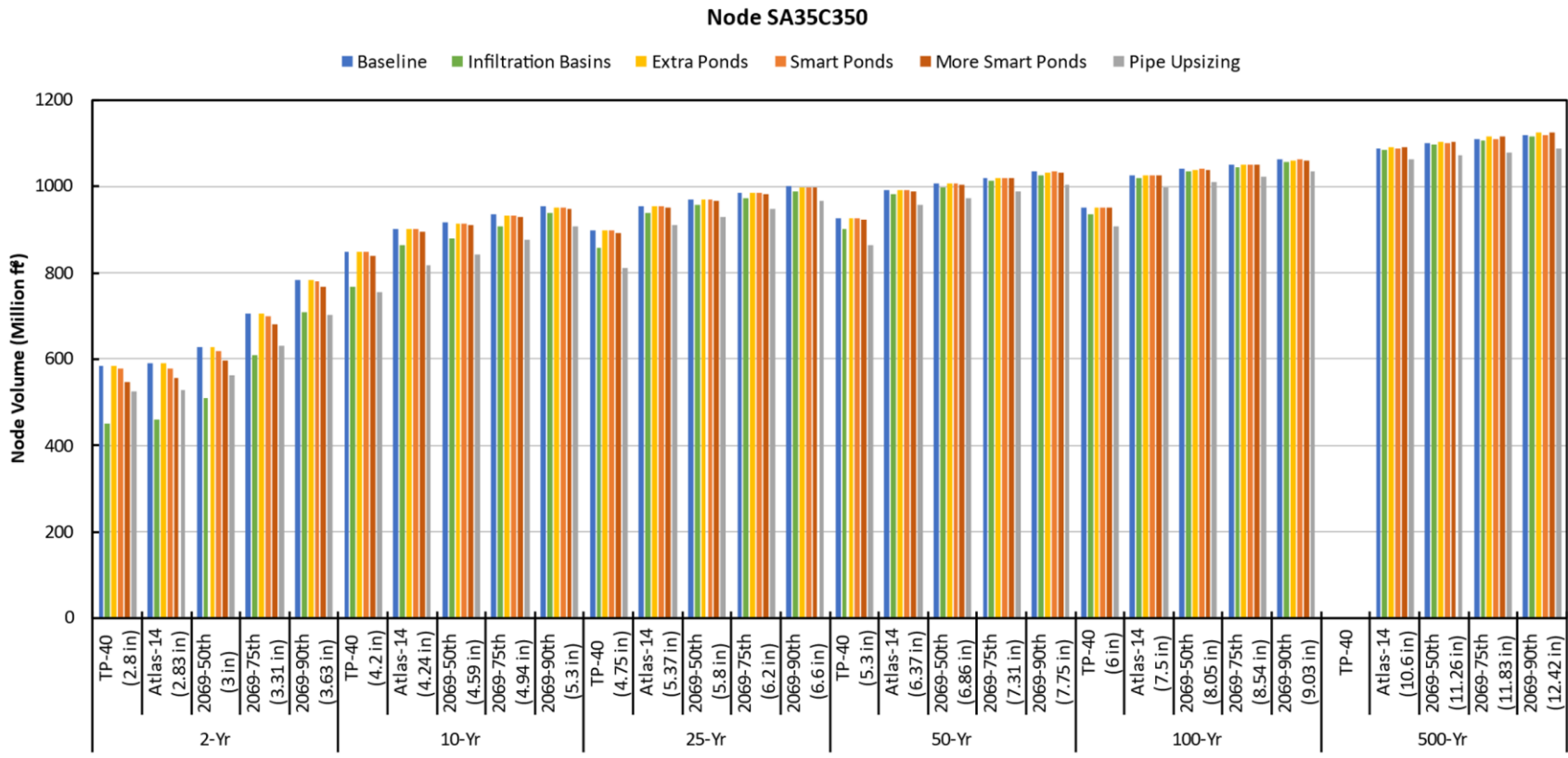


Figure A-21: Cumulative Node volume in million ft³ for the 2-, 10-, 25-, 50-, 100-, and 500-year storms at SA35C350 in Minneapolis.

Node SS512682

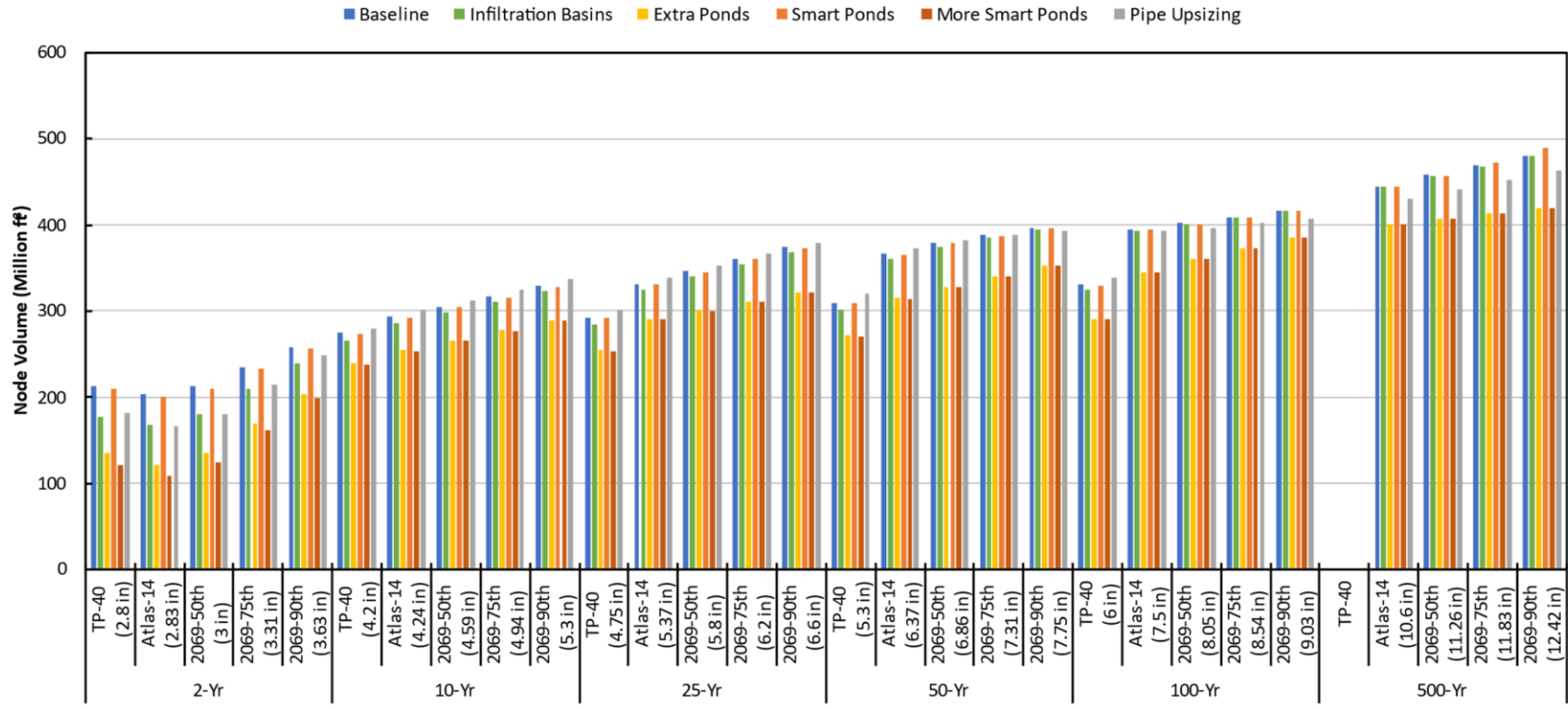


Figure A-22: Cumulative Node volume in million ft³ for the 2-, 10-, 25-, 50-, 100-, and 500-year storms at SS512682 in Minneapolis.

Node SA999039

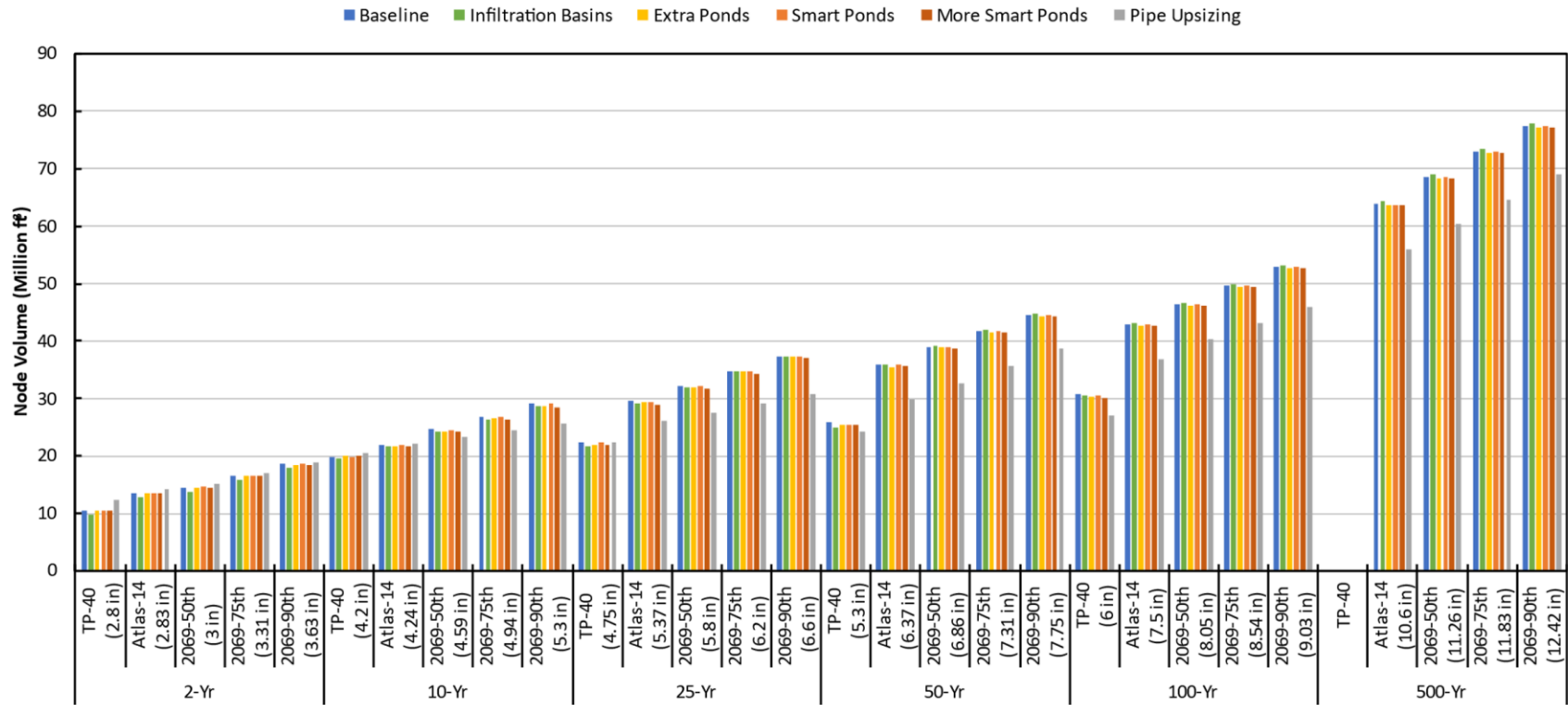


Figure A-23: Cumulative Node volume in million ft³ for the 2-, 10-, 25-, 50-, 100-, and 500-year storms at SA999039 in Minneapolis.

Node OF441270

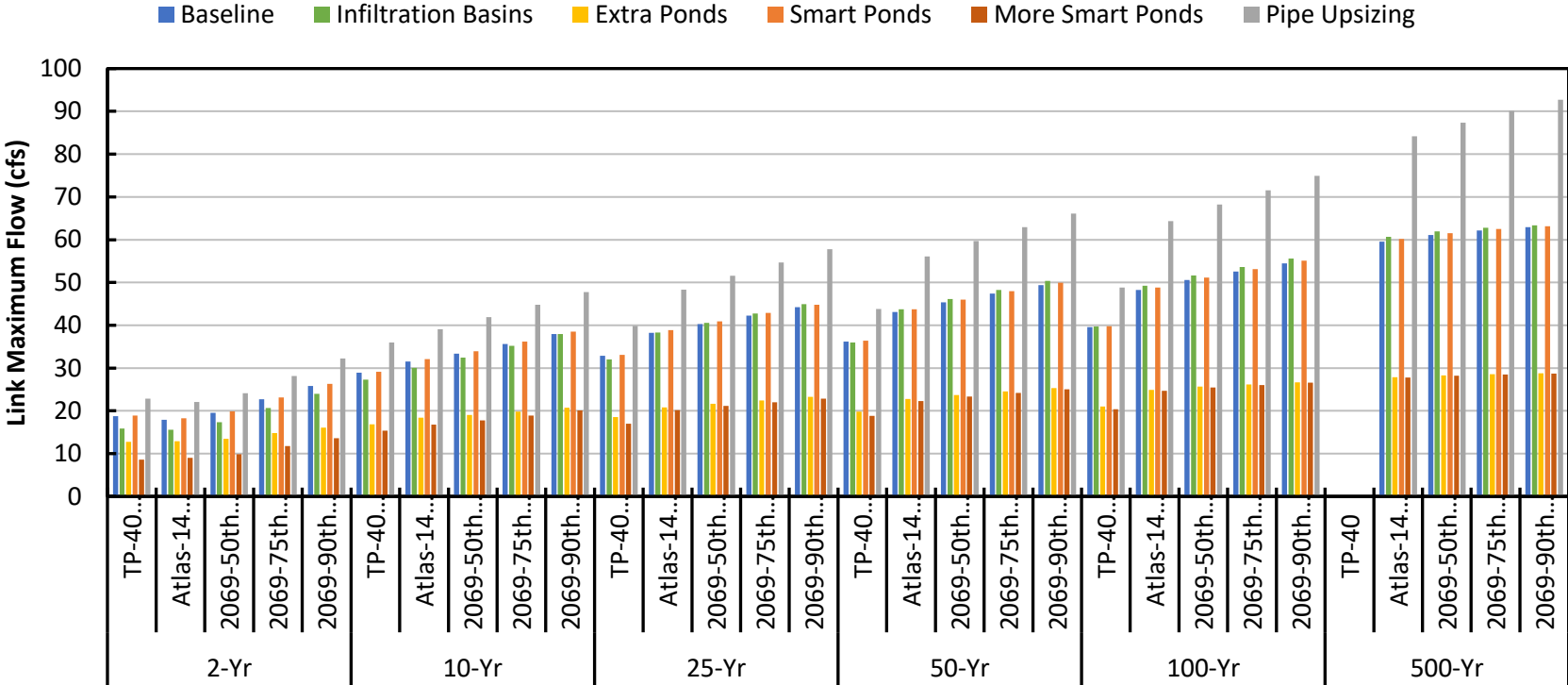


Figure A-24: Maximum Flow Rate (cfs) for the 2-, 10-, 25-, 50-, 100-, and 500-year storms at the outlet (OF441017) of the 1NE watershed in Minneapolis.

Node OF441270

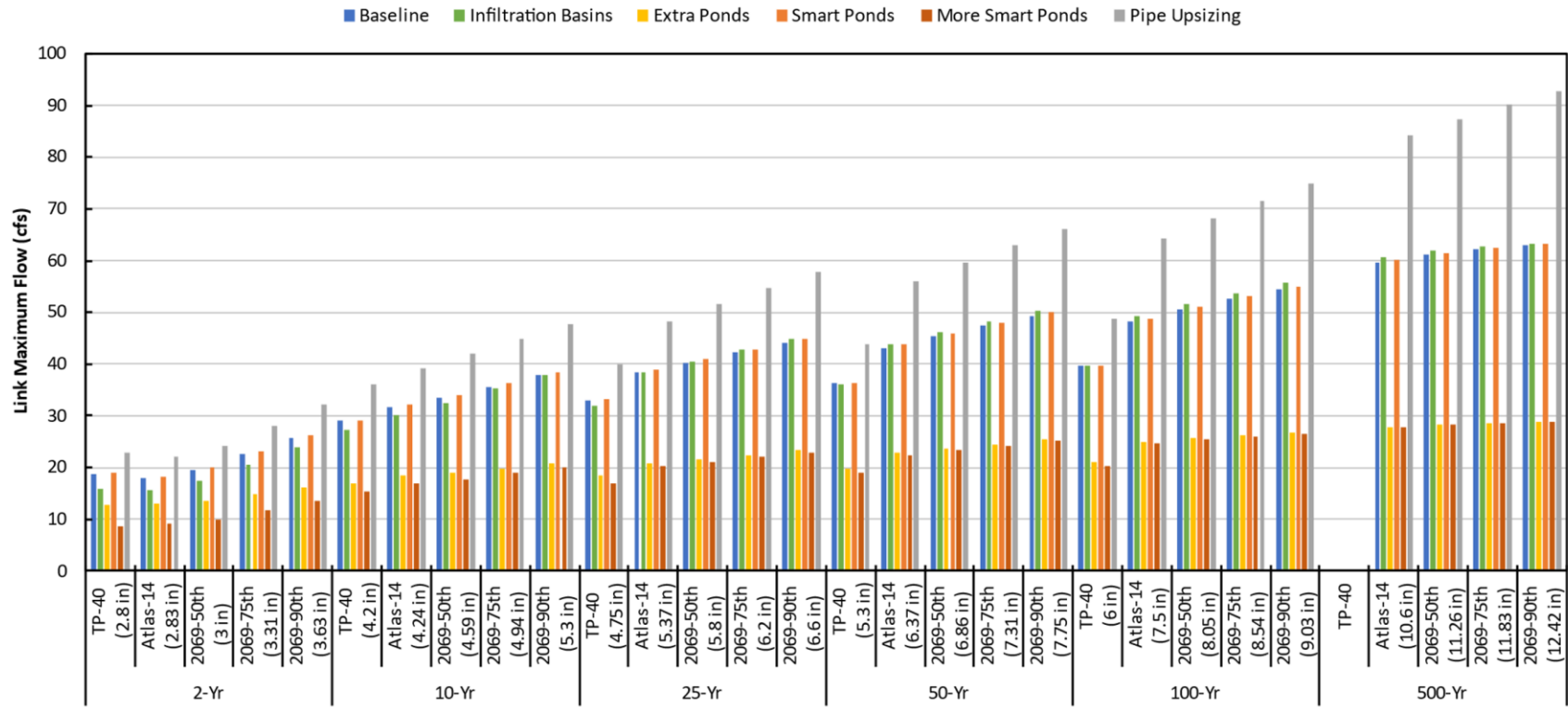


Figure A-25: Maximum Flow Rate (cfs) for the 2-, 10-, 25-, 50-, 100-, and 500-year storms at the outlet (OF441270) of the 1NE watershed in Minneapolis.

Node MH420743



Figure A-26: Flood duration in hours for the 2-, 10-, 25-, 50-, 100-, and 500-year storms at node MH420743 in Minneapolis.

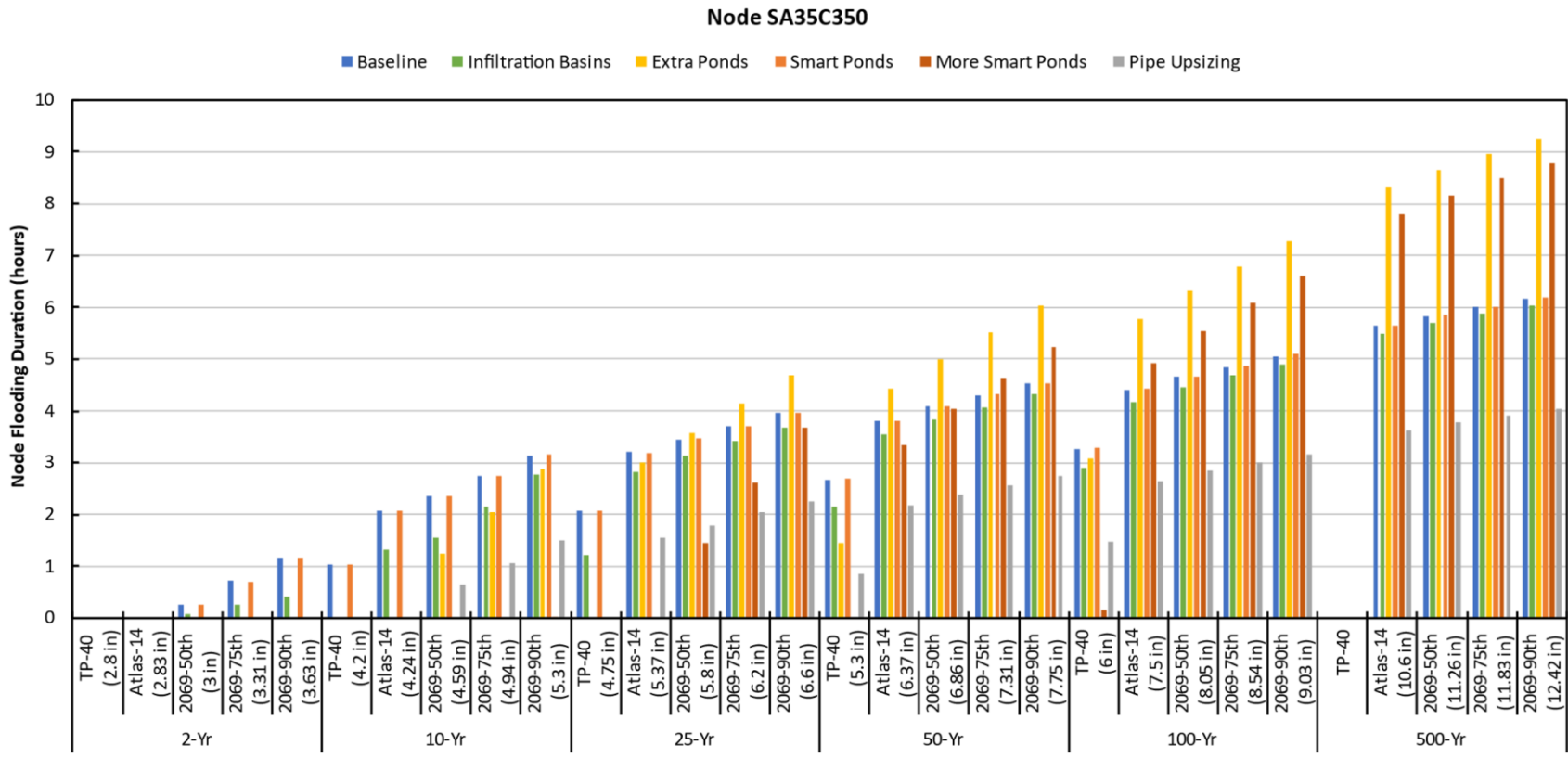


Figure A-27: Flood duration in hours for the 2-, 10-, 25-, 50-, 100-, and 500-year storms at node SA35C350 in Minneapolis.

Node SS512682



Figure A-28: Flood duration in hours for the 2-, 10-, 25-, 50-, 100-, and 500-year storms at node SS5120682 in Minneapolis.

Node SA999039

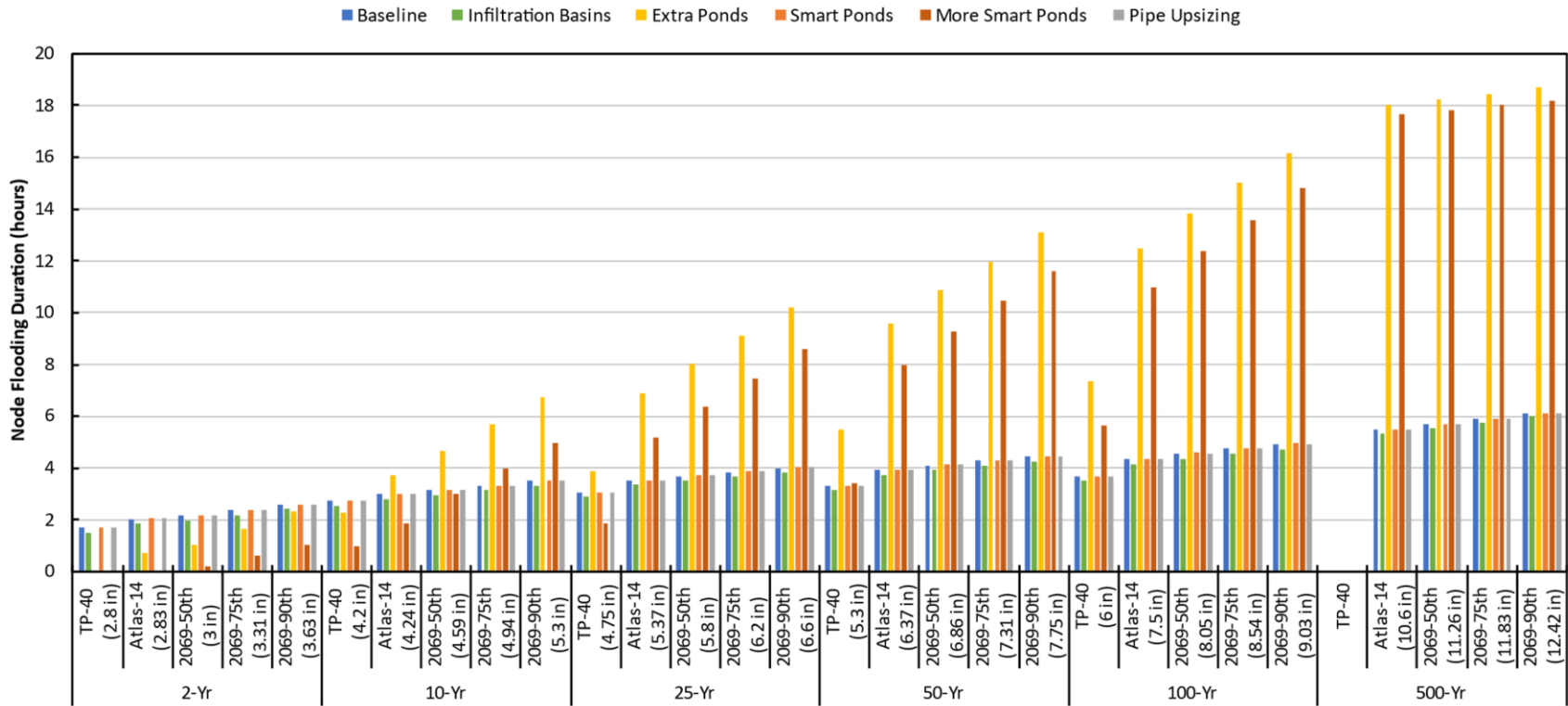


Figure A-29: Flood duration in hours for the 2-, 10-, 25-, 50-, 100-, and 500-year storms at node SA999039 in Minneapolis.

Hydrograph OF441017 Flow during 100 -year Atlas 14 Storm

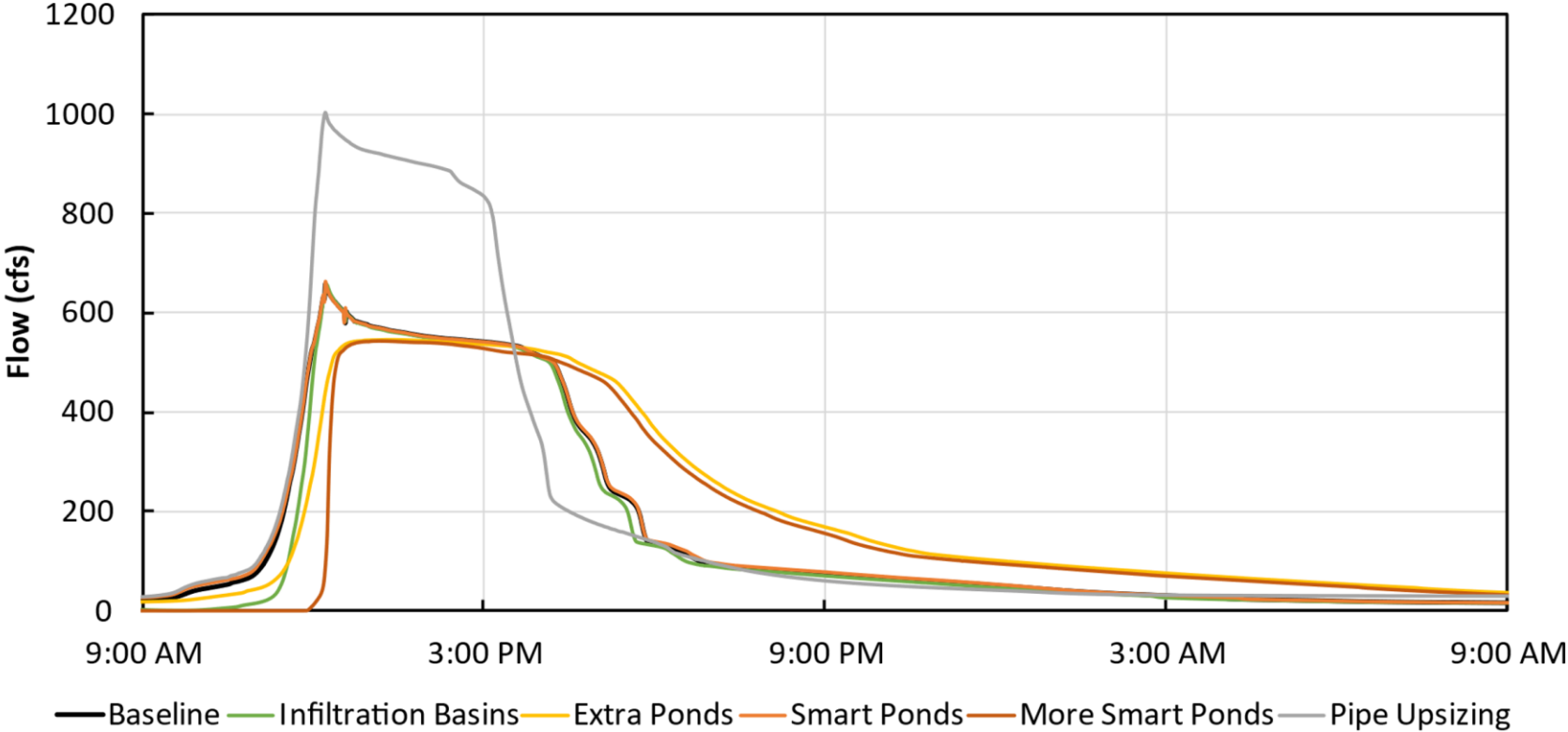


Figure A-30: 1NE Outlet (OF441017) Hydrograph (flow in cfs) for the 100-year Atlas 14 event (7.5 inches)

Hydrograph OF441270 Flow during 100 -year Atlas 14 Storm

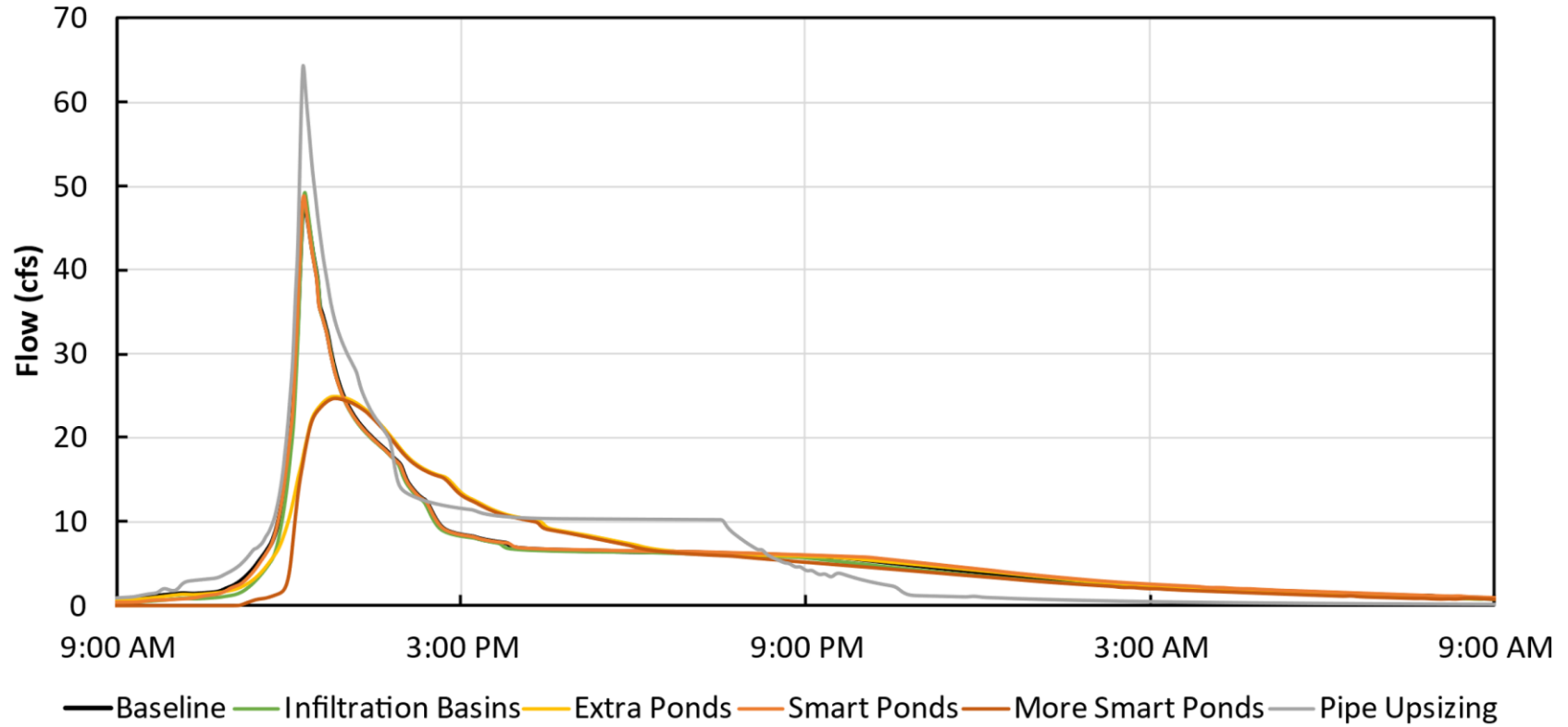


Figure A-31: 1NE Outlet (OF441270) Hydrograph (flow in cfs) for the 100-year Atlas 14 event (7.5 inches)

A.3 SWMM Simulation Results for Kings Run, Rochester

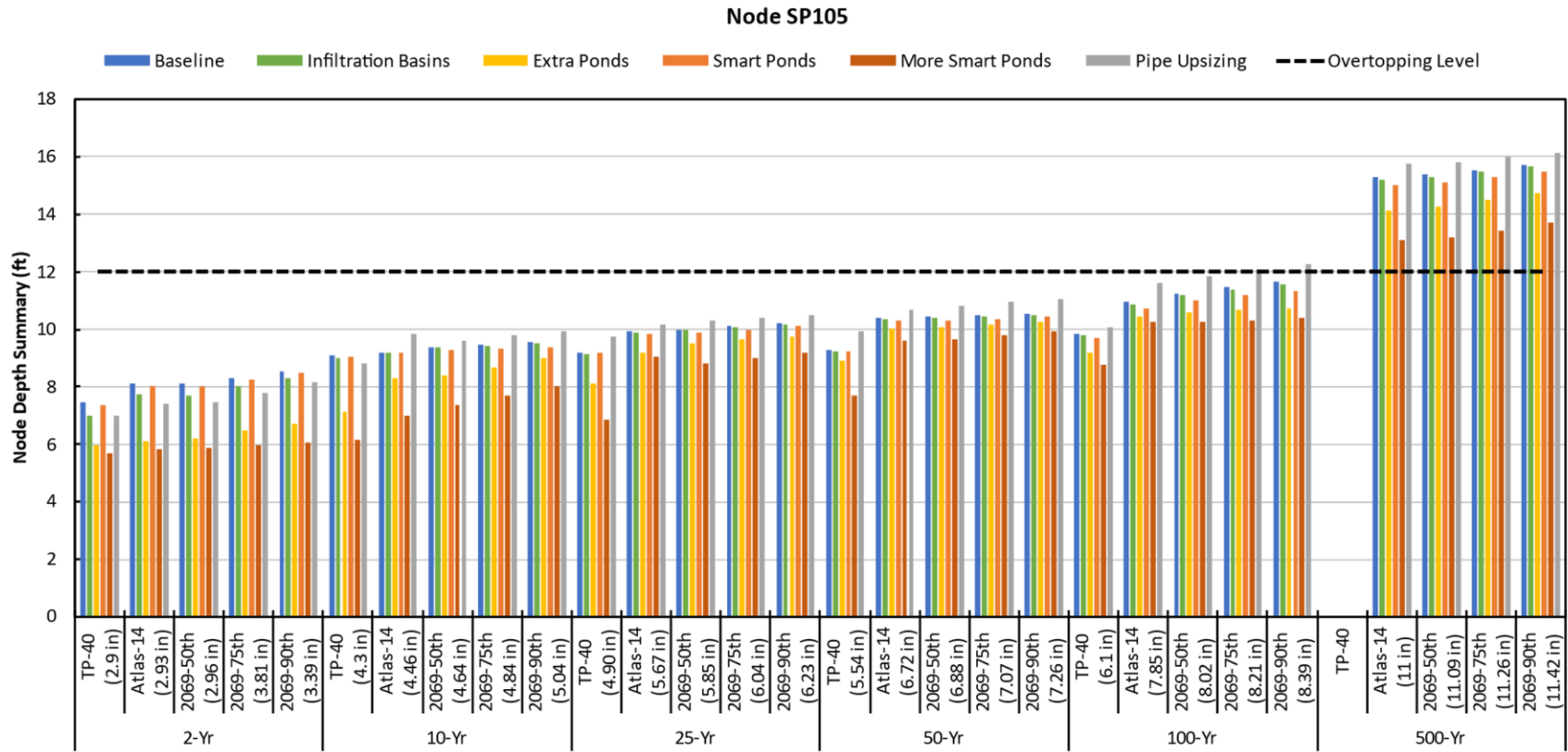


Figure A-32: Node Depth in ft for the 2-, 10-, 25-, 50-, 100-, and 500-year storms at node SP105 in Rochester.

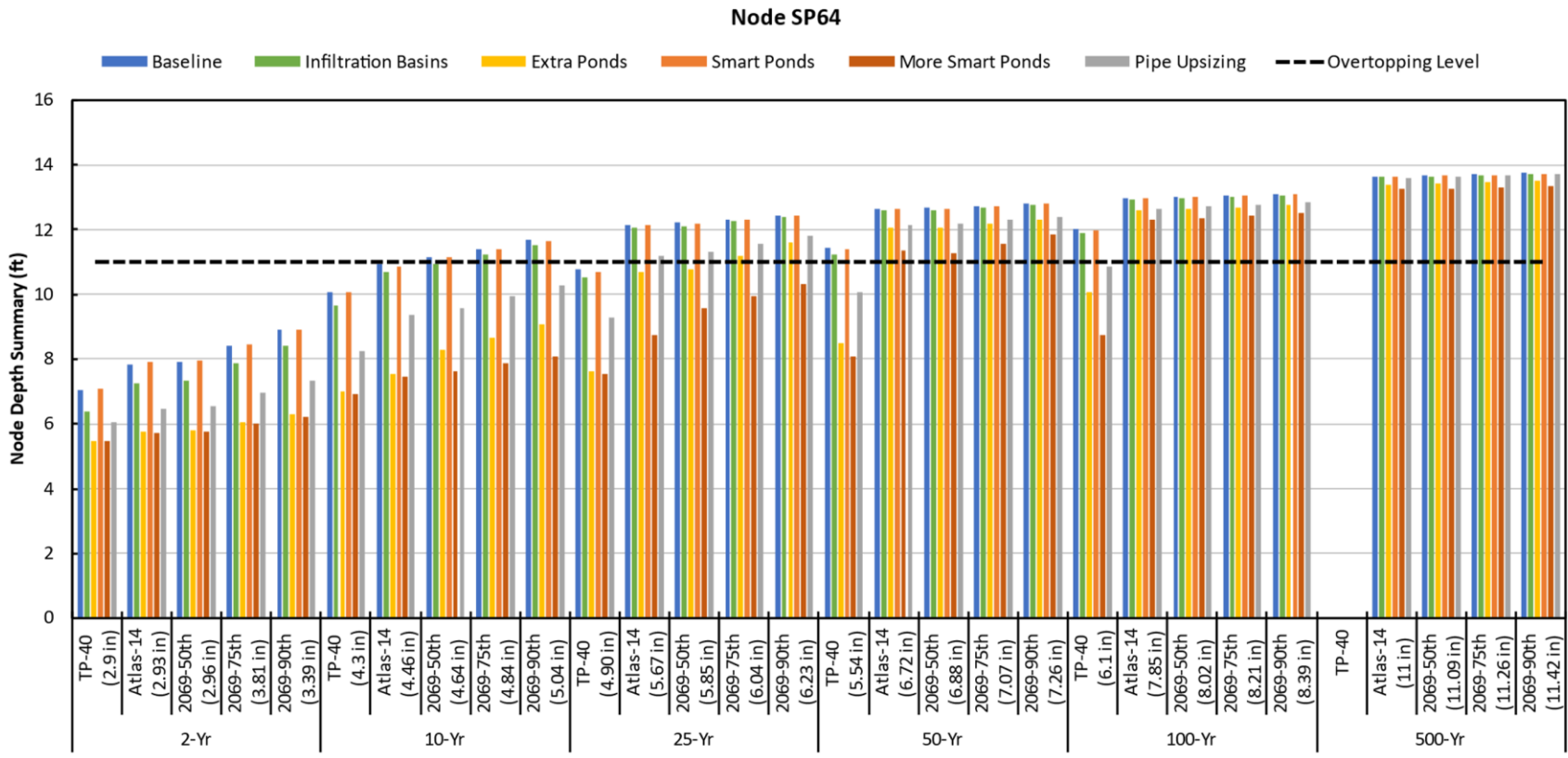


Figure A-33: Node Depth in ft for the 2-, 10-, 25-, 50-, 100-, and 500-year storms at node SP64 in Rochester.

Node RN176248



Figure A-34: Node Depth in ft for the 2-, 10-, 25-, 50-, 100-, and 500-year storms at node RN176248 in Rochester.

Node SP113



Figure A-35: Node Depth in ft for the 2-, 10-, 25-, 50-, 100-, and 500-year storms at node SP113 in Rochester.

Node SP105

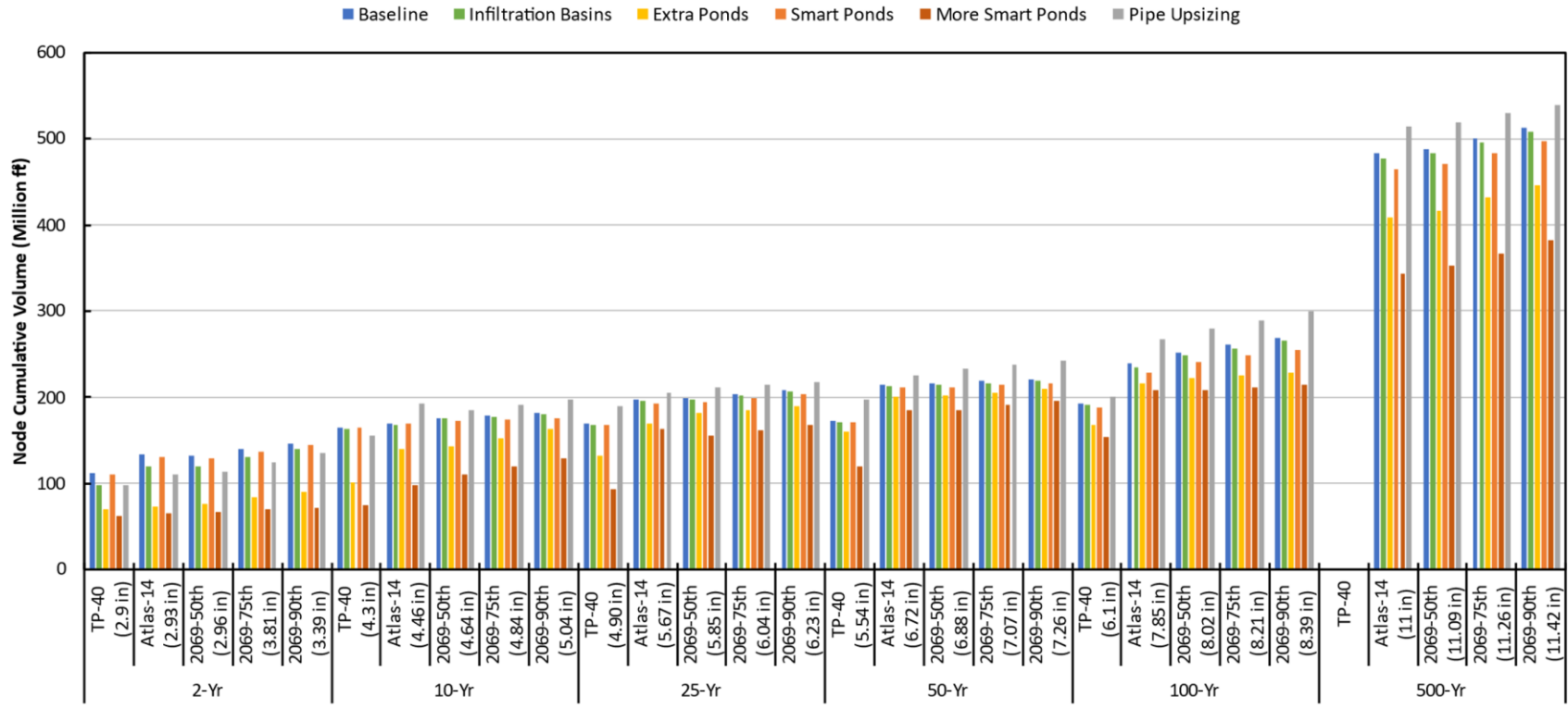


Figure A-36: Cumulative Node volume in million ft³ for the 2-, 10-, 25-, 50-, 100-, and 500-year storms at SP105 in Rochester.

Node SP64

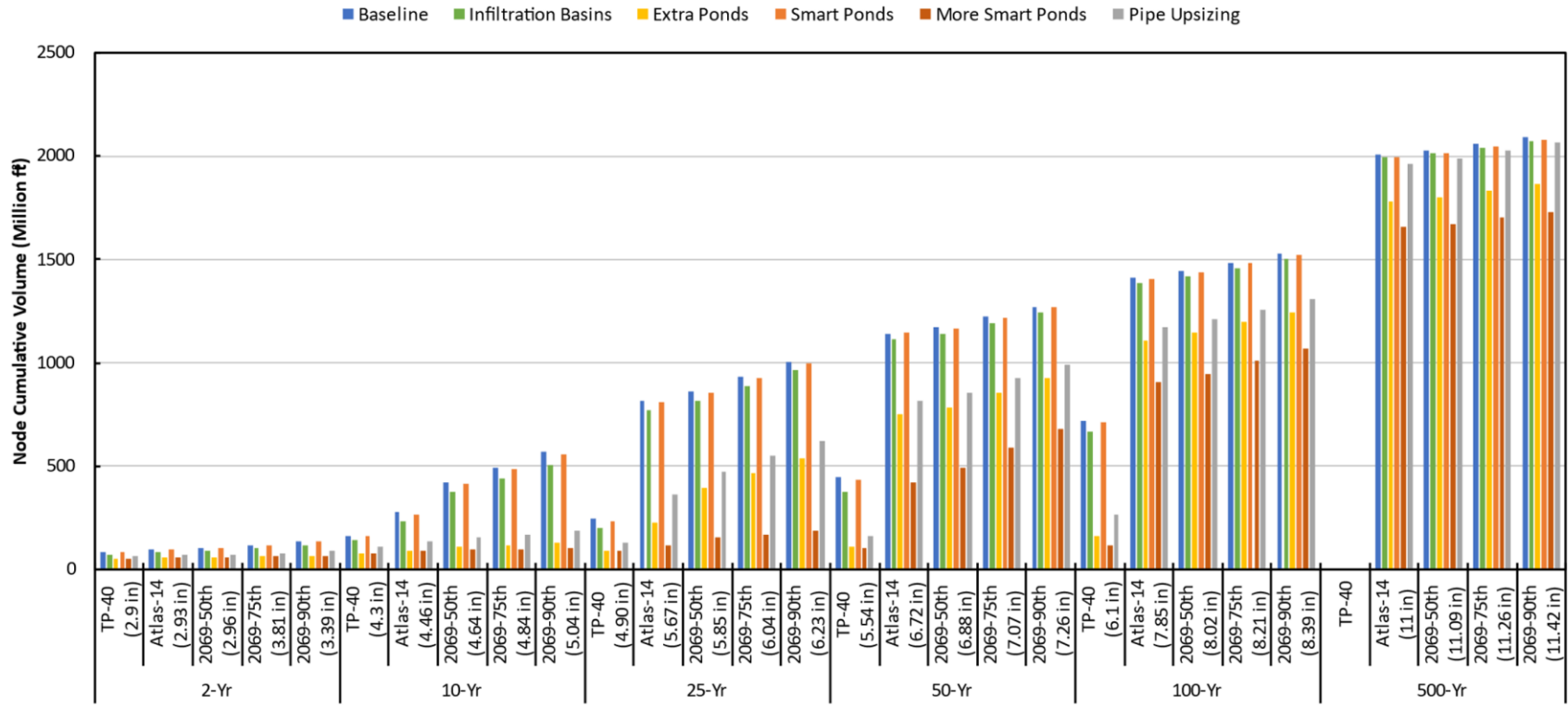


Figure A-37: Cumulative Node volume in million ft³ for the 2-, 10-, 25-, 50-, 100-, and 500-year storms at SP64 in Rochester.

Node RN176248

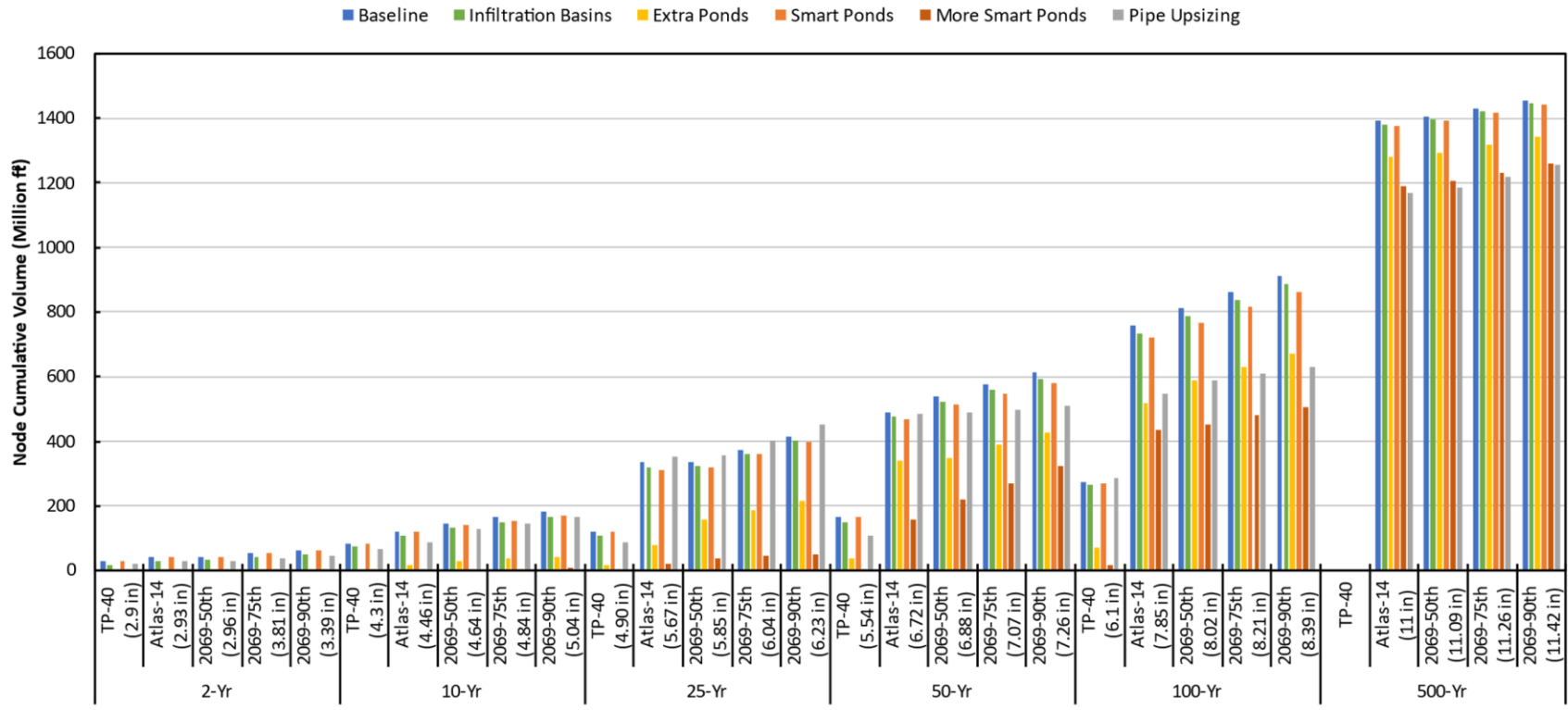


Figure A-38: Cumulative Node volume in million ft³ for the 2-, 10-, 25-, 50-, 100-, and 500-year storms at RN176248 in Rochester.

Node SP113

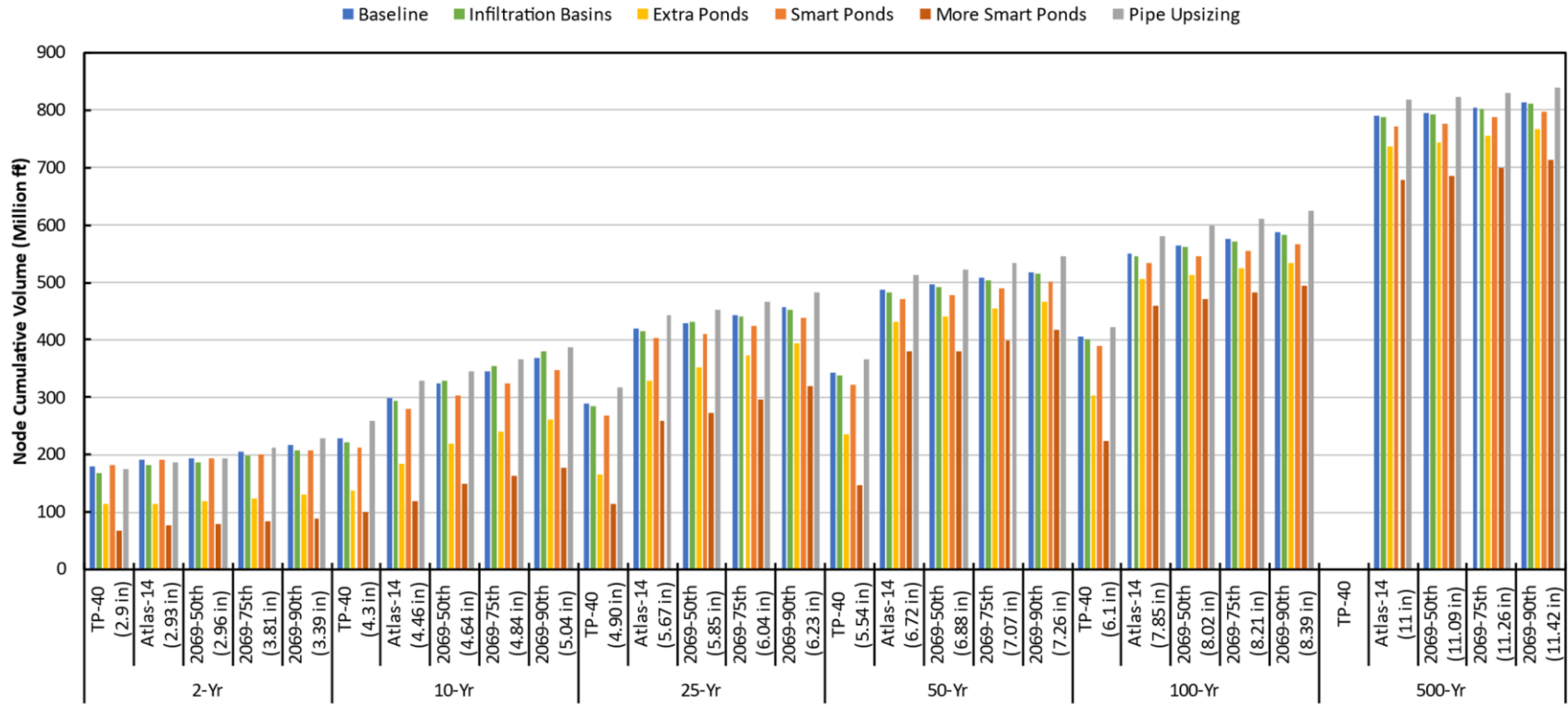


Figure A-39: Cumulative Node volume in million ft³ for the 2-, 10-, 25-, 50-, 100-, and 500-year storms at SP113 in Rochester.

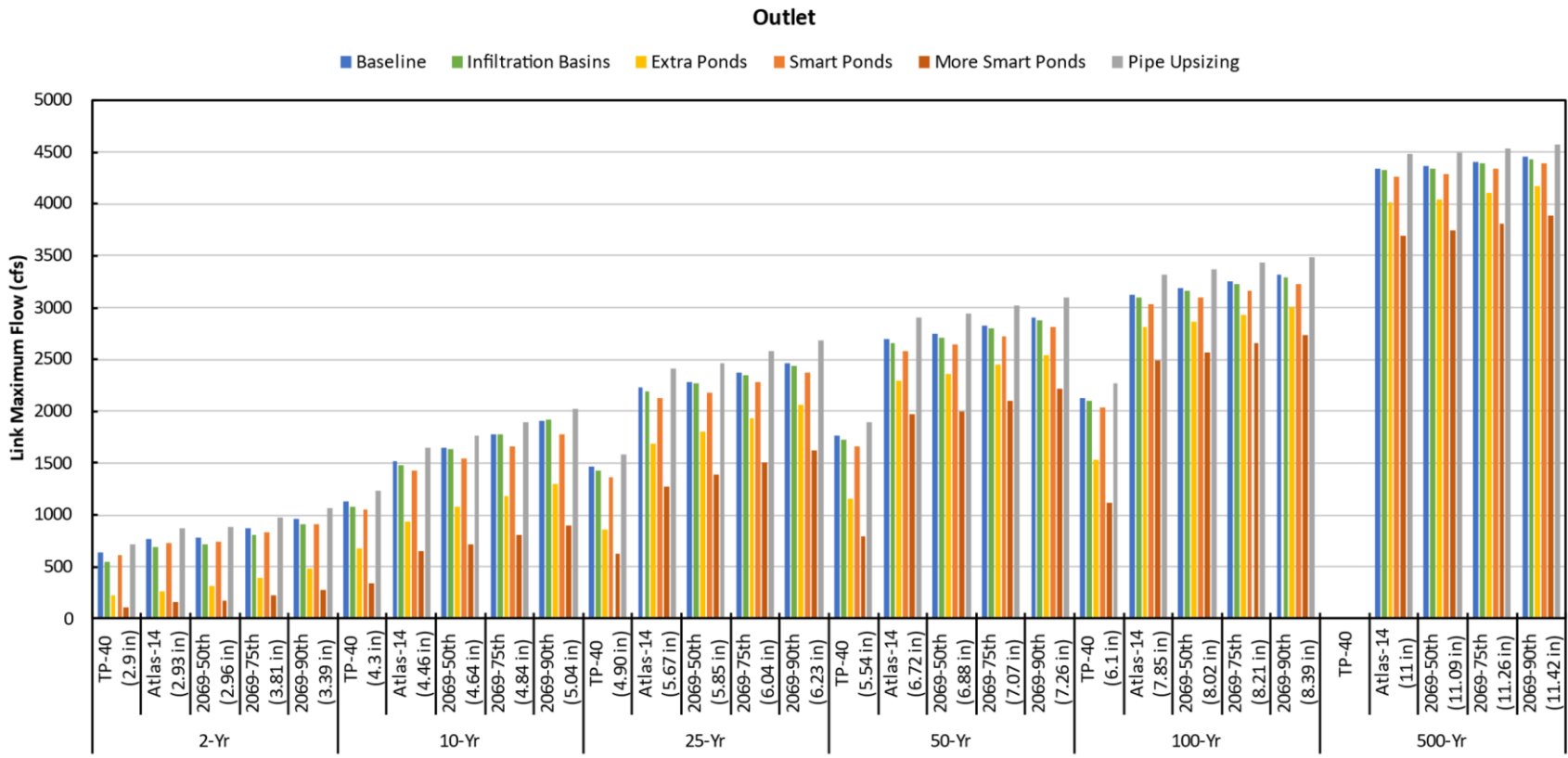


Figure A-40: Maximum Flow Rate (cfs) for the 2-, 10-, 25-, 50-, 100-, and 500-year storms at the outlet (Temp) of the Kings Run watershed in Rochester.

Node SP105

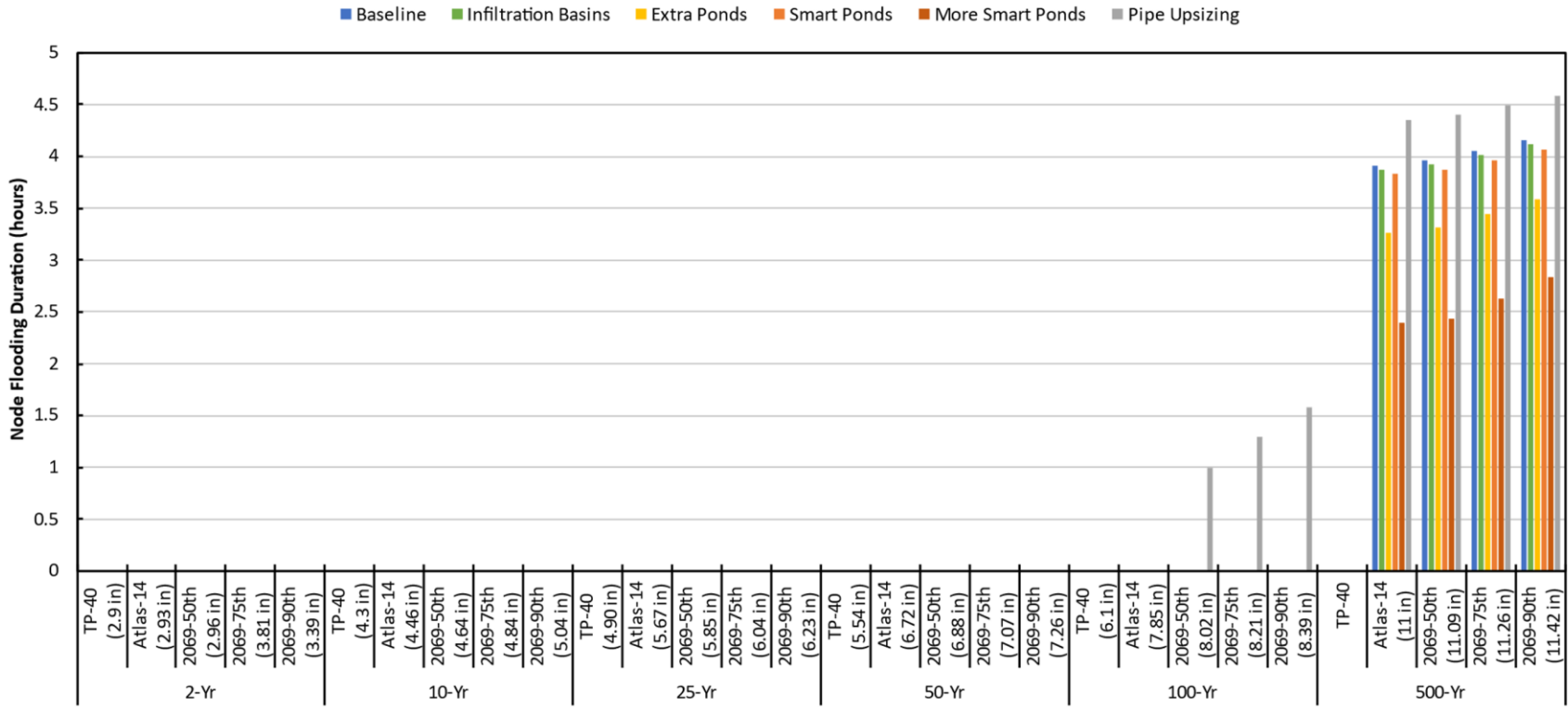


Figure A-41: Flood duration in hours for the 2-, 10-, 25-, 50-, 100-, and 500-year storms at node SP105 in Rochester.

Node SP64



Figure A-42: Flood duration in hours for the 2-, 10-, 25-, 50-, 100-, and 500-year storms at node SP64 in Rochester.

Node RN176248

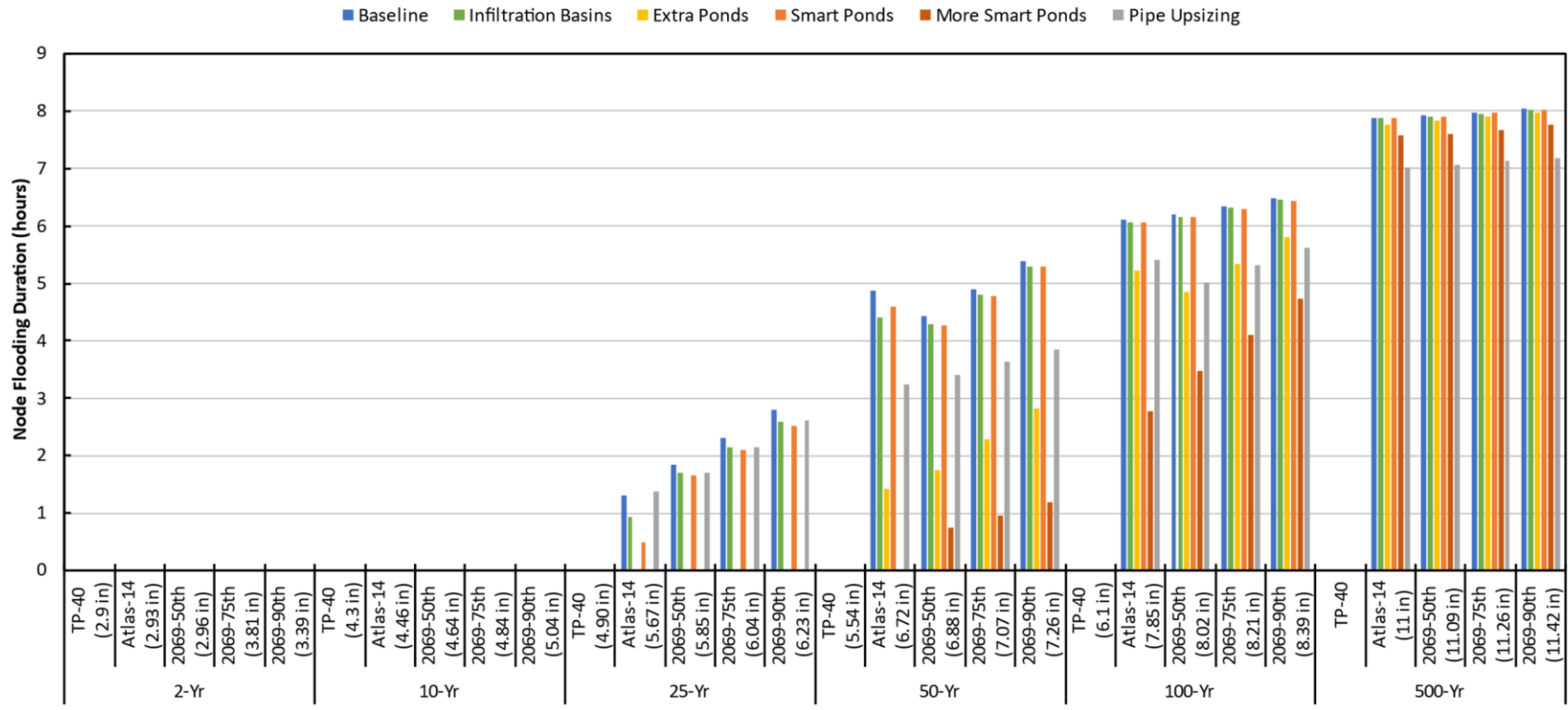


Figure A-43: Flood duration in hours for the 2-, 10-, 25-, 50-, 100-, and 500-year storms at node RN176248 in Rochester.

Node SP113

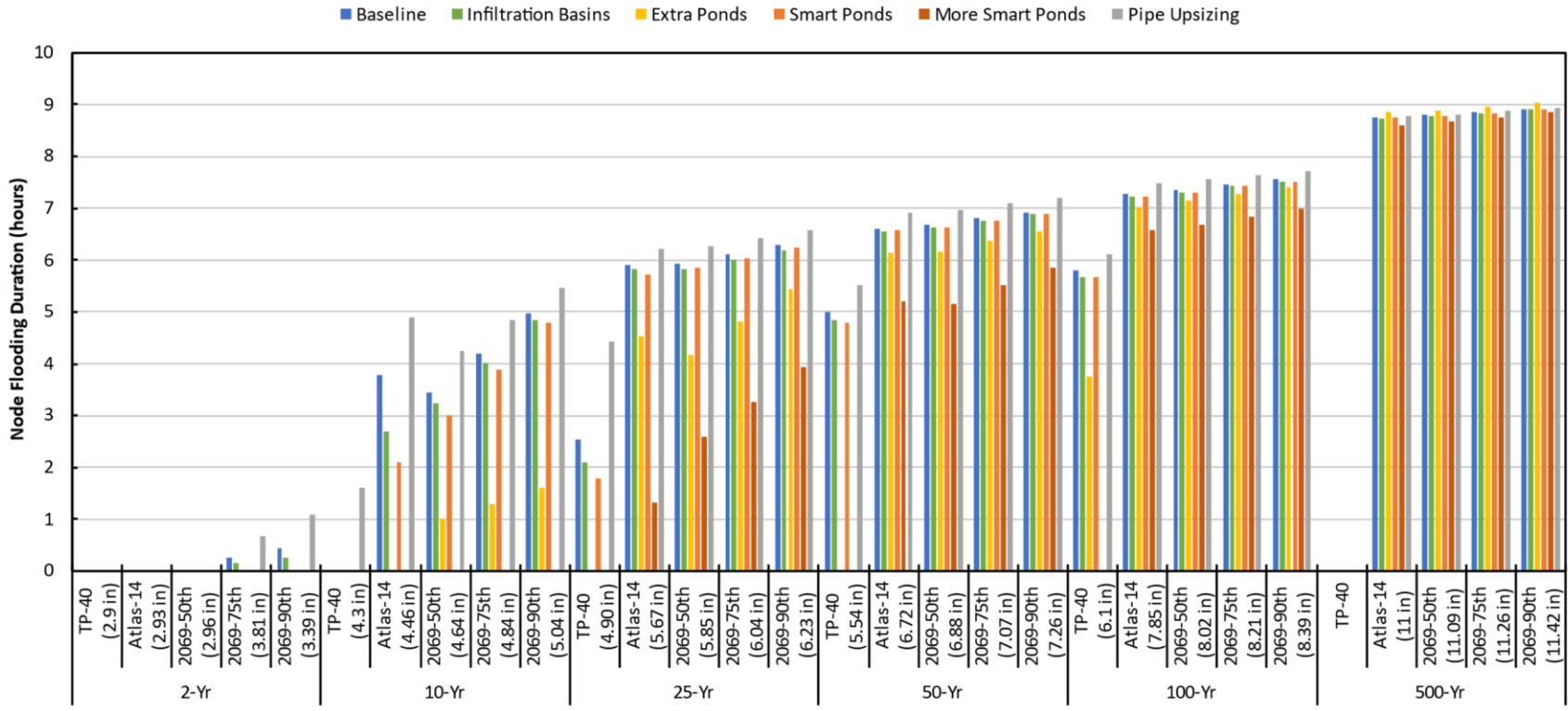


Figure A-44: Flood duration in hours for the 2-, 10-, 25-, 50-, 100-, and 500-year storms at node SP113 in Rochester.

Appendix B: Climate Predictions

B.1 Introduction

The goal of this section is to describe and evaluate methods to determine the 24-hour rainfall depths and the sub-daily rainfall distributions for future climate conditions. These rainfall characteristics are of fundamental importance for assessing adaptations to our stormwater infrastructure to handle larger runoff events. Projections of daily rainfall depths for storms with return periods from 2 to 500 years under different climate change scenarios created by WSP (Dorney and Miller, 2020) are an important part of the analysis. The emphasis of this section is on the methods to determine the depth-duration-frequency (DDF) of sub-daily rainfall distributions. An overview of possible methods has been identified in the literature review completed as part of Section 2. Analyses are limited to our three evaluation sites of Minneapolis-St. Paul, Duluth and Rochester, Minnesota.

This section first provides the general theoretical structure for our method. A summary is then given of the observed data sets and general circulation models and their coupled downscaling algorithms. Different observed data sets are used for daily precipitation, hourly precipitation and 15-minute precipitation. We are primarily interested in the frequency analyses using the annual maximum time series for durations of 15 min to 24 h. A brief description of the trends of the general circulation models (GCMs) of interest for this study is also given. These trends are important in interpreting GCMs in our study. Of greatest interest, however, are the predicted DDF values using the quantile method. The quantile method is evaluated using data sets corresponding to pre-climate conditions (approximately 1950-1979) and current conditions corresponding to a climate change (approximately 1988 to 2017). The predicted DDF values using the quantile method are then compared to those obtained using NWS Atlas 14 (Perica et al, 2013). To illustrate the use of quantile method for this project, design storms are developed for the time period of 2040 to 2069.

B.2 Theoretical Framework

B.2.1 Frequency Analysis of Sub-daily Precipitation Depth

Frequency analyses of precipitation depths are often summarized using DDF curves or tables. These analyses are generally done by fitting probability density functions to annual maximum or partial duration time series. We limit our analysis to annual maximum series. For annual series, the cumulative probabilities are conveniently related to return periods as:

$$T = \frac{1}{1 - F(x)} \quad 1$$

where T is the return period and F(x) is the cumulative probability for a depth of x.

Two different probability density functions were considered to represent the frequency of depths for different duration. One of the distributions is the extreme value type I (EV1) distribution. This distribution was used for DDF of TP-40 (Hershfield, 1961) and was the distribution for the seminal work

of Srivastav et al. (2014) on the quantile method. The probability density function of the EV1 is defined as:

$$f(x) = q \exp[(-q(x-w) - \exp(-q(x-w)))] \text{ for } -\infty < x < \infty \quad 2$$

where $f(x)$ is the probability density function and where the statistical parameters of q and w are defined using the mean and standard deviations of the observed data as:

$$q = \frac{\pi}{s\sqrt{6}} \text{ and } w = \bar{x} - \frac{0.5572}{q} \quad 3$$

The EV1 cumulative distribution, $F(x)$, and its inverse are defined as:

$$F(x) = \int_{-\infty}^x f(x) dx = \exp[-\exp(-q(x-w))] \quad 4$$

$$x = F^{-1}(x) = w - \frac{\ln(-\ln(F(x)))}{q} \quad 5$$

If two points are known for $F(x)$ and x , we can rearrange and solve for the statistical parameters of q and w . By using the inverse function, we have:

$$x_1 = w - \left(\frac{\ln(-\ln(F(x_1)))}{q} \right) \quad 6$$

$$x_2 = w - \left(\frac{\ln(-\ln(F(x_2)))}{q} \right) \quad 7$$

where the depths x_1 and x_2 are known for the cumulative probabilities of $F(x_1)$ and $F(x_2)$.

For our applications, x_1 and x_2 are the depths corresponding to the 10-y and 100-y return periods. We can rearrange and solve for q and w as:

$$q = \frac{\ln(-\ln(F(x_1))) - \ln(-\ln(F(x_2)))}{x_2 - x_1} \quad 8$$

$$w = x_1 + \left(\frac{\ln(-\ln(F(x_1)))}{q} \right) \quad 9$$

The other probability density function of interest is the generalized extreme value distribution (GEV). This distribution is used for the DDF analysis of Bulletin 71 (Huff and Angel, 1992) and Atlas 14. The probability density function is defined as:

$$f(x) = \frac{1}{\beta} \left(1 - \frac{\gamma(x-\alpha)}{\beta} \right)^{-1+1/\gamma} \exp \left(- \left(1 - \frac{\gamma(x-\alpha)}{\beta} \right)^{1/\gamma} \right) \text{ for } -\infty < x < \infty \quad 10$$

where α , β and γ are parameters fitted to observed or GCM data.

The statistical parameters of α , β and γ are estimated using L-moments defined using theoretical concepts of ordered statistics (Landwehr et al., 1979; Hosking, 1990). Data are first ordered from smallest to largest. Definition of the first three L-moments are:

$$L_1 = \bar{x}, \quad L_2 = 2 b_1 - \bar{x}, \quad L_3 = 6 b_2 - 6 b_1 + \bar{x} \quad \text{and} \quad t_3 = \frac{L_3}{L_2} \quad 11$$

where b_1 and b_2 are defined using the ordered x values as:

$$b_1 = \frac{1}{n} \sum_{i=1}^N \left(\frac{i-1}{n-1} \right) x_i \quad \text{and} \quad b_2 = \frac{1}{n} \sum_{i=1}^N \left(\frac{(i-1)(i-2)}{(n-1)(n-2)} \right) x_i \quad 12$$

Parameter values for the GEV are now determined as:

$$z = \frac{2}{3 + t_3} - \frac{\ln(2)}{\ln(3)} \quad \text{and} \quad \gamma \approx 7.859 z + 2.9554 z^2 \quad 13$$

$$\beta = \frac{L_2 k}{(1 - 2^{-k})\Gamma(1+k)} \quad \text{and} \quad \alpha = \bar{x} + \beta \left(\frac{\Gamma(1+\gamma) - 1}{\gamma} \right) \approx 7.859 z + 2.9554 z^2 \quad 14$$

The cumulative distribution of the GEV is determined as:

$$F(x) = \int_{-\infty}^x f(x) dx = \exp \left(- \left(1 - \frac{\gamma(x-\alpha)}{\beta} \right)^{1/\gamma} \right) \quad 15$$

The above equation can be rearranged to solve for x for a given cumulative distribution. The inverse of the GEV is then obtained as:

$$x = F^{-1}(x) = \alpha + \frac{\beta (1 - [-\ln(F)]^\gamma)}{\gamma} \quad 16$$

The three parameters of the GEV can be estimated from three known return period depths corresponding to inverse functions, that is:

$$x_1 = \alpha + \frac{\beta (1 - [-\ln(F_1)]^\gamma)}{\gamma}, \quad x_2 = \alpha + \frac{\beta (1 - [-\ln(F_2)]^\gamma)}{\gamma}, \quad x_3 = \alpha + \frac{\beta (1 - [-\ln(F_3)]^\gamma)}{\gamma} \quad 17$$

We generally use the 2-y, 10-y and 100-y return period depths for x_1 , x_2 , and x_3 . By subtracting x_2 from x_3 and x_1 from x_2 , we have:

$$\beta = \frac{\gamma (x_{100} - x_{10})}{(-\ln(F_{10}))^\gamma - (-\ln(F_{100}))^\gamma} = \frac{\gamma (x_{10} - x_2)}{(-\ln(F_2))^\gamma - (-\ln(F_{10}))^\gamma} \quad 18$$

By rearranging terms, we obtain:

$$\frac{(-\ln(F_2))^\gamma - (-\ln(F_{10}))^\gamma}{(-\ln(F_{10}))^\gamma - (-\ln(F_{100}))^\gamma} - \frac{x_{10} - x_2}{x_{100} - x_{10}} = 0 \quad 19$$

This relationship is used to determine γ . An iterative solution is required. For a known γ , we can solve for β and α as:

$$\beta = \frac{\gamma (x_{100} - x_{10})}{(-\ln(F_{10}))^\gamma - (-\ln(F_{100}))^\gamma} \quad \text{and} \quad \alpha = x_2 - \frac{\beta (1 - [-\ln(F_2)]^\gamma)}{\gamma} \quad 20$$

B.2.2 Quantile Method

As discussed in the literature review of Section 2, the quantile method is often used to estimate the frequency of the sub-daily precipitation depth. With this method, we are interested in the observed cumulative distributions for the sub-daily depths and the predicted daily precipitation depths for the current and future conditions obtained by GCMs. Once again, we are using the annual maximum series. The cumulative distribution for the observed data set is represented by the notation of:

$$F_o(X_{oj} | \theta_{oj}) \quad \text{and} \quad X_{oj} = F_o^{-1}(X_{oj} | \theta_{oj}) \quad 21$$

where the subscript o is for observed, subscript j represents different durations varying from 0.25 h to 24 h and θ_{oj} is the parameters of the probability density function (q and w for EV1 or α , β and γ for GEV).

The corresponding notation for the current and future cumulative distributions of daily precipitation from our GCM is:

$$F_p(X_{p24}^c | \theta_{p24}^c), X_{p24}^c = F_p^{-1}(X_{p24}^c | \theta_{p24}^c) \quad \text{and} \quad F_p(X_{p24}^f | \theta_{p24}^f), \quad 22$$

$$X_{p24}^f = F_p^{-1}(X_{p24}^f | \theta_{p24}^f)$$

where the superscripts “c” and “f” are used to represent the current and future conditions and the subscript “p” for predicted daily depths.

The quantile method is shown graphically in Figure B-. The left-sided cumulative frequencies correspond to those obtained from the GCM for the current conditions (solid line) and future conditions (dotted line). These distributions are therefore known. The solid lines for the sub-daily duration for the right-sided graphs correspond to the frequency analysis obtained using the current data sets. These distributions are also known. The quantile method is used to estimate the future distributions by using the shift in cumulative probability obtained from the GCM.

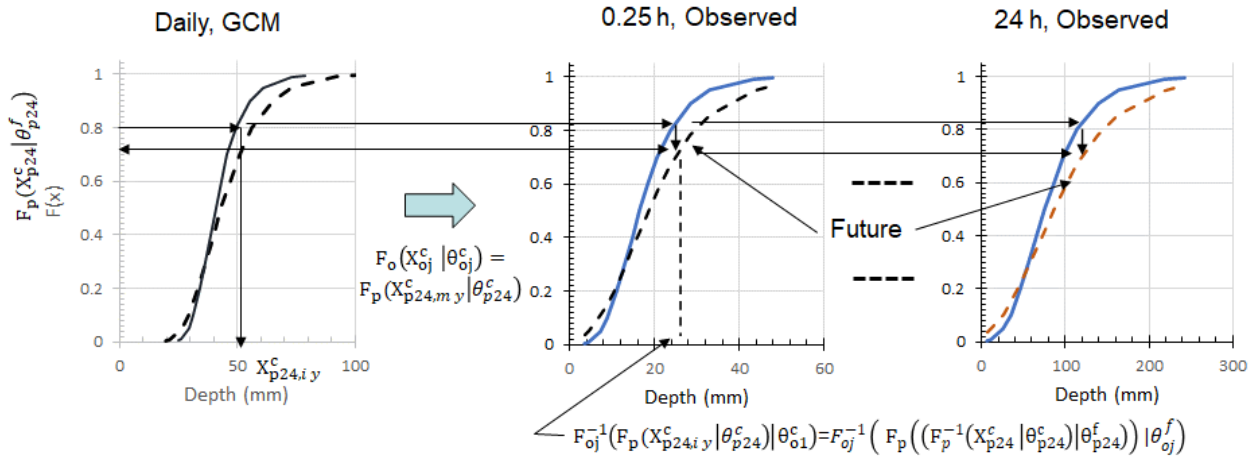


Figure B-1: Illustration of the Quantile Method

B.2.2.1 Key steps for the quantile method

1. Compute the statistical parameters of probability density functions of the maximum sub-daily time series of observed 15-min and 1-h data sets. We examine sub-daily durations of 15 min, 30 min, 45 min, 1 h, 2 h, 4 h, 6 h, 12 h and 24 h. The set of parameters for the current conditions is represented by the notation of θ_{oj}^c .
2. Adjust the observed data set for consistency between different duration. This step is necessary because of the limitations of observed data.
3. Compute the statistical parameters of probability density functions of the maximum daily time series of GCM. Sets of parameters for the current and future conditions are represented by the notation of θ_{p24}^c and θ_{p24}^f .
4. Select different cumulative probabilities for the evaluation rainfall depths for future conditions. We report results for probabilities corresponding to the 2-yr, 10-yr and 100-yr return period events. However, trends shown in graphs are based on twenty-two rationally spaced cumulative probabilities between $F(x) = 0.001$ and $F(x)=0.999$.
5. For the daily GCM using current conditions, compute the current depth corresponding to each of the cumulative probabilities. This depth is represented by $X_{p24}^c = F_p^{-1}(X_{p24}^c | \theta_{p24}^c) = F_p^{-1}(0.8)$ in Fig. 1.
6. For each depth in Step 5, compute the cumulative probability corresponding to the future using GCM predictions. In Fig. 1, this probability is $F_p(X_{p24}^c | \theta_{p24}^f) = 0.67 = F_p((F_p^{-1}(X_{p24}^c | \theta_{p24}^c) | \theta_{p24}^f))$.
7. For the observed distributions of the sub-daily durations (including 24 h), compute the depths for the cumulative probabilities defined in Step 4. For each j sub-daily duration, these depths are represented by the notation of $X_{oj}^c = F_{oj}^{-1}(F_p(X_{p24}^c) | \theta_{oj}^c)$.
8. Determine the future cumulative distributions for the sub-daily depths of Step 7 by using the shift in cumulative distribution of GCM given in Step 6. For the illustration in Fig. 1, the depth

originally defined cumulative distribution of 0.8 ($X_{oj}^c = F_{oj}^{-1}(0.8)$) corresponds to the depth of cumulative distribution of 0.67 under future conditions ($F_{oj}(X_{oj}^c | \theta_{oj}^f) = 0.67$).

9. Compute the statistical parameters for cumulative distributions under future conditions (θ_{oj}^f) using Eqs. 8 and 9 for EV1 distributions and Eqs. 19 and 20 for GEV distributions. For the EV1, the current depths of 10-yr and 100-yr return periods were used for x_1 and x_2 and the shifted cumulative distributions were used $F(x_1)$ and $F(x_2)$. For the GEV distribution, the current depth of 2-yr and the corresponding shifted cumulative probability were also included in computing its parameters.
10. By using the statistical parameters under future conditions of Step 9, compute the depths for each of the cumulative probabilities of Step 4 for each of the sub-daily durations.

B.2.3 Temporal Storm Pattern

The quantile method of the previous section allows us to determine DDF values for future conditions for sub-daily durations. These values are used to determine the distribution of rainfall depths within the design storms necessary for the SWMM simulations. We use a synthetic pattern where the return period for each duration within the storm is equal to the design return period. This approach is also used for the widely used SCS Types I and II patterns (Soil Conservation Service, 1972). We organize the pattern such that the maximum rainfall depth occurs at the midpoint of a 24-hour storm. The storm pattern is tied to the frequency analysis of WSP by normalizing the quantile results using the 24-hour depth, that is:

$$P_j^* = \frac{P_j^f}{P_{24}^f} \tag{23}$$

The normalization increases the robustness of the approach. If fractional change in the precipitation depth for duration j ($P_j^f = kP_j^c$) is the same as that for the 24-h depth ($P_{24}^f = kP_{24}^c$), then the normalized depth doesn't change under future conditions. The precipitation depth for a design event is obtained by multiplying the normalized depth by the return period of the daily depth obtained by WSP.

B.3 Data and GCM Predictions

B.3.1 Acquisition of Observed Climate Data

Observed precipitation and air temperature data for the three study sites (Minneapolis, Duluth, Rochester) were obtained for daily, hourly, and sub-hourly time steps. The daily and hourly data sets were obtained for the Minneapolis, Duluth, and Rochester international airports (MSP, DLH, RST) from the Midwestern Regional Climate Center (<https://mrcc.illinois.edu/CLIMATE/>). The hourly weather data were downloaded for the full record available, 1945-2020, 1948-2020, and 1948-2020, for MSP, DLH, and RST, respectively. The daily weather records were downloaded for the same time periods, although longer records are available.

The hourly precipitation data were not complete, with many missing records and some years with 3 hour, rather than 1 hour, data. To help select years with relatively complete hourly precipitation data for analysis, the total annual rainfall for each year was calculated using both the hourly and daily data, and the ratio of the two (hourly total/daily total) was calculated. The precipitation ratio for Minneapolis is shown in Figure B-2. As discussed later, the years 1965-1969 were discarded (3-hour precip data), and the year 2003 was corrected by noting the presence of three 6.0 inch rainfall events in December that do not appear in rainfall records from another source.

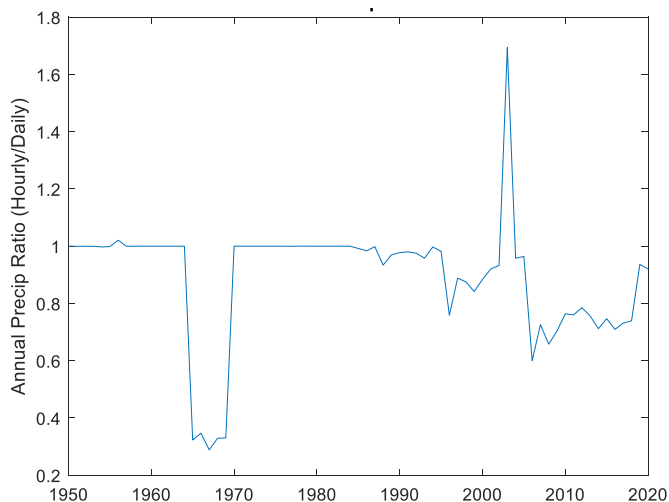


Figure B-2: Ratio of total annual precipitation calculated from hourly and daily precipitation data for Minneapolis.

The 15-min data were obtained from the NOAA webpage of <https://www.ncdc.noaa.gov/>. The WINDS model (Wilson and Sheshukov, 2011) was used to determine annual maximum series of depths corresponding to different durations. The sites of the 15-min data are different than the hourly and daily data. We used the data at Golden Valley (GV), MN for MSP, at Holyoke, MN for DLH and Spring Valley, MN for RST. The analyses were performed for 1972 through 2013. Some of the years had significant missing data and were not used in the analysis.

B.3.2 Acquisition of Downscaled Global Climate Model Data

Several sources of downscaled global climate precipitation and air temperature data were outlined in Section 2. For this analysis, LOCA (Localized Constructed Analogs, Pierce et al., 2014) data based on the CMIP5 (Climate Model Intercomparison Project, 5th exercise) were used, the same data source (https://gdo-dcp.ucllnl.org/downscaled_cmip_projections/) used by WSP in their analysis of future storms in Minnesota (Dorney and Miller, 2020). Downscaled air temperature and precipitation data were downloaded as daily time series from 1950 to 2099 for locations corresponding to the Rochester, Minneapolis, and Duluth international airports. Data were downloaded for all available GCMs (32) and CO₂ emission scenarios (RCP4.5 and RCP8.5, Figure B-3). The two GCM/CO₂ emission scenarios used by

WSP in their storm analysis (mpi-esm-mr rcp4.5 and mpi-esm-mr rcp8.5) were emphasized in this analysis, but some results from other GCMs are included in this report to show the variability between GCMs. The deliverables for the WSP project that were available for this study included maps of future storms depths for the mpi-esm-mr rcp4.5 and mpi-esm-mr rcp8.5 GCM projections, and maps of the % change in future storm depths for 32 GCMs and 2 CO₂ emission scenarios.

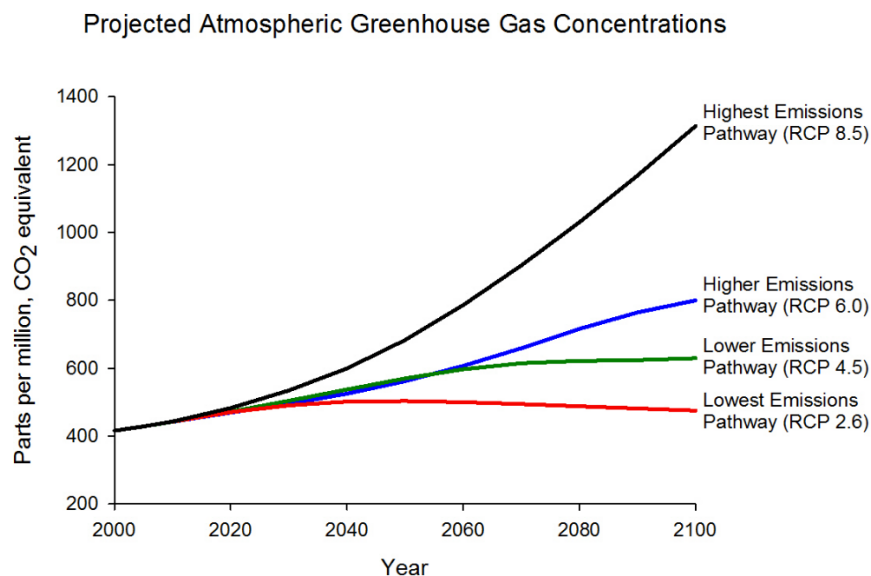


Figure B-3: Equivalent CO₂ emissions for the RCP 2.6, 4.5, 6.0 and 8.5 scenarios using in CMIP5 (source epa.gov).

B.3.3 Analysis and Comparison of Observed and Downscaled GCM Climate Data

The analysis of observed and simulated (downscaled GCM) climate data included the following:

1. Analysis of annual precipitation for historical periods (mean, standard deviation, trends)
2. Analysis of annual maximum daily precipitation (mean, trends, probability density functions). Generalized Extreme Value (GEV, see Theoretical Framework section) analysis was used to examine the distribution of daily precipitation data for historical and future periods.
3. A comparison of the probability of wet days for observed and simulated data. The probability of a wet day was calculated from the simulated and observed daily precipitation time series, with a wet day defined as any day with measurable precipitation. In addition, the probability of wet day following a wet day was calculated, to help inform antecedent conditions for storm events.
4. Relationships between precipitation intensity and air temperature were examined, based on previous work which found that storm intensity systematically increases with increasing air temperature (Lenderink et al. 2010, Lepore et al. 2015). Hourly precipitation data were binned by mean daily air temperature, the percentiles (or return periods) of the hourly precipitation values were calculated for each bin, and trends in the precipitation data with temperature were examined and compared to theoretical relationships.

B.3.4 Results: Comparison of Observed and Simulated Precipitation Data

B.3.4.1 Annual Precipitation

Observed and simulated annual precipitation statistics were compiled for the three study sites. The GCM precipitation statistics matched the mean and standard deviation of the observed precipitation fairly well for the period 1950-2020 (Table B-). However, the slopes (trends) of the observed annual precipitation were not reproduced by the GCMs, with the GCMs underpredicting the observed slope for Minneapolis (Figure B-4) and Rochester, and overpredicting the observed slope for Duluth. Over the period 1985-2099, the two GCMs projected increasing annual precipitation of 0.28 to 1.68 mm/year (Table B-).

Table B- gives results for the mpi-esm-mr rcp4.5 and mpi-esm-mr rcp8.5 GCM simulations. Analyzing all 64 GCM simulations for the Minneapolis site, the slope of annual precipitation for the period 1950-2020 varied from -0.066 in/year to 0.092 in/year. Therefore, none of the 64 GCMs reproduced the observed slope of 3.3 mm/year (0.13 in/year). For the period 1985 to 2099, the slope varied from -1.3 mm/year to 2.5 mm/year over the 64 GCM outputs.

Table B-1: Summary of observed and simulated annual precipitation statistics for the three study sites.

Location	Data Source	Average (mm)	Stan. Dev. (mm)	Slope, 1950-2020 (mm/year)	Slope, 1985-2099 (mm/year)
Minneapolis	Observed	739.1	155.0	3.30	n/a
	mpi-esm-mr rcp4.5	754.4	142.2	0.18	0.53
	mpi-esm-mr rcp8.5	751.8	142.2	0.17	1.09
Rochester	Observed	800.1	177.8	3.81	n/a
	mpi-esm-mr rcp4.5	787.4	152.4	1.27	1.32
	mpi-esm-mr rcp8.5	807.7	147.3	-0.023	1.68
Duluth	Observed	774.7	129.5	0.28	n/a
	mpi-esm-mr rcp4.5	800.1	149.9	1.88	0.28
	mpi-esm-mr rcp8.5	792.5	137.2	1.42	0.79

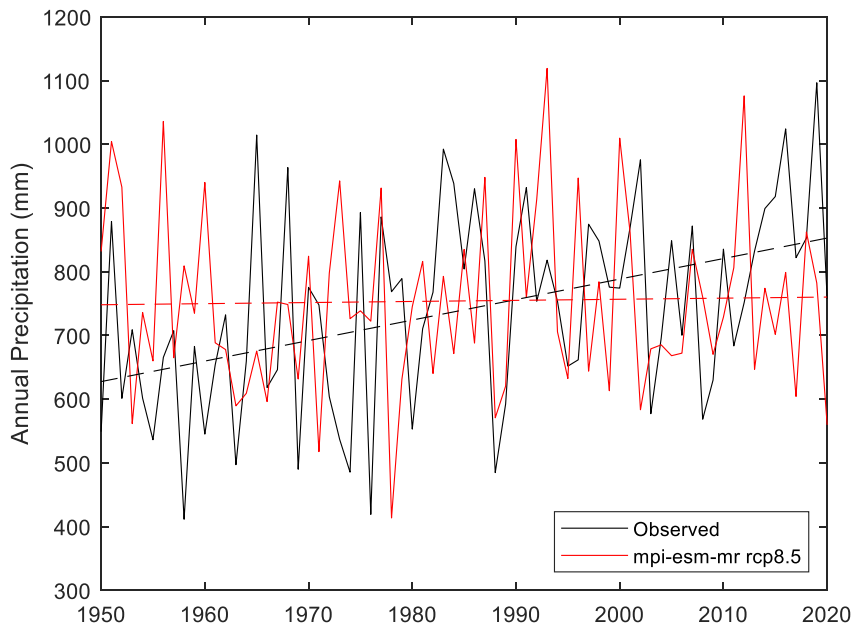


Figure B-4: Observed and simulated (mpi-esm-mr rcp8.5) annual total precipitation, 1950-2020, and linear trend fits, Minneapolis.

B.3.4.2 Annual Maximum Precipitation

Times series of the annual maximum daily precipitation depth were calculated for each GCM output and for the observed daily precipitation. For all three sites, the annual maximum daily precipitation simulated by GCMs underpredict the observed precipitation maxima, and the GCM outputs do not capture the positive slope of the observed annual maxima from 1950 to 2020 (Table B-2, Figure B-5). Minneapolis was the only station of the three where the slope of observed annual maxima was significant (Figure B-5), based on the Mann-Kendall test ($p=0.05$).

Table B-2: Summary of observed and simulated annual precipitation statistics for the three study sites, based on observed and simulated daily precipitation.

Location	Data Source	Mean (mm)	Stan. Dev., (mm)	Slope, 1950-2020 (mm/year)
Minneapolis	Observed	59.5	30.7	0.30
	mpi-esm-mr rcp4.5	41.0	11.7	0.0042
	mpi-esm-mr rcp8.5	41.0	11.7	0.0042
	All GCMs (range)	41.0 to 47.5	10.1 to 14.8	-0.23 to +0.19
Rochester	Observed	65.2	30.1	0.20
	mpi-esm-mr rcp4.5	53.5	25.6	-0.023
	mpi-esm-mr rcp8.5	53.5	25.6	-0.023
	All GCMs (range)	47.4 to 62.3	13.7 to 33.6	-0.63 to 0.65
Duluth	Observed	57.5	17.9	-0.05
	mpi-esm-mr rcp4.5	46.0	14.0	0.10
	mpi-esm-mr rcp8.5	46.0	14.0	0.10
	All GCMs ((range)	44.6 to 51.4	11.0 to 18.7	-0.22 to 0.26

For Minneapolis and Rochester, there is a general shift upward in the GEV distribution of the observed daily precipitation between 1950-1979 and 1988-2017, indicating an increase in storm sizes (Figure B-6 and Figure B-7), while there was relatively little change in GEV distribution in Duluth (Figure B-8). For all three sites, GEVs of the GCM-simulated precipitation shifted upwards between 1950-1979 and 1988-2017 (Figure B-6 - Figure B-8), with the best agreement between the observed and simulated data at Rochester (Figure B-7). The underprediction of observed annual maximum precipitation depths by the mpi-esm-mr model for the three study sites apparent in Table B-2 was also apparent in the GEV analysis (Figure B-6 - Figure B-8).

For longer time periods, the GEV precipitation distributions continued to shift upward to 2100, but the relative positions of the mid-century (200-2049) and late-century distribution (2050-2099) varied between the three sites (Figure B-9 - Figure B-11).

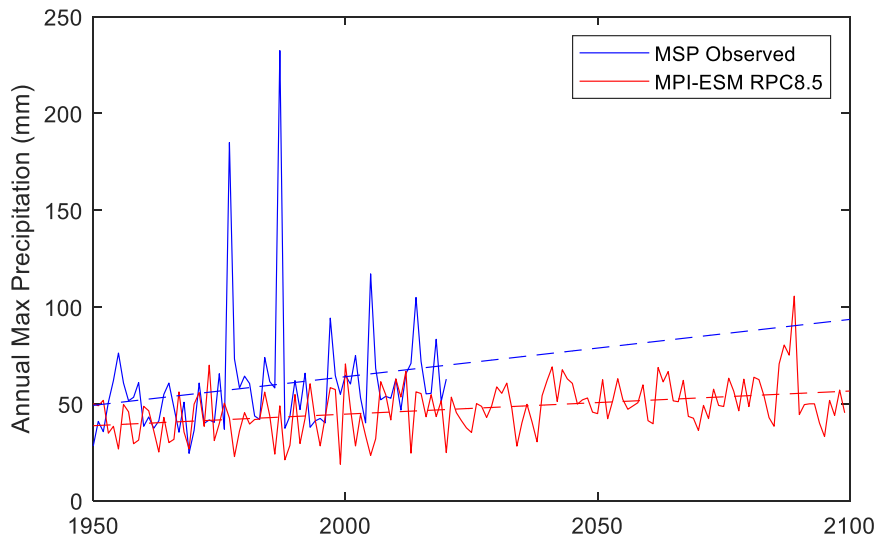


Figure B-5: Observed and simulated (mpi-esm-mr rcp8.5) annual maximum daily precipitation time series and fitted trendlines, for Minneapolis.

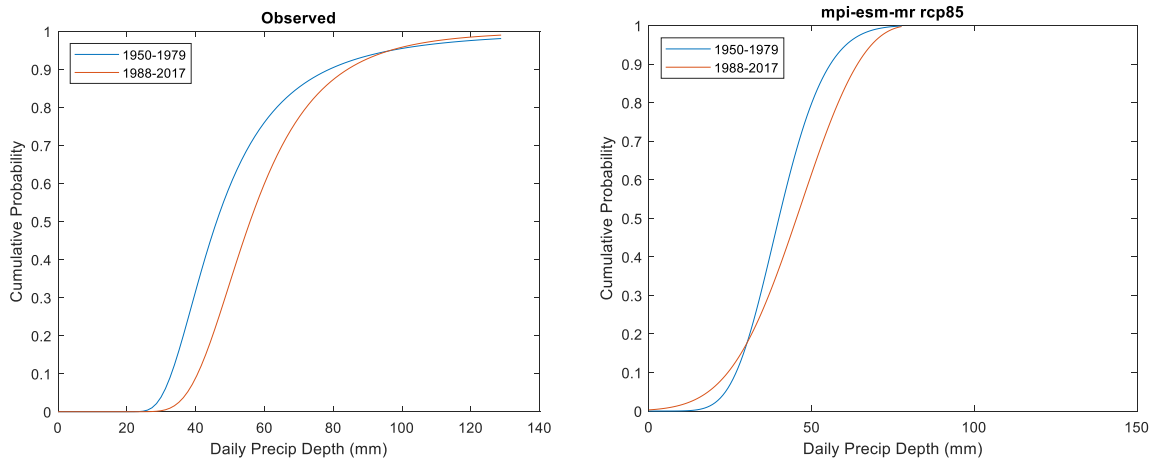


Figure B-6: GEV distributions of observed and simulated annual maximum daily precipitation for the time periods 1950-1979 and 1988-2017, Minneapolis.

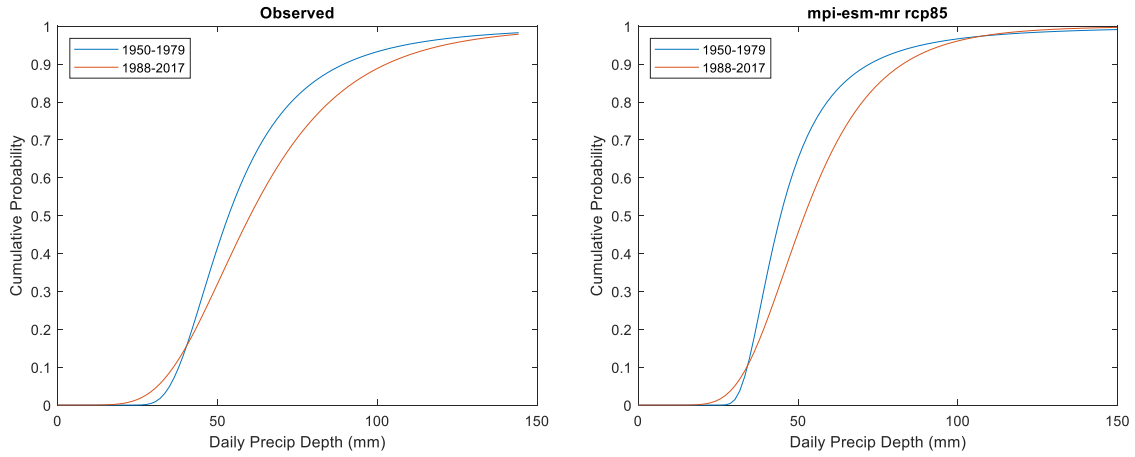


Figure B-7: GEV distributions of observed and simulated annual maximum daily precipitation for the time periods 1950-1979 and 1988-2017, Rochester.

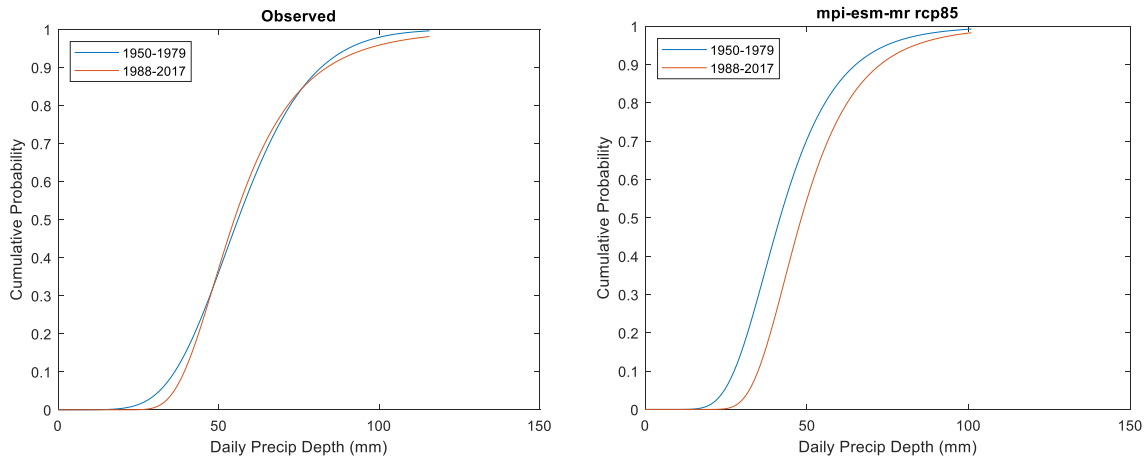


Figure B-8: GEV distributions of observed and simulated annual maximum daily precipitation for the time periods 1950-1979 and 1988-2017, Duluth.

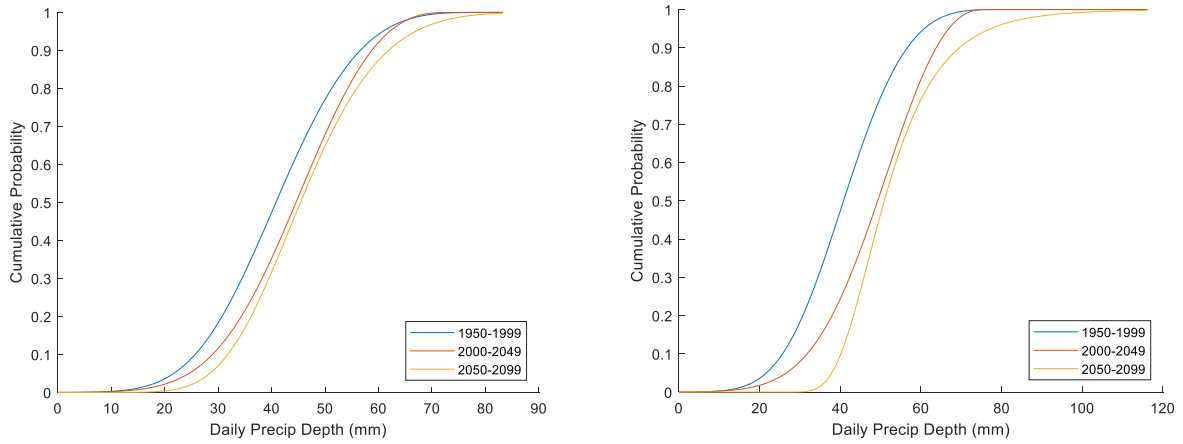


Figure B-9: Historical and future GEV precipitation distributions for 50-year blocks of data, MPI-ESM-MR, RCP4.5 (left) and RPC8.5 (right), Minneapolis.

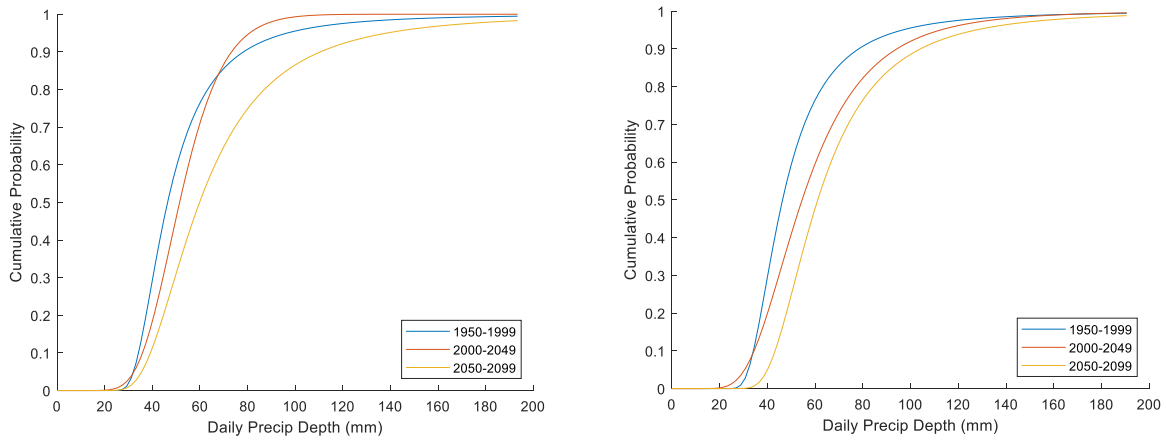


Figure B-10: Historical and future GEV precipitation distributions for 50-year blocks of data, MPI-ESM-MR, RCP4.5 (left) and RPC8.5 (right), Rochester.

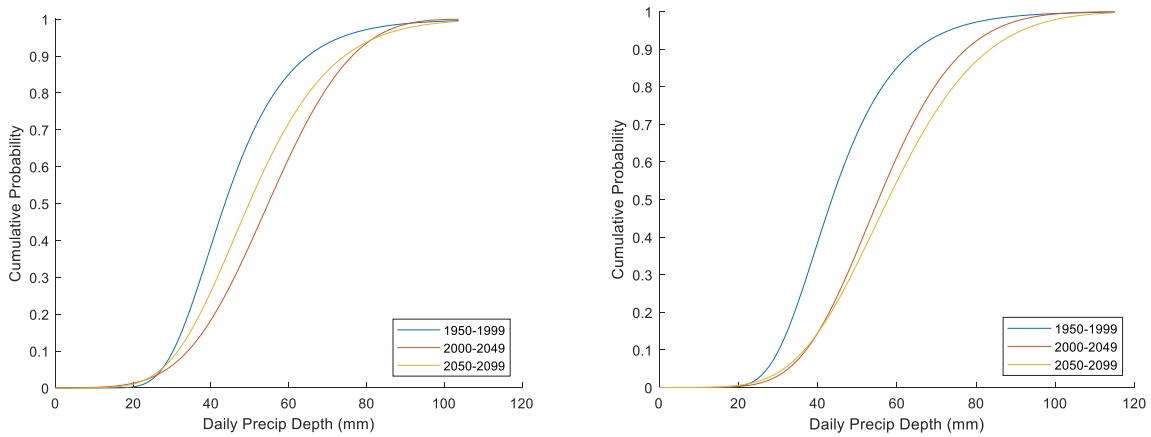


Figure B-11: Historical and future GEV precipitation distributions for 50-year blocks of data, MPI-ESM-MR, RCP4.5 (left) and RPC8.5 (right), Duluth.

B.3.4.3 Probability of Wet Days

The GCM outputs had a significantly higher probability of a wet day (mean=0.55) compared to observations (0.31) at Minneapolis, with similar results for Duluth (Table B-3). Agreement was better for Rochester, with a probability of wet days based on the GCM outputs and observed data of 0.41 and 0.31, respectively. The probability of a wet day following a wet day was also higher in the GCM outputs than observed at all three sites (Table B-3). For both the GCM outputs and observations, P(W) and P(W/W) changed only slightly between 1950-1979 and 1988-2017. For Minneapolis, the mpi-esm-mr GCM outputs showed modest changes in P(W) and P(W/W) out to 2100, with both emission scenarios showing changes less than 10% in P(W) and P(W/W) (Figure B-12).

Table B-3: Probability of a wet day P(W) and probability of a wet day following a wet day P(W/W) for the GCM outputs and observations at Minneapolis, Duluth, and Rochester.

Location	Data Source	P(W)		P(W/W)	
		1950-1979	1988-2017	1950-1979	1988-2017
Minneapolis	Observed	0.313	0.320	0.438	0.445
	mpi-esm-mr rcp45	0.542	0.548	0.667	0.670
	mpi-esm-mr rcp85	0.542	0.563	0.667	0.684
	Mean, all GCMs	0.548	0.547	0.673	0.672
	Stan. Dev., all GCMS	0.0070	0.0084	0.0092	0.010
Duluth	Observed	0.372	0.362	0.502	0.481
	mpi-esm-mr rcp45	0.529	0.540	0.651	0.655
	mpi-esm-mr rcp85	0.529	0.556	0.651	0.667
	Mean, all GCMs	0.539	0.538	0.658	0.660
	Stan. Dev., all GCMS	0.0066	0.0068	0.0079	0.0098
Rochester	Observed	0.310	0.331	0.435	0.458
	mpi-esm-mr rcp45	0.414	0.431	0.581	0.598
	mpi-esm-mr rcp85	0.414	0.433	0.581	0.597
	Mean, all GCMs	0.425	0.425	0.589	0.591
	Stan. Dev., all GCMS	0.0053	0.0080	0.01	0.0091

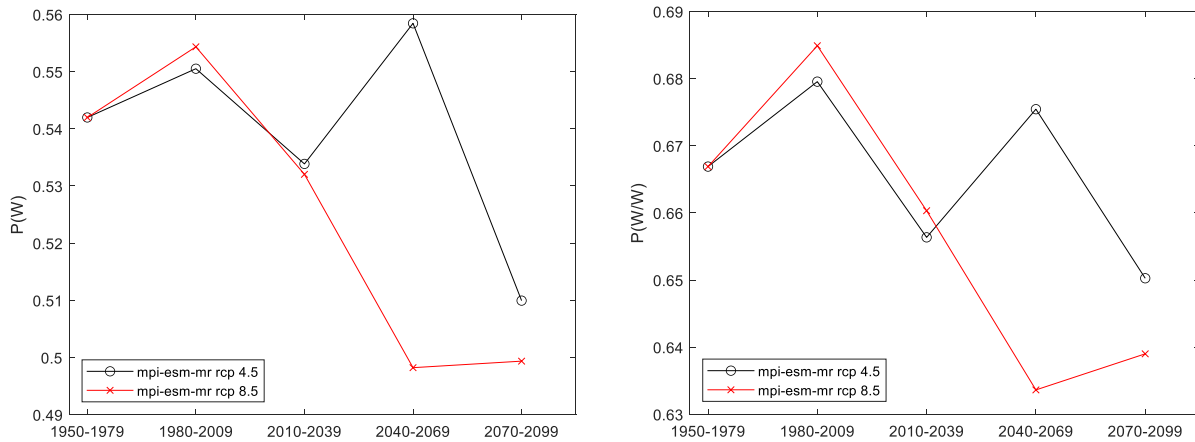


Figure B-12: Probability of a wet day (P(W)) and probability of a wet day following a wet day (P(W/W)) for the mpi-esm-mr RCP4.5 and RCP8.5 GCM outputs, for 30-year blocks from 1950 through 2099.

B.3.5 Relationships of Precipitation to Temperature

Observed hourly precipitation data for MSP, DLH, and RST were binned according to the mean daily air temperature, per Ledereck et al. (2010). The 90th, 99th, and 99.9th percentile hourly precipitation depth was then calculated for each bin and plotted against temperature on a semi-log scale. Figure B-13 gives an example of the precipitation-air temperature relationship for Minneapolis. The log slope parameter (α) of the three exponential fit lines in Figure B-13 are 0.054, 0.076, and 0.097, where the fit is of the form $d = \beta \cdot \exp(\alpha \cdot T)$, where d is precipitation depth (mm), and T is temperature ($^{\circ}\text{C}$). These log slopes can be compared to a theoretical increase in saturated water vapor content with temperature, which varies with temperature, but is, for example, 0.065 at 14 $^{\circ}\text{C}$ (Boer 1993). A similar analysis of daily precipitation depths was also performed, showing a similar relationship with temperature, but with lower slopes (Figure B-13) of 0.028, 0.031 and 0.045 for the 90th, 99th, and 99.9th percentile daily depths, respectively.

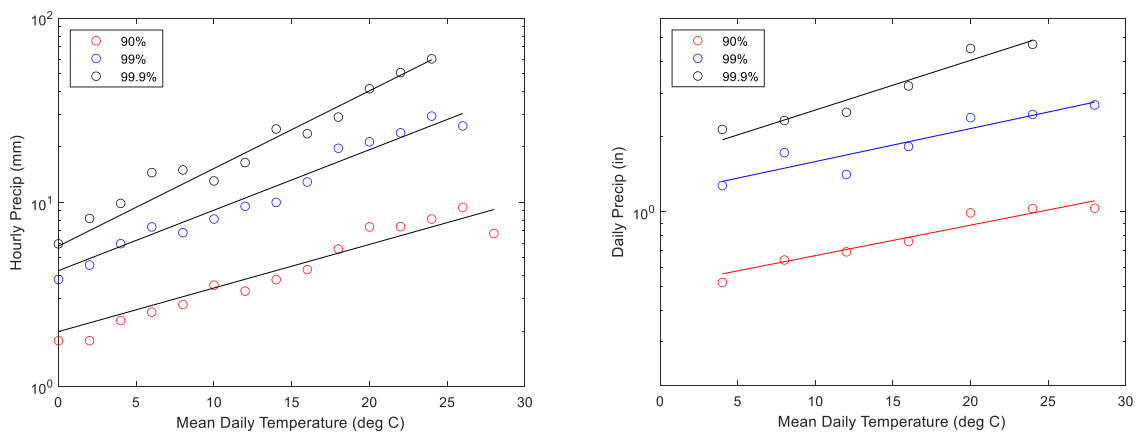


Figure B-13: 90th, 99th, and 99.9th percentile hourly (left panel) and daily (right panel) precipitation depth vs. mean daily air temperature based on observed MSP data, 1950-2020

B.3.6 Discussion

The analysis in this section shows the limitations of the downscaled GCM outputs. While the GCMs reproduce the mean and variability of annual precipitation in the historical period, finer scale details such as the annual maximum precipitation and historical trends in precipitation are not captured as well. Overprediction of the number of wet days by the GCMs leads to underprediction of the annual maximum daily rainfall. Future changes in the distribution of daily precipitation at mid-century and end-of-century vary significantly between GCMs and between locations – this will be a large source of uncertainty for future projected storm sizes at daily and sub-daily time scales.

The air temperature precipitation relationships found are in the same range as previous research, and could provide the basis for an alternate method for projecting future changes in extreme storms based on projected increases in air temperature. A temperature-based method for projecting future storm sizes was used for the future storm database in the USEPA Climate Resilience Evaluation and Awareness Tool (USEPA 2016).

B.4 Frequency Analysis

B.4.1 Preliminary Analysis

The first step in our data analysis was the selection of the data sets and the probability density function to represent the sub-daily duration data. We limit our analysis to Twin Cities using annual maximum series. Both hourly (at MSP) and 15-minute data (at GV) are available for 1972 through 2013. The annual maximum 1 h, 2 h, 4 h, 6 h, 12 h and 24 h depths were computed for both sets of data. Limited screening of raw data was done with these data sets. The cumulative distributions were estimated using the plotting position and the EV1 and GEV distributions.

Frequency analyses for the 1-h duration and 6-h duration are shown in Figure B-14 and Figure B-15. Symbols correspond to the plotting values, solid lines to the GEV distribution and dotted lines to the EV1 distribution. The GEV data better represents the plotting position values. It is selected for the remaining analyses. The GV and MSP data provide similar results for 6-h duration. The GEV data resulted in larger depths for the 1-h duration. Since the MSP data set is longer, this data set is the primary source of frequency analysis of sub-daily depths.

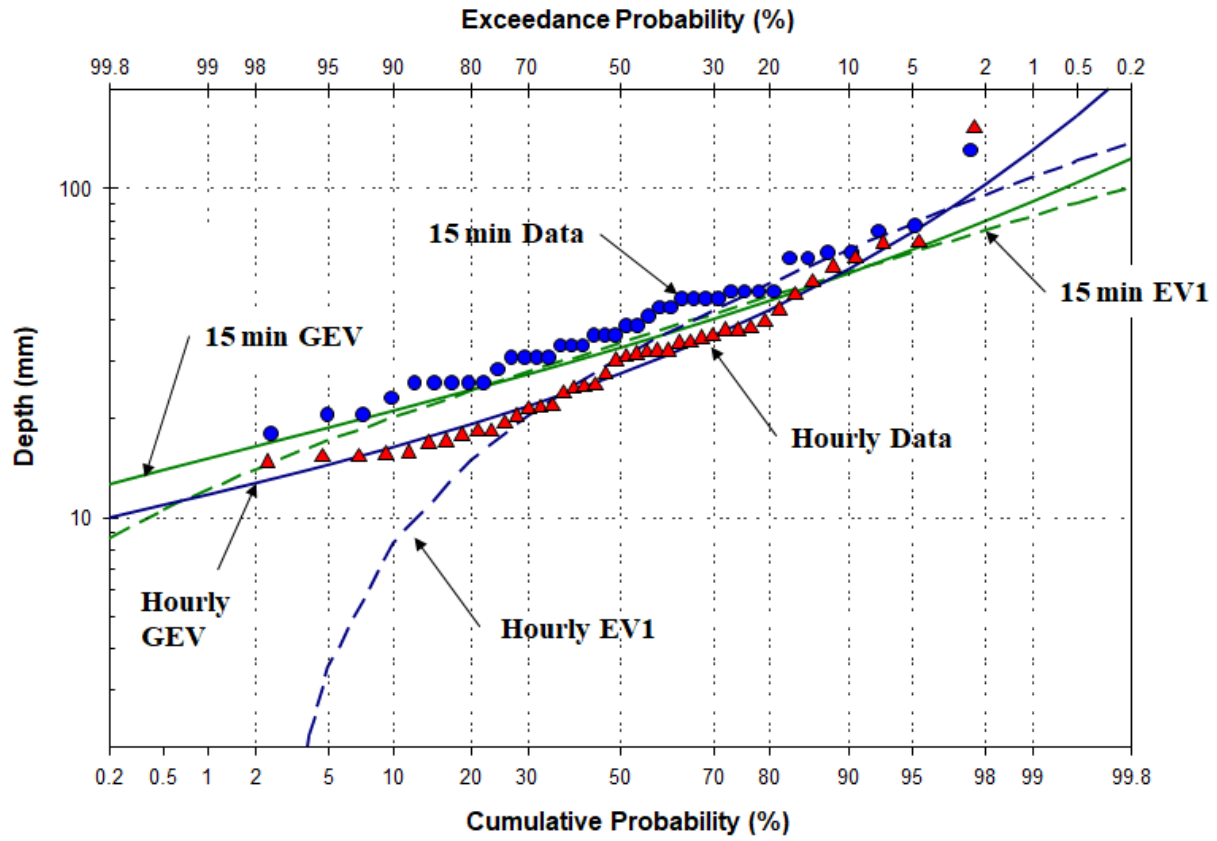


Figure B-14: Frequency Analysis for 1-h Duration.

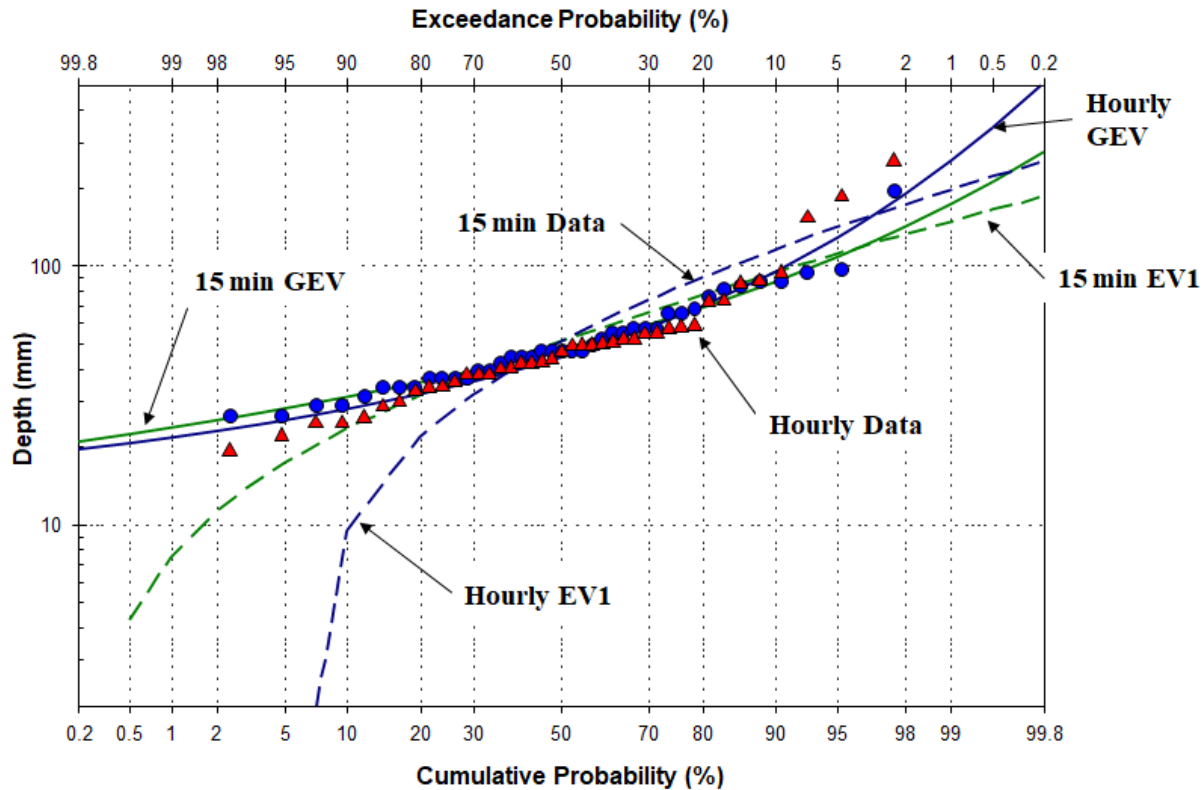


Figure B-15: Frequency Analysis for 6-h Duration.

For durations less than 1-h, the ratios of depths of the 15-min, 30-min and 45-min to the 1-h depth from the GV data set are used. These ratios are computed for return periods of 2-yr, 10-yr and 100-yr. By multiplying each ratio by the corresponding 1-h depth for MSP data set, the sub-hour depths can be estimated. The statistical parameters of the GEV can then be estimated using Eqs. 19 and 20. The ratios are given in Table B-4.

Table B-4: Ratios Used to Compute Depths for Sub-hour Durations

Return Period	Ratios		
	$P_{0.25}/P_1$	$P_{0.5}/P_1$	$P_{0.75}/P_1$
2 yr	0.54	0.77	0.91
10 yr	0.56	0.80	0.91
100 yr	0.53	0.85	0.93

B.4.2 Sub-Daily Analysis

For the overall goal of the project, the observed current conditions will be determined using the analysis of Atlas 14. To evaluate the quantile method, however, frequency analyses were performed of the observed data for the pre-climate change conditions (approximately 1950-1979) and the current conditions with climate change (approximately 1988 to 2017). Depths obtained using the quantile

method for these two time periods are compared to those given by Atlas 14. Statistical parameters for Atlas 14 were determined using depths corresponding to the 2-yr, 10-yr, and 100-yr and Eqs. 19 and 20.

As discussed in the data section, observed data were screened to remove years with potential errors in the sub-daily depths. This screening was done by comparing the annual maximum 24-h depth to the annual maximum daily depths. Based on this analysis, four years of data were removed in the 1960s for pre-climate analysis. These four years were replaced with data prior to 1950 and additional years prior to 1985. Data were also removed for the current climate conditions. These data were replaced with estimates corresponding to the 15-min data set and additional hourly data by including years between 1981 and 1988.

Frequency plots for the 1-h duration and the 24-h duration are shown in Figure B-16 and Figure B-17. For the 1-h duration, the plotting position points are generally larger for the current data than the pre-change data. We therefore have a larger mean and median for the current data. However, the variance of the pre-change data is larger than that of the current data. Because of this larger variance, and a shift in the non-symmetry parameter γ , the 100-yr, 1-h depth for the pre-climate change (pre-change) condition is greater than that of the climate-change conditions. This outcome is likely caused by the uncertainty in estimating statistical parameters with only 30 years of data. It is difficult to estimate 100-yr depths with a record length of 30 years. Also shown in Figure B-16 and Figure B-17 are the depths obtained from Atlas 14. The 100-yr depths from Atlas 14 are larger than those obtained using the pre-change data for both 1-h and 24-h durations.

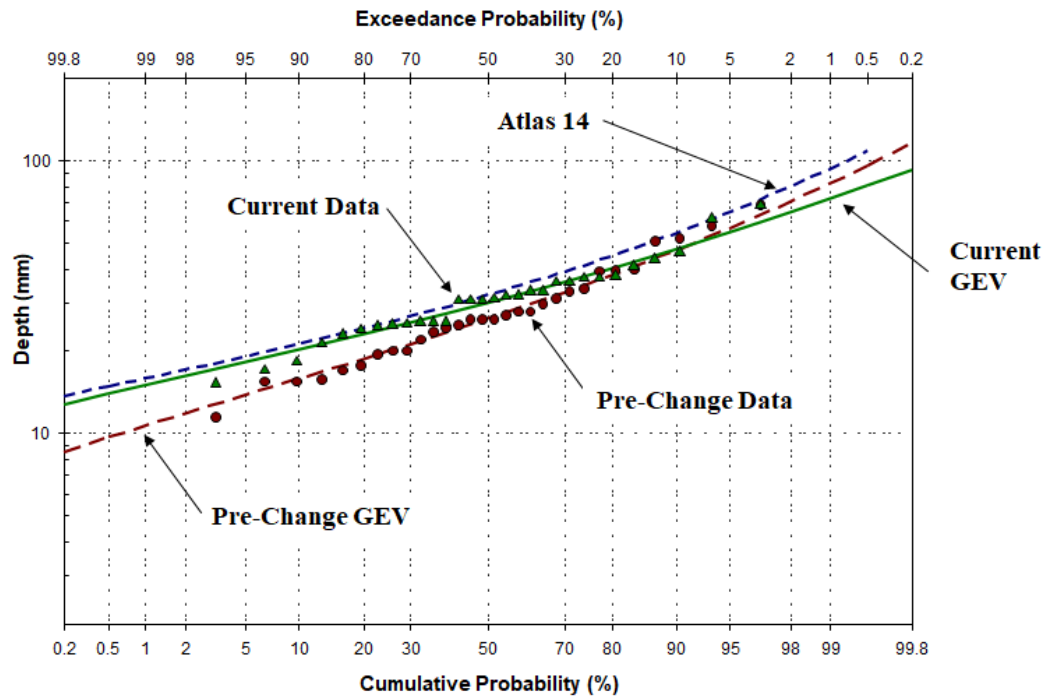


Figure B-16: Frequency Analysis for 1-h Duration for Pre-Change and Current Conditions.

For the 24-h duration, the variance is smaller than that of the 1-h duration. Once again, the plotting position points are generally larger for the current conditions than pre-change values. The current GEV predicts a larger 100-yr depth than those obtained from Atlas 14 and pre-climate change conditions. These trends need to be considered with the context of issues previously discussed of observed data and the inherent uncertainty in estimating the 100-yr value using 30 years of data. Since 100-yr depth of the pre-change using GEV is similar to that of Atlas 14, it is useful to consider what the pre-change depth would have been if the EV1 distribution was used instead of GEV. Once again, EV1 distribution was used to estimate 100-yr depths in TP-40. The difference between the two distribution is approximately 15 mm.

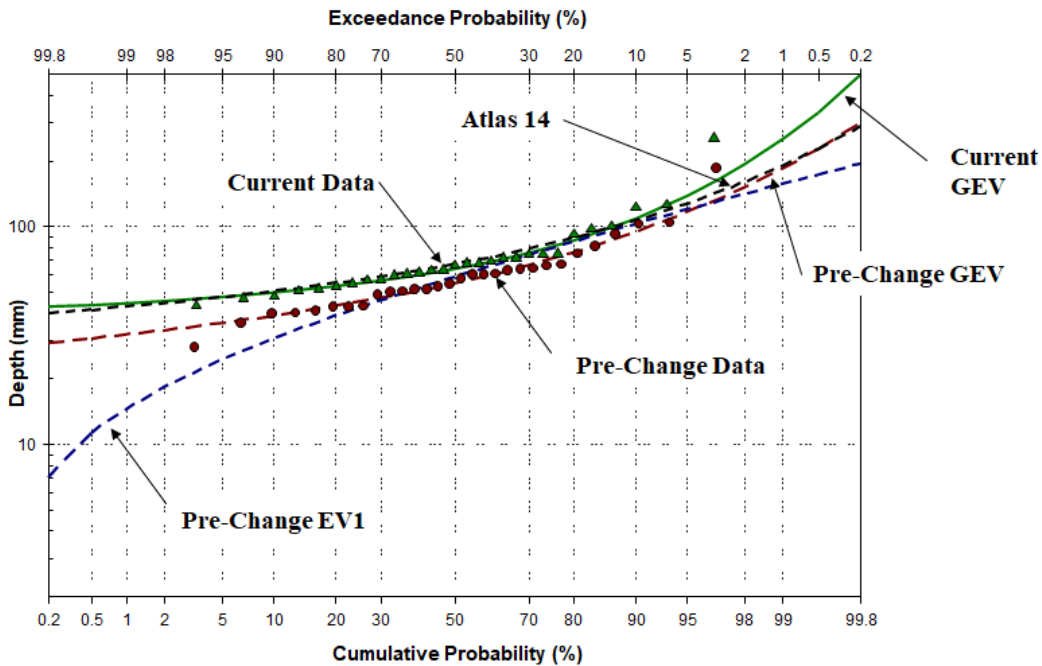


Figure B-17: Frequency Analysis for 24-h Duration for Pre-Change and Current Conditions

Greater insight into trends of return period depths of different duration is obtained by examining the mean and standard deviation. Trends in these statistics for the pre-change data are shown in Figure B-18 for durations between 1-h and 24-h. As expected, the mean increases with duration. However, the standard deviation decreases between the 6-h duration and the 24-h duration. The uncertainty in sample estimate of the standard deviation is greater for 30 years of data than the sample estimate of the mean. Similar issues occur when considering the non-symmetrical parameter γ .

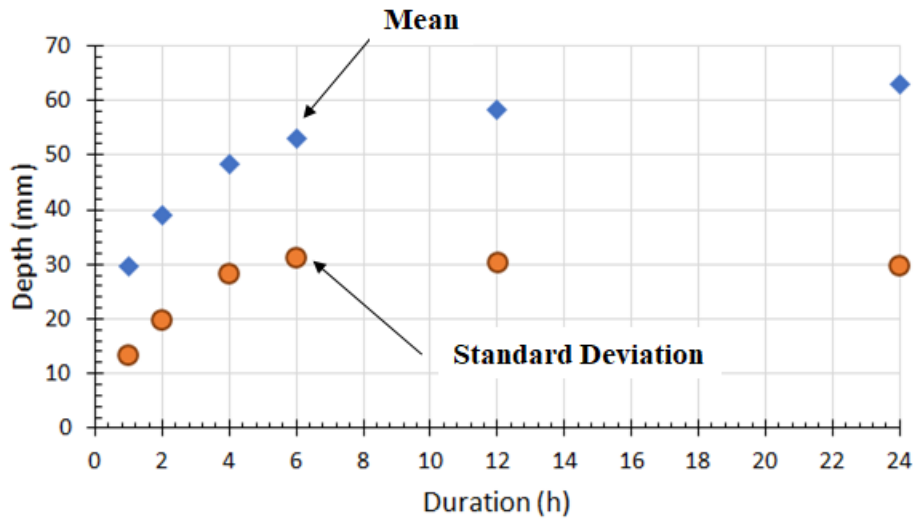


Figure B-18: Mean and Standard Deviation Trends with Duration for pre-climate change conditions.

Let's now consider the trends of 100-yr depths for pre-change conditions shown in Figure B-19 for durations between 1 h and 24 h. As expected, the 100-yr depths increase to a duration of 6 h; however, the 100-yr depth decreases for the durations of 12-h and 24-h. Since the annual maximum depths for the 12-h and 24-h must be at least as large as that of the 6-h duration, additional adjustments are required. These adjustments are necessary because of the limitations of the observed data and issues in estimating statistical parameters with only 30-years of data.

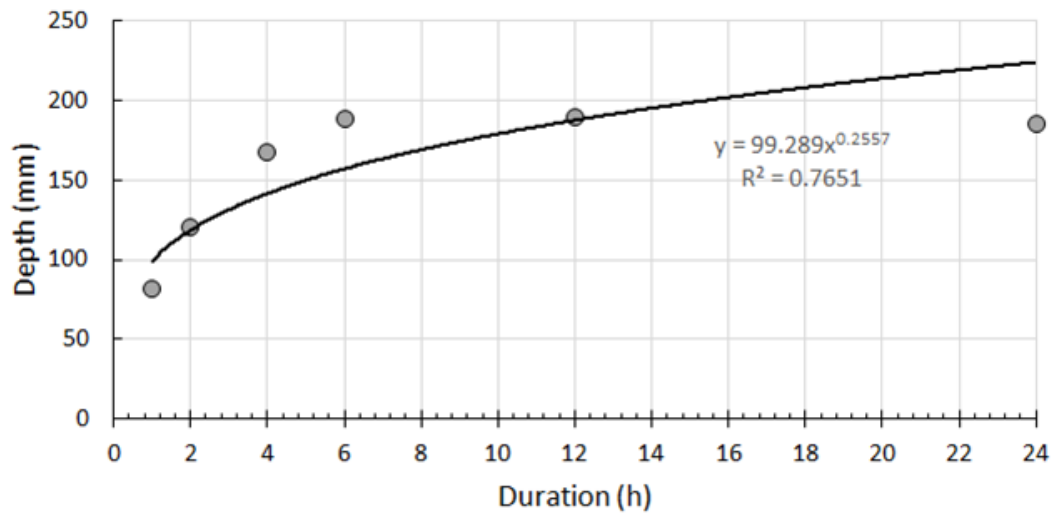


Figure B-19: Trends in 100-hr Depths with Durations for Pre-climate change Conditions

Adjustments to the pre-change data were obtained by replacing the 100-yr depths for each duration obtained from GEV distribution with values obtained by the power function shown in Figure B-19. No changes were made in the 2-yr and 10-yr depths. The GEV statistical parameters were then recomputed using Eqs. 19 and 20 with the new 100-yr depths. The original and the adjusted cumulative distributions

for 6-h, 12-h and 24-h durations are shown in Figure B-20. The dotted lines correspond to the original GEV and solid lines for the adjusted GEV. The 24-h adjusted GEV have a larger depth than the 6-h and 12-h durations for all return periods. The adjusted GEV are used as the cumulative distribution of the sub-daily depths in the quantile method.

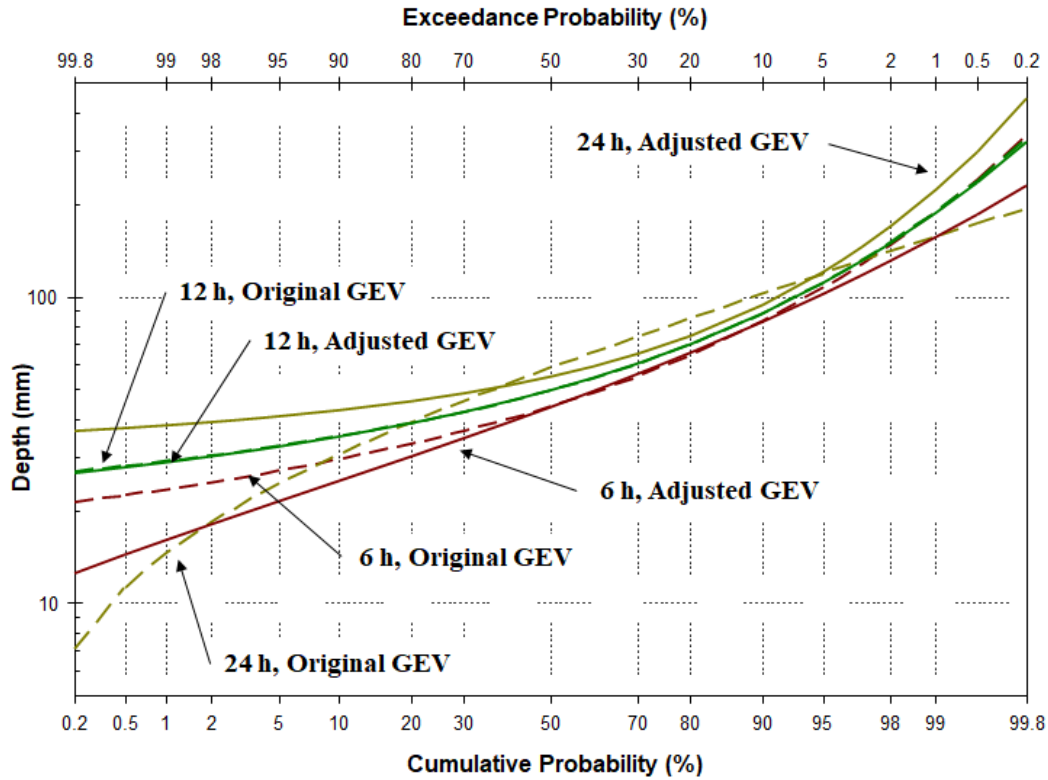


Figure B-20: Original and Adjusted GEV for 6-h, 12-h and 24-h Durations.

B.4.3 Analysis of GCM Simulated Data

The frequency analysis of daily depths obtained from the GCM for the pre-change climate conditions and for current conditions using RCP of 8.5 and 4.5 has been previously discussed. Key results are summarized in Figure B-21 with the addition of plotting position values obtained for the data between 1950 and 1979. Once again, the GCM model substantially underpredicts the observed annual maximum series values. The simulated annual maximum daily depths for return periods greater than 2-yr are larger for the current conditions than pre-change conditions. The increase is greater for RCP8.5 than RCP4.5.

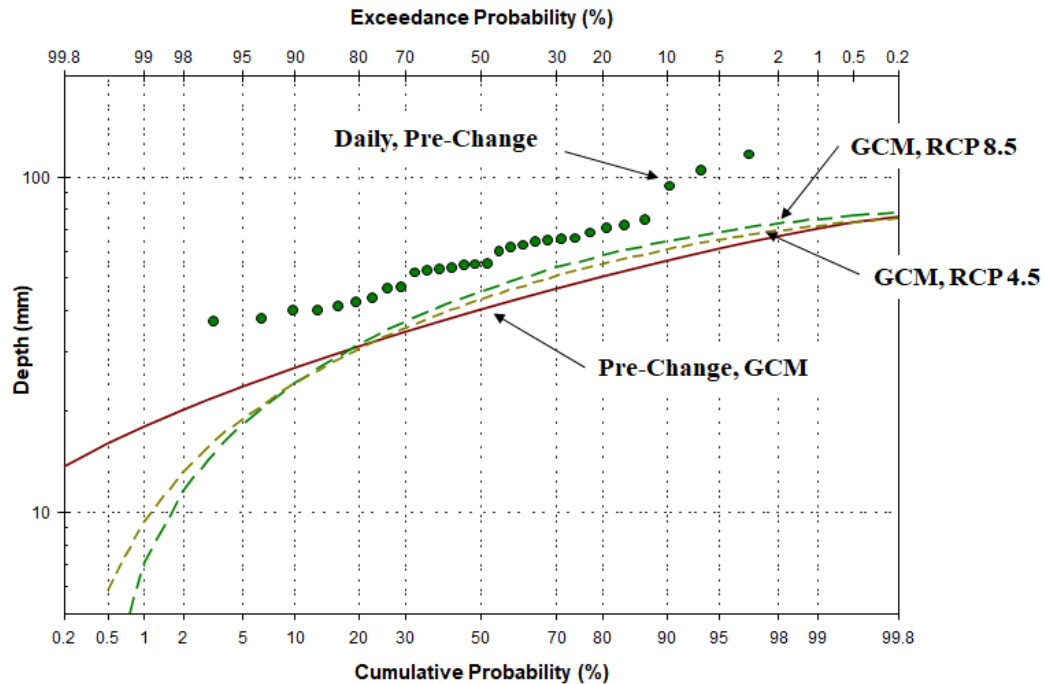


Figure B-21: Frequency Analysis of Daily Depths Using GCM simulations mpi-esm-mr rcp4.5 and mpi-esm-mr rcp8.5.

B.5 Future DDF for Sub-daily Durations

B.5.1 Evaluation of Quantile Method

Based on the results of the previous subsection, we know the statistical parameters of the observed pre-change sub-daily durations and the GCM under pre-change conditions and for future conditions using RCP of 4.5 and 8.5. The current sub-daily depths can now be determined using the quantile method. The results are summarized using DDF plots. To simplify the plots, only return periods of 2-yr, 10-yr and 100-yr are shown. These return periods adequately capture trends of the quantile method.

A comparison of DDF values by different methods are shown in Figure B-22. Depths obtained from the frequency analysis of the pre-change data are shown as solid lines. Atlas 14 depths are represented by symbols. Depths from the quantile methods are given for GCM RCP4.5 (long-dashed lines) and for GCM 8.5 (short-dashed lines). The quantile method resulted in consistent estimates of the Atlas 14 depths for 2-year return periods. The predicted depths using RCP4.5 were also consistent with Atlas 14 values. Less accurate results were obtained for the 100-yr return period depths. Limitations of the observed data sets have the smallest impact on the 2-year depths and the greatest impact on the 100-year values. The observed 100-year depths were also adjusted by the power function given in Figure B-19. Because of these uncertainties, we have the least confidence in using the quantile method for 100-year depths.

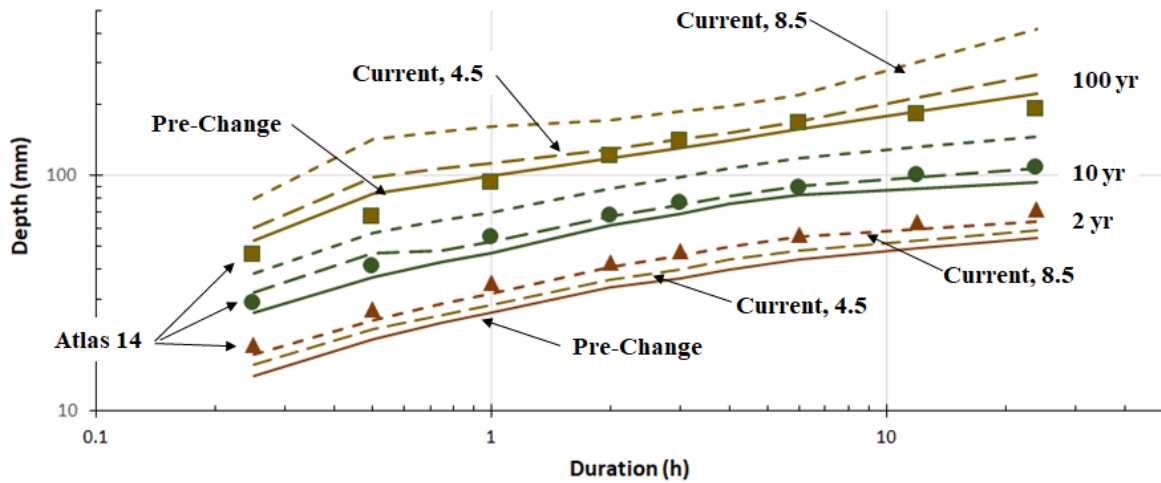


Figure B-22: DDF Depths Using Quantile Method and Depths from Atlas 14.

To tie the sub-daily analysis to the WSP results, our interest lies in the sub-daily depth normalized by the 24-h depth. These ratios were computed for the data of Figure B-22 and are shown in Figure B-23. With exception of the 100-yr values, the ratios are consistent with the pre-change and Atlas 14 values. Considering the uncertainties in the quantile method, the Atlas 14 values may be adequate to determine the temporal distribution of depths for analysis of engineering projects using a design storm.

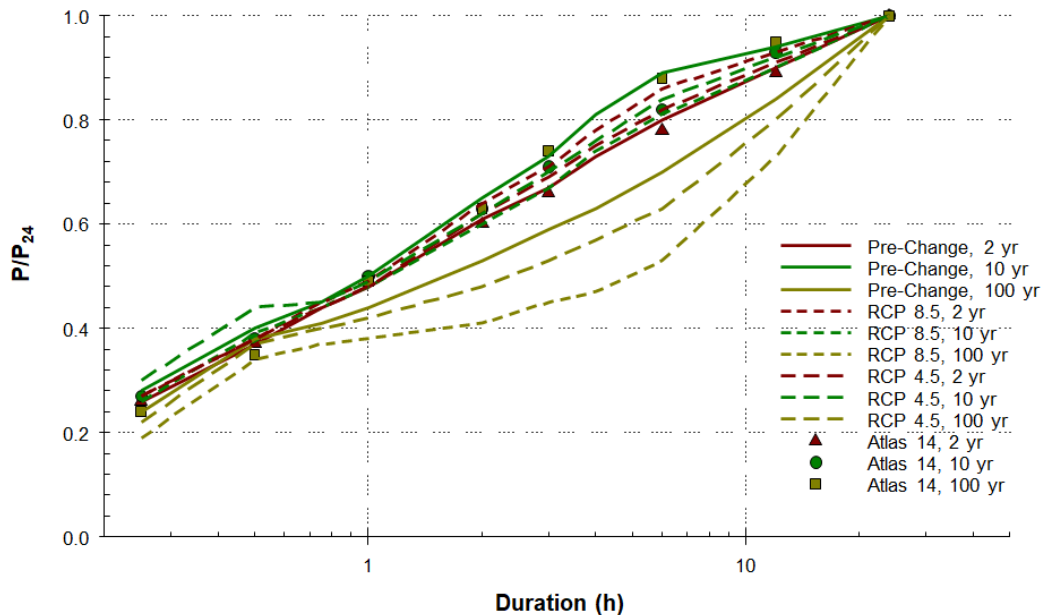


Figure B-23: Summary of Normalized Depths for Different Durations.

B.5.2 Application of Quantile Method

To illustrate the application of the quantile method to the overall goals of the project, the method was used to determine temporal patterns of 2-yr, 10-yr and 100-yr design storms. These patterns are inputs into the SWMM model. For our illustration, the statistical parameters for the cumulative distributions of sub-daily depth of current conditions were evaluated using Atlas 14 data and Eqs. 19 and 20. The annual maximum daily depths for current conditions were obtained from the GCM for RCP8.5 (mpi-esm-mr rcp 85) for a simulation period of 1980 to 2009. The annual maximum daily depths for future conditions were obtained using the same model for a simulation period of 2040 to 2069.

The 2-yr, 10-yr and 100-yr depths using the quantile method are shown in Figure B-24. Also shown in this figure are the depths of Atlas 14 (current condition), which are shown as solid lines. The future depths are nearly identical to the current conditions. The sub-daily depths for the 100-yr return periods are considerably larger than those obtained using Atlas 14. The sub-daily depths for the 10-yr return period for 2040-2019 are only slightly larger than those obtained for 1980-2009.

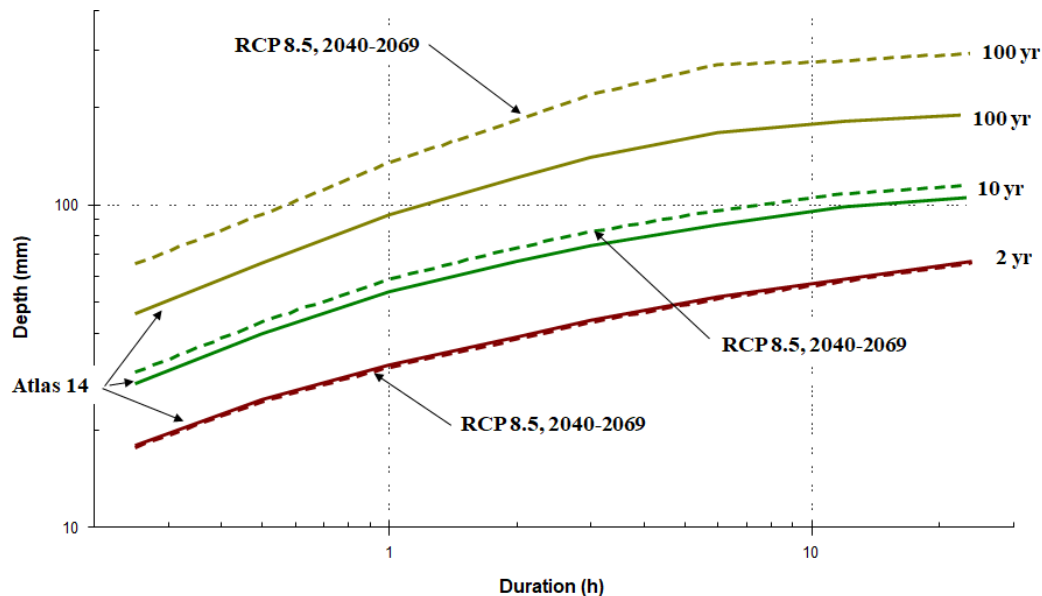


Figure B-24: DDF Analysis for MSP using RCP8.5 for 2040 to 2069.

The normalized depths necessary for the temporal rainfall patterns are shown in Figure B-25. The ratios are similar using Atlas 14 for the 2-yr and 10-yr return periods. The future ratios are noticeably different than those of Atlas 14 for the 100-yr events.

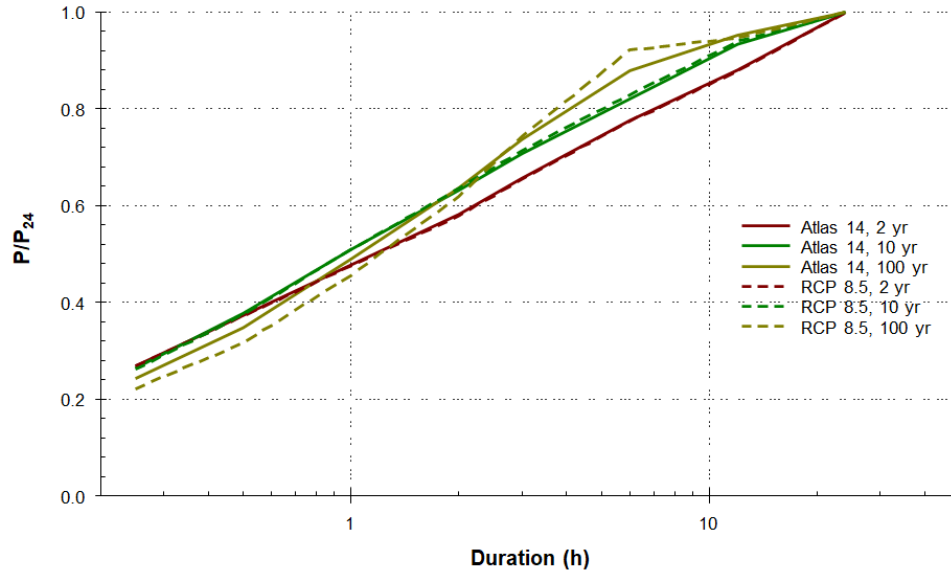


Figure B-25: Normalized Sub-daily Depths Using GCM for 2040 to 2069.

The temporal pattern necessary for SWMM simulations is obtained by assuming that depths within the storm corresponding to different durations have the same return period. Similar to the SCS Type II storm, the most intense part of the storm occurs at 12 hours. The storm pattern using these criteria are shown in Figure B-26 for the 2-yr, 10-yr and 100-yr return period events. Other return periods can be obtained using the same approach. A greater fraction of the storm occurs at 12 hours as the return period increases from 2-yr to 100-yr.

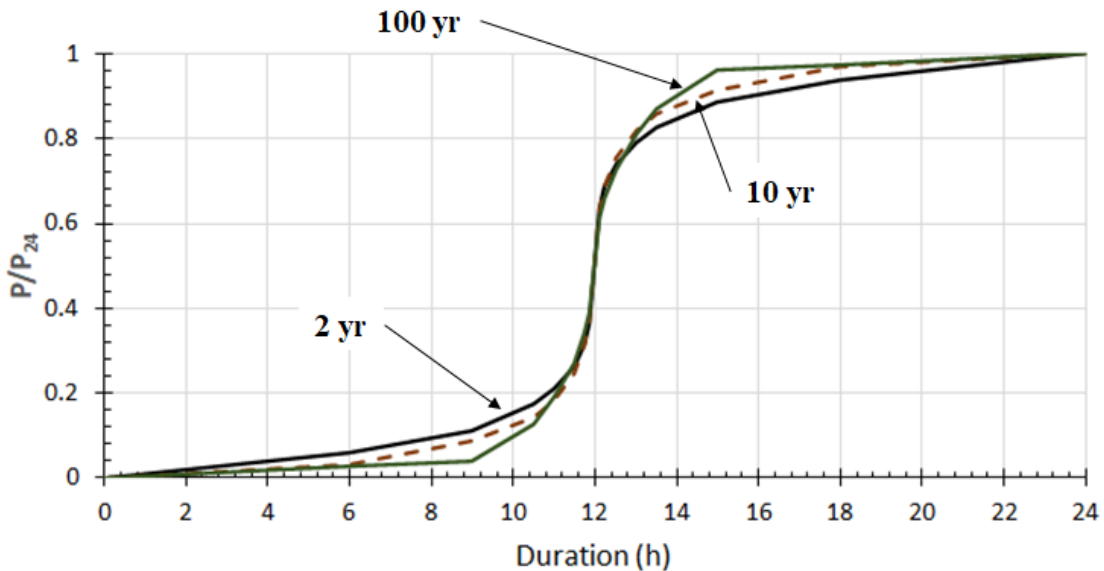


Figure B-26: Design Storms for 2-yr, 10-yr and 100-yr Return Periods for 2040 to 2069.

B.5.3 Annual and Partial Duration Series

Our analysis was done using maximum annual series corresponding to the quantile methods of Srivastav et al. (2014) and Butcher and Zi (2019). Frequency analysis is often done using the partial duration series. As shown in Figure B-26, the design storm patterns are defined using the ratio of the depths of different duration to that of the 24-hour. Differences between depths of the partial duration and maximum annual series occur in both the numerator and denominator of the ratio. Depths from Atlas 14 for different duration and different return periods were obtained using the maximum annual series and partial duration series for MSP, RST and DLH. Only the results for MSP are reported. Similar trends were obtained for RST and DLH.

Table B-5: Comparison of P_x/P_{24} Using Annual and Partial Duration Series for MSP.

Return Period	Type	Durations						
		15 min	30 min	60 min	2 h	3 h	6 h	12 h
2 y	Annual	0.261	0.368	0.477	0.591	0.655	0.769	0.875
	Partial	0.265	0.375	0.488	0.597	0.664	0.777	0.887
	% Diff	1.39	1.80	2.12	1.05	1.36	1.09	1.34
5 y	Annual	0.269	0.384	0.500	0.616	0.686	0.799	0.910
	Partial	0.269	0.384	0.500	0.619	0.689	0.802	0.912
	% Diff	0.01	0.12	0.00	0.38	0.47	0.35	0.28
10 y	Annual	0.266	0.380	0.505	0.629	0.703	0.823	0.928
	Partial	0.267	0.380	0.505	0.630	0.705	0.823	0.929
	% Diff	0.36	-0.18	-0.01	0.08	0.26	0.02	0.11
25 y	Annual	0.258	0.371	0.502	0.635	0.721	0.848	0.942
	Partial	0.257	0.371	0.503	0.635	0.721	0.847	0.942
	% Diff	-0.56	-0.06	0.18	0.03	-0.04	-0.12	0.03
50 y	Annual	0.250	0.360	0.497	0.635	0.730	0.863	0.947
	Partial	0.250	0.359	0.498	0.636	0.730	0.865	0.948
	% Diff	-0.16	-0.16	0.16	0.09	0.06	0.21	0.17
100 y	Annual	0.241	0.348	0.491	0.633	0.735	0.877	0.949
	Partial	0.241	0.348	0.491	0.633	0.735	0.877	0.949
	% Diff	0.00	0.00	0.00	0.00	0.00	0.00	0.00
200 y	Annual	0.233	0.336	0.483	0.630	0.740	0.888	0.951
	Partial	0.233	0.336	0.483	0.630	0.740	0.888	0.951
	% Diff	0.00	0.00	0.00	0.00	0.00	0.00	0.00
500 y	Annual	0.222	0.322	0.474	0.626	0.745	0.902	0.953
	Partial	0.222	0.322	0.474	0.626	0.745	0.902	0.953
	% Diff	0.00	0.00	0.00	0.00	0.00	0.00	0.00

The ratios of the depths of different duration and the 24-h depths for the annual series and partial duration series for MSP are shown in Table B-5. Percent differences in the ratios are less than one

percent for return periods greater than 2 years. Percent differences for the 2-y return periods is less than 2.5%. Because of the small differences between the two types of analysis, it is unnecessary to adjust the results obtained for the annual duration series to partial duration series.

B.6 Climate Predictions: Summary and Conclusion

Sub-daily depths are needed to assess the performance of stormwater infrastructures for a changing climate. Since these depths are not predicted by current GCMs, the goal of this section is to evaluate methods for estimating sub-daily depths. The analysis is conducted so that it can be tied directly to WSP daily depths obtained for different climate change scenarios. The theoretical framework is based on the quantile method. This method requires the annual maximum cumulative distributions of the sub-daily depths corresponding to current conditions. It also required the annual maximum simulated daily from GCMs for the current conditions and future conditions.

Three sources of observed precipitation data are used in the analysis. Data were downloaded for 15-min intervals, 1-h intervals and daily depths. The record length for the 15-min data was 1972 and 2013. The record length for the 1-h data was 1948 and 2020. Both data sets were used to determine the annual maximum depths for durations of 1 h, 2 h, 4 h, 6 h, 12 h and 24 h. The 15-min data set was also used for the annual maximum depths for durations of 15 min, 30 min and 45 min. Missing data and other inconsistency made the analysis more difficult. Some years were not used because of these difficulties. GCM simulations were selected for consistency with the WSP study.

An evaluation of the quantile method was done by considering a pre-climate change period (approximately 1950 to 1979) and current conditions with climate change (approximately 1988 to 2017) using the MSP site. The accuracy of the quantile method was assessed by comparing its predicted depths to those reported in Atlas 14. Statistical parameters of sub-daily depths were determined for both periods and used to estimate the cumulative distributions. The sub-daily depths obtained from the quantile method were consistent with the depths of Atlas 14 for the return periods of 2-yr and 10-yr. Depths were less consistent for the 100-yr return period events.

The quantile method was used to determine the design storm for climate conditions corresponding to 2040 to 2069. These storms provide inputs into preliminary SWMM simulations to assess alternative infrastructure designs. The sub-daily depths were normalized by the 24-h depth. The storm pattern was more intense at 12 hours for the 100-yr return period event.